Analysis *of the* Compartment Fire Parameters Influencing *the* Heat Flux Incident *on the* Structural Façade

Presented by

Cecilia Abecassis Empis

MEng (Civil Engineering) • The University *of* Edinburgh • 2004

For the degree of

Doctor *of* Philosophy

in

Structural Fire Engineering

THE UNIVERSITY *of* EDINBURGH

2010

Optimæ familiæ, cārissimīs amīcīs, sapientissimō magistrō, amantissimō spōnsō

Declaration

This thesis and the research work detailed herein has been solely conducted by the author, Cecilia Abecassis Empis, at the BRE Centre for Fire Safety Engineering, under the helpful supervision of Professor José L. Torero and Professor Asif Usmani at The University of Edinburgh and that of an industrial supervisor, Dr. Debbie Smith at BRE. Where others have contributed or other sources are quoted, adequate references are provided.

Cecília Abecassis Empis

October, 2010

Abstract

In recent years several high-profile building fires have highlighted shortcomings in the way we design for the complex interaction of structures and fire. These weaknesses appear to arise from a combination of gaps in knowledge of some of the more intricate aspects of compartment fire dynamics and from limitations in the engineering applications developed to date from hitherto established fundamentals. In particular the One Meridian Plaza Fire (1991), the Madrid Windsor Tower Fire (2005) and the Lakanal House Fire (2009) have emphasised the need for further study in the field of post-flashover compartment fires and the often consequent external fires that emerge from the compartment openings. External fire plumes impinge upon the structural façade, causing added structural stress, and often result in external fire spread and secondary ignition in upper level compartments. Hence a better understanding of the effect had by the internal compartment fire on the development of external flaming and the insult of the plume to its surroundings is beneficial for Structural Engineers, Fire Protection Engineers and Emergency Response Personnel alike. This research explores existing correlations, identifies their limitations and proposes a simplified methodology that links key parameters found to govern the internal post-flashover compartment fire to the heat flux potentially imposed on the exterior façade.

Existing correlations addressing the effect of compartment fires on the insult to the external structure have largely been compiled by Law and are summarised in the form of a design manual for bare external structural steel [1]. Formulated in the 1970s, these correlations are based on the combined findings of several different experimental tests devised to investigate component phenomena of compartment fires and external flaming, forming an *analytical model* which is mostly empirical in nature. The methodology is convoluted and has several inherent assumptions which give rise to various limits of applicability however it is currently still used in structural-fire design, but best known as Annex B of both Eurocodes 1 and 3 [2,3]. As part of the present research, full-scale fire tests are conducted *in situ*, in a highly instrumented high-rise building, to provide high-resolution measurements of several internal compartment fire characteristics during a post-flashover fire in a modern,

realistically-furnished compartment. External high resolution instrumentation in the main test also provides detailed measurements of the external flaming and distribution of heat flux incident on the façade. The tests provide *realistic benchmark scenario* data for comparing physical measurements against the analytical Law Model, the difference in which allows for an evaluation of the assumptions used in the model, which are often defined as 'conservative' in nature from the perspective of structural design.

A detailed sensitivity study of the main input parameters in the Law Model allows for the identification of parameters of pivotal influence on the resultant heat flux incident on the plane of the external façade. Analysis of the Law Model and its underlying experimental basis also enables the identification of several limits of applicability of the model. Combined, these assessments show the analytical model can be stripped of unnecessary complexity and a *Simplified Model* is proposed with clear bounds of applicability. The proposed model describes the distribution of heat flux to the façade above a compartment opening and features only parameters of key importance, where low-dependency parameters are grouped into associated error bars. This results in a model that can be applied in the design of several building components that fall in the plane of the façade, such as structural elements, façade cladding and window arrangements. Its ease of implementation renders the model more widely accessible to different factions of the Fire Engineering Community.

Furthermore, analysis of the Law Model identifies further parameters of potential importance that have, as of yet, not been addressed. A preliminary investigation conducted using Computational Fluid Dynamics (CFD) tools shows that variation in some parameters – that are not individually accounted for in the Law Model – may influence the compartment fire conditions, the consequent external flaming and the resultant external heat exposure. Therefore, it is recommended that further comprehensive experimental research be conducted into the potential influence of the identified parameters.

Keywords: Enclosure Fire Dynamics, External Flaming, Heat Flux to Façade, External Fire Spread, Dalmarnock Fire Tests.

Publications

Journal Papers

Abecassis-Empis, C. and Torero, J.L., Analysis of the compartment fire parameters affecting the heat flux incident on the building façade: A simplified model with distinct bounds of applicability. *To be submitted to Fire Safety Journal*.

Cowlard, A., Jahn, W., **Abecassis-Empis, C**., Rein, G. and Torero, J.L., Sensor assisted fire fighting, *Fire Technology* 46 (3), pp. 719-741, 2010.

Abecassis-Empis, C., Cowlard, A., Valenzuela, M., Jahn, W., Lange, D., Rein, G., Torero, J.L., Forensic analysis of fire induced structural failure, *Forensic Engineering: From failure to understanding*, Institution of Civil Engineers, London, 2009. ISBN: 978-0-7277-3613-0.

Rein, G., Torero, J.L., Jahn, W., Stern-Gottfried, J., Ryder, N.L., Desanghere, S., Lázaro, M., Mowrer, F., Coles, A., Joyeux, D., Alvear, D., Capote, J.A., Jowsey, A., **Abecassis-Empis, C**. and Reszka, P., Round-robin study of modelling blind-predictions using the Dalmarnock Fire Test, *Fire Safety Journal* 44 (4), pp. 590-602, 2009.

Abecassis Empis, C., Reszka, P., Steinhaus, T., Cowlard, A., Biteau, H., Rein, G., Welch, S., Torero, J.L, Characterisation of Dalmarnock Fire Test One, *Experimental Thermal and Fluid Science* 32 (7), pp. 1334-1343, 2008.

Book Chapters

Abecassis Empis, C., Cowlard, A., Welch, S., Torero, J.L., Test One: The 'Uncontrolled' fire, Chapter 3, The Dalmarnock Fire Tests: Experiments & Modelling, Edited by Rein, G., Abecassis Empis, C. and Carvel, R., School of Science and Engineering, The University of Edinburgh, U.K., 2007. ISBN 978-0-9557497-0-4.

Reszka, P., **Abecassis Empis, C**., Biteau, H., Cowlard, A., Steinhaus, T., Fletcher, I., Fuentes, A., Gillie, M. and Welch, S., Experimental layout and building description, Chapter 2, The Dalmarnock Fire Tests: Experiments & Modelling, Edited by Rein, G., Abecassis Empis, C. and Carvel, R., School of Science and Engineering, The University of Edinburgh, U.K., 2007. ISBN 978-0-9557497-0-4.

Cowlard, A., Steinhaus, T., **Abecassis Empis, C**. and Torero, J.L., Test Two: The 'Controlled fire', Chapter 4, The Dalmarnock Fire Tests: Experiments & Modelling, Edited by Rein, G., Abecassis Empis, C. and Carvel, R., School of Science and Engineering, The University of Edinburgh, U.K., 2007. ISBN 978-0-9557497-0-4.

Conference Papers

Cowlard, A., Jahn, W., **Abecassis-Empis, C**., Rein, G. and Torero, J.L., Sensor assisted fire fighting, Suppression and Detection Research and Applications – A Technical Working Conference (SUPDET), Orlando, U.S.A., 2008.

Deeny, S., **Abecassis Empis, C**., Stratford, T., Gillie, M., Torero, J.L., The Dalmarnock Fire Tests on a cast in-situ concrete structure, FIB Workshop on Fire Design of Concrete Structures: From Materials Modelling to Structural Performance, Coimbra, Portugal, 2007.

Rein, G., **Abecassis Empis, C**., Amundarain, A., Biteau, A., Cowlard, A., Chan, A., Jahn, W., Jowsey, A., Reszka, P., Steinhaus, T., Welch, S., Torero, J.L., Stern-Gottfried, J., Hume, B., Coles, A., Lázaro, M., Alvear, D., Capote, J.A., Desanghere, S. Joyeux, D., Ryder, N.L., Mowrer, F., Round-robin study of fire modelling blind-predictions using the Dalmarnock Fire Experiments, Fire Computer Modelling, Edited by Jorge A. Capote, presented at Advanced Research Workshop on Fire computer Modelling, Spain, 2007, pp.65-81. ISBN 978-84-8102-468-5

Jahn, W., Snorrason, D., **Abecassis Empis, C**., Rein, G., Welch, S., Torero, J.L, A posteriori modelling of the Dalmarnock Fire Tests, Fire Computer Modelling, Edited by Jorge A. Capote, presented at Advanced Research Workshop on Fire computer Modelling, Santander, Spain, 2007, p.169-199, ISBN 978-84-8102-468-5

Abecassis Empis, C., Reszka, P., Steinhaus, T., Cowlard, A., Biteau, H., Rein, G., Welch, S., Torero, J.L, Characterisation of Dalmarnock Fire Test 1, The Fifth International Mediterranean Combustion Symposium, Monastir, Tunisia, 2007.

Abecassis Empis, C., Snorrason, D., Lee, J., Reszka, P., Steinhaus, T., Cowlard, A., Biteau, H., Stratford, T., Gillie, M., Rein, G., Welch, S., Torero, J.L., The Dalmarnock Fire Tests, IFE AGM, Cambridge, 2007.

Jowsey, A., Rein, G., **Abecassis Empis, C**., Cowlard, A., Reszka, P., Steinhaus, T., Torero, J.L., Usmani, A., Lane, B., An analytical approach to define surface heat fluxes to structural members in post-flashover fires, 5th International Seminar on Fire and Explosion Hazards, Edinburgh, 2007.

Rein, G., **Abecassis Empis, C**., Amundarain, A., Biteau, A., Cowlard, A., Chan, A., Jahn, W., Jowsey, A., Reszka, P., Steinhaus, T., Welch, S., Torero, J.L., Stern-Gottfried, J., Hume, B., Coles, A., Lázaro, M., Alvear, D., Capote, J.A., Desanghere, S. Joyeux, D., Ryder, N.L., Mowrer, F., Round-robin study of fire modelling blind-predictions using the Dalmarnock Fire Experiments, 5th International Seminar on Fire and Explosion Hazards, Edinburgh, 2007.

Awards

IFE Bodycote Warrington Fire Research Prize for the Best Fire Safety Engineering Paper 2007

This is a joint award from the Institution of Fire Engineers (IFE) and Bodycote Warrington Fire Research for the "Best Fire Safety Engineering paper" of 2007. The best paper is selected, from a very wide range of subject areas including case studies, technical fire engineering and general fire safety issues, by an expert panel from the fire engineering community. The award consists of a £1000 contribution from Bodycote Warrington Fire Research and a trophy presented by the IFE.

This award was presented for the paper co-authored by Abecassis Empis *et al*., entitled "The Dalmarnock Fire Tests" and presented at the IFE AGM in Cambridge in July 2007. Apart from the authors, this paper was a culmination of work from several other contributors from the BRE Centre for Fire Safety Engineering, The University of Edinburgh and others further afield, who helped make the Dalmarnock Fire Tests possible.

FM Global Award for the Best Paper at the 5th International Seminar on Fire and Explosion Hazards 2007

FM Global, a leading commercial insurance company with a specialised Fire Technology Laboratory, boasts years of experience dedicated to high-end research in Fire Science and Fire dynamics. At the 5th International Seminar on Fire and explosion Hazards, FM Global granted several awards for "Best Papers" presented at the conference. The 1st Prize award was £500.

The 1st Prize for Best Paper was awarded for "Round-robin study of fire modelling blind-predictions using the Dalmarnock Fire Experiments", a paper co-authored by Rein *et al*., presented at the 5th International Seminar on Fire and Explosion Hazards, held in Edinburgh in 2007.

Best Poster award at the Annual Poster Day for PhD Students in the School of Engineering and Electronics, The University of Edinburgh 2007

> *Every year, the School of Engineering - previously known as the School of Engineering and Electronics – at The University of Edinburgh, holds a Poster session to publicise research work undertaken by their postgraduate students. The exhibition of a poster in this session is compulsory for students during their 2nd year of study towards a PhD degree. The event is open to the public and all those in attendance can cast a vote towards their Best Poster of choice.*

During the 2007 Annual University of Edinburgh, School of Engineering Poster Day, the prize of Best Poster was awarded for "Fire Properties Characterising External Spill Plumes and the Subsequent Effect on Structural Stability" presented by Abecassis Empis and respective research supervisors.

Acknowledgements

First and foremost I'd like to thank my Professor, supervisor and friend, Prof. José Luis Torero for his expert guidance, continual support and insurmountable amount of patience as well as for all the amazing opportunities he gave me throughout this research. Had it not been for José I think I can safely say that I would have never: (*i*) spent a night sleeping on the floor of a disused tower block in the Dalmarnock area of Glasgow, where I had previously found two spent bullets on clearing the room for some experiments; (*ii*) been woken up by a surprise visit from the Glasgow Housing Authority in the middle of the night demanding to know the whereabouts of the building's security guard (only to find him at the local pub with half a bottle of vodka in him); (*iii*) used a bathroom that was 'under surveillance' by our hardworking team of security guards; (*iv*) driven a big white van at 6 am on our way to being filmed for a BBC documentary; (*v*) spent such 3 great weeks working *together* with Adam, Thomas, Hubert and Pedro; (*vi*) had the opportunity to help plan, design and manage such a large-scale project; (*vii*) travelled so extensively and attended so many conferences; and, (*viii*) had the chance to work on such interesting projects with such brilliant minds; (*ix*) enjoyed the process of getting my Ph.D. and learnt so much about life in the process. The list of previously unimaginable activities is clearly endless and for all of this I thank him. On a more technical level however, I would like to thank José for having so much faith in me and for supporting the decisions I made throughout this work, even when they were not what he had envisaged.

I'd also like to thank Prof. Asif Usmani, my second supervisor, for having introduced me to this exciting field of research (together with Prof. Torero) during my Master's studies and for his guidance during my contribution to the FireGrid project. Over the course of this research I also worked closely with Dr. Stephen Welch and Dr. Guillermo Rein, particularly over the Dalmarnock Fire Tests project, and would like to thank them for the very fruitful interactions.

I am equally grateful to Dr. Debbie Smith, my industrial supervisor, who helped me keep on top of things by ensuring I had annual progress reviews and to her

colleagues at BRE for providing much needed assistance on a number of occasions. I would also like to express my gratitude to BRE Trust for providing the financial backing to this work, in the form of a studentship.

To Prof. Fred Mowrer, my external examiner, I am indebted for having travelled from the USA to attend my Viva Examination and for his pertinent comments and recommendations. To Prof. Dougal Drysdale, my internal examiner, I owe a very, very big thank you for all the time he spent helping me review this document and for all his advice and continued patience. Without Dougal's generous help, this wouldn't be half as readable.

On a more general level, thanks go out to all my 'Fire Group' colleagues at the BRE Centre for Fire Safety Engineering, both those with whom I've worked and those who have simply helped by providing entertainment when I most needed to relax – you know who you are, you are far too many to name, but for your part in this I am truly grateful. Content-wise however, this work would not have been possible without the help those Fire Group members involved in the Dalmarnock Fire Tests, inclusive of James Lee and David Snorrason who helped me analyse some of the data as part of their Master's degree. Most pertinently, the contributions of Dr. Adam Cowlard, Dr. Thomas Steinhaus, Dr. Hubert Biteau, Dr. Wolfram Jahn and Thomas French – both towards providing technical assistance and helping further my understanding of Fire Dynamics – must be acknowledged, although foremost I'd like to thank them for engaging in many a late-night ludicrous discussion and for being such good friends throughout.

Over the last few years, I have been rather self-indulgent and have not been able to leave 'work behind' very often, so I'd like to thank my friends and family for being so very understanding and for giving me both the space I needed to 'get on with things' and the support I needed to 'get through them'. These thanks go particularly to my dear childhood friends, Sofia d'Orey, Barbara de Castro Guimarães and Carolina Empis Cid as well as all my flatmates who put up with me throughout the course of this research, in particular Thomas French, Hubert Biteau and Adam Cowlard who were unfortunate enough to live with me through the (worst) final

stretch. Thank you all for the great, long chats and for helping to keep me sane. The Cowlard family have also been very kind, supportive and understanding over the last few years, as has my extended family, and I didn't see near as much of them as I would have liked.

Thanks also go to my family for not being too upset (or surprised!) when I called to say their long-serving car had burst in to flames while I was driving it, part-way through this research. No matter how much I have maintained that I was not doing "research" on the car, there is no doubt an element of dubiousness about my account, given the circumstances. They were also surprisingly unfazed when I singed a pile of clothes by draping them over the back of a chair against tiles that provide backing for a fireplace thinking it would be a better way to warm them up than to leave them sitting in front of the fire place unattended. It was only when my clothes caught fire *while* I and wearing them (and attempting to cook!) that my family began to question my choice of career…particularly when my first thoughts weren't "Aaargh! I'm on fire!" or "I better run in the shower", but rather "I can't believe the fire alarm hasn't gone off! Useless.", quickly followed by "I should use the fire extinguisher", only to quickly be replaced with "by the time I've worked out how to use it, I'll be completely alight" and "forget it, if I use it I'll have to get it replaced and I really don't have time to deal with such things at the moment!". On a more serious note, I can not express how grateful I am to both my parents, my sister, my brother and his family and to Adam, who accompanied me through the struggles, the little successes and the daily antics that feature in the life of a Ph.D student. You are all a great source of inspiration, *thank you* for all the encouragement, for listening, for being so patient, for 'bringing me back to reality' when needed and for putting up with me! If I survived this process, it was because of you.

Contents

List of Figures

List of Tables

Nomenclature, Acronyms and Terminology

Notation

A_F Compartment floor area [m^2]

A_{sp} Perimeter of the cross-section through the structural steel element [m]

A_T Area of the enclosure surfaces excluding opening areas [m^2]

A_w Area of openings [m^2]

a Ratio of h'/S' [*dimensionless*]

b Ratio of w'/S' [*dimensionless*]

C Dimension (width or length) of the compartment core [m]

c Specific heat [kJ/kg.K]

D Depth of compartment [m]

d Characteristic length scale for the convective heat transfer coefficient [m]

e Euler's Number, ~2.718 [*dimensionless*]

f_{ex} Excess fuel factor [*dimensionless*]

g Acceleration due to gravity, ~9.81 [m/s^2]

H Height of compartment [m]

h Height of an opening [m]

$h_{neutral}$ Height from the neutral axis to the soffit of the opening [m].

h' Effective height of radiating surface [m]

k Heat loss by conduction [kW/m^2]

L Fire load [kg]

L'' Fire load density (average per unit floor area) [kg/m^2]

l Local length measurement taken along the external flame axis [m]

M Mass of steel per unit length [kg/m]

$\dot{m}$ Rate of burning [kg/s]

n Aspect ratio of the upper half of a compartment opening [*dimensionless*]

P Point of interest on radiation receiver surface [*dimensionless*]

P' Point on radiation emitter surface, where the normal to point P intersects the emitter plane [*dimensionless*]

$\dot{Q}$ Rate of convective heat flow from an opening [kW]

$\dot{q}''$ Total heat flux incident on façade [kW/m^2]

r_o Characteristic length scale of the external plume heat source [m]

S' Distance between radiant emitter and receiver [m]

T Temperature [K; ^{o}C]

t Time [s]

u Draught or Wind Velocity [m/s]

$V_{ND,To}$ A combination of variables, as defined by Chapter 3, Equation (3.33) [*dimensionless*]

W Width of compartment [m]

w Width of opening [m]

w' Effective width of the radiating surface [m]

X Flame length along its axis from the opening to the flame tip (Chapter 3) [m]

X Coordinate axis used as part of the Global Coordinate System used in the Dalmarnock Fire Tests (Chapter 4, Appendices C and D); S*ee* Chapter 4, Figure 4.3 for GCS origin [m]

x Horizontal flame projection, from façade to the axis of the flame tip [m]

Y Coordinate axis used as part of the Global Coordinate System used in the Dalmarnock Fire Tests; S*ee* Chapter 4, Figure 4.3 for GCS origin [m]

Z Vertical distance along façade from opening soffit (Chapter 6) [m]

Z Coordinate axis used as part of the Global Coordinate System used in the Dalmarnock Fire Tests (Chapter 4, Appendices C and D); S*ee* Chapter 4, Figure 4.3 for GCS origin [m]

z Vertical component of flame height above the opening soffit [m]

α Convective heat transfer coefficient [kW/m^2**.**K]

ε Emissivity [*dimensionless*]

η Reciprocal opening factor [m$^{-1/2}$], Chapter 3, Equation (3.4)

Θ Yokoi temperature term [*dimensionless*]

θ Angle between radiation emitter and receiver planes [rad]

θ_f Temperature difference [°F]

λ Flame thickness [m]

ρ Gas density [kg/m^3]

σ Stefan-Boltzmann constant, 5.7 x 10^{-8} [W/m^2**.**K^4]

τ Fire duration [s]

ϕ	Configuration (or 'view') factor [*dimensionless*]
ψ	Compartment scenario parameter [kg/m^2], Chapter 3, Equation (3.5)

Other Subscripts

a	Pertaining to ambient conditions
dr1	Dalmarnock Fire Tests compartments' door leading to the hallway
dr2	Dalmarnock Fire Tests compartments' door leading to the kitchen
F	Free-burning fire
Fuel	Fuel-controlled, free-burning fire
f	Pertaining to internal compartment fire conditions
max	Maximum realistic value
mo	Modified opening values
o	Pertaining to conditions at the pane of the opening
s	Pertaining to the steel element
Vent	Ventilation-controlled fire conditions
win	Pertaining to the Dalmarnock Fire Test compartments' window
x	Flame Tip location
z	Pertaining to the external flame

Acronyms

BRE	(*formerly*) Building Research Establishment UK
CIB	Conseil International du Bâtiment
CFD	Computational Fluid Dynamics
DFT	Dalmarnock Fire Tests
DFT1	Dalmarnock Fire Test One
DFT2	Dalmarnock Fire Test One
FirExHeat	Computational implementation of Law Model with some adaptations
FDS	Fire Dynamics Simulator
FRP	Fibre Reinforced Polymer
GCS	Global Coordinate System
HRR	Heat Release Rate
ND	No Through Draught
ToFD	Through or Forced Draught

Terminology

Ambient	General conditions pre-ignition and in the far-field to the compartment fire
External Flaming	Flames emerging from a compartment opening to the exterior of the building
Fire	Refers to the *internal* compartment fire
Flame	Refers to *external* flaming
Incident Heat Flux	Combined radiative and convective (*i.e.* total) heat flux falling incident on a given point or surface
Local	Conditions at a given point along the axis of the external flame
Reciprocal Opening Factor	Ratio of area of enclosure surfaces to ventilation factor (*cf.* Chapter 3, Equation (3.4))
Sill	Lower ledge of the window opening
Soffit	Upper ledge of the window opening
Window plane	The 2-D plane defined by the normal to the window pane
Weight-averaged height	Height averaged relative to the heights and areas of other openings (*cf.* Chapter 3, Figure 3.1 (ii))

Foreword

A Note on the Philosophy of Engineering Research

With the arrival of the computer era came a desperate frenzy of research in all fields with an ever increasing urge to quantify, discretise and explicitly pick apart nature enabling its eloquent description using the languages of mathematics and physics. This very urge appears to be our largest limitation in attaining a precise representation of nature. Nature is, by nature, a continuum with an infinity that can not be quantified as much in the infinite immensity of the universe's expanse as in the infinite minuteness into which things can be dissected and in the natural continuum of anything in between, exemplified by the naturally recurring but non-recurrent irrational numbers of Pi, Euler and Fibonacci.

Nevertheless intrinsic to human nature is a desire to group things, categorise, to box knowledge into entities we can comprehend and computers have allowed us to do this more quickly. Part of this process requires an evaluation of what is to be done and what it is to be used for. Be it an equation that represents the physics of electricity, the theories that describe types of intelligence or music that depicts the dance of the bees, the limits of its "accuracy" always lie within the bounds of the assumed scale, an agreement of the axioms of compliance.

Engineering is precisely the art and craft of deciphering such problems. The skill lies in evaluating the scope of the conundrum and identifying the critical players. In outlining the discrete pieces of this puzzle, engineers have to untangle the fundamentals from the peripheral fillers. They then stand back and reason the rules of the game using them to discard unnecessary detail and weave back together the key pieces creating an optimal solution. Engineering is a mere translation tool that allows for the interpretation of nature in a way we can fathom.

It is important however to distinguish a "solution" from "natural reality". With the computing world fast-appealing to more and more of our senses, it is often tempting to indulge in smaller and smaller dissections of our problems. As we become

increasingly obsessed with intricate dependencies we run the risk of creating a solution that is self-fulfilling without realising it has departed so far from its application that it has become a mere representation of the human ego with little or no use beyond the amusement of a select few curious minds. Detail can lead to a false sense of proximity to nature whereas the very nature of engineering is to accept that any attempt to model nature will always fall short of perfect. Instead engineering embraces the asymptotic nature of complex solutions and opts for providing simple and effective shortcuts that are perfect if they solve the particular problem at hand within the scope of its axioms. Hence an engineer must be humble and not lose sight of the problem objectives, the initial assumptions and the scale delineating the limitations and applications of engineering work.

Engineering research aims to provide rational solutions that make daily life just a little bit easier in order to make time for sitting back, relaxing and to enjoy the awesomeness of the irrational, chaotic magnificence of nature.

In this light it is hoped this work will make a useful contribution.

Cecilia Abecassis Empis

Chapter 1

Introduction

http://splendidmarbles.com/wp-content/gallery/culture/cromag_fire_0.png [*accessed 18/02/2010*]

- Cartoon juxtaposing the two historic approaches to Fire Safety Engineering -

1.1 Early Humans and the 'Control' of Fire

Since the dawn of our time, fire has proved vital for the survival of humankind. In fact, recent archaeological finds have uncovered what is believed to be evidence of fire use by the predecessors of *homo sapiens*, circa 790,000 years ago [4]. Throughout the millennia, humans have gradually improved their 'control' of fire and have learnt to use fire as a tool for their advantage. The ability to make 'controlled' use of fire had a remarkable influence on the development of civilisation. As a somewhat portable source of heat and light, fire allowed humans to cook food, broadening their nutritional intake and allowed them to move to cooler climes by providing warmth at night and deterring potential predators. So important was fire to the essence of ancient civilisations that it became hailed worldwide as one of a handful of key elements deemed to be the fundamental building blocks of the foundations of life [5].

Adversely, fire has always posed a potential danger to humankind. Initially natural and accidental wildland fires posed the biggest threat, however as humans gained increased 'control' of fire they began to use it malevolently, as a weapon of war, setting vegetation alight to burn their enemies and devastate their crops. Hence the level of human 'control' of fire has had to become progressively more sophisticated. Potentially one of the most notable leaps in widespread use of fire in a significantly 'controlled' fashion was at the onset of the industrial revolution in the 18th-19th Centuries, when 'fire-powered' machinery became commonplace [6]. At this point, the main threat of fire shifted from one of general, multiple building conflagrations to a more building- and contents-specific concern, particularly as factories drew the need for large, often multi-storey, open-plan areas and for bulk storage warehouses [6]. However, it was only in the late 18th century that the process of combustion was found to involve a reaction with oxygen, by one Antoine Lavoisier. Up until then the essence of fire was believed to be solely due to a substance called *phlogiston* contained within all combustible materials [6]. Methods of fire-fighting, fire prevention, fire protection and even fire-warning had been developed however, even then, the 'control' of fire was mainly based on experience and trial-and-error alone. Fire-related quantification was limited to the classification of materials as combustible, flammable, non-combustible, or non-flammable [6].

1.2 The Dawn of Fire Science

Perhaps surprisingly, given the centuries of coexistence and increasing dependence on fire, it was not until relatively recently, in the mid-20th Century, that fire dynamics began to be studied in depth scientifically and moulded into a subject in its own right [6-8]. According to Howard W. Emmons - "the father of modern fire science" [9] - at this time "the realization of the importance of developing a fundamental understanding of fire through the methods of science was developing" [7] and information from other fields was gathered to form the basis of the discipline that became known as Fire Dynamics [6]. Much of this realization came from the heightened exposure to fire during World War II, allowing for comparable observation of the range of fire involvement, inter-building fire spread and resultant levels of devastation caused by conventional weapons [6]. Conveniently, by this time, the level of understanding of many of the component phenomena (*i.e.* classical dynamics) and development of necessary tools (*i.e.* computers) were at a stage that allowed for the simpler problems of fire science to be solved [7].

In 1962, in the USA, representatives from across all fields of science potentially related to fire safety engineering gathered for four weeks with leaders in fire prevention and protection and with fire insurers, to discuss prospective solutions to the main problems in fire safety. The scientists concluded an intensive federal research program should be established however the fire protection community and the insurers staunchly opposed this suggestion, recommending instead that efforts be made to employ the already sufficient existing knowledge into common practice [6]. By then "there was a well developed public awareness of the seriousness of fire and a procedure of city fire codes and variously approved tests and standards", however "these were almost entirely empirical" [7], according to Emmons' part-historical, part-speculative account. Although nothing official resulted from the scientists' recommendations this conference was critical in that it "generated consensus in the scientific community that there was a potential to mathematically describe (model) fire phenomena and the impact of fire on the environment within buildings" [6] and hence allow for improvement in the 'control' of fire.

1.3 Fire and the Built Environment

In the pursuit for the 'control' of fire, there have always been two main threats: *wildland* fires and *enclosure* fires. *Wildland* fires involve the complex interaction between several different types of fuel, continually variable air movement, moisture content and often uneven terrain [10]. *Enclosure* fires on the other hand, ranging from building to vessel fires, involve many of the same complex interactions as wildland fires but have a further degree of complexity rooted in the interaction between the fire and the enclosure itself. Hence in aiming to scientifically understand the behaviour of fire in enclosures - both fuel and ventilation controlled fires – understanding of both the main fire threats was advanced simultaneously. By the 1980s, scientific knowledge obtained in the laboratories began to be applied in the practice of fire protection engineering [6] and there was a healthy interaction where feedback from real fires guided the need for further scientific research [7].

As the common abode evolved and grew in complexity from the cave to multi-compartment adobe brick buildings and eventually to composite material skyscrapers, the 'controlled' fires within evolved from an open bonfire type arrangement to fireplaces which were eventually replaced by boilers and kitchen stoves. Often it was architectural innovation compounded with advances in material science and resultant changes in civil engineering applications that led "fire engineers" to strive for ever increasing 'control' of fire. Over the last half-century, fire dynamics research into the complex interaction between fire and structures – 'the effect of structural geometry and material properties on fire development' and 'the fire development effect on the structural reaction, resultant structural geometry and material properties' – has lead scientists and fire engineers to identify several parameters that govern this intricate inter-related behaviour [6]. To date, the research effort has made impressive progress in identifying component phenomena in fire dynamics and has been successful in modelling these phenomena for practical application in elementary cases [10]. However, as predicted by Howard W. Emmons in 1984 [7], these models are presently not yet capable of fully supporting performance-based design [11]. Nevertheless the research conducted to date was a "necessary preliminary since without an adequate quantitative understanding of the building blocks of a fire, the overall fire phenomena itself could not be put together" [7].

Ideally, the field of fire engineering, encompassing fire dynamics, fire prevention and protection and fire suppression, would continually be on par with innovation in the fields of architecture, material science and civil engineering. However, although an extreme case, the events witnessed on September 11th, 2001 during the attacks on the World Trade Centre Twin Towers in downtown New York, were a stark reminder of the existing disparity between the level of progress made in these three affiliated fields and that of fire engineering. To best illustrate this disparity succinctly, two scenes are juxtaposed. Both settings depict fire-fighters tending to fires in buildings however the scenes, the buildings and the fire-fighting tools are characteristic of different eras. Figure 1.1 shows the fire-fighters of 1776 tending to a fire in a typical 18th Century building while Figure 1.2 shows the fire-fighters of 2001 tending to a fire in a building representative of the pinnacle of 20th Century architecture and use of then novel materials in construction. While the construction materials, furnishing materials and structural-architectural layout of the buildings have distinctly changed over the past three centuries, the fire-fighting methods and the techniques available to control fires once they break out appear not to have changed significantly.

Figure 1.1. Depiction of 18th Century fire-fighting in tenement buildings typical of the time [12].

Figure 1.2. Photographs depicting fire-fighters in standard equipment arriving at the scene of a large fire in the upper floors of a skyscraper over 400 m high, taken at the World Trade Centre site in New York after the attacks on September 11th 2001 [13].

In the 18th Century, fire-fighters with step-ladders, helmets and water hoses had most of the tools needed to access and combat commonplace fires. With the advent of skyscrapers running several hundred metres high, with large atria and a vast variety of materials used for construction and furnishings, fire-fighters armed with helmets, pike poles and water hoses appear rather ill-equipped by comparison. Although fire-fighting equipment has evolved more than first meets the eye – fire engine pumps are no longer manually operated, and often replaced by fire hydrants and in-built standpipes; ladders reach several stories higher; breathing apparatus is a requirement; building fire detection, suppression and management systems such as fire alarms, sprinklers and smoke extractors help deal with the fire and aid evacuation from the outset – this modernisation still seems orders of magnitude behind the exponential innovation witnessed in the built environment. Architectural design has evolved from the single standard compartment to large volume compartments with high aspect ratios; innovation and development in construction materials now allows for open-plan offices to be supported by light-weight long-span composite-material beams;

furnishings have evolved from mainly cellulosic materials to plastics, foams and complex composite materials. The level of disparity in the progress made in fire-fighting compared to that in the structural-material areas may be different to that witnessed in other areas of fire engineering, however it serves as a clearer example of the disparity exists between other more technical areas of fire engineering.

On September 11th, 2001, the gap between these fields was further emphasised by both WTC1 and WTC2 having remained standing for 1-1.75 hours, after being penetrated by large commercial aircraft but later collapsing after prolonged exposure to fires on multiple floors, killing hundreds of occupants and fire-fighters [14,15]. The extent of the gap between structural-material innovation and fire dynamics knowledge has varied considerably over the past few decades with periods of intensive fire research leading to a significant narrowing of the gap. Nevertheless since the field of fire science is still comparatively young, fire engineering is not yet able to keep up with the successive exponential surges in architectural and material science innovation, and resultant civil engineering practice. While it appears certain areas of fire engineering are more advanced than others, perhaps the scientific developments in the area of enclosure fire dynamics have not yet been fully integrated into practical fire prevention, protection, suppression, and management strategies.

1.4 Describing the Phenomenon of Fire

Several factors are thought to contribute to what is often perceived by laypeople as the ‘chaotic’ behaviour of fire. At present, the number of variables identified stands in the order of 30 parameters [16]. Several intensive experimental programmes, conducted mainly since the 1950s, have allowed the parameters identified to be pieced together to form correlations, many of which are based on empirical data that are potentially tied to the specific experimental scenarios. These many correlations steadily evolved into analytical models and were subsequently implemented in both Zone models and Computational Fluid Dynamics (CFD) models, often with a steady increase in complexity and number of parameters involved. Although the more complex models are rooted in conservation of mass and energy, their success in simulating realistic fire behaviour is varied and most often depends on the scenario the models are applied to.

In many cases the disparity appears to lie in the intricacies of the fire-specific correlations.

When a scenario consists solely of a pre-mixed flame, such as that in a household boiler or kitchen stove, the combustion process and resultant fire can be robustly described using analytical models and accurately simulated using CFD. When considering a simple pool fire, which has the added complexity of air entrainment among other parameters, both analytical models and CFD models can simulate the fire behaviour with reasonable accuracy. Often the discrepancy between the model predictions and the measured *data are* within the bounds of experimental error and the error involved in measuring the different aspects of the fire [17]. On the other hand, when considering a more complex scenario, such as a regular household living room fire involving several types of fuel, complex air entrainment and re-radiation, analytical models, zone models and CFD models all compare fairly poorly to thorough experimental measurements by comparison [18,19]. Unfortunately the latter is a better representation of the everyday threat posed by 'uncontrolled' fire.

CFD models involve the most complex level of interaction between the numerous parameters identified to date and represent the state-of-the-art of current knowledge in the field of fire dynamics. While these tools enable the user to set up a complex multi-compartment scenario, visually comparable to an architect's depiction, and to assign temperature-dependent material properties to different items of enclosure boundaries, furniture, *etc*., it is clear they can not yet model the intricate detail involved in an 'uncontrolled' household or office fire. In current practice the discrepancy between the output of a tailored model and detailed experimental data pertaining to the same scenario can still be large. For example, a study concerning the *a priori* modelling of the Dalmarnock Fire Test One (a full-scale, realistic scenario) showed that even for a generalised representation of enclosure fire events, such as the modelled time to flashover, output varied from 80-850 s, which is a significant variation from the actual 300 s recorded time to flashover [18]. Although the level of detail obtained from a CFD model is tied to the resolution of the computational domain, with high resolution models often requiring currently unfeasible computational effort, studies have shown higher resolution does not necessarily equate to more accurate results [18]. Hence, it seems reasonable to conclude that perhaps not all the parameters and parameter

interactions involved in the complex phenomenon of enclosure fire dynamics have yet been identified. It is possible that many of these are still hidden within the empirical constants used in several of the correlations embedded in fire models. Therefore, CFD models and all other models used in fire dynamics should only be used for scenarios that fall within the bounds for which they have been validated.

Since the limitations of the models currently available are well known, practitioners tend to concentrate on implementing conservative approaches in design, such as the extensive use of compartmentation to prevent fire and smoke spread to other parts of a building. Although there are some models of multi-compartment smoke flow, correlations for fire spread are still limited to simplistic scenarios [20,21]. Yet with architects', material scientists' and civil engineers' continual innovation, we have reached a point where the time to fully evacuate the tallest buildings has become comparable to the time taken for the fire to have adverse effects on the structure, as exemplified in the World Trade Centre towers on September 11th, 2001. In order to further advance the fire dynamics models such that they can indeed be used for detailed performance-based design and eventually allow for an all-encompassing fire-structural behaviour model, it is vital that the fundamental parameters and correlations in fire dynamics are comprehensively explored.

In order to study the complex phenomenon of fire dynamics, it is useful to break fire down into component phenomena. These components can be specific scenarios or aspects of fire however all originate from a large set of fundamental governing parameters. The arrangement of these inter-related components is best represented by an inverted tree-like structure, with fire at the base and the fundamental parameters at the extremities. An example of a segment of such a tree is given in the upper half of Figure 1.3, where the yellow background shows a section of the larger triangle that encompasses all the potential branches of the 'fire dynamics' tree. The fundamental parameters are represented by a set at the extremities of the yellow tree. These individual parameters come together by way of correlations to describe several different phenomena involved in different aspects of a fire. In turn, these can be further grouped to describe specific scenarios, eventually to culminate in the complete description of "fire" at the root of the tree. Open-ended arrows allude to further branches that are not depicted in this tree segment.

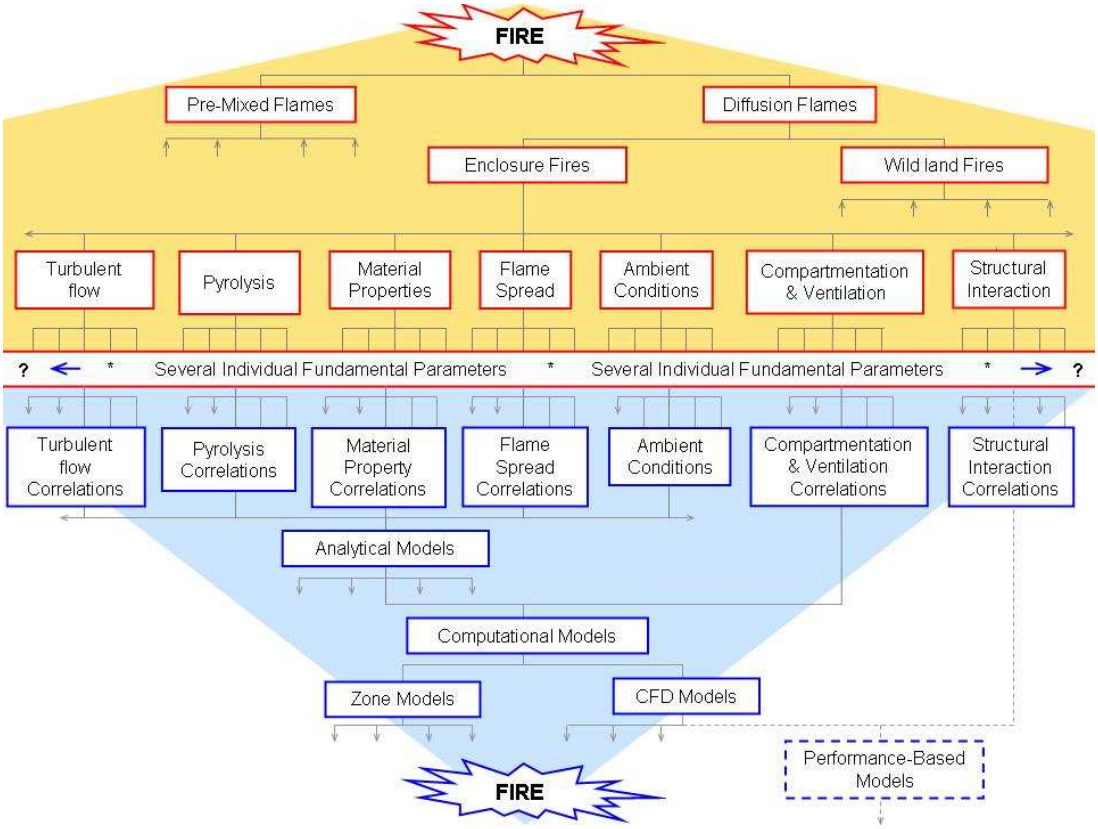

Figure 1.3. A segment 'branch' of the potential 'tree' of component phenomena (red boxes) that contribute towards the global phenomenon of fire dynamics is explored in the upper section (yellow background), while the lower section (blue background) contains some of the components that have been identified and compiled using correlations and models (blue boxes) in the efforts made to date towards the understanding of fire dynamics (dotted lines represent work in progress).

Conversely, the lower half of Figure 1.3 shows an upturned tree set over a blue background, the extremities of which also originate from the fundamental parameters that govern fire dynamics. This tree represents the body of knowledge we currently hold in the field. We have identified many but perhaps not all of the fundamental parameters that govern fire dynamics and have formulated correlations that describe particular aspects of a fire. These correlations have been combined to allow for analytical models that describe a number of phenomena, which in turn have been built on to produce computational models capable of describing specific fire scenarios. Since these models still provide limited accuracy when simulating certain fire scenarios and given that many model components still rely on empirical data, it seems reasonable to assume that somewhere down the 'branch', certain component phenomena have not yet been identified or included. These potentially 'unknown'

components and inter-relations are qualitatively represented by open-ended connections (arrows) in the lower half of the diagram. Similarly the blue background encompassing the tree of the 'known' components in fire dynamics alludes to a smaller tree than the upper section, however the components illustrated in both trees are not exhaustive and structural behaviour is only on the edge of the field, with changes in compartment geometry affecting the fire and 'real' performance-based design being a complex integration of knowledge in the fields of fire and structural engineering and material science.

There is no doubt that the last 50-60 years of research have offered a tremendous insight into what was previously a little understood phenomenon. However technological advances over the last half-century mean we are now more equipped that ever to revisit the recommendations of the scientific body of the 1960s, by delving further into the fundamentals of fire dynamics. Ideally, experimental programmes would be set up to explore the limitations and assumptions inherent in the early experimental scenarios to establish whether there are any further governing parameters and correlations in fire dynamics that can replace much of the empirical data and allowing for more robust models that can be more generally applied. Nevertheless in order to keep at some pace with architectural, structural and material science innovation, there is also a patent need to develop innovative approaches in applying what is already known into practical solutions, allowing current buildings to be effectively fire engineered.

1.5 Practical Applications of Fire Science

The current range of practice in fire engineering is broad. Regular building design and retrofit involves mainly the implementation of standard codes which are based on fundamental principles, a significant amount of empirical data and a notable qualitative contribution based solely on 'past experience'. This type of design is usually approved by an authorising body. In the U.K. this usually constitutes approval by the local authorities following a site inspection by the fire brigade [22,23]. An alternative approach is taken for some of the more innovative structures that fall outwith the building and occupancy categories stipulated in the standard codes. Most of these cases require engineers to devise tailored fire engineering solutions often

integrating elements from fundamental principles, fire dynamics models and standard code recommendations extrapolated past their usual limits of application. For complex structures, these designs tend to undergo a third party review by highly regarded fire engineers before the respective authorities give their approval. Although this type of design is commonly coined ‘performance-based’ design, it can only account for performance under the ‘known’ fire dynamics phenomena and subsequent structural behaviour and hence is more of a ‘scenario-tailored engineering-based’ design. Only once a complete, thorough and holistic understanding of all parameters governing enclosure fire dynamics is attained will *actual* ‘performance-based’ models be possible, allowing for full integration of *precise* fire-structural interaction once detailed structural-fire behaviour is also better understood.

Given the current level of fire dynamics knowledge, all design approaches aim to considerably err on the safe-side. However when the scenarios presented are at the limit of our current understanding, what constitutes a conservative choice might not be evident, hence innovative structures often suffer greater structural damage from accidental fires than regular buildings. Across the board of fire engineering design, the tendency is to frequently feature compartmentation, as an attempt to contain any potential fire, as much as possible, to a restricted area. Even if the intricate fire dynamics of the single standard compartment are not yet fully understood, it best represents the vast majority of experimental scenarios leading to the current knowledge, so it is better understood than travelling fires which potentially involve more parameters. Compartmentation restricts the air inflow which in turn reduces the fire growth and it minimises smoke outflow, while aiming to prevent multi-compartment fire spread, all of which contribute towards better conditions for the egress of occupants. It also minimises the heated area of a structure, however whether this is less adverse than more generalised heating is highly dependent on the individual scenario and specifics of the structure itself. Nevertheless, architectural innovation witnessed over the past decades has the tendency to increasingly feature open-plan and atrium spaces that often span several stories in height.

In the meantime, technological advances have allowed for several types of sensors that are now compact and affordable, yet accurate enough to make permanent sensor integration within buildings feasible. Should buildings be fitted with such sensors, the

structural health of the building could be continuously monitored but most pertinently, should a fire arise they could be used to detect it, and to monitor its development and consequent structural behaviour. Data gathered on the development of a fire could be remotely collected and fed into fire models that in turn would attempt to predict its development in super-real time. The outcome of these models could then be continuously checked against recorded fire data such that the real fire data would help steer the fire model predictions, enabling them to become increasingly accurate [24]. Eventually this could allow for 'intelligent' automated building interaction with the fire, guided by recommendations from expert systems. Essentially this is a more sophisticated use of 'smart buildings' that currently simply involve sensor-based automation. In turn the sheer amount of data such a system would collect for a wide variety of fire scenarios could also help further the research into the fundamental principles of fire dynamics and fire-structural behaviour. This could subsequently then be re-implemented into the expert system steering models. The feasibility of the implementation of such a system has been explored in the FireGrid Project [24,25] which forms part of the context of the present work.

1.6 Outline of the Aspect of Concern

Although most current buildings are highly compartmentalised, one of the biggest problems faced in building fires is still multi-compartment fire spread. Fires within confined compartments can lead to a rapid temperature increase, particularly during the flashover and post flashover period. This often results in shattering of windows and fire breach of the intended compartmentation. Post-flashover compartment fires tend to be ventilation-controlled resulting in partially combusted fuel which subsequently flows out of the broken windows and leads to external flaming. Frequently this external flaming is the main cause of multi-storey fire spread, mostly by simply breaching the windows of the compartment above. However at times the façade cladding may ignite which can lead to rapid multi-storey fire spread. Should there be a gap between the structural perimeter wall and an external curtain wall façade or should the compartment open out to an external louvre, the mode of fire spread due to external flaming can involve more complex interactions between the fire and the structure.

In order to successfully prevent external flame spread, it is vital to understand the behaviour of external flaming. Investigative work to determine the characteristics of external flames was conducted in Japan by Yokoi as early as the 1950s [6]. Several parameters thought to govern the internal fire dynamics, the compartment ventilation and the consequent external flaming are still based on this early research. Others have since built upon this research. The most commonly used analytical model involving external flaming was compiled in the form of a design manual for "Fire Safety of Bare External Structural Steel" by Margaret Law in collaboration with Turlogh O'Brien, in the late 1970s [1,26]. This model, henceforth referred to as the *Law Model*, brings together several correlations that define different aspects of the problem. These range from internal fire dynamics to the affect of wind or a through draught on the heating of external structural elements. Soon after Law first formulated this model in the late 1970s, it was applied in the design of the external steelwork used in the *Centre Georges Pompidou* in France [27]. The model forms the basis of Eurocode standards, having been integrated into Eurocode 1 – Annex B, where the calculations for "Thermal Actions for External members" [2] are detailed, and Eurocode 3 – Annex B, outlining the calculations for "Heat Transfer to External Steelwork" [3]. Hence the Law Model is now commonly employed in buildings that feature external steelwork.

1.7 Scope of the Research

The success of the Law Model has not yet been thoroughly tested as there is little evidence to date of large fires having occurred in buildings where it has been applied. Nevertheless the model itself appears to present scope for simplification, as Law and O'Brien envisaged that "as more use is made of the method it is likely that more straightforward rules will be worked out" [1]. The present work aims to analyse the model, which involves over 14 root parameters, in order to determine whether the model's complexity is justified or whether there are a smaller number of key parameters that fundamentally govern the overall exposure of external structural elements to fire. In essence a global analysis of the model is conducted in the form of a parameter sensitivity study, allowing for the 'tree branches' that link the fundamental parameters and correlations to the analytical model (as exemplified in Figure 1.3) to be evaluated such as to engineer out any 'branches' that provide unjustified complexity. The inclusion of such 'filler' parameters may provide extra

scope for potentially misleading results when applied to particular scenarios and hence unnecessarily limit the application of the Law Model. In addition, revisiting the importance of the fundamental parameters at the base of the Law Model allows for an assessment of the assumptions inherent in the model and a thorough evaluation of its limits of applicability.

The present research particularly focuses on the heat flux imposed by external flaming on the plane defined by the external façade, due to the importance of preventing external fire spread and fire-induced external structural damage. Although the Law Model allows for calculation of heat flux to external structural steelwork, all of the examples given are based on structural elements that are not flush with the façade rendering it unclear as to whether the model is directly applicable to scenarios requiring heat flux to elements in the plane of the façade (*i.e.* façade cladding, spandrel beams, perimeter columns, window pane glass, *etc*.). In order to facilitate assessment of the Law Model and that of the subsequent simplified model in reproducing heat fluxes to an external façade, full-scale tests were conducted with extensive measurements of both the internal and external fire characteristics and external heat flux to the façade. CFD modelling has also been employed to further explore the affect of some of the assumptions inherent in the Law Model and the importance of the definition of some of its main governing parameters.

The simplification of the Law Model by removal of unnecessary complexity and provision of clear limits of applicability, allows for a quicker evaluation of the external heat flux likely experienced by the various elements of the façade during a specific compartment fire. This facilitates the design of adequate cladding systems and vertical window spacing such as to minimise inter-storey fire spread and provides external fire loading for the adequate design of spandrel beams and perimeter columns. Apart from design, the appeal of a simplified model is also relevant for the respective authorities in charge of verification of compliance and adequate fire safety provision for project approval.

Chapter 2

Literature Review

http://www.thisislondon.co.uk/standard/article-23803983-assembly-launches-inquiry-into-fire-safety-of-tall-buildings.do [accessed 18/02/2010]

- The Lakanal House Fire, London, 2009 -

The study of Fire Dynamics attempts to decipher the apparently chaotic behaviour of fire and determine the various relationships between the tens, hundreds or potentially more parameters that govern the time evolution of a fire. As the field of Fire Science is relatively young, several of these parameters have been pinpointed over the last few decades of research but due to the scale of the parametric relationships, many "known" relationships still rely on empirical correlations to account for the, as of yet, "unknown" parameters. Add to this the placement of a fire within the confines of a building and several other parameters governing the fire dynamics emerge due to the interaction between the compartments, their material properties, the complex flow currents developed due to geometry and the relative location of the fire itself. Hence, any attempt to determine the behaviour of a given fire within a building and the behaviour of the building subject to this fire is, from the outset, not a simple task.

In the case of compartment fire parameters influencing the heat flux incident on the external structure, it is vital to understand the research methodologies used to identify the parameters and correlations which eventually lead to the development of the Law Model. This allows an insight into the origin of the empirical values used and to identify the scenarios the correlations are valid for and the source of the limits of applicability.

2.1 Review of Incidents Involving External Flaming

The study of external flaming is important for understanding some of the mechanisms of fire spread, particularly in the case of high-rise buildings, where evacuation times are longer and inter-storey fire spread can pose a significant threat to a large number of occupants. While compartment fires can spread inside a building due to openings, shafts and other breaches in internal compartmentation, rapid inter-storey fire spread is often the consequence of external flaming.

As a compartment fire reaches flashover conditions, the temperature rise often leads to cracking and eventually fall-out of compartment windows panes. The ventilation-controlled fire then tends to move towards the openings, with a plentiful supply of air.

The consequent external flaming and hot gases tend to rise due to the effects of buoyancy, imposing a heat flux on the surroundings. This heat flux can lead to the cracking and fall-out of upper-storey windows and the eventual ignition of compartment fires in the floors above and in cases when the radiant heat flux is high enough, ignition of items in upper-level compartments can sometimes occur prior to the window fall-out. Eventually the upper-level compartment fire might result in external flaming and the fire continually spreads up the building. In cases where the external cladding ignites, fire can rapidly spread up the façade and result in fires in several-storeys within a short space of time. The study of external flaming is also allows for the evaluation of heat flux to external structural elements (both those at a distance from and those forming part of the façade), such that adequate fire loading can be considered as a boundary condition used in their design.

While there are more complex scenarios where the study of the external flaming is important, such as buildings that have curtain walls [28] or where the external cladding has inadequate fire stops such that can fire spread vertically through the cavities between the façade wall and the cladding [29], external flaming into 'confined' spaces is not considered as part of this research. Similarly, downward flame spread and fire spread to adjacent buildings [30] due to external flaming is also important but outwith the scope of this work.

Over the years, several high-profile building fires have highlighted the importance of understanding external flaming and the associated risk of fire spread. While in many well-known high-rise building fires – such as the Joelma Building fire in 1972 [31], the One Meridian Plaza fire in 1991 [32] and the Windsor Tower fire in 2005 [33] – the external fire spread from floor to floor, the images available for the TVCC Building fire in 2009 [34] and the Melia Hotel fire in 2010 [35,36] appear to indicate fire spread mostly along the façade, with little damage to the interior of the buildings. Nevertheless, all cases involved external fire spread, which has been in the case in several other high-rise buildings. Table 2.1 lists a number of high-rise building fires where external fire spread was one, if not the sole, mechanism of fire spread. Often these fires resulted in a large number of casualties so the understanding of external flaming and mechanisms of external fire spread have been of continued interest over the years.

Building	Location	Year	Details
Andraus	São Paulo, Brazil	1972	16 dead. 375 casualties. 28 floors on fire. External inter-storey fire spread [37]
Joelma	São Paulo, Brazil	1974	179 dead [31]. 320+ casualties. [38] 1.5hrs. 14 floors on fire [31]. Internal and external inter-storey fire spread [31] [38,39]
Las Vegas Hilton	Las Vegas, U.S.A.	1981	8 dead. 350 casualties. 22 floors on fire. External inter-storey fire spread. [40]
First Interstate Bank	Los Angeles, U.S.A.	1988	1 dead. 40 casualties. 4hrs. 5 floors on fire. External inter-storey fire spread. External inter-storey fire spread [33].
One Meridian Plaza	Philadelphia, U.S.A.	1991	3 dead. 24 casualties. 19+hrs. 8 floors on fire. Primarily external inter-storey fire spread [32]
World Trade Centre	New York, U.S.A.	2001	Several diff. buildings, all featured external flaming at some point [39]
Parque Central Complex (East Tower)	Caracas, Venezuela	2004	28 casualties. 12+hrs. 23 floors on fire. External fire spread [41]
Windsor Tower	Madrid, Spain	2005	7 casualties. ~22hrs. 30 floors on fire. Both external and internal inter-storey fire spread [33].
Golden Tower Plaza	Taiwan	2005	4 dead. 3 casualties. 1.5hrs. ~5 floors on fire. External inter-storey fire spread [33].
Beijing Television Cultural Centre (TVCC)	Beijing, China	2009	1 dead. 7 casualties. 5-6hrs. External ignition source [34]. Mostly façade fire spread (?).
Lakanal House	Camberwell, U.K.	2009	6 dead. 15 casualties [42]. 2+hrs. 6 floors on fire. External inter-storey fire spread.
Melia Hotel	Braga, Portugal	2010	No casualties. 1.5hrs. 16 floors. Façade fire spread. [35,36]

Table 2.1. Historic high-rise building fires that involved external flaming. A number resulted in inter-storey fire spread, others in fire spread up the façade. Some also involved internal fire spread. Where

available, details are given for the number of dead and the number of casualties caused by the fire, as well as fire duration, number of floors on fire and the main mode of fire spread.

Although the fire protection and suppression systems available have development significantly over the last few decades, many of the fires listed in Table 2.1 are recent and occurred in modern buildings, indicating that perhaps more needs to be done to mitigate external fire spread, starting by enforcing the use of non-combustible façades [29].

2.2 The Compartment Fire and External Flaming

The study of enclosure fires began with investigating the dynamics of compartment fires. Hence in this context, the term 'compartment fire' often refers to a cuboid-shaped compartment with aspect ratios close to unity and a fairly standard size, of the order of 100 m^3 [21] or so. While a large portion of enclosure fire dynamics research concerns compartments of such a description, it has been found fire behaviour in much larger or much smaller compartments, as well as those with large aspect ratios and irregular geometries, can vary significantly from that in a 'regular' compartment. Most compartment fires, however, undergo three specific stages: the growth period, the fully-developed period and the decay period [21]. External flaming is chiefly associated with the fully-developed fire [21], as is most of the fire-induced structural damage [26] hence the fire dynamics pertaining to this period are of greatest interest.

2.2.1 Compartment Fire Dynamics

Several phenomena are known to govern fully-developed compartment fire dynamics. Beyond the compartment geometry, the "ventilation and the nature, distribution and quantity of fuel all have a significant effect" [21] on the duration and severity of a fire. Ingberg, in the 1920s, was the first to begin to quantify the effect of fire load density, L'' – as a measure of fire load per unit floor area – to the severity of a fire, [43]. The importance of ventilation was identified and Fujita quantified it in terms of the ventilation opening area, A_w and height, h, which in this case referred to a window [44]. It was Kawagoe, however, who conducted the first systematic study of fully-developed compartment fire behaviour. In the late 1940s, Kawagoe and his team conducted several full-scale and small-scale compartment fire tests with various different compartment opening sized. Using wood cribs as fire load, they found the

rate of burning to be strongly dependent on the size of the ventilation opening, such that [45]:

$$\dot{m} = 0.09\, A_w h^{\frac{1}{2}} \quad \textbf{(2.1)}$$

where $\dot{m}$ (kg/s) is the burning rate and A_w (m^2) and h (m) are the area and height of the opening, respectively. This led to the understanding that fully-developed fires are ventilation-controlled, while fires in the growth period are fuel-controlled. The correlation however was semi-empirically deduced and was later found to hold only for roughly cubical compartments [46] and within a limited range of the ventilation parameter, $A_w h^{\frac{1}{2}}$ [47].

In 1958 a large cooperative research study sponsored by the Conseil International du Bâtiment (CIB) formed to undertake a thorough study of the parameters influencing compartment fire behaviour. Due to the scale of the problem, it was decided that the fully-developed compartment fire regime would be investigated first. Over 400 experiments were carried out over 8 different institutions using model-scale compartments with various aspect ratios and heights varying between 0.5 m, 1 m and 1.5 m [47]. Besides the compartment geometry, several other parameters such as the ventilation opening size, the flammability of the wall lining and the fire load density (*i.e.* mainly 20 kg/m^2, 30 kg/m^2 and 40 kg/m^2) were systematically varied, in order to establish the effect of such parameters on the post-flashover fire [47]. Most tests were carried out under natural fire conditions, without any forced ventilation however some explored the effect of wind on the internal compartment fire. The aim was to identify "the relative importance of various features, notably compartment shape, and scale, which had not hitherto been studied" [47]. The group reported that "the effects of scale were found to be minor, justifying the use of small-scale compartments" [47]. Although Thomas and Heselden emphasise that "fire is so complex a phenomenon that it was not possible to model in one fire the effects of more than a very few factors", the experiments were used to identify the effect of compartment geometry and fire load on the mean burning rate, the mean intensity of radiation and the mean compartment temperature [47].

The study identified the importance of the compartment scenario parameter, the ratio of fire load, L to the parameter $(A_w A_T)^{\frac{1}{2}}$, where A_w is the area of the opening and A_T is the area of the enclosure surfaces excluding the opening area. Similar to Kawagoe's research, the $\dot{m}/\mathrm{A_w} h^{\frac{1}{2}}$ ratio was found to have an *average* value of 0.1 kg/s.m$^{5/2}$ in the tests conducted however it was found to be tied to compartment geometry and hence only a "gross approximation" [47]. Instead a new correlation for rate of burning was later suggested (*cf.* Chapter 3, Equation (3.7)), with additional parameters such as the compartment width, W and depth, D and the reciprocal opening factor, η which equates to $A_T/\mathrm{A_w} h^{\frac{1}{2}}$, used to represent the area of the compartment surfaces relative to the opening ventilation parameter [48]. While most of the compartments conventionally used in experiments fall within a small range of the reciprocal opening factor, it was found that for significantly higher values, such as those representative of typical compartments in larger buildings, the ratio $\dot{m}/\mathrm{A_w} h^{\frac{1}{2}}$ of is nearly double [47].

The average compartment temperature was also found to be a function of the compartment geometry and size of the opening and a maximum compartment fire temperature was found to correspond to a certain range of reciprocal opening factor values [47]. While the time-averaged parameter values (taken over the period of fire load reduction from 80% to 30% of its initial mass, where rate of mass loss was found to be approximately steady) have "enabled many important conclusions", no analysis has been conducted on the time-variation of the data collected which could provide further refinement of the correlations identified [47]. Although others have developed other correlations for the evaluation of post-flashover compartment fire burning rates and resultant temperatures [49,50,51], the work conducted by the CIB is most pertinent to the methodology used in this study.

2.2.2 External Flaming

External flaming has been found to be a characteristic of the fully-developed, ventilation-controlled fire. The internal compartment fire characteristics deemed to be most important in determining external fire exposure are "the rate of burning which affects flame size and fire duration" and "fire temperature which affects the radiation from the window [26].

2.2.2.1. Experimental research leading to the development of the Law Model

A comprehensive study of external flaming was first carried out by Yokoi [52] in the late 1950s. Yokoi was interested in the risk of vertical external fire spread and his research produced the pioneering trends used to describe the behaviour of external plumes. Having initially investigated the temperature and velocity distribution in the plume of hot gases arising from alcohol-based pool fires, Yokoi then derived similar correlations for the external plumes emerging from a 0.4 m by 0.4 m by 0.2 m model-scale compartment fire, where alcohol was also used as fire load. The size and aspect ratio of the opening at the top of one of the compartment walls was systematically varied, while ensuring the compartment was well-ventilated such that combustion was assumed to occur only inside the enclosure. The aspect ratio of the opening was found to have an important effect on the plume projection. Yokoi derived a series of plume shapes corresponding to different opening aspect ratios, treating the upper half of the opening as the heat source and hence using the parameter *n* [52]:

$$n = \frac{2w}{h} \tag{2.2}$$

where *w* (m) is the opening width and *h* (m) is the opening height. Yokoi also investigated the effect of having a vertical wall above the window on the temperature distribution and trajectory of the plume. It is found that when no wall is present above the opening, the plumes tilt away from the wall as they are projected outwards from the opening before the effect of buoyancy becomes dominant. However with a wall above the opening, for larger values of *n* where the opening is wide relative to its height, the plume is found to tilt back towards the wall. While the wall absorbs heat, it also restricts air entrainment to the 'back' of the plume, such that for relatively wide openings the plume is found to adhere to the wall as it rises from the opening. Conversely, for smaller values of *n* where an opening is relatively narrow, the plumes are found to tilt further away from the wall, again projecting outwards before the effect of buoyancy become dominant. Therefore a wall above the opening only has a significant effect on the trajectory of a plume emerging from a 'wide' opening [52].

The plume trajectories found by Yokoi are plotted in Figure 2.1, where z (m) is the height of the plume above the opening soffit, x (m) is the horizontal projection of the plume away from the opening wall and $h_{neutral}$ (m) – the height from the axis of neutral pressure that divides the opening into inflow and outflow of gases (Yokoi assumed this to be half the opening height) to the opening soffit – is used to normalise the values of reference. Good agreement is then found between the results from the model-scale tests and the data obtained from tests conducted in four full-scale test conducted in three concrete compartments using a wood-based fire load: one compartment measured 13.35 m by 9.7 m by 3.5 m, another 4.3 m by 3.48 m by 2.47 m and a third 5.0 m by 2.5 m by 1.67 m [52]. Nevertheless Yokoi points out that theoretically adjustments should be made for the differences in fuel and material used for enclosure surfaces, namely due to the difference in emissivity of flames and thermal properties of the enclosure material. It is also noted that incomplete combustion inside the compartment resulting from ventilation-controlled fires could lead to combustion outside the opening, which again would affect the correlations derived [52].

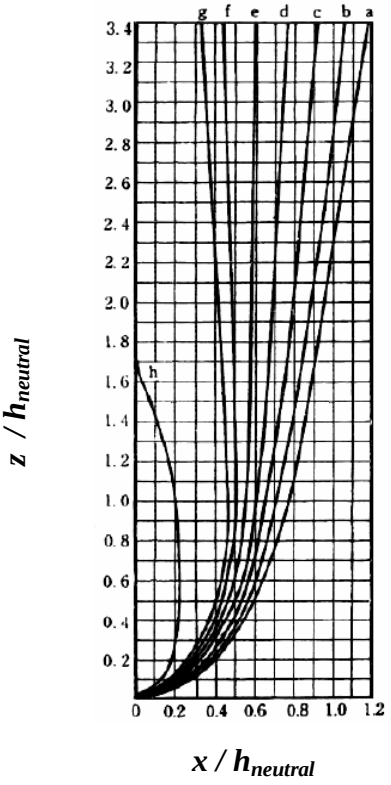

Curve Label	Opening Ratio, *n*
a	No wall above
b	1
c	1.5
d	2
e	2.5
f	3
g	3.4
h	6.4

Figure 2.1. The trajectory of the hot plume emerging from opening of the model-scale compartment used in Yokoi's experiments, where the aspect ratio of the opening is varied according to the key provided. This image has been extracted from Yokoi [52].

In developing a correlation for the temperature of the external plume, Yokoi used a characteristic length scale to represent the external plume 'heat source' as the area of the opening corresponding to the outflow of hot gases. This opening area is expressed in terms of the radius of a circle of equivalent area, such that the characteristic length scale of the heat source, r_o is [52]:

$$r_o = \sqrt{\frac{h\,w}{2\pi}} \qquad \textbf{(2.3)}$$

where h and w are the opening dimensions, as defined above. Yokoi also used a non-dimensional temperature parameter to collate the plume temperature data. This non-dimensional temperature parameter, Θ is described as [52]:

$$\Theta = \frac{(T_z - T_o) r_o^{\frac{5}{3}}}{\sqrt[3]{\frac{\dot{Q}^2 T_a}{c^2 \rho^2 g}}} \qquad \textbf{(2.4)}$$

where T_z (K) is the temperature at a certain point along the external plume axis, T_o (K) is the temperature of the plume at its axis and at its point of origin on the opening plane, $\dot{Q}$ (kW) is the rate of convective heat flow at the opening, T_a (K) is ambient temperature, c (kJ/kg.K) the specific heat and ρ (kg/m^3) the local density of the hot gases, and g (m/s^2) acceleration due to gravity. Plotting the data collected from his model-scale fire tests, using the non-dimensional temperature parameter against the vertical distance from the opening soffit, normalised against the characteristic length scale of the heat source, Yokoi obtained a very good match between the data pertaining to tests with different opening aspect ratios, as shown in Figure 2.2.

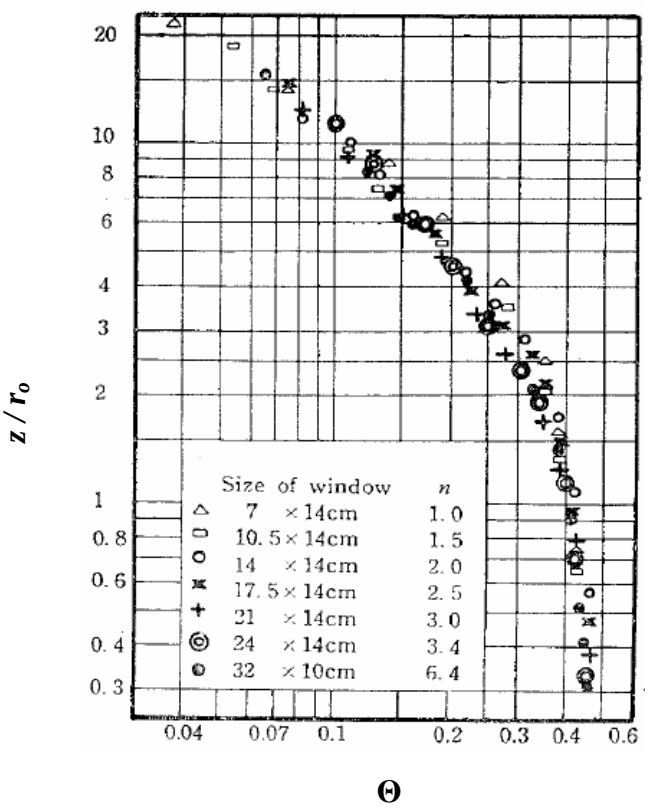

Figure 2.2. Non-dimensional distribution of temperature along the axis of hot plumes emerging from openings (window) with different aspect ratios, where there is a vertical wall above the opening. This image has been extracted from Yokoi [52].

Apart from studying the effect on the external plume of a vertical wall above the opening, Yokoi also studied the effect a horizontal projection above the window has on the plume trajectory. A projection, such as an awning or balcony, is found to deflect the flame away from the opening wall, although beyond the projection the flame is seen to deflect back to its original trajectory. The overall flame length however is seen to be relatively unaffected as the temperatures along the axis fall somewhere between those recorded with a wall above the opening and those without. Nevertheless Yokoi determined that the further away the projection is placed from the opening soffit, the lesser its effect on the flame trajectory. The inter-storey opening separation necessary to prevent inter-storey fire spread is also investigated, where a temperature of 500 ^{o}C is defined as the likely temperature for window glass fallout and hence the temperature at which there would be risk of inter-storey fire spread [52].

Around the same time Webster *et al*. conducted a series of experiments, mostly model-scale, in which visual estimates of the external flame heights were recorded [53-55]. Cubical compartments were used, with one wall completely open and no wall above the opening, using wood cribs as fire load. Thomas later used dimensional analysis, similar to that employed by Yokoi, to correlate the data collected by Webster *et al*. Although Yokoi refers only to temperature measurements of external plumes, described as 'upward currents', the point at which the axis temperature has reduced to 500 ^{o}C is defined as equivalent to the flame height, on the basis that at this temperature radiation has mostly ceased [52]. In applying this temperature to Webster *et al*.'s data Thomas was able to compare the data recorded against that reported by Yokoi. While Thomas recognises there are clear differences in the two systems, several reasons are given to justify the comparison and although in places there is significant scatter, Thomas reports reasonable agreement is found between the two sets of data, provided a temperature rise is used to define the flame tip. Thomas suggests simplifications to some of the Yokoi's correlations "without sacrificing too much accuracy" [56]. Both Yokoi and Webster *et al*.'s experiments considered only a single-storey fire, so the temperature distribution correlation is only valid for such scenarios.

In the 1960s Seigel reported on some large-scale tests conducted at the Underwriter's laboratories in which air was forcibly supplied to the fire test compartment, beyond that provided by the opening, in most tests. The opening size and aspect ratio was systematically varied and it appears there was no wall above the compartment opening. Fire load consisted of wood cribs. Flame temperature measurements were taken and visual estimates of flame height were made, although Seigel also reports the flame tip at a measured temperature of 540 ^{o}C. The added air supply (of up to 2.25 m^3/s) created a forced draught which simulated 'free-burning', fuel-controlled conditions, increasing the rate of burning and the external flame length. In this case, the flames are treated as forced horizontal jets and Seigel excludes the effect of buoyancy [57]. The flames projecting from the openings under these *Forced Draught* conditions were observed to widen with distance from the opening and the flames were observed to project from the whole are of the opening [57].

Thomas and Law [46] analysed Seigel's data by comparing it to the data collected by Yokoi and Webster *et al*. Despite the differences between the three experimental set-ups and the lack of some key data measurements, not reported by Seigel, which had to be estimated, they derived the first correlation for external flame height:

$$(z+h)=18.6\left(\frac{\dot{m}}{w}\right)^{\frac{2}{3}} \quad \textbf{(2.5)}$$

where z (m) is the vertical component of the flame height above the opening soffit, h (m) is the opening height, $\dot{m}$ (kg/s) the rate of burning (wood-equivalent) and w (m) the width of the opening. This was found to hold, with little loss of accuracy (considering the significant data scatter and the estimates made), for most scenarios that were compared, whether the external flame was considered as a jet or a plume [46]. This correlation was later adapted by Law [26] as a better fit to the general trends in data collected from a number of large-scale tests [52,57-64] and is in wide-spread use, recommended by both Drysdale [21] and Buchanan [65]. Law [26] developed separate correlations for natural *No Through Draught* and for *Through or Forced Draught* scenarios. Details of these correlations are given in Chapter 3, Sections 3.2.2.1.2 and 3.2.2.2.2, respectively and the large-scale experiments used are further discussed in Section 3.3. Under both draught conditions, the rate of burning, $\dot{m}$ is found to be important in determining the external flame height. Law [26] also provides correlations for the horizontal projection of flames, measured from the opening wall to the flame axis at the flame tip, for both types of draught conditions. Thomas [66] reports on the effect of wind on external flames, finding that wind speed has little effect of the length of the flames, however it the flame trajectory is deflected in the direction of the wind.

The experimental work conducted by Yokoi [52], Webster *et al*. [53-55] and Seigel [57] and the subsequent interpretations of this data conducted by Thomas [56,66] and Law [26,46] discussed above form the basis of the Law Model which is examined in detail in Chapter 3. As part of this model, Law developed a methodology for determining the heat flux to external structural members based on the characteristics of the external flame and the temperature within the fire compartment, which imparts

a radiant heat flux on external surfaces that are in the direct line of sight of the compartment opening [1,26]. While the methodology and correlations defined in this model are still in mainstream use in codes and standards today [2,3], further research has since been conducted on several aspects of external fire exposure. These individual research studies mainly investigate one or two aspects of the problem, although a few address several components at once. Although the present research mostly concerns a thorough analysis of the Law Model, research conducted post the development of the Law Model in some ways corroborates the correlations proposed and also highlights some areas of importance that do not feature in the Law Model.

2.2.2.2. Experimental research conducted post development of the Law Model

In the 1970s, Bullen and Thomas [67] conducted some fire experiments in compartments using non-cellulosic fuels. It was found that fires involving liquid or thermoplastic materials resulted in an increase in external fire exposure due to an increase in external combustion. The concept of an excess fuel factor, f_{ex} was used to quantify this external combustion. It was noted that external heat transfer due to fire exposure can not solely be defined in terms of the opening geometry and compartment temperature but that external combustion and flame emissivity should also be considered. It is also observed that external flames are seen to widen as they emerge from narrow openings and that the heat flux to a wall above the opening decreases with vertical distance from the opening soffit. While the flame emissivity is taken into account in the Law Model [1,26], the excess fuel factor is not directly incorporated into the calculations and widening of flames is only described under *Through or Forced Draught* conditions as described by Seigel [57].

In the 1980s, Bohm and Rasmussen [68] further investigated the relationship between the external flame height and radiative heat flux to the façade to the rate of heat release due to external combustion. Model-scale tests were conducted using propane gas burners under *Forced Draught* conditions where the rate of forced-air supply was regulated. The rate of heat release in the internal compartment was measured and that in the external flame was calculated by measuring oxygen concentration both in an exhaust duct and at the compartment opening, which was located high on the wall, close to the ceiling. Temperatures and heat flux both within and outside the

compartment were also measured. While this is a thorough collection of data and external heat fluxes are reported, the data are not extensively analysed and hence little new insight is provided into the role of external combustion in determining heat flux to external surfaces.

In the late 1980s to early 1990s, Oleszkiewicz conducted a series of full-scale fire experiments to investigate external fire exposure [69-71]. A single compartment size was used and the size and aspect ratio of the opening was varied. Measurements were taken of the external heat flux to the wall above the opening. In some tests, a propane gas burner was used and its flow rate was varied. It was found that the heat flux to the external structure increased with the increasing rate of gas flow. The heat flux to the wall above the opening was also reported to decrease with vertical distance from the opening soffit, as previously observed in experiments where the external heat flux was measured. Differences in external heat flux were also noted when changes were made to the compartment opening geometry, corroborating Yokoi's finding of the effect of opening geometry on the external flame shape and Law's correlations for determining the external heat flux from the external flames. Similar tests conducted using wood cribs resulted in higher heat fluxes to the external wall than those using propane gas with a similar burning rates. This is attributed to the lower emissivity of the propane flames, as earlier described by Bullen and Thomas [67].

Also in the early 1990s, Gottuk, Roby and Beyler [72] undertook model-scale tests with a hexane gas burner in order to determine the effect of external combustion on the downstream yields of carbon monoxide and soot. Several distinct modes of external flaming (varying intensity and duration) are identified and compared to the compartment equivalence ratio – the ratio of *actual* fuel/air mass ratio in the compartment to that of the *stoichiometric* fuel/air mass ratio [21]. It is reported that external flaming does not occur when the fire is fuel-controlled and occurs when it is ventilation-controlled. Nevertheless, while theoretically excess fuel will travel out through the opening when the equivalence ratio is greater than one, external combustion is only observed when the equivalence ratios are significantly higher (~1.7 on average for sustained external flaming). It is concluded that external combustion is therefore dependent not only on the equivalence ratio (which

determines the excess fuel factor) but also on an ignition source which itself is dependent on the opening geometry and fire size.

Others such as Ohmiya *et al*. [73-75] have also investigated the effect of external combustion. In carrying out model-scale tests with varying opening dimensions, similar to those of Yokoi's, it is noted that Yokoi's method could underestimate the risk of external fire spread as the heat release rate from external combustion is not taken into account. Ohmiya *et al*. propose a model to predict the heat release rate due to external combustion of excess fuel. It is also reported that external flames arise not only from compartments under ventilation-controlled conditions, but from those with fuel-controlled conditions as well, where long flames inside the enclosure are seen to emerge out of the opening. The risk of external fire spread due to external combustion is emphasised as a complex function of the opening dimensions the compartment dimensions, the fire load and the fire location. This is an important point as in previous tests, fire load was often uniformly distributed throughout the compartment, with uniform internal conditions of combustion, as is assumed in the Law Model [1,26].

More recently Lee, Y.-P. *et al*. [76,77] conducted a series of model-scale tests in which internal and external heat release rates and temperatures were measured. External flame heights and heat flux to the spandrel wall above the opening are also reported. In using a gas burner and systematically varying the compartment dimensions, the opening dimensions and the burner location, uniform temperatures were reported inside the compartment and previous relationships for air inflow and heat release rate inside the compartment were verified. Hence the burner location is deemed to not have an effect on the resultant external heat exposure. New length scales are proposed based on the effective area of outflow and the length after which the external plume changes from horizontal to vertical (due to the effects of buoyancy). These are used in proposed correlations for flame height and heat flux to the façade above an opening. Goble [78] on the other hand, also investigated the properties of the external flame and resultant heat flux using model-scale compartments and proposes new correlations for the external flame length and heat flux to the façade using non-dimensional expressions.

In the late 1990s to early 2000s, Klopovic and Turan [79-81] conducted a series of eight full-scale fire tests in a 3.6 m by 5.3 m by 2.4 m compartment with a 2.4 m by 1.5 m window opening (and a 0.8 m by 2 m door in some cases). The tests are set up to further investigate the effect of ventilation (*No Through Draught and Through Draught*) and wind on the external flaming and on the heat flux to the façade wall above the opening. Furniture is used as fuel with a wood-equivalent fire load density of circa 23-29 kg/m^2. Taking the flame tip at a flame axis temperature of 540 ^{o}C, the flames dimensions recorded measured noticeably more than would be predicted using the Law Model correlations [1]. In line with this observation, the glass in the upper storey compartment window was breached in every test, even though the length of the spandrel wall between the two openings was close to three times that recommended by Yokoi [52] in order to prevent vertical fire-spread. These findings suggest that perhaps previous work underestimates the risk of vertical fire-spread in realistic fire scenarios. This is potentially due to the difference in fuel used in these tests (*i.e.* non-cellulosic) compared to the wood cribs used in the derivation of many of the Law Model correlations. However beyond the increase in external combustion found by Bullen and Thomas to be characteristic of non-cellulosic fuel fires [67], the distribution of fuel throughout the compartment may also be an underlying cause of the high heat flux to the façade.

In terms of obstructions and deflection of external flames, back in the late 1980s Oleszkiewicz [70] also investigated the effect of external projections. It was found that horizontal projections significantly reduced the heat flux to the façade above the opening, in line with the deflection in flame trajectory reported by Yokoi [52]. Vertical projections on either side of the opening lead to higher heat flux to the façade as the flames became elongated [70]. Oleszkiewicz also reported on the necessary heights of spandrel walls above openings to prevent inter-storey fire spread [71]. Alterations to the flame shapes of constant thickness used by Law and O'Brien [1] (*cf.* Chapter 3, Figure 3.2) are also proposed as these are deemed to be "conservative". Oleszkiewicz recommends instead that a tapered, triangular-shaped flame be used for determining the flame thickness, which affects the correlation for flame emissivity at a particular point along its axis (*cf.* Chapter 3, Section 3.2.2.1.3).

Over the years, others have also investigated the effect of external projections on the internal and external fire behaviour. Using model-scale experiments with gas burners, Suzuki *et al*. [82-84] showed the presence of balconies lead to an increase in the internal compartment fire temperature, while the temperature along the external plume axis is reported to decrease faster than when no balcony is present. Apart from this, deflected flame trajectories reported were similar to those found by Yokoi [52]. Using full-scale tests with a wood crib fire load, Hakkarainen and Oksanen [85] investigated the effect of the opening width on the ignition of a wooden façade as well as that of horizontal projections of varying lengths. An increase in internal compartment fire temperature with increase in opening width is reported and longer horizontal projections above the compartment opening are again seen to reduce the heat flux incident on the façade above. Notably, it was also found that horizontal projections increase the risk of horizontal fire spread to adjacent compartments due to an increased exposure to radiant heat flux. Sugawa and Takahashi [86] furthered the work done by Thomas [66] on the effect of wind on the external flame by defining several different plume trajectories depending on the wind direction, where a frontal wind was seen to push the flame back towards the spandrel wall.

The work conducted to date has been diverse and at times even inconsistent, as is the case with observations of external flaming under fuel-controlled conditions. While there are several instances where the work conducted prior to the development of the Law Model is corroborated, research has also shown that other parameters of importance might not have been considered at the time. Although some new correlations have been proposed, most are only relevant to specific scenarios, with particular draught conditions or with the presence of a spandrel wall. The measurements made by Klopovic and Turan [80,81] indicate also that further investigation is still necessary to ensure correlations for external flaming and external heat exposure are adequate for realistic scenario such that they can be confidently used in design. On the other hand, no thorough investigation appears to have yet been conducted on the effect of varying the location of an opening, the number and dimensions of openings on different walls (*i.e.* openings as windows *and* doors) and of varying the location of the fuel within the compartment in a large-scale setup where the fuel is either wood cribs or furniture, as well as combustible wall-lining. Hence, to date, the Law Model is still the most comprehensive model linking the internal

compartment parameters to the characteristics of the external flame and heat flux to the external surroundings. It is therefore appropriate to revisit the model and to conduct a thorough sensitivity analysis of the parameters it takes into account. This enables the identification of the parameters that have the greatest influence on the resultant external heat exposure, in order to focus the direction of further research.

Chapter 3

The Analytical Law Model

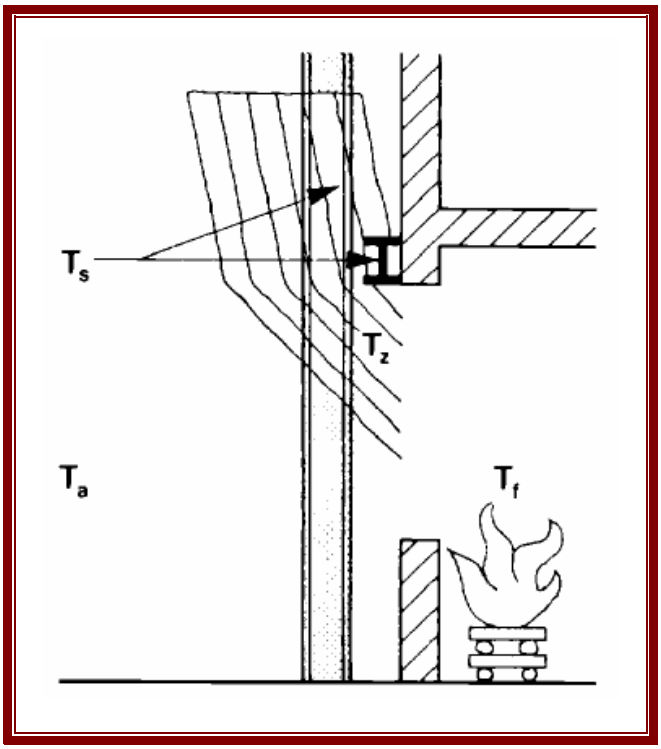

Extracted from Law and O'Brien [1].

- External flaming from a compartment fire with reference temperatures indicated -

The main analytical model describing external flaming and linking its development to the characteristics of an internal fire can be found in the form of a design manual for "Fire Safety of Bare External Structural Steel" [1]. The model - herein referred to as the Law Model – is based on fundamental fire science, balance of heat and mass transfer and experimentally derived empirical correlations [26,46,52-57] and hence has some inherent assumptions and limits of application.

3.1 Overview of the Law Model

The Law Model comprises a detailed analytical model devised to determine whether external structural steel members require passive fire protection or whether the steel can remain 'bare' and provide adequate performance in the event of a post-flashover compartment fire. As an advocate of practical engineering solutions, Law aimed to develop a model that could be understood and employed by the wider non-specialist community [87]. The Law Model was developed as a tool for structural design to help determine the resultant temperature of external steel members when exposed to a regular compartment post-flashover fire, hence it involves a fire component and a structural-heat transfer component. One of the main design manual requirements stipulated by Law was that "the correlations of fire and flame behaviour should be based on parameters which can be readily identified by the designer" [26]. Although the model is theoretically based on fundamental fire science, fire dynamics and balance of mass and heat transfer [21,88], its translation into an engineering tool for design [1,26] means many of the fundamental principles have been converted into component correlations based on simple input parameters. Most of these correlations are derived from experimental data [46,52-57] and hence involve empirical values which to some extent may be tied to the specific set of experimental scenarios used.

In discretizing the problem several assumptions were made, inevitably leading to limitations in the application of the model. Nevertheless, where specific knowledge was not available, assumptions were devised to err on the conservative side. This approach was deemed to allow for conservative structural design [1,26].

Although several assumptions and limitations of the model are stipulated by Law [1,26], these appear not to be exhaustive. In order to study the limits of application of the Law Model in detail, it is necessary to understand the intricacies of the model and to appreciate the experimental work [52-55,57] many of the correlations are based on, as well as the assumptions made in analysing the experimental data [46,56].

3.2 The Law Model Methodology

The Law Model is composed of two main calculation sections: fire development leading to an external heat insult to the surroundings and a structural heat transfer section where the heat flux from the fire is applied to a given external structural steel member in order to obtain a resultant steel temperature. Heat flux to the external elements arises from a combination of "radiant heat from the windows" of the compartment fire and both "radiation and convection from flames projecting from these windows" while the elements are also "free to lose heat to the surrounding air". Hence the amount of heat flux impinging on external structural members is highly dependent on the location of the member relative to the window (or windows) and the external flaming [1].

If the external steel member is engulfed in flame, the heat balance per unit surface area of the steel surface can be expressed as a combination of components:

Convection from External Flames	+	Radiation from External Flames	+	Radiation from Fire (through windows)	+	Radiative Heat Loss to Surroundings	=	Rate of Heat Gain per Unit Surface Area

These components are respectively defined by Law and O'Brien [1] as:

$$\alpha_z(T_z - T_s) + \varepsilon_z\varepsilon_s\sigma(T_z^4 - T_s^4) + \varepsilon_f(1-\varepsilon_z)\varepsilon_s\phi_f\sigma(T_f^4 - T_s^4) + (1-\varepsilon_z)\varepsilon_s(1-\phi_f)\sigma(T_a^4 - T_s^4) = \frac{Mc_s}{A_{sp}}\frac{dT_s}{dt} + k \quad \textbf{(3.1)}$$

where α (kW/m^2.K) is the convective heat transfer coefficient, T (K) represent temperatures, ε is a measure of emissivity, σ (W/m^2.K^4) the Stefan-Boltzmann

constant, ϕ a configuration, or 'view' factor, M (kg/m) the mass of steel per unit length, c (kJ/kg.K) the specific heat of the steel, A_{sp} (m) the perimeter length of the steel cross-section, t (s) represents time and k (kW/m^2) the heat loss by conduction. Throughout the Law Model, the internal compartment fire is mainly referred to as the 'fire' and related to the subscript *f*, while the external flaming is referred to as the 'flame' related to subscript *z*, 'ambient' external conditions are given subscript *a*, and properties of the 'steel' are referred to by the subscript *s*.

Nevertheless, the emissivity of the steel surface, ε_s is deemed to be high, so it is approximated as unity. The emissivity of the internal fire, ε_f is also expected to be high, so for simplicity, it too is taken as unity. Radiative heat transfer from the ambient surroundings to the steel, σT_a^4 is deemed to be relatively small and hence negligible, particularly in comparison with heat loss from the steel to the ambient. Conduction is also assumed to be negligible as little temperature gradient is expected within the region of the section engulfed in flame. Additionally, steady-state conditions are assumed for the heat transfer process as they lead to a maximum steel temperature which is of interest for design purposes. These approximations and assumptions allow for a simplified heat balance for steel members engulfed by flame [1,26]:

$$\alpha_z(T_z - T_s) \;+\; \varepsilon_z \sigma T_z^4 \;+\; (1-\varepsilon_z)\phi_f \sigma T_f^4 \;-\; \sigma T_s^4 \;=\; 0 \qquad \textbf{(3.2)}$$

Similarly, when a steel member is not engulfed by external flame and hence no longer in the convective stream of the flame and hot gases, the heat balance can be expressed as a combination of the following components:

Radiation from External Flames	+	Radiation from Fire (through windows)	+	Radiative Heat Loss to Surroundings	+	Convective Heat Loss to Surroundings	=	Rate of Heat Gain per Unit Surface Area

Taking the same approach and making the same assumptions as for the scenario engulfed in flame, these heat transfer components are described by Law [1,26] under steady-state conditions as:

$$\varepsilon_z \phi_z \sigma T_z^4 \quad + \quad \phi_f \sigma T_f^4 \quad - \quad \sigma T_s^4 \quad - \quad \alpha_s (T_s - T_a) \quad = \quad 0 \qquad \textbf{(3.3)}$$

where individual terms represent the same variables as described above. Note that under transient conditions, the right-hand side of Equation (3.3) would include the same expression as that in Equation (3.1) for rate of heat gain per unit area of steel and conduction losses.

Hence, in order to determine the heat transfer to the steel, the fire and resultant external flaming have to be characterised for each particular scenario, such that each necessary parameter can be quantified. This renders the two main 'fire development' and 'structural heat transfer' calculation sections sequential, as are their individual components. Nevertheless the first step is to define the scenario by identifying the compartment parameters.

3.2.1 Defining the Scenario

The Law Model allows only for simple right-angle cuboid-shaped compartments with the possibility of defining an additional internal core. There can be any number of openings in the compartment, provided there is at least one. The compartment width, W (m) is taken as the length of the wall containing the largest opening area, the length of the perpendicular wall is taken as the compartment depth, D (m) and the compartment height, H (m), is defined from floor to ceiling. Opening dimensions are characterised by their width, w (m) and their height, h (m). Should there be a core within the compartment its dimensions are labelled relative to the wall they face (*cf.* Figure 3.1 (iv)). These are the key parameters defining the geometry of a specific scenario.

The key geometric dimensions can be used to obtain further parameters characteristic of the scenario, such as the compartment floor area, A_F (m^2) the sum of area of openings, A_w (m^2) and the total surface area of the enclosure, A_T (m^2) including the walls, floor and ceiling but excluding the area of the openings. The ratio D/W also forms a further parameter to be employed in the model's correlations. Under scenarios

with specific characteristics, the definition of some of these parameters is modified when used in the Law Model correlations. Figure 3.1 illustrates four main potential scenario characteristics and the respective definitions of several parameters in each specific case. The parameter calculations for a compartment scenario with just one opening, seen in Figure 3.1 (i), are straightforward. Nevertheless, should there be multiple openings of different dimensions, as is the case in Figure 3.1 (ii), an overall opening width, w_{mo} is taken as the sum of all the individual opening widths and an equivalent area-weight-averaged value of opening height, h_{mo} is used in subsequent calculations. If the multiple openings lie on more than one wall, as depicted in Figure 3.1 case (iii), the total opening area calculation will remain straightforward however the total area of the openings on each individual wall are used to enable a weighted calculation of the compartment depth-to-width ratio, D/W_{mo}. Similarly if the compartment has a core, as in the case of Figure 3.1 (iv), the compartment depth-to-width ratio, D/W_{mo} is also adjusted, as are the floor area and total enclosure surface areas. These same definitions and modified definitions of the main geometrical parameters are given in the Eurocode [2].

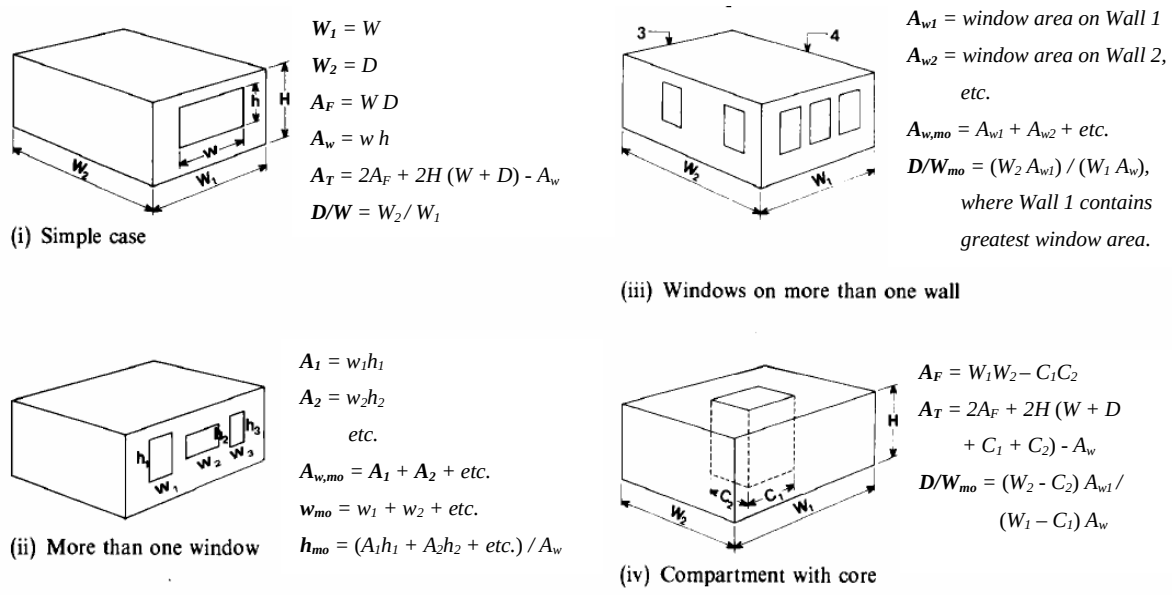

Figure 3.1. Depiction of the key characteristic dimensions of the compartment and its openings for four different types of scenario. The definition of further characteristic parameters, respective to each scenario, is given in the form of simple equations. Where modified definitions of w, h, A_w and D/W are given, the new definitions are referred to as h_{mo}, w_{mo}, $A_{w,mo}$ and D/W_{mo}. These images have been extracted from Law and O'Brien [1].

The parameters shown in Figure 3.1 are used to calculate the reciprocal opening factor, a parameter found to have significant effect on the fire conditions in particular scenarios [47,48]. In this case, the reciprocal opening factor, η ($m^{-1/2}$) is defined as [1]:

$$\eta = \frac{A_T}{A_w h^{\frac{1}{2}}} \quad \textbf{(3.4)}$$

The reciprocal opening factor is the ratio of the enclosure solid surface area relative to the main ventilation parameter, the product of opening area and weight-averaged height of the enclosure openings. For the case of multiple openings of varying sizes, the values of A_w and h are defined as per the modified values defined for the respective scenario defined in Figure 3.1.

3.2.2 Describing the Fire

The main purpose of the model is to evaluate whether any fire protection is required on external structural steelwork, hence the fire is only characterised in its fully developed, post-flashover stage, when it is most expected to produce external flaming. Additionally the steady-state conditions assumed for the heat transfer calculations to the external steel are more likely to be found during the post-flashover stage of fire development, than in the growth and decay stages.

Beyond the dimensions of the compartment and its openings, the only other input parameter required is the fire load, L (kg). This is a measure of the total amount of combustible fuel within the compartment, expressed in terms of "equivalent amounts of wood which would evolve the same amount of heat [as the actual fuel] when burnt" [1]. For a particular scenario, this is often defined in terms of the fire load density, L'' (kg/m^2), an average of the fuel content per unit floor area expressed as the quotient of the fire load, L and the total floor area, A_F (m^2). Together with the properties of the enclosure geometry, the fire load parameter, L is found to affect the conditions of the internal compartment fire [47], particularly in the form of the compartment scenario parameter, ψ (kg/m^2):

$$\psi = \frac{L}{(A_w A_T)^{\frac{1}{2}}} \quad \textbf{(3.5)}$$

which subsequently features in several equations [1]. Within the model, the internal fire is mainly described by a uniform burning rate and a single resultant fire temperature. Consequent external flaming is then characterised in terms of flame dimensions, flame projection and temperature distribution along its axis. Characteristics of the fire and external flame, such as emissivity and the convective heat transfer coefficient, are also defined.

There are two main sets of calculations for fire development for two distinct scenarios. The potential variation in amount of air that can reach and take part in the fire has been found to influence fire behaviour [44-66]. Hence, if the scenario includes openings on only one wall or two adjacent walls, the scenario is expected to have "*No Through Draught*" (*alias* natural draught) conditions. If there are openings on opposite walls or if there is an alternative supply of air fed into the compartment, "*Through or Forced Draught*" conditions are considered [1,57]. The prospective effect of wind [66] is considered separately.

3.2.2.1. No Through Draught (ND)

3.2.2.1.1. The Internal Fire (ND)

Under *No Through Draught* (ND) scenarios, there are two distinct conditions that may characterise the internal fire. If the compartment is well ventilated, the fire is expected to burn freely under *fuel-controlled* conditions, with a different burning rate and fire temperature than a compartment which is under-ventilated, burning under *ventilation-controlled* conditions. In order to identify which of these two conditions the scenario falls under, the rate of burning, $\dot{m}$ (kg/s) is calculated for both conditions. For a fuel-controlled fire, the rate of burning is defined as [1,26,46]:

$$\dot{m}_{Fuel} = \frac{L}{\tau_F} \quad (\textit{fuel-controlled} \text{ fire}) \quad \textbf{(3.6)}$$

where L (kg) is the fire load in equivalent kilograms of wood and τ_F (s) is the free burning fire duration, whereas for a ventilation-controlled fire, the rate of burning is defined as [1,26,48]:

$$\dot{m}_{Vent} = \frac{0.18\left(1 - e^{-0.036\eta}\right)}{\left(\frac{D}{W}\right)^{\frac{1}{2}}} A_w h^{\frac{1}{2}} \qquad (\textit{ventilation-controlled} \text{ fire}) \quad \textbf{(3.7)}$$

where only compartment geometry and ventilation parameters feature. These parameters are defined relative to their corresponding scenario as defined in Figure 3.1. It should be noted that Equation (3.7) has been derived from a best-fit through data pertaining to a number of both model-scale [47,48] and large-scale [58,59,89] tests. Since the units of the parameters featured in Equation (3.7) are not consistent, it is implicit that the coefficient 0.18 has units ($kg.m^{-2.5}$), therefore there may be further parameters of importance within this coefficient that are yet to be found.

The *actual* burning rate of a specific scenario, $\dot{m}$ is then defined by the *lowest* of the two burning rates, hence $\dot{m} = \min(\dot{m}_{Fuel} ; \dot{m}_{Vent})$. Nevertheless, subsequent fire and flame calculations are identical for both fuel-controlled and ventilation-controlled conditions, differing only by the value of rate of burning used.

The internal compartment fire temperature, T_f (K) is given by [1,26]:

$$T_f = \left(6000 \left[\frac{\left(1 - e^{-0.10\eta}\right)}{\eta^{\frac{1}{2}}} \right] \left(1 - e^{-0.05\psi}\right) \right) + T_a \qquad \textbf{(3.8)}$$

where the previously defined reciprocal opening factor, η and compartment scenario parameter, ψ are used and the ambient temperature, T_a is input in degrees Kelvin (K). As this correlation was also empirically derived, the coefficient 6000 must have units ($K.m^{-0.25}$) and again may be composed of several other parameters that have not yet been identified. This fire temperature, T_f is an important parameter that features in the 'radiation from the fire' component, as expressed in Equations (3.2) and (3.3).

3.2.2.1.2. The External Flame Shape and Temperature Distribution (ND)

Consequent external flame conditions are defined using 'notional flame shapes' as a geometrically simpler, idealised representation of the actual emerging flames. The flames are defined in 3D with temperature varying mainly with distance from the opening, along a central axis. Figure 3.2 illustrates the notional flame shapes used to describe external flames under *No Through Draught* conditions, the main dimensions of which are described below.

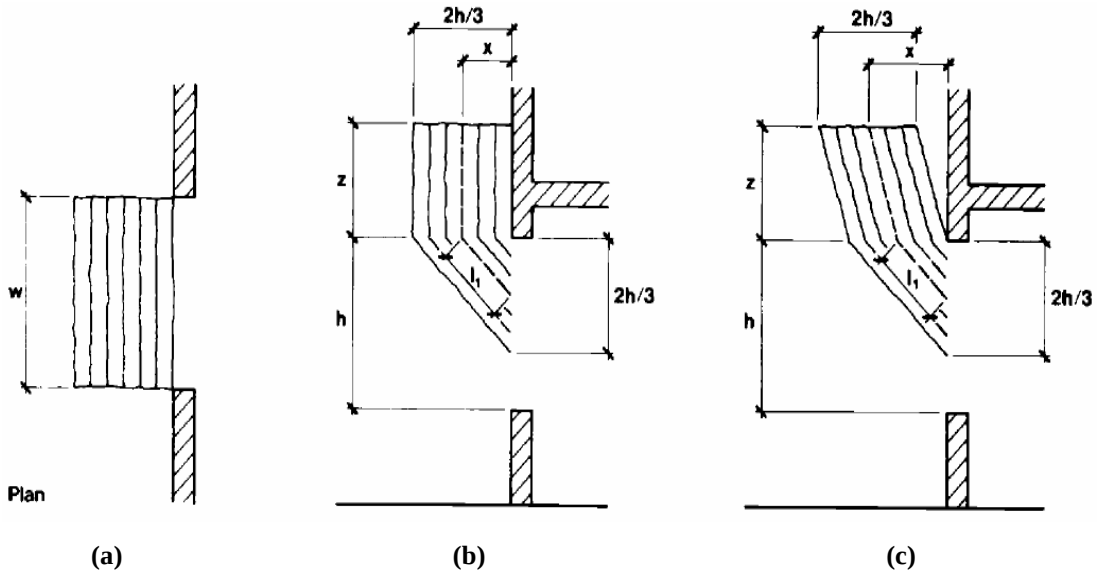

Figure 3.2. External flame geometry under *No Through Draught* conditions: (a) a plan view of the flame protruding from the façade; (b) an elevation of the flame when there is a wall above the window and the conditions are satisfied for an adhered flame; (c) an elevation of the flame when there is no wall above the window or when other conditions cause the flame to protrude away from the wall. Key characteristic dimensions are labelled, the flame axis is shown as a dotted line and l_1 indicates the flame axis length below the opening soffit. The flame is assumed to project from the compartment at an initial angle of 45^o to the horizontal. These images have been extracted from Law and O'Brien [1].

The flame height, z (m) is defined from its base, at the opening soffit (top sill), vertically to its tip where the flame temperature has decreased to 813 K (~540 ^{o}C), as depicted in Figure 3.2. The flame height is expressed as [1,26,46]:

$$z = 16h\left(\frac{\dot{m}}{A_w \rho [gh]^{\frac{1}{2}}}\right)^{\frac{2}{3}} - h \qquad \textbf{(3.9)}$$

where a buoyancy term features where ρ (kg/m^3) is the density of the gases flowing out of compartment, g (m/s^2) is acceleration due to gravity and h is the window opening height, as defined above, together with parameters $\dot{m}$ and A_w. Although the units within this expression are consistent, the correlation is empirical in nature, having been derived as a best-fit through a number of data from model-scale tests [47,52-55] for which data scatter was significant. For design purposes, Law simplifies Equation (3.9) by taking the gas density to be 0.45 kg/m^3 (taken at 540 ^{o}C) and gravitational acceleration to be 9.81 m/s^2 [1,26]:

$$z = \left(12.8 h^{\frac{2}{3}} \left[\frac{\dot{m}}{A_w} \right]^{\frac{2}{3}} \right) - h \qquad \textbf{(3.10)}$$

and then further simplifies this to [1,26]:

$$z = \left(12.8 \left[\frac{\dot{m}}{h} \right]^{\frac{2}{3}} \right) - h \qquad \textbf{(3.11)}$$

Although Law makes no further comment on this latter simplification, its validity is discussed in Section 3.4. The flame width is simply taken to be the same as the width of the window, w, even as it projects outwards, while the flame depth is described as two-thirds of the window height, $2h/3$ [1,26], equivalent to the height of the neutral plane down from the opening soffit, which describes the area of outflow. For the case of multiple windows, particularly when these are different sizes as in Figure 3.1 case (ii), w and h are redefined as w_{mo} and h_{mo}. It is unclear both in the Law Model [1] and the related literature detailing its derivation [26], if the window width, w and opening height, h used to define the flame width and depth refer to the modified values described in Figure 3.1 case (ii), or whether they refer to dimensions of a specific window. Hence, since the rate of burning for such a case is defined by $A_{w,mo}$ for multiple windows, these values have been assumed to refer to the modified dimensions, resulting in an averaged flame height, h_{mo} for all windows. In any case, the full expression given in Equation (3.9) is given in the Eurocodes hence in these mainstream standards the simplification expressed in Equation (3.11) is not used [2].

The horizontal projection of the external flame may vary in accordance with the external geometry. It is measured horizontally from the façade to the flame axis, as depicted in Figure 3.2. A wall above the compartment window is defined as a vertical surface that will retain its "integrity" during a fire and "exceeds 2z/3 in height" [1]. If these conditions are not met, the window is deemed not to have a wall above it. The presence of a wall limits the amount of air that can be entrained into the back of the plume and hence the flame tends to adhere to the wall, limiting its projection. However, the width of the window can also affect the flame projection, as very narrow windows lead to narrow flames. In this case, provided there aren't any other windows close by, the presence of a wall provides limited restriction to the air entrainment behind the plume as some air can be entrained from the sides. Hence, if there is no wall above the window or if the window is narrow and well spaced from other windows, the flame will be projected outwards from the façade.

For a scenario with a wall above a window that is not narrow and/or has no windows at a distance closer than 4*w*, the flame adheres to the wall hence the flame projection is simply half the flame depth [1]:

$$x = \frac{h}{3} \qquad \forall \quad h \leq 1.25w \tag{3.12}$$

If there is a wall above the window but the window is narrow and other windows, if any, are at a distance greater than 4*w* away, the flame projection is defined as [1,26]:

$$x = 0.3h\left(\frac{h}{w}\right)^{0.54} \qquad \forall \quad h > 1.25w \tag{3.13}$$

On the other hand, when there is no wall above the window of interest, the flame projects further, and its horizontal distance from the façade to the flame axis is defined by [1,26]:

$$x = 0.6h\left(\frac{z}{h}\right)^{\frac{1}{3}} \tag{3.14}$$

This defines the basic geometry of the external flame, illustrated in Figure 3.2, allowing for a definition of flame temperature distribution within the flame. Flame temperature, T_z (K) is assumed to vary only along the flame height and is defined along the flame axis [1,26]. Thus the axis temperature at any point represents the flame temperature through the cross-sectional plane provided it intersects the point and its normal is parallel to the flame axis. The flame axis is simply defined as running through the centre of the flame as depicted by the dotted line in Figure 3.2 (b) and (c). With the distance along the flame axis denoted by l (m), running from the plane of the window to the flame tip, the temperature distribution is defined as [1]:

$$\frac{T_z - T_a}{T_o - T_a} = 1 - 0.027\frac{lw}{\dot{m}} \qquad \textbf{(3.15)}$$

where the subscript '*o*' describes conditions just at the 'window plane'. Nevertheless, in order to pin-point a flame temperature, T_z (K) at any particular point along the flame, T_o (K) must be known. The temperature at the base of the flame, T_o is found by benchmarking against the total flame length along its axis, X (m) and the temperature at the flame tip, T_x (K) assumed to be 813 K (~540 ^{o}C) [1,26,46,57]:

$$T_o = \left(\frac{813 - T_a}{\left[1 - 0.027\left(\frac{X\,w}{\dot{m}} \right) \right]} \right) + T_a \qquad \textbf{(3.16)}$$

where the length of the flame axis, X (m) is found by simple trigonometry. The temperature just at the plane of the window, T_o can be found to exceed the internal fire temperature, T_f. This is expected as often a significant portion of partially combusted fuel emerges from the compartment and burns outside the window as described by Bullen and Thomas [67]. The temperature T_o is input into Equation (3.15) enabling the flame temperature, T_z to be defined for any point along the flame axis, defined by length l (m). This provides yet another input variable for the heat balance Equations (3.2) and (3.3).

At times, obstructions may be present between the window soffit and the spandrel wall above. Awnings, balconies and other projections above the window may affect the flame shape if they are deemed to be fire resistant. If such an obstruction lies in the regular path defined for the flame, it deflects the flame away from the façade as found by Yokoi [52]. The flame will follow the length of the projection and then its height, if applicable, however once past the obstruction, the flame will then deflect back to its original trajectory at an assumed angle of 45^o provided it is long enough. Although the flame shape changes, the length along its axis remains constant, so the calculation for the flame height, z and flame projection, x should be adjusted accordingly.

3.2.2.1.3. Flame Emissivity (ND)

The emissivity of the external flame, ε_z is related to the flame thickness, λ (m) in a relationship described by the Beer-Lambert law [1,21]. In turn, the flame thickness is defined relative to the location of the steel element of interest [1,26]. It is taken as the dimension of the flame perpendicular to the surface of the steel member of interest, hence normal to the flame face the surface 'sees' directly. This can vary depending on whether the steel member of interest is a column or a beam and also if the member is engulfed in flame. In the latter case, the thickness is calculated as just the portion of the flame the specific surface 'sees'. In any case, the thickness should be calculated individually for each face of the steel member and the thickness is cumulative if a given surface 'sees' several flames emerging from different windows. Once the flame thickness has been specified for each face of the steel member, it is used to find the emissivity of the flame relative to the faces the steel 'sees', as [1,21,26]:

$$\varepsilon_z = 1 - e^{-0.30\lambda} \tag{3.17}$$

where the emissivity is dimensionless. The flame emissivity is another variable that features in the heat balance Equations (3.2) and (3.3). In some specific cases the flame emissivity from the exposed faces of a steel member are averaged, however further details are given by Law and O'Brien [1] for specific scenarios.

3.2.2.1.4. The Convective Heat Transfer Coefficient (ND)

A simplified approach is taken for the calculation of the convective heat transfer coefficient, α (kW/m^2.K). Details of the simplification are given by Law in a paper that explains the development of the model [26]. The approach relates the convective heat transfer coefficient to the ratio of the burning rate to the area of the opening as this has been found to be proportional to the mass flow of hot gases per unit area of the opening. The coefficient α is also related to a characteristic dimension of the steel member cross-section, d (m). The steel member's surface orientation is taken to be perpendicular to the flow as this yields a maximum value for the coefficient, α. This is deemed to be a conservative assumption, particularly for a fuel-controlled fire [26]. For a case with multiple windows of varying sizes, the value of A_w used is that redefined in Figure 3.1 case (ii) as $A_{w,mo}$ as this will provide a generalised estimate of the coefficient [1,26]:

$$\alpha = 0.026\left(\frac{1}{d}\right)^{0.4}\left(\frac{\dot{m}}{A_w}\right)^{0.6} \qquad \textbf{(3.18)}$$

Irrespective of the cross-sectional shape of the steel element, for the purposes of the model, a rectangular geometry is used, its dimensions defined by closely enveloping the real steel shape, as illustrated in Figure 3.3.

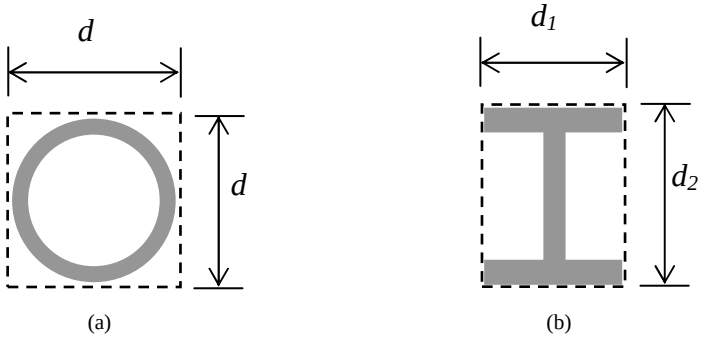

Figure 3.3. A cross-section through sample structural steel members, where the characteristic dimensions, d (m) are shown for both: (a) a circular section; and (b) an I-section. The dimensions are obtained by taking a rectangular envelope around the sections, the dimensions of which are taken as the characteristic dimensions of each section.

For cases where the rectangular envelope around the steel section is square, where both sides are of the same dimension, d as in Figure 3.3 (a), then d is simply the characteristic dimension of the section. On the other hand, although not explicitly

mentioned by Law and O'Brien, example cases provided [1] show that when the rectangular envelope around the section has sides of two differing lengths such as d_1 and d_2 in Figure 3.3 (b), an average of both lengths (*i.e.* $(d_1 + d_2)/2$) is taken as the characteristic dimension, d. Although this approach mainly applies to the convective heat transfer coefficient for steel elements engulfed in flame, α_z it is also used for the coefficient of elements that are not directly engulfed in flame, α_s where heat from the steel is lost by natural convection [1]. The use of Equation (3.18) to define both α_z and α_s is justified by the *assumption* that "the air in the region of the windows" (pertaining to α_s) "will be similar to that in the flame" (pertaining to α_z) as "the velocity of hot gases out through the window and the velocity of the wind (ambient air) are [taken to be] similar" [1]. While some gross approximations are made in defining the convective heat transfer coefficient for the Law Model, most are made to err conservatively, allow for a single coefficient of general applicability to be used such as not to over-complicate the model. The significance of these assumptions is further discussed in Section 3.4. Both these parameters feature in heat balance Equations (3.2) and (3.3).

3.2.2.2. Through or Forced Draught (ToFD)

For *Through or Forced Draught* conditions, where there is an extra supply of air, be it through openings on opposite walls or via an alternative supply of air fed into the compartment (*i.e.* a fan inlet), the calculation procedure is similar to that described in Section 3.2.2.1 however several equations are slightly modified.

3.2.2.2.1. The Internal Fire (ToFD)

Contrary to *No Through Draught*, under the *Through or Forced Draught* scenario only free-burning, fuel-controlled conditions prevail as it is assumed there is always sufficient ventilation. Hence the burning rate is [1,26,46]:

$$\dot{m} = \frac{L}{\tau_F} \qquad \textbf{(3.19)}$$

where the variables are the same as those described in Equation (3.6) above. Law and O'Brien assume this to be appropriate for "most types of furniture found in buildings"

[1] (*N.B.* Building contents have changed considerably since this work was undertaken). The fire temperature however appears to be only dependent on the compartment scenario parameter, ψ and the ambient temperature, T_a:

$$T_f = 1200\left(1 - e^{-0.04\psi}\right) + T_a \qquad \textbf{(3.20)}$$

where all temperatures are described in degrees Kelvin (K). The fire temperature is one of the variables required in order to conduct the heat balance described in Equations (3.2) and (3.3).

3.2.2.2.2. The External Flame Shape and Temperature Distribution (ToFD)

Analogous to the *No Through Draught* scenario external flame conditions under the *Through or Forced Draught* scenario are defined using 'notional flame shapes' and the flame temperature is defined as varying only along the flame axis. At any point along the axis, the axis temperature defines a uniform temperature through the cross-section of the flame, normal to the axis. Figure 3.4 illustrates the notional flame shape used to represent external flaming under *Through or Forced Draught* conditions. The key dimensions labelled are described below and the flame axis is indicated by a dotted line.

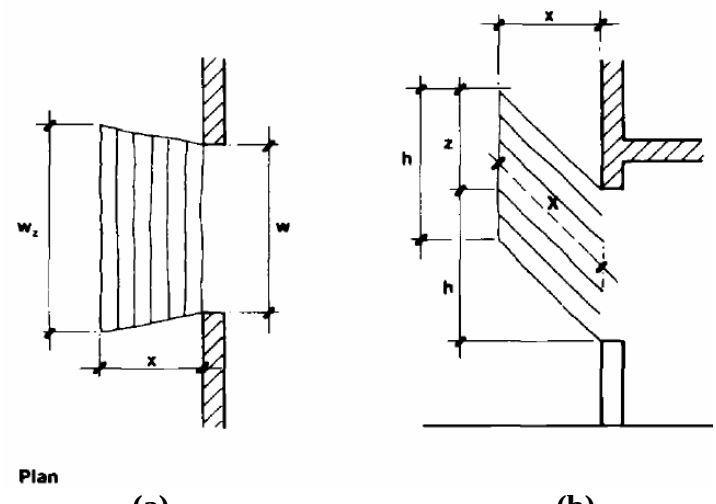

Figure 3.4. External flame geometry under *Through or Forced Draught* conditions: (a) a plan view of the flame projecting from the façade showing the flame widening with distance from façade, and (b) an elevation of the jet-like flame seen to project away from the façade. Key characteristic dimensions are labelled, with *X* (m) indicating the flame axis length. These images have been extracted from Law and O'Brien [1].

The flame height, z (m) is again defined from the opening soffit (top sill) vertically to where the flame temperature has decreased to 813 K (~540 ^{o}C), however under *Through or Forced Draught* conditions the flame is more jet-like and the effects of buoyancy and turbulent mixing are not as significant [1,57] so the flame shape is slightly different. Under such conditions, the flame height, z is defined as:

$$z = \left(23.9 \left[\frac{1}{u} \right]^{0.43} \left[\frac{\dot{m}}{A_w^{\frac{1}{2}}} \right] \right) - h \qquad \textbf{(3.21)}$$

where u (m/s) is the draught velocity, taken to be the same as the general wind velocity. Since the Law Model is intended for design, a wind velocity of 6 m/s is suggested and justified by Law and O'Brien [1], however other values can be used if deemed more appropriate for a specific scenario. While the total opening area, A_w is identical to that defined in Section 3.2.1 and specified in Section 3.2.2.1 for either single or multiple openings, under *Through or Forced Draught* conditions the flames are assumed to only project from "half" of the windows [1]. It is assumed the draught is drawn in through the openings on one wall and flames emerge only out of the opening on the opposing wall, occupying the whole opening area. Although Law specifically designates the flames as projecting from "half" the number of windows, it is thought they will project out of all windows on one of the walls regardless of whether the openings are equally distributed throughout the compartment walls. Since the wind direction is unknown in a design scenario, the calculation should be repeated for all main wind directions necessary, depending on how many walls have openings with structural steel members on the outside. It should be noted that Equation (3.21) is empirical hence the coefficient 23.9 has units ($m^{2.43}s^{0.57}kg^{-1}$) in order that the correlation is dimensionally correct.

The jet-like properties of the emerging flames, caused by the draught flow, mean the flames always project outward from the façade, irrespective of whether there is a wall above the window and other opening conditions that affected the flame projection under *No Through Draught* conditions. The projection, x (m) hence becomes a function of the draught velocity, u and is defined as [1,26]:

$$x = 0.605\left(\frac{u^2}{h}\right)^{0.22}(z+h) \quad \textbf{(3.22)}$$

where it is measured horizontally from the façade to the flame tip. The definitions of flame height and flame protrusion relative to draught velocity mean an increased wind velocity will result in a decrease in flame height but an increase in flame projection and vice-versa. It should again be noted that this is an empirical correlation therefore the coefficient 0.605 must have units ($m^{-0.22}s^{0.44}$) to enable adequate dimensional consistency.

Under these *Through or Forced Draught* conditions, the flame width is assumed to occupy the width of the window as it exits the compartment, however experimental observation has shown it to widen as it gets further from the opening [57]. The widening is found to bear no correlation to any specific parameter, so the average angle of widening observed (11^o) [57] is used, by relating the width of the outermost flame face to the flame projection, x [26]. This flame shape widening effect can be seen in Figure 3.4 (a), in plan view. At its widest, at the flame face furthest from the façade, the flame width, w_z (m) is [1]:

$$w_z = w + 0.4x \quad \textbf{(3.23)}$$

The main dimensions of the notional flame shape allow for calculation of the flame axis length, X (m) by means of simple trigonometry, such that the flame temperature distribution can then be specified. As is the case for the *No Through Draught* scenario, the external flame temperature is defined as a distribution between two known temperatures, one at the flame base in plane with the window, T_o (K) and the other the temperature at the flame tip, T_x (K), defined as 813 K (~540 ^{o}C). Hence, in order to determine the temperature at the base of the flame, the flame axis length and the flame tip temperature are used as a benchmark [1]:

$$T_o = \left(\frac{813 - T_a}{\left[1 - 0.019\, A_w^{\frac{1}{2}}\left(\frac{X}{\dot{m}}\right)\right]}\right) + T_a \quad \textbf{(3.24)}$$

where all temperatures are in degrees Kelvin (K), A_w represents the total area of the openings and all parameters have been previously defined. This is an empirical correlation and the coefficients have units to account for the dimensional disparity between the parameters specified. It is expected that the temperature just at the window, T_o is found to be smaller than the fire temperature, T_f due to the excess of air inside the compartment and the subsequent free-burning conditions expected. In turn, the flame temperature, T_z (K) can be defined at any distance, l (m) from the window pane along its axis, as [1]:

$$T_z = \left(\left[1 - 0.019 A_w^{\frac{1}{2}} \left(\frac{l}{\dot{m}} \right) \right] \left[T_o - T_a \right] \right) + T_a \qquad \textbf{(3.25)}$$

where again all temperatures are in degrees Kelvin (K) and all parameters are defined in this section, above. This flame temperature is also one of the parameters required to conduct the heat balance described in Equations (3.2) and (3.3).

Although the general flame shape differs under *Through or Forced Draught* conditions to that under *No Through Draught* conditions, the presence of an external obstruction above the opening soffit may also have a significant effect. As specified for the *No Through Draught* scenario in Section 3.2.2.1.2, an awning or balcony projecting from the façade just above the window would deflect the flame, provided the obstruction is fire-resistant. The flame trajectory would be altered just as described in Section 3.2.2.1.2, however beyond the obstruction the flame would tilt back to its original angle of projection. Similarly, the dimensions of the flame height and flame projection would change accordingly but the length of the flame axis would remain constant [1]. Furthermore should the obstruction be at a distance above the window soffit, simple trigonometry must be employed to determine whether it would still intersect the flame trajectory and hence deflect it.

3.2.2.2.3. Flame Emissivity (ToFD)

The emissivity of the external flame remains unaffected by the draught conditions. Therefore Equation (3.17) and the definition described in Section 3.2.2.1.3 also apply under *Through or Forced Draught* conditions.

3.2.2.2.4. The Convective Heat Transfer Coefficient (ToFD)

The convective heat transfer coefficient, on the other hand, is affected by the *Through or Forced* draught velocity, *u*. Although its derivation and application is similar to that described in Section 3.2.2.1.4, under *Through or Forced Draught* conditions the convective heat transfer coefficient, α (kW/m^2.K) is defined as [1,26]:

$$\alpha = 0.0098\left(\frac{1}{d}\right)^{0.4}\left(\frac{\dot{m}}{A_w}+\frac{u}{1.6}\right)^{0.6} \quad \textbf{(3.26)}$$

where the rate of burning, $\dot{m}$ (kg/s) is defined above and draught velocity, *u* (m/s) is taken as the draught or wind velocity, which Law and O'Brien recommend be taken as 6 m/s for design purposes [1], but can in fact be specified for any given scenario. While the parameters featuring in Equation (3.26) appear to present dimensional inconsistency, it should be noted that, as before, this is an empirical correlation and the denominator 1.6 has units (m^3kg^{-1}) as does the coefficient 0.0098 ($J.K^{-1}kg^{-0.6}s^{-0.6}m^{-0.2}$). The definition of the characteristic length scale, *d* discussed at length in Section 3.2.2.1.4, should also be referred to for the *Through or Forced Draught* condition.

As is the case for the *No Through Draught* section, this approach applies both to steel elements engulfed in flame, α_z and those not directly engulfed in flame, α_s and the assumptions made throughout the steps outlined above are more thoroughly discussed in Section 3.4 below.

3.2.2.3. The Effect of Wind

The potential effects of 'through' wind have already been considered in the *Through or Forced Draught* section, however 'lateral' wind may also have a potential affect on the flame shape. Since Law and O'Brien [1] assume a draught velocity in the 'through' direction for a case where there are openings on two opposite walls, the effects of a 'lateral' wind are only considered under *No Through Draught* conditions. Since it is difficult to quantify the general effect of 'lateral' wind on an external flame, particularly for design conditions, a maximum sideways deflection of the flame by 45^o is assumed due to the effect of wind [1]. Hence the basic flame shape is taken from the notional flame shape defined in Section 3.2.2.1.2 and then modified by tilting it sideways by 45^o using simple trigonometry as shown in Figure 3.5 below.

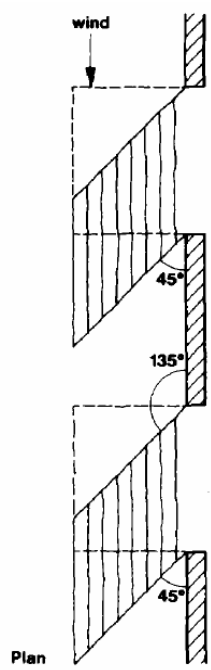

Figure 3.5. Plan view of the external flame geometry tilted sideways by 'lateral' wind. This image has been extracted from Law and O'Brien [1].

In design, it is prudent to allow for a worst-case scenario however the worst-case conditions for structural steel heat exposure may vary depending on the location of the member relative to the compartment openings. Thus the calculation should always be carried out for both *still* conditions and the effects of *wind* such that the worst-case can be identified and designed for [1]. Under windy conditions, the side to which the flame tilts should be taken as that which brings the flame closer to the steel member. The effects of gusting are not accounted for as the heat balance described in Section 3.2 describes steady-state conditions which require "time for equilibrium to be established" [1]. In any case, over a period of time, gusting should average out.

3.2.3 Heat Transfer to the Structure

The heat transfer from the internal fire and external flame to a structural steel element can be determined once the fire and flames have been thoroughly described. Section 3.2.2 provides all the parameters required for the heat balance Equations (3.2) and (3.3) for steel members both engulfed and not engulfed by flame, respectively, with the exception of the configuration factor, ϕ and the resultant steel temperature, T_s. Therefore, once the configuration factor is defined, the heat balance equations can be rearranged to determine the resultant steel temperature.

3.2.3.1. The Configuration Factor

The configuration factor is a 'view' factor that quantifies the portion of radiant energy leaving an emitting surface that arrives at a receiver point at a certain distance and orientation away. Therefore the configuration factor can vary from zero to unity, with potential for having a significant effect on the radiation components of the heat transfer equation.

In the Law Model simplified notional flame shapes are used and only rectangular openings are allowed such that all radiating surfaces are rectangular in shape. The window shape is taken as the surface emitter for the internal fire while the flame faces 'seen' by the different faces of the steel member are taken as the surface emitters for the external flames [1]. A point, P is chosen on the steel element surface as the receiver so the heat transfer calculation can be made to that point. If the point is on a surface that is parallel to the emitting surface, the configuration factor is described as [1,90,91]:

$$\phi = \frac{1}{2\pi}\left(\left[\frac{a}{\left(1+a^2\right)^{\frac{1}{2}}}\tan^{-1}\left(\frac{b}{\left(1+a^2\right)^{\frac{1}{2}}}\right)\right] + \left[\frac{b}{\left(1+b^2\right)^{\frac{1}{2}}}\tan^{-1}\left(\frac{a}{\left(1+b^2\right)^{\frac{1}{2}}}\right)\right]\right) \quad \textbf{(3.27)}$$

where $a = h'/S'$ and $b = w'/S'$, where h' (m) is the effective height of the radiating surface, w' (m) the effective width of the radiating surface and S' (m) the distance between the point and its perpendicular projection on the emitting surface, P' as shown in Figure 3.6 (a). The effective height and width measurements define the radiating surface and one of its corners must lie on the effective projection of the steel point, P'. Should the radiating surface location not match this directly, the surface can be divided into component rectangular radiant surfaces, all of which have a corner centred on point P', as shown in the lower half of Figure 3.6 (a). Individual configuration factors are then calculated for each component panel and they are simply added together to determine the overall configuration factor for that specific arrangement. Should the projected point P' fall entirely outwith the radiating surface, a similar composition of component panels centred on P' can be made and the individual component configuration factors can be added or subtracted as necessary to represent the overall configuration factor for that arrangement [1,91].

Similarly, should the emitting surface and the surface the point receiver is on be at an angle θ (rad) to each other, the following equation is used to describe the configuration factor [1,90,91]:

$$\phi = \frac{1}{2\pi}\left(\tan^{-1}(a) + \left[\frac{(b\cos\theta)-1}{(1+b^2-2b\cos\theta)^{\frac{1}{2}}} \right] \tan^{-1}\left(\frac{a}{\left[1+b^2-2b\cos\theta\right]^{\frac{1}{2}}} \right) \right.$$

$$\left. + \frac{a\cos\theta}{(a^2+\sin^2\theta)^{\frac{1}{2}}} \left[\tan^{-1}\left(\frac{b-\cos\theta}{\left[a^2+\sin^2\theta\right]^{\frac{1}{2}}} \right) + \tan^{-1}\left(\frac{\cos\theta}{\left[a^2+\sin^2\theta\right]^{\frac{1}{2}}} \right) \right] \right) \quad \textbf{(3.28)}$$

where again $a = h'/S'$ and $b = w'/S'$, where h' (m), w' (m) and S' (m) are shown in Figure 3.6 (b) and (c). The angle, θ (rad) is taken as the angle between the planes where the emitter and receiver lie. Again, an effective point, P' is taken at a distance, S' along the plane on which the receiver point P lies, at the point where the two planes intersect. If the radiating panel does not have a corner that lies directly on point P', component rectangular surfaces are again used to determine the component configuration factors, that are then a added or subtracted as appropriate, to find the overall configuration factor. The key dimensions are labelled in examples illustrated in Figure 3.6, where the case of a receiver perpendicular to the emitter (b) is a specific example of the general case (c), in which the angle between the two planes is $\pi/4$ rad (90^o).

The location of the point on the steel member is usually taken where the heat exposure it expected to be at its greatest. Experiments have shown that this is often the point on the steel member nearest the opening soffit and this is the point recommended by Law and O'Brien [1] for most scenarios described. However this may vary and the user may decide to conduct the heat balance at a few different points in order to identify the worst-case scenario. In most cases, Law then recommends the configuration factor be calculated for central points on each face of a steel element at a certain cross-sectional level and a combined use of these configuration factors weighted over the length of each face is employed to obtain an average temperature for the section [1].

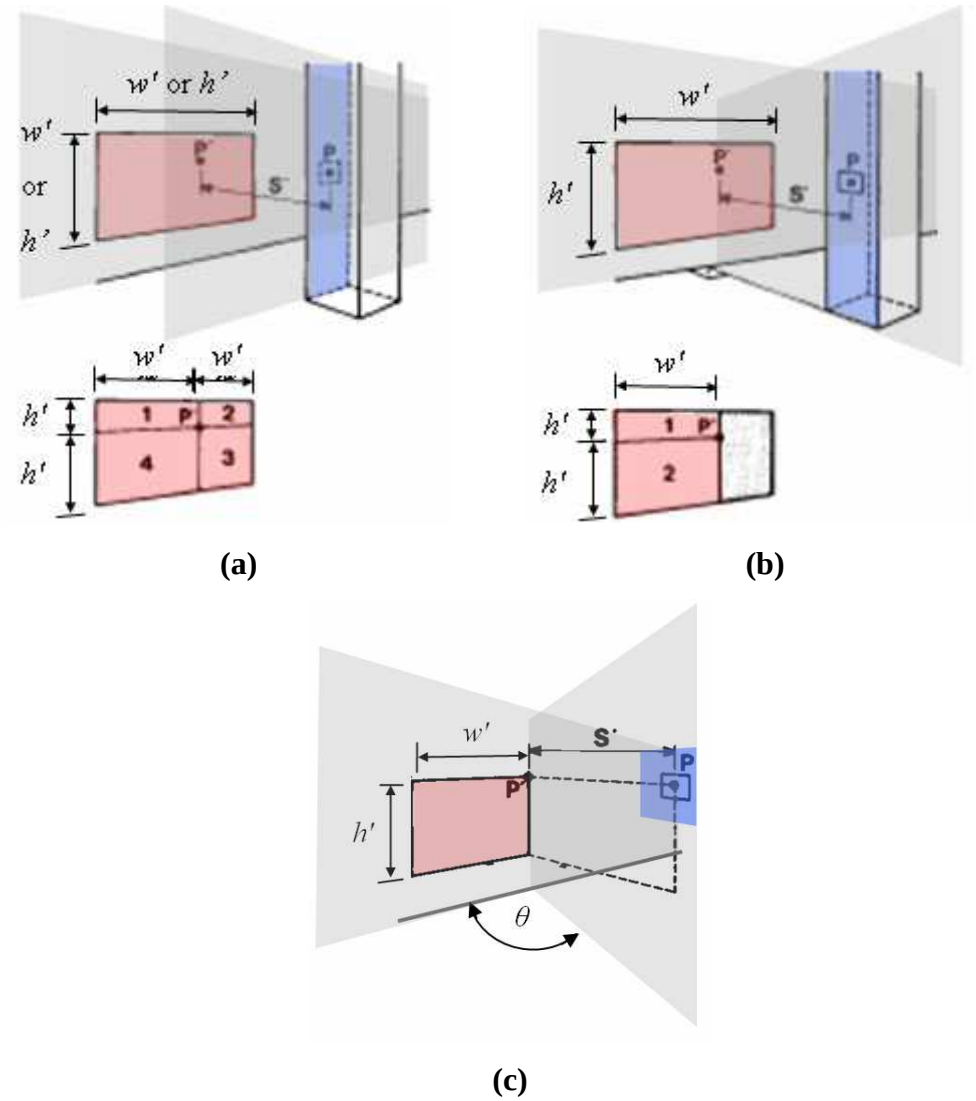

(a) **(b)**

(c)

Figure 3.6. Example configurations of radiative emitter surface (pink) and receiver point *P* on steel surface, with key dimensions labelled accordingly, where: (a) emitter and receiver surfaces are parallel; (b) emitter and receiver surfaces are perpendicular, a subset of the general case; (c) emitter and receiver are at an angle, θ which is the general case. These images have mostly been extracted from Law and O'Brien [1] with some slight alterations.

3.2.3.2. Steel Temperature

The heat balance equations for steel elements engulfed (*cf.* Equation (3.2)) and not engulfed (*cf.* Equation (3.3)) in flame can be rearranged such that the unknown steel temperature terms are shown to equate to a combination of terms with parameters that are defined in Sections 3.2.2 and 3.2.3.1 above. Equations (3.29) and (3.30) show the total heat flux incident on the steel - from radiation from the fire and external flame and convective heat transfer from either the flame, if element is engulfed, or from the

surroundings if it is not engulfed in flame – equating to the total heat loss from the steel by both radiation and convection as steady-state conditions are assumed. If the steel is engulfed in flame, the heat balance can be rearranged to show:

$$\varepsilon_z \sigma T_z^4 + (1-\varepsilon_z)\phi_f \sigma T_f^4 + \alpha T_z = \sigma T_s^4 + \alpha T_s \qquad \textbf{(3.29)}$$

and if the steel element is not engulfed in flame:

$$\varepsilon_z \phi_z \sigma T_z^4 + \phi_f \sigma T_f^4 + \alpha T_a = \sigma T_s^4 + \alpha T_s \qquad \textbf{(3.30)}$$

where in both cases ϕ_f is the configuration factor for the fire with respect to a point on the steel surface and in the case of steel not engulfed in flame ϕ_z is the configuration factor for the flame with respect to that point. All parameters are known except for the resultant steel temperature at steady-state, T_s (K), which can be solved for using an iterative process. Although for most cases Law and O'Brien state the model is "insufficiently sensitive" to render separate calculations for the temperature on each face of a steel member, the case of a deep spandrel beam provides an exception [1]. Since its orientation is usually horizontal, the temperature variation between the beam's upper and lower flanges can be significant. This temperature difference may be considerable as the height of the beam web may equate to a significant temperature change along the flame axis and the upper flange of the beam will also not receive a radiation component from the compartment fire as its fire 'view' factor would be zero.

In the Law Model the steel temperature reached at steady-state is the parameter used to evaluate whether a structural element will fail to perform under fire conditions. Law takes the average steel temperature of 550 ^{o}C (hence ~823 K in the model) as the average failure criteria [92-94] in tests standard resistance tests carried out according to BS476: Part 8 [95], however a different value can be taken if it is justified, for example by the use of different grades of steel [1,26]. Should the resultant steel temperature be higher than that specified in the failure criteria, the scenario has to be adjusted by either shielding the steel member, by moving it or by rearranging the dimensions and location of the compartment openings. Any new arrangement should be rechecked using the Law Model before any external structural steel is left bare [1].

The suitability of defining a single temperature as the failure criteria for a structural steel element – under stress from loading and temperature gradients and with the potential for different types of support conditions and end restraints at the structural connections – can be questioned [21,65] however this is outwith the scope of the present research.

3.2.3.3. Total Incident Heat Flux

Although the Law Model has been developed to calculate the temperature of external structural steel elements resultant from insult from a compartment fire and consequent external flaming, the theory expressed in Section 3.2 has wider applications. The total incident heat flux described by the left-hand-side of Equations (3.29) and (3.30) can be applied to other external elements. While it is unclear whether the Law Model was devised to allow for structural members partially embedded in the façade or even encased in the façade flush with its surface, the model at no point specifically states that it is inappropriate for such calculations. Although example cases are given for spandrel beams and external columns, the members shown are external to the building façade, at most with one single face flush with the façade, but generally at a distance from it. Nevertheless there is no reason to assume the model could not be similarly applied to a member that is encased in the façade with only one of its faces exposed, externally flush with the façade. Such a case would enable calculation of heat flux to a point on the façade, which could in turn be applied to a 'receiver' material, be it the external cladding or the glass from the window in the compartment above. Further discussion of the application of the model to elements on the plane of the façade can be found in Chapter 5 where the model is analysed in detail.

3.3 The Experiments used to validate the Law Model

The overall model methodology described in Section 3.2 has been justified by its authors through comparison of calculated model results and a variety of test programs carried out in the years prior to its development [26]. Since many of the correlations in the model were derived empirically from model-scale experiments, as described in Chapter 2, it is vital to appreciate the characteristics of the large-scale tests against which the model was then validated by Law [26].

Moreover many of the correlations used in the Law model derive from tests devised to investigate *fundamental* correlations between the several parameters identified. It appears many of these correlations, although empirical in nature, were not particularly developed with the concept of their application for *design* in mind. Hence, most correlations derive from a line of 'best-fit' through data points rather than taking a 'conservative' fit that ensures *all* data are accounted for by an over-estimate. This, unavoidably, has the potential to carry through some 'un-conservative' trends in to the Law Model which is mostly geared toward conservative design. It is therefore of particular interest to analyse the discrepancy between the large-scale data obtained from the tests listed in Table 3.1 and the Law Model correlations.

3.3.1 The large-scale experiments used for model validation

The Law Model is intended for use in 'full-scale' compartment design therefore in analysing the model it is important to consider the scale and characteristics of the large-scale experiments used for model validation. Table 3.1 contains a summary of the main characteristics of the large-scale experiments Law [26] used to conduct circa 50 experiments, the data of which was then compared against the correlations developed for the Law Model.

The large-scale experiments summarised in Table 3.1 cover a significant range of compartment sizes, comparable to those for which the Law Model may currently be employed in design. The largest experimental compartment against which the Law Model was validated is 12.6 m by 6.6 m by 2.7 m high and the average compartment size used is 6 m by 6 m (and 2.6 m high), with the largest number of compartments measuring about 3.6 m by ~4 m (and ~2.5m high). While these are all fairly standard compartment sizes, they do not cover large open-space type compartments that often feature in modern building design.

On the other hand, the opening sizes used in these compartments mean the range of reciprocal opening factors investigated was only between 5.4 $m^{-1/2}$ (3 $ft^{-1/2}$) and 40.8 $m^{-1/2}$ (22.5 $ft^{-1/2}$). Furthermore, 23 out of the 50 tests fall in the 5.4-14 $m^{-1/2}$ range, 21 tests in the 14-18 $m^{-1/2}$ range and only 6 out of 50 tests fall in the larger 18-40.8 $m^{-1/2}$ range (*cf.* Figure 3.7). Hence, the adequacy of the Law Model correlations for

compartments with reciprocal opening factors over 18 $m^{-1/2}$ has not been thoroughly explored and for compartments with reciprocal opening factors over 40.8 $m^{-1/2}$ it is not known at all. Nevertheless Law assumes the correlations generally apply, justifying the value of the model by stating that if "a design approach is adopted, it not only obviates the need for these *ad hoc* tests, but also extends to sizes of fire well beyond the limits of size of practical fire tests" [26].

Test	**Depth** (m)	**Width** (m)	**Height** (m)	**Type of Fire Load**
Yokoi 1 [52]	9.7	13.4	3.5	Timber
Yokoi 2 [52]	3.5	4.3	2.5	Timber
Yokoi 3 [52]	2.5	5.0	1.7	Timber
Yokoi 4 [52]	2.5	5.0	1.7	Timber, plywood linings on walls and ceiling
Trenton [96]	7.3	17.1	2.7	Wood cribs of sticks 38mm thick
Disney World [60]	8.5	4.3	2.6	Wood cribs of sticks 88.9mm thick @ 24.5 mm spacing
Borehamwood [58,61]	3.7	7.6	3.0	Wood cribs of sticks 45mm thick @ 45 mm spacing; Fire insulating board on walls and ceiling Test S
Tranas I [63]	12.6	6.6	2.6	Mixed Furniture
Tranas II [63]	12.6	6.6	2.7	Mixed Furniture
Carteret [59]	3.7	3.0	2.4	Wood cribs
Kordina [64]	5.1	3.6	2.7	Office Furniture
Webster *et al*. [55]	2.4	2.4	2.4	Wood cribs of sticks 24.5mm thick
Underwriters [62]	3.7	3.0	3.0	Wood cribs of sticks 38.1mm thick
Metz [89,97]	3.7	3.4	3.0	Wood cribs of sticks 70mm by 45mm thick @ 45mm spacing

Table 3.1. Information detailing the main compartment dimensions and types of fuel used to conduct several large-scale fire tests which were then used to validate most of the Law Model correlations [26].

One thing that stands out from the collection of large-scale tests listed in Table 3.1 is that most involved only wood cribs as fuel. Although some data are available for experiments using office furniture as fire load, Law states that "strictly speaking, the

information derived is only applicable to fires involving mainly wood fuel" [26]. Hence, the Law Model is only *assumed* to "give reasonable correlation with domestic, office, and similar types of fire load" [26]. The tests covered a significant range of fire load densities (*cf.* Figure 3.7) with the Borehamwood tests alone comprising load densities, L'' of 7.5 kg/m^2, 15 kg/m^2, 30 kg/m^2 and 60 kg/m^2 [58], which covers the range expected in regular building occupancies. The fuel distribution however was mostly homogenous throughout the compartments. Although in some cases the fire load was varied from one single large crib to several smaller, equally spaced cribs, the fuel distribution was always fairly even throughout the compartment floor.

In terms of ambient conditions, most tests were conducted under *No Through Draught* conditions. Only the Underwriters' Laboratories [57,62] test were conducted under *Forced Draught* conditions and some of Webster's tests [55] under *Through Draught* conditions, although it is unclear which tests, if any, where conducted under *Through Draught* conditions generated by the presence of openings on opposite walls. The relative positioning of the openings with respect to distance from the ceiling was also not specifically investigated. Although it is not deemed to be of great importance, none of the tests were conducted under particularly high ambient temperatures, such as those expected in warmer climes.

3.3.2 Validation of the Internal Compartment Fire Correlations

The model correlations for rate of burning, $\dot{m}$ and internal fire temperature, T_f under *No Through Draught* conditions were derived from a large sample of model-scale experiments coordinated by the Conseil International du Bâtiment (CIB) [47], as discussed in Chapter 2. The reciprocal opening factor, η (*cf.* Equation (3.4)) was identified as a parameter found to influence both these properties of the internal compartment fire. In defining the correlation for the measured burning rate, $\dot{m}$ against the reciprocal opening factor, η a best-fit line was plotted through the data collected from the model-scale tests, resulting in a data scatter of circa $\pm 15\%$ [26]. A few samples of large-scale tests data plotted on the same graph are in good agreement with the correlation and appear to fall within the same error bound at that of the model-scale data such that the discrepancy is still circa $\pm 15\%$ [26].

The plot obtained from fire temperature, T_f against the reciprocal opening factor, η for CIB test data [47], shown in Figure 7.3, is more well-known and the trendline is sometimes referred to as the "Thomas curve" [26]. It is often used to define the reciprocal opening factor range which equates to a maximum compartment fire temperature for a given scenario under *No Through Draught* conditions and also to define the limit of a fuel-controlled fire *vs.* a ventilation-controlled regime [21].

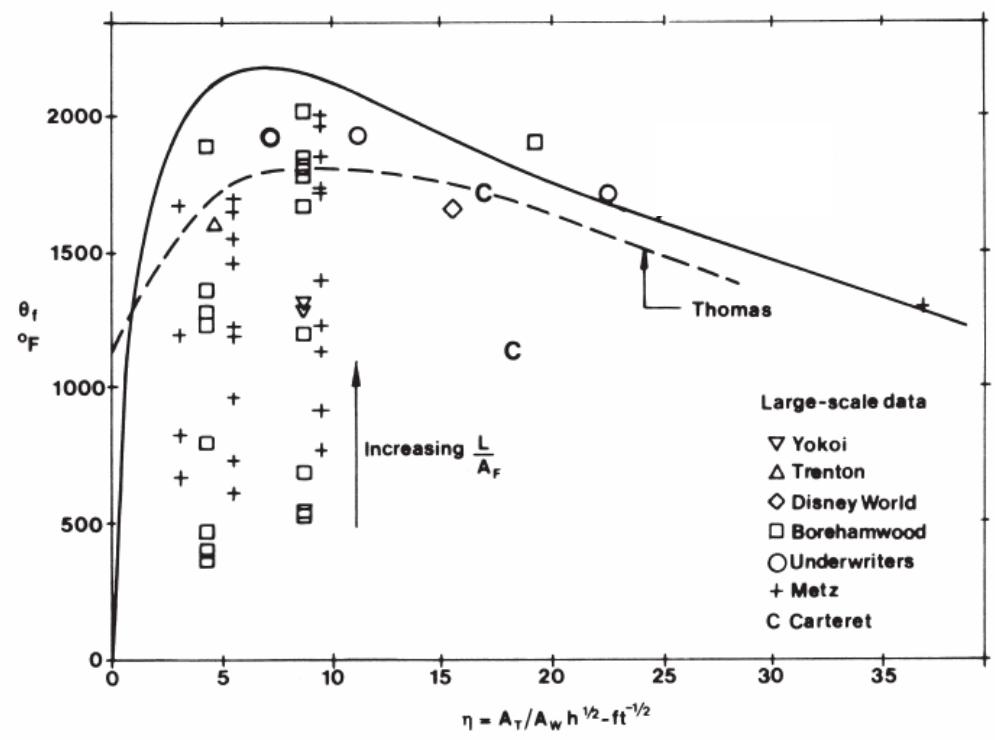

Figure 3.7. The 'Thomas curve' developed as a best-fit through the model-scale CIB test data is plotted as a dashed line, showing average compartment temperature rise against compartment reciprocal opening factor for *No Through Draught* conditions. Data from several large-scale tests are plotted for comparison and an adjusted curve (solid line) seen to envelope most of the data is proposed by Law [26]. This image has been extracted from Law [26]. Note the units are Imperial – for a similar version of this graph showing the model-scale CIB test data but in S.I. units, refer to Drysdale [21].

Figure 3.7 illustrates the large-scale data obtained from several of the tests listed in Table 3.1, where the average rise in compartment fire temperature, θ_f (*i.e.* $T_f - T_a$) is plotted against the reciprocal opening factor values for each scenario. The data shows a considerably large scatter compared to the equivalent Thomas curve, which is a trendline of best-fit through the CIB test data (dashed line). Law instead provides a modified trendline, as shown in Figure 3.7 (solid line), which assumes there is an

"upper limit" to the compartment fire temperature rise [26] and conservatively accounts for most of the large-scale data shown. Nevertheless the average temperature rise is found to be a function of the fire load density, L'' so the correlation is further modified by Law [26] to include the compartment scenario parameter, ψ (*cf.* Equation (3.5)). The compartment fire temperature T_f is thus defined in the form of Equation (3.8) above, reducing the error between the correlation and the measured data to +10%, -30%. Similar correlations were made with data from the large-scale tests conducted at Underwriters' Laboratories [62] under *Through or Forced Draught* conditions and the error between the data and correlations is again found to fall around $\pm 20\%$ [26].

Thus, the correlations used by Law to describe the parameters that define the internal compartment fire conditions have in several cases derived from best-fit lines through test data. While the discrepancy between the correlation and the test data that falls beneath is only important in terms of the cost that could be saved by reducing this over-estimate if the model were employed for the design of such a scenario, it is the test cases for which the data falls above the correlations that are of concern for life-safety. While the data from experiments conducted surely has a degree of error associated with the measurements taken, the trendlines used by Law could potentially not always be conservative for every design scenario. This decision to often take best-fit lines instead of conservative trendlines that envelope *all* the experimental data is of particularly importance as the correlations are empirically-based and further parameters that may affect the internal compartment fire conditions might not be accounted for in the Law Model.

3.3.3 Validation of the External Flame Correlations

As described in Chapter 2, Yokoi pioneered the research into the properties of the external plume. The correlations Yokoi developed, from a series of model-scale tests, for temperature and velocity distribution in the external plume showed reasonable agreement with data collected from four further large-scale, wood-fuelled tests Yokoi conducted [52].

Thereafter, Thomas and Law developed correlations for the dimensions and projection of external flames under the *No Through Draught* scenario, mainly based on experiments carried out by Yokoi [52], Seigel [57] and Webster *et al*. [53-55] (*cf.* Chapter 2). While the scatter of these data has been described as "large" [21], Thomas is said to have obtained "reasonable agreement" between the data collected by Yokoi and Webster *et al*. when correlated using dimensional analysis [26]. External flame height data obtained from some of the large-scale tests listed in Table 3.1 were plotted against the correlations obtained from the model-scale tests. The scatter of the large-scale test data was significant, which can perhaps be explained by the fact that "most large-scale experiments specifically designed to study flame projection" have been described by Law as "*ad hoc*" [26]. The large-scale test flame height scatter ranged between + 10% to - 90% from the model-scale-based correlation [26], thus Law deems the correlation to generally overestimate the flame height. The correlation was adjusted to provide a 'best-fit' through the large-scale data, rendering a scatter of circa $\pm 50\%$ [26]. It should be noted, however, that many of the flame heights within the lower range were obtained from some of the Underwriters' Laboratories *No Through Draught* tests [62] where the flame height was only visually estimated. Therefore, while this correlation is used to define the flame height used in the Law Model (*cf.* Equation (3.9)), its derivation does not appear to have followed a very 'conservative' approach. Similarly, other correlations for the characteristics of the external flame, plotted against large-scale experimental data by Law [26], are seen to have a comparable range of error.

For *Through or Forced Draught* conditions, the external flame correlations were derived by Seigel from large-scale tests carried out at Underwriters' Laboratories [62], under the assumption that a forced draught would increase the rate of burning of an other-wise ventilation controlled fire to 'free-burning' conditions [57]. Law however found that "the effect on 'free-burning' fires was insignificant for the range of forced ventilation used", which had a mean of circa 1 m/s [26]. Nevertheless the forced draught was observed to have an effect on the emerging external flames and therefore "for a given rate of burning, a wind may also affect the flame size and direction" [26]. On conducting dimensional analysis of the large-scale test flame height data, similar to the analysis conducted on the data pertaining to tests under *No*

Through Draught conditions, Law used data regression to introduce a Froude number (*i.e.* u^2/gh) into Seigel's correlation. The correlation used by Law, described in Equation (3.21), results in a $\pm 35\%$ scatter of the measured data [26], although it should be noted that during these tests, the external flame height was only visually recorded. Similar data regression leading to the flame projection correlation suggested by Law (*cf.* Equation (3.22)) results in a + 50%, -40% scatter of the data [26].

Law [98] independently compares the Law Model against large-scale test data from fire experiments conducted at Lehrte by Kordina in 1978 [64]. The fuel types used in these tests vary from wood cribs to domestic and office furniture, thus potentially not solely wood-based fuel. The results show a reasonably good agreement with the correlation developed for the external flame temperature distribution however data for flame height was again found to have "considerable scatter" and the external steel column temperatures measured had a few under-predictions and interestingly, a couple of very high over-predictions [98]. This discrepancy indicates that there are potentially other parameters of influence on the external fire conditions that have perhaps not been taken into account in the Law Model, such as the fuel type and fire load distribution which was not completely uniform due to the use of furniture as fire loading.

In terms of the measurements taken for radiation (from fire and flame) to a point on an external column, the Law Model calculations seem to compare fairly well, with graphs plotted by Law [26] showing the calculation to err slightly on the conservative side. Conversely, comparison of Law Model calculations with external steel temperatures measured in a number of the large-scale tests often features an under-prediction of the temperature by the model [26]. This discrepancy is however dismissed as "of little interest" as it occurs mostly at measured steel temperatures over 550^oC (1020^oF), which equates to the temperature taken by Law as the failure criterion for design [26]. Yet *crucially* what fails to be addressed is that in consequence of this under-prediction, it is at these very *measured* temperatures that the Law Model would predict a value deemed to be "appropriate" for the design of bare steel, which in the case of such a fire would result in the failure of the steel member, according to the failure criteria defined.

3.4 Law Model Assumptions and Limitations

In the Law Model [1], several assumptions are clearly summarised at the start so the user can gauge if the model is applicable to their design scenario. These assumptions are discussed below, together with other more subtle assumptions that are inferred both in the design manual and in the supporting papers that describe the derivation of the model in more detail. These assumptions have allowed Law to develop a simplified tool however some of them limit the applicability of the model.

3.4.1 General assumptions

The Law Model was intended as a general method for design hence the assumptions "must always be made to err on the side of safety" [1]. Law and O'Brien state "it is likely that with some combinations of conservative assumptions, unrealistic fire conditions may be found, with excessively large emerging flames, for example" and that it may be reasonable in some cases to vary these assumptions, provided this is done with caution as correlations are very closely inter-linked [1].

In the design manual, some values are suggested for parameters that may otherwise be known for specific scenarios or for which better estimates may be available. Examples include the fire duration, τ where a value of 20 min is suggested for design, the ambient temperature, T_a with 20 ^{o}C built into simplifications of several correlations (such simplifications were excluded from the model description in Section 3.2) and wind velocity, u for which a value of 6 m/s is suggested [1]. Although the values of these parameters are assumed for design, the input can be varied from that suggested, should a better estimate be available. Direct input assumptions such as these can easily be made to 'err on the conservative side', however as discussed in Section 3.3 above, it is questionable whether some of the empirical correlations themselves are in fact 'conservative'.

The general approach to the model is that the heat transfer occurs under steady-state conditions. This affects the assumptions made for definitions of the internal fire, the external flame properties and the structural heat transfer. Although Equation (3.1) contains a transient term for the heating of the steel and Law states that under

"transient conditions […] T_s can then be calculated by iterative methods", other parts of the model affected by the steady-state assumption remain. It is the assumption of steady-state that allows for a clear definition of whether the scenario falls under *No Through Draught* or *Through or Forced Draught* conditions and whether particular elements are engulfed in flame or not, whereas in reality the scenario may vary throughout the course of the fire.

The distinction between two main scenarios dependent on draught conditions may render it difficult to classify a scenario, in some cases. For the case of a compartment with openings on opposite walls – normally classified as a *Through Draught* scenario in the Law Model – if there is little or no wind, the scenario could potentially be closer to *No Through Draught* conditions. Similarly, for the case of a compartment with openings on two adjacent walls, a strong wind, potentially at 45^o to these openings, could render the scenario closer to that described for *Through or Forced Draught* conditions. In fact, Law and O'Brien clearly state that "fire behaviour is influenced by the amount of air that can be reached and take part in the fire" [1]. Hence it is rather unclear why the distinction is made between windows on opposite walls and adjacent walls for the potential presence of a *Through Draught*, other than that wind in the 'through' direction of windows on opposite sets of walls is likely to cause a worst-case scenario flame projection. The *No Through Draught* scenario also emulates somewhat artificial conditions as the buoyancy effects of a fire would also induce air flow and hence create a natural 'through' draught. Nevertheless the values of a buoyancy induced natural draught are likely to be considerably lower than those present under wind conditions. Furthermore, the intricacies of the definition and distinction between detailed scenarios are not significant for design conditions. Designing for the worst of two extreme case scenarios (plus the possible effects of wind) should result in a conservative design for all cases that lie somewhere in between these two bounds. Although this might not always be the case, it is the best possible assumption without over-complicating the simplified method considerably.

For *No Through Draught* conditions it is assumed the scenario can burn under either of two regimes used to define the burning rate. The burning rate, $\dot{m}$ is specified as the lower of the *fuel-controlled* regime burning rate, $\dot{m}_{Fuel}$ – characteristic of a free-

burning fire – and the *ventilation-controlled* regime burning rate, $\dot{m}_{Vent}$ as described in Section 3.2.2.1.1. Although these two distinct burning regimes are known to be characteristic of the internal compartment fire only the latter regime tends to be associated with external flaming. In *fuel-controlled* fires the air supply to the compartment is sufficient to allow for free-burning of the fuel hence even if compartment openings are breached, the importance of the exchange of gaseous fluid at the openings tends to be much lower than that witnessed under the *ventilation-controlled* regime. The hot gases and potential flames that may emerge from a *fuel-controlled* fire are not likely to be realistically described using the same correlations as those for *ventilation-controlled* external flames, nevertheless implementing $\dot{m}_{Fuel}$ in these correlations is likely to provide a rather conservative steel temperature for design compared to the actual external heat insult resulting from a free-burning fire. Under the *ventilation-controlled* regime the partially-combusted fuel that typically emerges from the openings results in increased external combustion and hence more elevated flame temperatures which would make both the radiative and convective heat transfer from the flame to the surrounding more significant than that under the *fuel-controlled* regime. In theory this discrepancy could potentially be more accurately accounted for using an excess fuel factor. Nevertheless it appears that Law describes a *fuel-controlled* regime of burning, $\dot{m}_{Fuel}$ not specifically to describe the threat posed to external structures from a free-burning compartment fire, but more so to provide an upper limit to the rate of burning. This is necessary as $\dot{m}_{Vent}$ is empirically defined and could other-wise describe a burning rate higher than that described by 'free-burning' conditions, which is not realistic.

3.4.2 Assumptions concerning the Scenario

The main implicit limitations of the Law Model are that it is only applicable to simple right-angle cuboid-shaped compartments and any openings must be rectangular and only on the vertical walls [1,21,26,50]. The model is also only applicable for fire safety design of external structural steel under insult from a single internal compartment fire. Insult from any potential fires external to the building, or heat flux to the structure resulting from ignition of external building materials (*i.e.* cladding) is not considered. Similarly, the model does not account for the insult from flames emerging from fires on multiple floors.

While the specification of the main compartment geometry is straight-forward, several assumptions have been made with regard to the openings. Throughout the Law Model, openings are regularly referred to only as "windows" [1], so it is not evident whether a door would classify as an opening for the purposes of the model. The importance of openings and the related ventilation opening parameter, $A_w h^{\frac{1}{2}}$ was first identified by Fujita with reference to "usually the window" [26,44], however no distinct definition of 'window' is given and the shapes and sizes of windows can vary significantly. In the extensive CIB experiments conducted at model-scale [47], from which many of the Law Model correlations derive, the openings extended "from floor to ceiling" and hence perhaps resemble the usual geometries of doors more than those of windows. For the purposes of quantifying the ventilation parameters in this research, openings were defined as potentially both doors and windows, depending on whether the doors lead to small finite volumes (*i.e.* small, closed compartments) or open spaces, with infinite ventilation (*i.e.* a compartment with another opening). If doors lead to small closed compartments, the main compartment geometry can be adjusted to describe this space, thus accounting for the volume of air readily available in the compartment beyond the door, but the door would not be considered as an opening. Should a door lead to a compartment that has an open window or to a compartment that is large relative to the main compartment of concern (*i.e.* an atrium), the door is taken as an opening as it can, in effect, provide an endless supply of air.

In the Law Model the ventilation parameters for scenarios with more than one opening are adjusted as described in Figure 3.1. Although Law states that "in practise, the correlations can be used for a variety of window sizes on one or more walls" [26] and Figure 3.1 (ii), extracted from the Law Model, illustrates such a case, the validity of the adjusted opening dimensions, h_{mo}, w_{mo}, $A_{w,mo}$ (*cf.* Figure 3.1 (ii)) has been disputed. Later work has in fact shown that "this is unlikely to apply to unusual ventilation conditions" [21], such as the case of several small openings positioned at varying heights [50]. Nevertheless, since this research comprises a detailed analysis of the model, the modified definitions of h_{mo}, w_{mo} and $A_{w,mo}$ are used throughout, as specified in Figure 3.1 for scenarios with multiple windows.

When there are multiple-sized windows, particularly if they are at different heights from the ceiling and under *No Through Draught* conditions, the area of the opening from which external flames emerge and through which ambient air enters may differ significantly and this is why the window heights are adjusted to a weight-averaged window height. Since the width of the windows are also added, the openings are in effect represented by one single large opening of dimensions h_{mo} by w_{mo}. This allows for the calculation of an emerging flame of average dimensions, which may differ significantly from the local flame dimensions at each window. This is particularly significant if the openings are of different dimensions, as the distinction between the calculations of flame projection for a 'wide' and a 'narrow' opening will not be accounted for. In some such cases there is also potential for the external heat flux to structural members to be under-predicted by employing a general definition of flame height. Nevertheless, even if all openings are at the same level from the floor, it is likely there will be some discrepancy between actual local flame dimensions and those represented by the average flame dimensions. However, this equivalent-opening-dimensions assumption allows for the model to be simplified and any attempt to reproduce the flame dimensions more locally for each opening would be impractical. Not only would it complicate the model, but it would also be likely to make little improvement on the accuracy of the representation as there has been no extensive experimental study to show the effects of multiple-shaped openings at different heights from the ceiling and from the fuel bed. What should however be noted is that the Law Model will thus provide only a crude estimate of local flame dimensions in scenarios with multiple openings, hence error bars involved in the heat transfer calculation can be considerable, compounded by those carried through from the correlations as described in Section 3.3.

Although the case of multiple openings at different heights is an extreme illustration of the level of sensitivity of the model, it is a very realistic scenario commonly encountered in cases with both windows and doors. Yet even for the case of multiple openings with identical geometry and at the same height from the ceiling, such as those depicted in Figure 3.1 (iii) some discrepancy between the calculated flame dimensions and the local dimensions is expected given all the assumptions made. In fact, the level of sensitivity the model is assumed to have to opening dimensions is further illustrated by the assumptions Law makes in undertaking crude

simplifications. This is exemplified in the definition of flame height under *No Through Draught* conditions which is simplified from the correlation defined by Equation (3.10) to that described by Equation (3.11). This simplification assumes that even in a case with multiple openings the modified opening area, $A_{w,mo}$ can be split into the product of h_{mo} and w_{mo}, which for opening of different dimensions is likely to be incongruous. The larger the difference between the shape of the openings, the greater the discrepancy between the product of h_{mo} and w_{mo} and the definition of $A_{w,mo}$ given in Figure 3.1 as the sum of all the *actual* opening areas. The dimension of this discrepancy gives an indication of the level of accuracy involved in the model, which is likely to then be further reduced by other assumptions and simplifications.

Another inconsistency in the model arises in the use of window width, w in the case of multiple-opening scenarios. A modified definition of window, w_{mo} is given (*cf.* Figure 3.1 (ii)), representing the openings as one large equivalent opening, rendering it unclear when the specific window width, w or the modified width, w_{mo} should be used in the equations described. While the model implies w_{mo} should be used, it then provides an illustration of the individual openings with individual flames [1], the local dimensions of which are used to calculate the flame thickness for flame emissivity, particularly when a steel member lies in between windows. Hence alternate uses of the window width definition are used throughout. Furthermore, although different ventilation geometry cases are given in Figure 3.1 are attributed distinct, modified definitions of the main opening parameters, it is unclear what the definition of these parameters would be for combinations of the cases shown, such a compartment with multiple windows of different sizes on more than one wall.

3.4.3 Assumptions concerning the Fire and External Flame

3.4.3.1. Internal fire

The description of the internal fire is greatly simplified. A single uniform burning rate, $\dot{m}$ is assumed throughout the duration of the fire until burnout [1,26]. This assumption allows for the use of steady-state conditions for the heat transfer calculation and derives from experimental observation of a relatively constant period of burning (usually post-flashover) between the 80-30% mass loss of fuel in the

experiments undertaken, as discussed in Chapter 2. This definition may appear conservative as during the initial burning period a fire tends to have a lower burning rate as it grows, external flaming most commonly occurs only post-flashover and the burning rate again tends to be lower during the decay period of a fire, close to burnout. Nevertheless, other components of this definition may not render the assumption as particularly conservative.

The Law Model is based on the assumption that fire load is homogenous throughout the compartment and that it all burns uniformly throughout the duration of a fire. Therefore the fuel is defined in terms of fire load density, L'' as a measure of uniform fire load, L per unit floor area, A_F of the entire compartment. Furthermore, the model correlations are based mostly on tests conducted using wooden cribs uniformly distributed throughout the compartment (*cf.* Chapter 2) and hence "strictly speaking, the information derived is only applicable to fires involving mainly wood fuel" [26]. The model is only *assumed* to apply to other typical furnishings. Since the usual contents of buildings can differ considerably from a uniform distribution of wood-base fuel, the fire load is instead expressed in terms of "total amount of wood-equivalent" that "would evolve the same amount of heat when burnt" [1]. Law and O'Brien admit this is only an approximate representation of the fire load but state that "it has been found by comparative experiments to be acceptable for the types of furnishings and contents normally found in buildings" [1]. Nevertheless, more recent experiments show this might in fact not be the case [79-81] as discussed in Chapter 2.

Conversely Thomas and Law [46] also found that for non-cellulosic fuels, particularly those with a low value of latent heat of evaporation, the Law Model correlations for external flame length and flame projection break down. In addition, hydrocarbon polymers have "a much higher air requirement [than] cellulosic fuels" rendering it almost inevitable that for such materials the "external flaming will be more significant, all other things being equal" [21]. Furthermore, fuel beds with a very large surface area tend to yield a higher rate of burning than that described by Equations (3.6), (3.7) and (3.19), in turn also resulting in longer external flames. Thermoplastics are one such example as they "tend to burn as pools" resulting in larger surface areas, however combustible wall linings can also have the same effect [21]. Hence, as material science has evolved considerably since the model was developed and the

contents and furnishings of buildings have changed significantly, the assumption of a uniformly distributed cellulosic fire load is perhaps no longer deemed to be 'conservative'. In fact, some of the issues related to different types of fuel have been investigated as discussed in Chapter 2 and some of the research findings, such as those by Bullen and Thomas [67], found the external flame size is further linked to an excess fuel factor, f_{ex}.

It is also worthy of note that the potential effects of highly localised concentrations of furniture items have not been considered. While the assumption of a homogenous fire might sound appropriate for design purposes – since it cannot be known where a fire might start and as it appears to be a good representation of post-flashover conditions when most fuel is alight – it is not necessarily representative of a 'worst-case' scenario and hence not necessarily a 'conservative' assumption for design. The heat insult to external structural elements from a fire load that burns in different localised areas may potentially be more severe than homogenous compartment fire conditions, depending on the local concentrations of fuel and relative position of ventilation openings. The fuel distribution likely to be found in modern buildings renders it likely that a fire scenario would result in conditions in the compartment that fall somewhere between homogenous burning and localised areas of intense burning throughout the fire. Hence it would perhaps be more 'conservative' to consider both the effect of fire load concentration in smaller areas and that of the uniform distribution over the entire floor area. Nevertheless, this would require extensive experimental investigation and could potentially render the model significantly more convoluted. Therefore, due to such unknown factors, it would be advisable to set limits of known-applicability of the Law Model which at present suggests that its application "extends to sizes of fire well beyond the limits of size of practical fire tests" [26].

For the analysis of the Law Model herein the definition of fire load density has been maintained, however the value of 25 kg/m^2 of wood equivalent suggested for design can be varied, provided it is justified by the scenario. In fact, the contents of common dwellings and regular office buildings has changed significantly over the last three decades, particularly with the digital computer era taking over paper and magazine records, replacing mainly cellulosic-based fuels with more plastic-based materials. There is now also a higher incidence of synthetic materials in furnishings and

upholstery, hence the recommendation of 25 kg/m^2 for design is again, no longer likely to be a 'conservative' assumption. Nevertheless, this can easily be adjusted as it is an input parameter in the Law Model.

Apart from the burning rate, the internal compartment fire is also defined by a fire temperature, T_f which significantly contributes to the external heat flux as it forms a key part of the fire radiation component ($\propto T_f^4$). In keeping with the steady-state assumption and that of a uniform rate of burning, a single fire temperature is used to represent the fire. This temperature is defined as the maximum compartment temperature as it is expected to affect the maximum external steel temperature attained. Although realistically the compartment fire undergoes a temperature evolution, varying both in time and in space, this assumption is justified as "the fire […] could easily reach the maximum temperature and maximum radiant energy at the window" where it would have most relevant effect on external members "even if other parts of the compartment are less hot" [1]. This assumption is regarded as a 'conservative' one for design, provided the temperature defined is not exceeded for a given period of time during an actual fire.

The temperature of the ambient surroundings, T_a is defined by Law and O'Brien [1] as 20 ^{o}C, to be used for design. Contrary to several other initial parameters, the value of 20 ^{o}C is actually built into the simplified form of some correlation rather than being left as an input variable at the discrepancy of the user. Although its use within the correlations in the Law Model is indicated, theoretically allowing for a different ambient temperature to be defined, in the Eurocodes only the simplified version of equations with an embedded ambient temperature of 20 ^{o}C feature, even though T_a appears as a variable elsewhere in these expressions [2]. Nevertheless Law and O'Brien specifically state that another choice of ambient temperature "will have a negligible effect within the normal ranges" [1].

3.4.3.2. External Flame Shape, Temperature distribution and Wind effects

The external flame shape is assumed to have distinct boundaries allowing for flame dimensions to be defined for a reasonably simplified geometry. These notional flame

shapes are in keeping with the steady-state assumption and enable calculation of other parameters using simple trigonometry. The flame temperature distribution is assumed to be constant across the width and through the depth of the flame, with temperature variation mainly in height, along the flame's central axis [1,26]. Although there is some temperature variation across the width and through the depth of the flame, the variation is more pronounced with height and assuming a constant temperature through the cross-section of the flame, taken at the flame axis where it is at a maximum, is a conservative assumption [1]. Nevertheless, Law states that this conservative assumption is "slightly offset by the assumption that the flame has distinct boundaries beyond which there is no convective heat transfer" [26] (*i.e.* the notional flame shapes). This approximation is illustrated in Figure 3.8 and again exemplifies the level of approximations taken in simplifying the model.

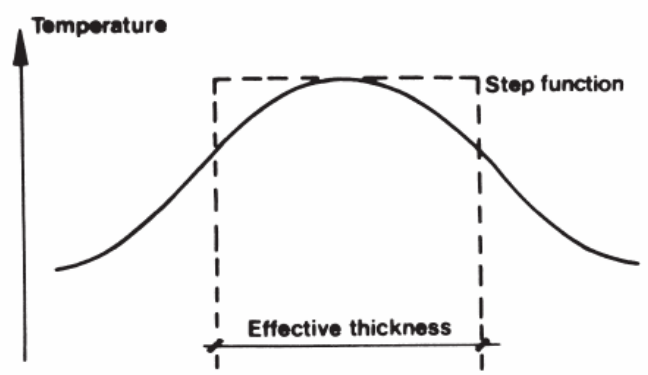

Figure 3.8. Normal distribution of actual flame temperature expected across the flame section with the step-function approximation used to describe the section temperature distribution in the notional flame shape flames used in the Law Model. This image has been extracted from Law [26].

Under *No Through Draught* conditions the flame depth is defined by the depth of hot gases emerging from the compartment at the window plane. Since the flame is assumed to occupy the top two-thirds of the window area (with ambient air assumed to be drawn in through the bottom third), the flame depth is defined as two-thirds of the window height ($2h/3$), unless there are several windows, in which case it is defined as two-thirds of the weight-averaged height ($2h_{mo}/3$) [1]. This assumption has been derived mostly from experimental observation and Law and O'Brien state "such evidence as is available suggests that [this assumption] will be a conservative one" [1]. For the case of *Through or Forced Draught*, the assumption that flames emerge from all of the opening area on half of the compartment, renders the flame depth the

same as the height of the openings, or the weight-averaged height if these vary in size. Again this assumption is an approximation derived from experimental observation.

While the flame width is simply assumed to be that of the opening width, varying only slightly for *Through or Forced Draught* conditions as per Equation (3.23), the flame height boundary is specified by a temperature. Law and O'Brien justify this by stating that a slight widening of the flame under certain conditions is compensated for by the assumption of a constant temperature throughout the specified width [1]. The flame height is taken at the point along the flame axis where the temperature reaches 813 K (~540 ^{o}C), which has been observed to roughly correspond to the temperature at which the flame "loses its luminous character" [1,57]. The buoyancy term associated with the flame is then defined using the gas properties at the flame tip, since all other temperatures along the flame can vary with the scenario. Hence a density of 0.45 kg/m^3 is assumed, corresponding to a 540 ^{o}C temperature [1,26]. The assumption is justified for general purposes given that the gas density within the plume is unlikely to vary significantly. The flame temperature variation along its axis, T_z is then based on a known distribution relative to the initial temperature at the base of the flame, T_o and that at the tip of the flame, T_x also defined from experimental measurements. Since the flame temperature varies along the length of the flame, an effective flame temperature must be estimated for the heat balance equation. The point along the flame axis, l (m) at which the flame temperature is taken can vary depending on the scenario. For columns not engulfed in flame, opposite a window, the point is usually taken opposite the window soffit where the steel is expected to experience its maximum temperature. Yet when a column is engulfed, it is recommended that a few different scenarios be checked at different heights along the column before the worst-case heating conditions are identified [1], as described in Section 3.2.3.1. The choice of location from which the flame temperature is taken is further discussed in Chapter 5, Section 5.4.

When defining the flame projection under the *No Through Draught* scenario, isolated narrow windows are found to have significant flame projection even when there is a wall above the openings. 'Isolation' is defined by Law and O'Brien as the "distance to any other window exceeding [four times the] width of individual window, *w*" [1]. For the purposes of this research "any other window" is interpreted to mean 'the closest

window is more than … away' rather than 'any window more than … away, even if other windows are closer'. This is justified as any plumes in the vicinity of the window would draw in air and the projection is a function of the amount of air that can get behind the plume.

Other assumptions regarding the flame projection involved deflection of the flame trajectory caused by external obstructions such as a balcony or an awning. These assumptions have been defined in Section 3.2.2.1.2 and are regarded as a simplified approximation of deflected flame trajectory, based on model-scale experimental observation by Yokoi [52]. However, in principle, these assumptions have been confirmed in large-scale tests [99-101]. Nevertheless, one main assumption which is not stated in the Law Model is that the model is valid only for cases where a single compartment is on fire and no fire exists in any compartment in the vicinity below. It has been found that if there is a fire on the floor below the flames emerging from the compartment lengthen due to oxygen depletion (by rising combustion products). Furthermore, flames emerging from lower floor fires have been observed to merge with flames emerging from floors above, as was observed in Sao Paulo, Brazil, in both the Andraus Building fire in 1972 [37] and the Joelma fire 1974 [31]. Both these phenomena render the correlations given in the Law Model invalid for calculation of external heat insult to the structure, under such conditions.

The external flame shape can also be affected by 'lateral' or cross-wind. This has been taken into account in the Law Model by calculating two extreme scenarios. The first involves the notional flame shape, undeflected by wind and the second, the notional flame shapes deflected by an angle of 45^{o} from the perpendicular to the façade, in keeping with the steady-state assumption. No mention is made of the deflection of the flame varying with height (defined by a vertical angle), so the whole flame geometry is merely deflected by an angle of 45^{o} in the horizontal plane, such that the flame face on the plane of the façade remains unaffected by wind and the front furthest away from the façade is most displaced. Although the effect of wind is more thoroughly discussed in Section 3.2.2.3, the assumption that two distinct cases can provide a 'conservative' representation of external fire exposure has the potential to under-predict external heat exposure because the worst-case flame location varies for each

distinct location of the structural member. In some cases a flame deflection of 20^o could provide heat exposure to a column that is more severe than that from both the undeflected flame and that of the flame deflected at 45^o. Nevertheless, for the purposes of design, since it can not be known how strong the wind will be in the event of a fire, and by how much it will deflect the flame, assuming a 45^o deflection is the simplest solution for emulating a potential worst-case condition for scenarios in general. Additionally, when considering the effects of wind on external flames, "a rule of thumb that is commonly used is that a 2 m/s wind will bend the flame by $\theta = 45^o$" [21] and this may not differ greatly under the suggested 6 m/s wind to be used for design. It has also been suggested that wind may reduce the length of the flame [46,88], however maintaining the longer flame description in this case is a conservative assumption.

3.4.3.3. Emissivity and Convective Heat Transfer Coefficient

The emissivity of the internal compartment fire is assumed to be "high" and hence is "taken as unity" [1]. While the environment in a post-flashover fire compartment is usually very sooty and hence highly emissive, it is still not a perfect black body radiator, particularly when emitting outside where temperatures are potentially lower. The emissivity will also vary throughout the duration of the fire and throughout the compartment as it is temperature dependent. Nevertheless, the overall average emissivity of the compartment post-flashover will be high and taking the emissivity as unity is a reasonable assumption, erring slightly on the conservative side. Similarly the emissivity of the external steel surface is assumed to be constant throughout the fire. It is assumed to be high, "of the order of 0.9" and hence is once again taken as unity as a conservative approximation [1]. While a clean, polished steel surface will typically have a much lower emissivity, the types of steel utilized in structural steelwork have rougher surfaces and the surface tends to oxidise over time, increasing its emissivity. Also, once the steelwork is heated its surface oxidises and exposure to fire can form a dark sooty surface layer, all adding to an increase in emissivity. Hence, it is reasonable to expect high emissivity of steel under steady-state conditions, particularly when the member is engulfed in flame.

The emissivity of the external flame is assumed to be a function of the flame thickness, which is assumed to be close to constant for any given face of the flame due to the notional flame shapes (*cf.* Figure 3.2 and Figure 3.4) adopted by Law. A single emission coefficient is assumed, regardless of the excess fuel factor [67], of possible variation in flame shape, such as those suggested by Oleszkiewicz [70,71], or whether the emerging flames are luminous or highly sooty. Therefore no distinction is made between *No Through Draught* and *Through or Forced Draught* flames [26]. This assumption, together with the configuration factor representation of the 'face' of the flame the member 'sees', allows for the whole body of the flame to be accounted for in the flame radiation calculation. For cases where the structural member of interest is a column at a distance away from the window, the flame face the member 'sees' is taken as the furthermost face of the flame from the window for the configuration factor calculation whereas the flame thickness is taken as its depth. Should a member be flush with the façade, to the side of a flame, it 'sees' the face of the flame facing the column and its thickness is taken as the flame width (or combination of flame widths if there are several other flames emerging from windows beyond the main window of consideration). For a case with a spandrel beam running above an opening external to the façade, the steel face of interest 'sees' the flame face it is facing and the flame thickness is defined as the dimension of the portion of flame perpendicular to that steel face. Hence, simple trigonometry can be used to calculate the flame thickness for these example cases, and any others, by employing the same definition of flame face and flame thickness.

The convective heat transfer coefficient between a travelling fluid and a solid object is often difficult to determine as it is a function of the boundary layer conditions [88]. These can be mainly expressed as the mass fluid flow velocity, its temperature, the angle of the flow relative to the solid surface and the shape of the solid, particularly in the vicinity of the 'receiver' point [1,26,88]. Hence, in the Law Model the definition of the convective heat transfer coefficient is grossly simplified and generalised to prevent over-complication of the tool. As such, a single convective heat transfer coefficient is calculated for each Law Model scenario. The mass flow of hot gases per unit area of a structural member is assumed to be proportional to the quotient of the rate of burning and the area of openings, $\dot{m}/A_w$ (or $\dot{m}/A_{w,mo}$ for the case of multiple

windows), together with the draught flow velocity, *u* under *Through or Forced Draught* conditions. The shape of the steel member is represented by a characteristic length scale taken as the average of the two main dimensions of the member's cross-section (*cf.* Figure 3.3). The proportionalities and the related constants linking these factors to the convective heat transfer coefficient were found by regression of experimental data. The orientation of the solid relative to the gas flow is assumed to be perpendicular to the member's cross-section throughout the fire as this yields a maximum value for the coefficient, rendering the assumption 'conservative'. Hence the assumptions inherent in the definition of the convective heat transfer blur the nuances of the heat transfer at edges with smaller characteristic length scales, such as around the flange edges of a steel section, as well as those of reduced heat transfer when gas flow is parallel the solid surface. However, this definition provides a reasonable estimate given the level of accuracy employed elsewhere in the model assumptions.

The definition of the convective heat transfer coefficient mainly applies to heat transfer between the hot gases in flames engulfing a structural member, as it is based on the flow rate of the hot gases emerging from the compartment windows. However for the purpose of simplicity, the velocity of ambient air in the vicinity of the openings is deemed to match that of the flow of the hot gases emerging from the compartment. This allows for the convective heat transfer coefficient for members not engulfed in flame to be assumed as equal to those engulfed in flame, as discussed in Sections 3.2.2.1.4 and 3.2.2.2.4. Hence, it is assumed that the flame transfers convective heat to steel members engulfed in flame with the same coefficient, as the steel members transfer convective heat to the ambient surroundings when they are not engulfed in flame. A distinction is nevertheless made in the definition of the coefficient under *No Through Draught* conditions and *Through or Forced Draught* conditions to account for the added velocity of the flow induced by the draught velocity. The case of a steel member only partially engulfed in flame is not addressed however a steel element engulfed in flame will always suffer a larger heat insult than an element surrounded by gases at ambient temperature, where the heat losses from the steel to its surroundings is more prominent.

For the case of a receiver element in plane with the façade, such as a spandrel beam or perimeter column embedded in the façade with only one face exposed, or the façade cladding or upper compartment window pane, the definition of the characteristic length scale for the convective heat transfer coefficient is not evident. The definition of the length scale for such a case is further discussed in Chapter 5, Section 5.4.1.

3.4.4 Assumptions concerning the Structural Heat Transfer

The Law Model is designed to be applied to external structural steelwork. Most steel section shapes can be used as a rectangular approximation is taken, as illustrated in Figure 3.3. The steel member used for the heat transfer calculation in the model is determined by enveloping the perimeter of the actual section with a rectangular-shaped section (*cf.* Figure 3.3). The heat transfer calculation is then made relative to points on the mid-point of each of the four faces of the steel section's cross-section. These values are used to determine an average temperature, so a single resultant temperature is assumed for the steel sections, ignoring any potential temperature gradients. This is enabled by the use of a surface-to-point definition of the configuration factors for radiation (*cf.* Section 3.2.3.1). As the heat flux to a structural element may vary along its length, particularly for vertically aligned members, taking a single point for heat transfer enables a 'worst-case heat flux' to be determined, resulting in a maximum steel temperature. Additionally, as steady-state conditions are assumed, there is no time-based pre-heating of the element. The latter is a reasonable assumption as during the less uniform fire growth period the fire tends to be restricted to within the fire compartment and usually only breaches the openings and emerges from the windows post-flashover, when conditions tend to be more uniform and closer to steady-state.

Nevertheless, the main heat balance equations (*cf.* Equation (3.1) for the 'engulfed' example) include a transient term. For cases involving a fairly massive section, where the cross-sectional area is large relative to the surface area, heat loss by conduction becomes more significant and steady-state conditions may not be reached. Steady-state may also not be achieved if the duration of flaming is short. In such cases the temperature gradient in the vicinity of the heating might warrant use of the transient calculation instead. Under transient conditions, all other fire and flame parameters are

assumed as per steady-state conditions but the steel temperature evolves in time and can be obtained from the main heat balance equations using an iterative process. Although the steady-state assumption is more justified for the case of a steel element engulfed in flame, due to a negligible temperature gradient in the steel section, for simplicity this assumption is also conservatively made for sections not engulfed in flame where the temperature gradient (and hence conduction) might be more pronounced [1]. For the case of heat transfer to an element on the façade plane, heat loss by conduction could potentially be more significant [21] however this depends on the properties of the material the steel section or point of interest is embedded in or attached to and the boundary conditions surrounding that element. Hence an incident heat flux is useful as it can be applied to any receiving surface with the resultant heat losses and solid temperature being separately calculated for individual materials and boundary conditions. In any case, while it is acknowledged that steady-state may not be attained, this assumption allows for the calculation of a maximum resultant temperature for each element (an upper bound) and thus results in a conservative solution [1,26].

The assumptions made allow for a single resultant steel temperature to be calculated and evaluated against the failure temperature criterion. A temperature of 550 ^{o}C, taken as the failure criterion for structural steel elements, is deemed to cause an element to either fail to carry its design load or to undergo excessive deformation due to loss of material strength [1,65]. The value of 550 ^{o}C is taken because under standard fire furnace testing (*i.e.* BS476: Part 8: 1972 [95]) of a single structural element, this is the average temperature at which failure is observed [92-94], however Law and O'Brien state that it is "possible to use any other limiting temperature…if it is judged that the grade of steel being used or the structural configuration involved justifies the use of a different value" [1].

Conversely, it is not evident whether a temperature-based failure criterion is a conservative solution. Recent research has shown differential heating of structural steel elements (only a portion of the section is heated as opposed to the quasi-uniform heating conditions in a test furnace) can induce structural stresses and cause thermal expansion [102,103]. These induced stresses can result in structural deformation and potentially lead to failure of load-bearing structural members (*i.e.* by buckling, *etc.*) at

temperatures lower than those specified by the BS476 furnace test [102,103]. The occurrence of such structural stresses under thermal gradients is also highly dependent on the element's end-restraints and support conditions [103]. Steel members with different end-connections and different ratios of slenderness can behave differently under thermal-induced stress and hence may also have the potential of failing before the specified failure temperature, under certain conditions. Both these particulars are thus highly dependent on the temperature gradients within the steel members, thus the step-function definition of flame temperature distribution (*cf*. Figure 3.8) could potentially disguise further nuances of the temperature induced in the steel. Nevertheless these particulars involve conditions that can not easily be replicated within a furnace test scenario as there are several potential variations and it is difficult to account for all of them. As such, the current Law Model failure criteria is deemed an appropriate approximation, in keeping with the simplifications made for other assumptions, however the designer of such elements should be aware of the potential issues involved in specifying certain types of connection, *etc*.

3.4.5 Numerical Limitations and Realistic Parameter Bounds

Apart from the model limitations imposed by the numerous assumptions, some of the experimentally-derived empirical correlations in the Law Model have numerical limitations. These include both singularities (point of discontinuity) and correlations that can potentially yield unrealistic values for specific parameters. Some of these numerical limitations have previously been discussed by Welch and Lennon [103] in a commentary to a draft version of part of the Eurocode [2] implementation of the Law Model, before it was published.

The definitions given for temperature at the opening plane, T_o in Equations (3.16) and (3.24) and for flame temperature, T_z in Equations (3.15) and (3.25), both under *No Through Draught* and *Through or Forced Draught* conditions, all include components involving a '(1 – *variables*)' term, where the *variables* term is composed of slightly different parameters and coefficients in each case. As such for both the *No Through Draught* and *Through or Forced Draught* scenario these equations can be expressed as:

$$T_o = \left(\frac{T_x - T_a}{1 - \text{variables}} \right) + T_a \qquad \textbf{(3.31)}$$

where the temperature at the flame tip, T_x has been defined as 813 K (~540 ^{o}C), and

$$T_z = \left(\left[1 - \text{variables} \right] \left[T_o - T_a \right] \right) + T_a \qquad \textbf{(3.32)}$$

For the case of the temperature at the plane of the opening, T_o under *No Through Draught* conditions (*cf.* Equation (3.16)) the *variables* term, $V_{ND,To}$ is:

$$V_{ND,To} = 0.027 \left(\frac{X\, w}{\dot{m}} \right) \qquad \textbf{(3.33)}$$

As the (1 - $V_{ND,To}$) term is the denominator of Equation (3.31), when $V_{ND,To} \rightarrow 0$, $T_o \rightarrow T_x$. This makes sense as $V_{ND,To}$ is a function of the length of the flame axis, X so that as the flame tends to be shorter, the flame tip tends to be closer to the window plane, however $V_{ND,To}$ is unlikely to ever realistically reach zero for any scenario of interest. On the other hand, as $V_{ND,To} \rightarrow 1$, $T_o \rightarrow \infty$, yielding non-physical temperatures due to the singularity. When $V_{ND,To} > 1$, T_o becomes negative and such values are unrealistic. Hence, as $V_{ND,To}$ grows the expression becomes an unrealistic representation of T_o and it is prudent to define a maximum value for $V_{ND,To}$. While the *variables* term for T_o under *Through or Forced Draught* conditions (*cf.* Equation (3.24)) is slightly different to that under *No Through Draught conditions*, the same limitations apply and a maximum value for its *variables* term should also be defined in order to limit the output of unrealistic values. Rearranging Equation (3.1) allows for a maximum value of the '*variables*' term to be defined:

$$\text{variables} = 1 - \left(\frac{T_x - T_a}{T_o - T_a} \right) \qquad \textbf{(3.34)}$$

where T_x is the temperature at the flame tip, 813 K (~540 ^{o}C) and a conservative value of 1573 K (~1300 ^{o}C) is assumed as the maximum realistic value of T_o for any given

scenario. Taking an ambient temperature range of $-60\ ^{o}C \le T_a \le 60\ ^{o}C$ as a conservative representation of the range expected for any given scenario, Equation (3.34) yields values of 0.56 and 0.61, respectively. Hence, an upper limit of the *variables* terms in Equations (3.16) and (3.24) should be set at ~0.6.

For the case of the flame temperature, T_z (*cf.* Equation (3.32)), the multiplier term is in the numerator hence as *variables* $\rightarrow$ 0, $T_z \rightarrow T_o$ which again is expected, as the temperatures at the window plane and the flame tip will be increasingly similar as the flame shortens. As *variables* $\rightarrow$ 1, $T_z \rightarrow T_a$ which is unrealistic since the external flame is defined by a minimum temperature of 813 K (~540 ^{o}C) in the model. Therefore it is also prudent to set an upper limit to the *variables* terms in Equation (3.15) and (3.25) to avoid unrealistically low values of T_z. Again assuming a conservative value of 1573 K (~1300 ^{o}C) and the same range of ambient temperatures as above, the same limits of 0.56 and 0.61 for *variables* term is obtained. Therefore, under both *No Through Draught* and *Through or Forced Draught* conditions the *variables* term in the flame temperature definition should be given an upper limit of ~0.6, particularly as it appears such values of the *variables* term can occur with fairly common combinations of parameters under ordinary scenarios [103].

The rate of burning, $\dot{m}$ is, in all four cases described above, the denominator in the *variables* term. The Law Model [1] suggests a value of 25 kg/m^2 of wood-equivalent be used for design, but specifies no lower limit to the fire load density for which the model is applicable. Although the Eurocode implementation of the Law Model specifies that the method is only applicable to fire conditions in compartments with a fire load density "higher than 200 MJ/m^2" [2], this equates roughly to 11 kg/m^2 of wood-equivalent, given 18.4 kJ/g heat of combustion of wood [21]. Therefore it is still possible in fairly regular scenarios for the *variables* term in the flame temperature, T_z and opening plane temperature, T_o parameters to exceed 0.6. In such cases, the correlations cannot be used for establishing an external structural steel temperature. This is a limitation of the Law Model due to the empirical nature of the correlations used rather than a limitation of the scenario itself.

The correlations describing the flame height, z seen in Equations (3.9) and (3.21) can also yield a negative value which is not realistic in a fire scenario. This results from the empirical nature of the correlations, the main function of which was experimentally correlated to a '$z + h$' term, both under *No Through Draught* and *Through or Forced Draught* conditions [26,46]. If the component parameters on the right-hand-side of Equation (3.9) render (Equation (3.9) + h) < h, then the flame height, z will be negative. The same applies to Equation (3.21). While the Law Model [1] defined no limit for this term, the Eurocode has limited this unrealistic outcome by defining the flame height for *No Through Draught* conditions as [2]:

$$z = \min\left(0 \; ; \; 16h\left[\frac{R}{A_w \rho (g h)^{\frac{1}{2}}}\right]^{\frac{2}{3}} - h\right) \tag{3.35}$$

and that for *Through or Forced Draught* conditions as [2]:

$$z = \min\left(0 \; ; \; \left[23.9\left(\frac{1}{u}\right)^{0.43}\left(\frac{R}{A_w^{\frac{1}{2}}}\right)\right] - h\right) \tag{3.36}$$

Due to the high degree of interactivity between the parameters described in the Law Model, this adjusted definition of the flame height parameter, z imposes limitations on several other parameters that are a function of z that could otherwise result in unrealistic or even non-physical values if z were calculated to be negative.

While it is possible that other physical parameters may also need upper or lower limits that prevent non-physical or unrealistic values from arising when these correlations are implemented, these limits can not be directly determined without further extensive experimental investigation beyond the tests these correlations have been based on. Other assumptions and limitation pertaining to parameters that comprise a combination of basic physical parameters, such as the reciprocal opening factor, η are further discussed in Chapter 5, Section 5.4.

3.4.6 Relevance of the Assumptions and Limitations

Any model based on empirical data obtained from an array of experiments is likely to be based on several assumptions, often inherent to the experimental setup since realistically only a number of parameters can be thoroughly varied, particularly with regards to large-scale experiments, most relevant to real-case scenarios. Nevertheless, in order to fully understand the application of a tool, it is necessary to clearly define its limitations. Therefore the assumptions and limitations described in this chapter have been taken into account during the detailed analysis of the Law Model conducted as part of this research and described in Chapter 5.

For the scenarios in which some parameters are close to or beyond the limits of their application, or involve a numerical limitation, such that they result in unrealistic values, Law and O'Brien [1] advise that certain assumptions be relaxed. Nevertheless Law and O'Brien recommend this be exercised with extreme caution as the model is highly "interactive" and varying an assumption may affect other parts of the calculation and other assumptions, together with the validity of certain empirical equations [1]. Hence while the manual lays out a specific method that has a limited, scenario-specific applicability due to the assumptions made to allow for a *simplified* model, the model can also be modified to allow for application to a wider range of scenarios. This aspect of the model, together with its numerous inherent assumptions, alter the notion of a potentially 'simple model' exposing it as a somewhat intricate tool that is reliant on several levels of interlinked parameters, empirical correlations and assumptions once a more general application of the model is considered.

3.5 Application of the Law Model

While the Law Model is geared towards the safe design of external structural steelwork under threat from a compartment fire, this research is primarily concerned with heat insult to any element on the plane of the façade, above the compartment openings. In both the Law Model design manual and its Eurocode implementation, it is not immediately clear whether the model is applicable to façade structural elements, hence in order to determine the level of application of the model to different scenarios

it is essential that the assumptions behind the different components of the model are clearly understood.

Many of the experiments the Law Model correlations are based on were primarily conducted to determine the parameters and correlations governing the behaviour of fire in the internal compartment and that of any resultant external flames. Although the structural heat transfer process detailed in the Law Model is particularly geared towards obtaining a resultant temperature of an external steel element outlying at a distance from the façade, the component of main interest is that of the heat flux incident on the element, such that the insult posed by the fire can be applied to other 'receivers'. Hence, it is assumed the calculations to determine the heat flux incident on the outlying structural elements can be applied to elements on the façade provided any necessary assumptions are adjusted and the appropriate configuration factors are used.

For the case of an element embedded in the façade above an opening, with only one face flush with the façade plane and exposed to fire, the main incident heat insult arises from radiation from the flame, convection from the flame and both radiative and convective heat losses from the element. Theoretically no radiation from the internal compartment fire arrives at the element as the plane of the façade does not 'see' the internal fire, hence this component is ignored. This heat flux falls incident on all elements in the plane of the façade, depending on their location relative to the compartment window, and provides a measure of the insult a given fire will inflict on these elements. Hence, it can be applied not only to structural load-bearing components such as spandrel beams and perimeter columns, but also to the façade cladding and to the glass panes of the windows of upper compartments. While the effects this incident heat flux has on the various elements of the façade are dependent on the individual properties of each element, should these properties be known, the corresponding heat losses can be calculated to ascertain a resultant element temperature or temperature evolution under transient conditions.

Compared to the outlying structural steel members used in the Law Model examples, conductive heat loses from elements flush-mounted within the façade can be significant depending on the material thickness, the material conductivity and the

boundary conditions. However conducting a heat transfer analysis under steady-state conditions (negligible conduction losses) will determine a worst-case resultant element temperature. This is justified for many cases, particularly with regards to a point on the façade that is engulfed in flame, where the temperature gradients to parts of the element outwith the engulfing flame are small, due also to low material thermal conductivity properties. Hence, assuming steady-state conditions, for any case, provides a conservative approach for design as such conditions should result in the highest possible temperature for a particular element.

In any case, the primary concern of this research is the total heat flux *incident* on the façade plane, such that it can be applied to any element of interest. For these purposes it is assumed the Law Model correlations can be directly employed, assuming the emissivity of any façade element can also be approximated to unity due to soot and oxidation from exposure to external flaming. Nevertheless, if these assumed properties differ greatly for a specific material, a fraction of the emissivity can be used. The intricacies of any further assumptions, such as the characteristic length scale for the convective heat transfer coefficient, the point along the flame axis at which the flame temperature is taken and the definition of the opening height *vs*. the modified opening height are discussed in Chapter 5 where the potential effect of the assumptions made is considered during a numerical analysis of the model.

Prior to conducting a detailed analysis of the Law Model in order to evaluate the sensitivity of the model to each of its constituent parameters, it is valuable to identify a benchmark scenario against which the effect of varying individual parameters is compared. It is of essence therefore that such a scenario falls within the assumptions and limitations imposed by the Law Model. In this case the benchmark scenario was based on Dalmarnock Fire Test One, the details of which are discussed in Chapter 4. The test compartment, a reasonably rectilinear mono-volume with rectangular openings, is of standard size and measurements were taken for most of the physical parameters described in the Law Model.

Chapter 4

The Dalmarnock Fire Tests

- *The External Plume during Dalmarnock Fire Test One* -

-

Ideally an evaluation of the applicability of the Law Model in the design of real, modern-day buildings would be assessed against a number of fire tests conducted in different compartments, representative of realistic scenarios. Unfortunately, conducting a multitude of full-scale tests is simply not feasible. An analysis of the model can however be undertaken by assessing the Law Model against a thorough set of data for a realistic scenario that can then be used as a benchmark for a parameter sensitivity study. This enables the analysis of the importance of different Law Model parameters under different scenarios.

The Dalmarnock Fire Tests provide detailed measurements of a realistic modern-day fire scenario, allowing for a global assessment of the current application of the Law Model as a measure of external exposure to heat for this particular scenario. These full-scale tests not only provide a thorough set of data against which to assess the various components of the model, but in serving as a benchmark scenario, they form the basis of the detailed analysis of the Law Model which enables the identification of the relative influence of individual parameters. Dalmarnock Fire Test One is of particular relevance as it was allowed to freely develop to post-flashover conditions and measurements of external flaming and heat flux to the façade were obtained throughout the duration of the fire. This chapter is mostly concerned with the characterisation of Dalmarnock Fire Test One such that it can be employed in the analysis of the Law Model.

4.1 Introduction to the Experiments

The Dalmarnock Fire Tests were conducted by the University of Edinburgh in July 2006, during the course of this research. The tests were undertaken *in situ* in a high-rise building with a non-combustible façade. Primarily devised to demonstrate the feasibility of the FireGrid Project [24,25], the tests involved a high density of data-gathering sensors. In Test One the fire was allowed to develop to post-flashover conditions and through most of the fully-developed fire stage hence the opportunity arose to conduct thorough measurements of the consequent external flaming. Test Two was conducted in a compartment with identical geometry and near-identical fuel

distribution to that of Test One, and both fires underwent a similar ignition process. Although Test Two was extinguished soon after flashover, its close correspondence to Test One allowed for an evaluation of the experimental repeatability of the tests while the slight variation between them highlighted the potential range of variability. This enables an error analysis to be conducted for the benchmarking and validation of some of the key characteristics of the fire [105]. A third test (Test Three) was conducted in a stairwell as part of a smoke management exercise hence it is outwith the scope of this research. Therefore any reference to the Dalmarnock Fire Tests henceforth refers mainly to the compartment fires of Test One and Test Two.

4.1.1 Context of the Dalmarnock Fire Tests

The fire tests were conducted in a 23-storey reinforced concrete building, constructed in 1964, in the Dalmarnock area of Glasgow, U.K. The multi-storey building was scheduled for demolition so sponsorship and authorisation were obtained to conduct fire tests within the unoccupied building. In conjunction with the FireGrid Project [25], the tests formed part of a BBC Horizon documentary on fire-fighting in high-rise buildings [13]. Although the tests were funded by various different organisations they were mainly designed and executed at the discretion of the BRE Centre for Fire Safety Engineering, at the University of Edinburgh.

4.1.2 Setup of the Experiments

Test One and Test Two were held in identical compartments within two-bedroom single family flats. In both cases, the common living area was set up as the main experimental compartment. Test One (DFT1) was held on the 4^{th} floor and the fire was allowed to grow 'uncontrolled' to fully-developed conditions. Test Two (DFT2) was held in a compartment directly two floors below and involved a more 'controlled' fire as the ventilation to the compartment was controlled remotely and the fire was not allowed to develop much past flashover. In both cases, the experimental compartments were identically furnished with typical household furniture for a room serving the dual purpose of living room and office work area. Both compartments were comprehensively instrumented with a variety of fire-monitoring sensors however Test One included a further set of sensors monitoring the evolution of the external

flaming and internal structural-monitoring sensors to measure the behaviour of the structure under insult from a large post-flashover fire.

The experimental setup and fuel layout were designed with the aim of creating a realistic scenario with a reasonable propensity to be repeatable. The main variant between both tests were the ventilation conditions. While the ventilation in Test One was set to provide the conditions required for flashover, in Test Two all the main openings to the compartment were operated remotely so the doors and windows could be opened and closed throughout the course of the fire. The remote operation of the openings was based on live information fed from the experimental monitoring sensors and aimed at exercising some control over the fire conditions within the compartment by controlling the smoke evacuation and air supply. Hence the 'uncontrolled' fire of Test One was allowed to burn freely until it began to have noticeably adverse affects on the structure, at which point the fire brigade intervened to extinguish the fire. On the other hand the Test Two fire was extinguished when remote operation of the ventilation conditions could no longer adversely affect the fire growth. Other discrepancies between the setup of the two tests involved mainly a series of independent demonstrations implemented in Test One. These demonstrations were undertaken as isolated studies of individual items under exposure to post-flashover compartment fire conditions [105] and hence were not directly associated to the development of the fire so are outwith the scope of this research.

4.1.3 General Application of the Experiments

These fire tests represent a typical fire scenario with realistic fire loading therefore the data recorded with the dense network of sensors used to monitor the evolution of the fire can be used to provide a thorough representation of the characteristics of a modern-day fire. This data can have immediate use as demonstrated by the live-stream to a remote command and control centre which made use of the interpreted data to make informed decisions in real-time, allowing for positive remote interaction with the fire as it evolved [106]. This interaction demonstrated the potential of sensor-assisted fire-fighting [24] and confirmed the feasibility of FireGrid [25]. The Dalmarnock Fire Tests also demonstrate the uses of structural health monitoring, both during a fire scenario and more generally over a building's lifetime.

In the long-term, this vast array of relevant fire data, compounded by the availability of two sets of comparable test data that allow for an assessment of the error involved in the repeatability of the fire scenario, provides a benchmark fire test setup against which models and correlations can be validated. Although the Dalmarnock Fire Tests' data are refined to a much smaller level of detail than is required to evaluate output from the Law Model, this data can easily be analysed to provide the best representation of each parameter. In fact, the data from the Dalmarnock fires is far more thorough than the measurements taken in any of the experiments the Law Model is based on (*cf.* Chapter 2 and Chapter 3). Hence, these data are likely to provide a better representation of the parameters theoretically identified by Law as contributing to the resultant external heat exposure.

The resolution of many of the Dalmarnock Fire Test measurements also renders the data exceptionally useful for validation of CFD models as the level of detail available is comparable to the grid-size dimensions used in computational models. An international 'blind' round-robin fire-modelling study of Test One was conducted *a priori* to the tests in order to evaluate the state-of-the-art of current CFD modelling in practice [18]. The results of the *a priori* study have lead to the need for an intensive *a posteriori* study in an attempt to further understand the discrepancies between the current implementation of available CFD models and the Test One data [19].

4.2 The Design of the Experiments

4.2.1 Layout of the Flat

The flats used were located on the north-west corner of the building, facing westward. They comprised a central flat hallway off which came two bedrooms, a bathroom and a common living area with a small kitchen off to its side, as shown in Figure 4.1. The characteristic dimensions of the main experimental compartment in both tests were an average width, W of 3.60 m, a depth, D of 4.75 m and a height, H of 2.45 m. Both compartments had identical openings – a window made up of two glass panes and two doors to other compartments – the characteristic dimensions of which are listed in Table 4.1. The location of the openings can be seen in Figure 4.1 where the window panes throughout the flat are shown in blue and the doors in red. Further details of the

compartment dimensions can be found in Appendix A and ventilation conditions are detailed in Section 4.2.4.

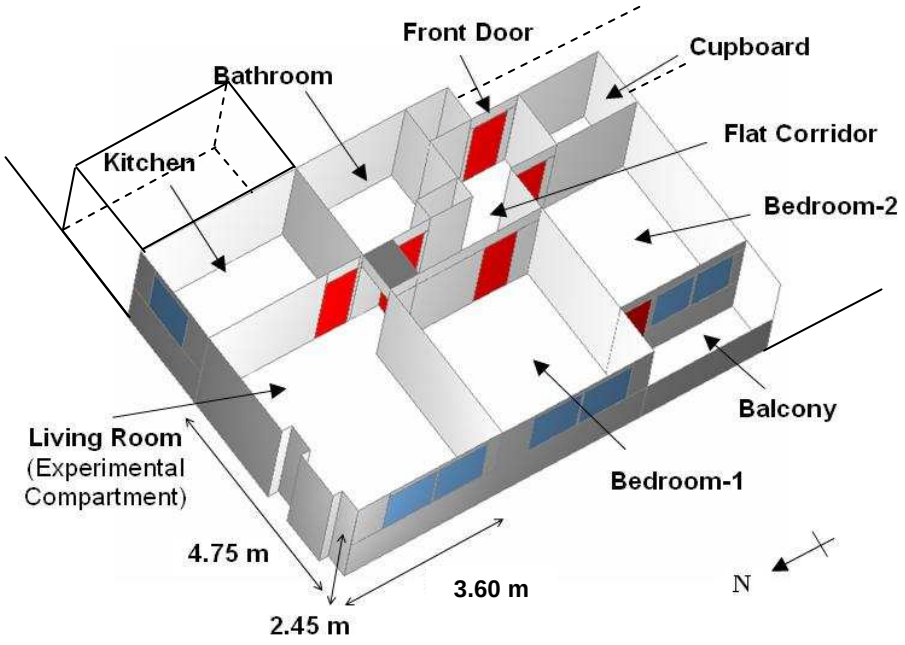

Figure 4.1. General layout of the flats in which Test One and Test Two were conducted. Key dimensions for the main experimental compartment are given in metres. The outline of the main data acquisition compartment is shown to the East, adjacent to the flat kitchen, together with the outline of the main flat access corridor leading to the front door.

Opening Reference	**Width, *w*** (m)	**Height, *h*** (m)
Window ($_{win}$)	2.35	1.18
Door 1 ($_{dr1}$) – to hallway	0.85	1.98
Door 2 ($_{dr2}$) – to kitchen	0.9	2

Table 4.1. Key dimensions of the openings in the experimental compartments.

4.2.2 The Fire Load Distribution

The fire load constituted a mixture of living room and office furniture, including several non-cellulosic, synthetic materials. The experimental compartments were stripped of their existing finishes and the flats were emptied of any existing contents. Identical carpeting was laid on the experimental compartment floors and all other compartments were left bare and unfurnished.

In the experimental compartments new, identical furniture was arranged to represent a realistic living room and study area, typically of a regular dwelling. A large portion of the fuel was concentrated towards the back of the compartment, in the NE corner away from the window, with a fairly even fire load distribution throughout the rest of the compartment. Figure 4.2 shows several photographs taken from different angle in the Test One fire compartment showing the experimental setup with the furniture layout used in both tests – labels indicate the main items of furniture. Figure 4.3 shows a scale outline of the experimental furniture in a plan view of the compartment where fire-monitoring sensors are also indicated.

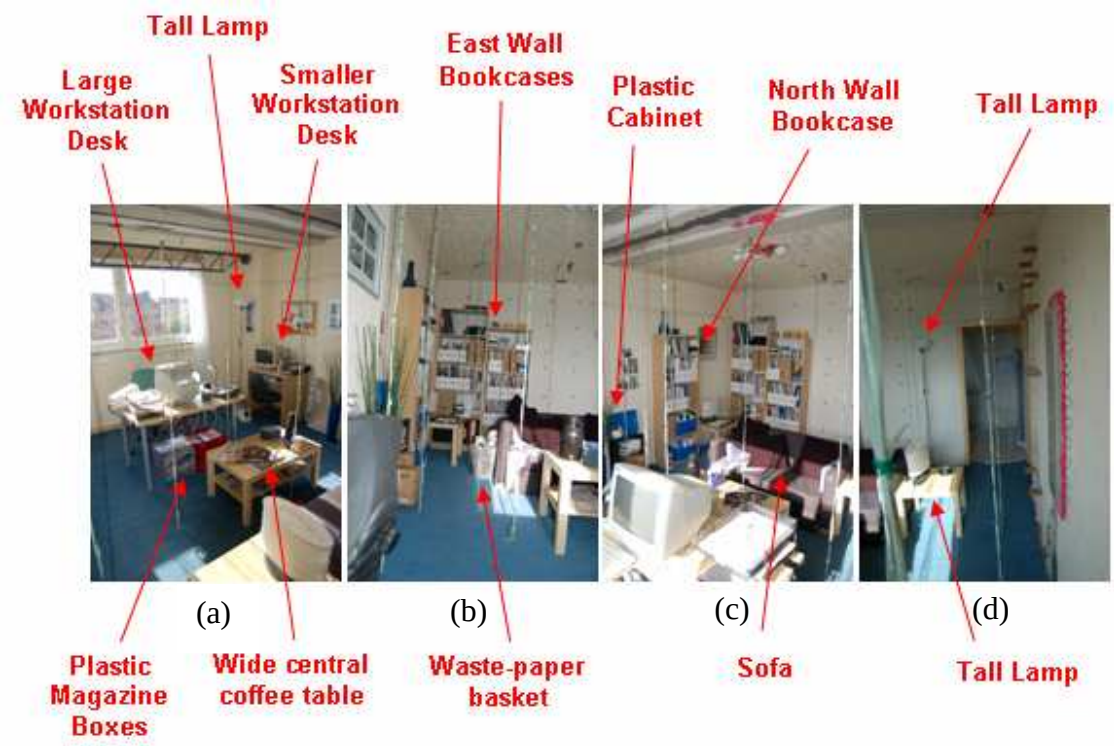

Figure 4.2. Photographs of the experimental setup in Test One, taken from several angles across the compartment, in the respective directions of: (a) NW from Door 1; (b) E along the North wall from the NW corner; (c) NE from the SW corner; and (d) E along the South wall from the SW corner. Labels indicate the main items of furniture.

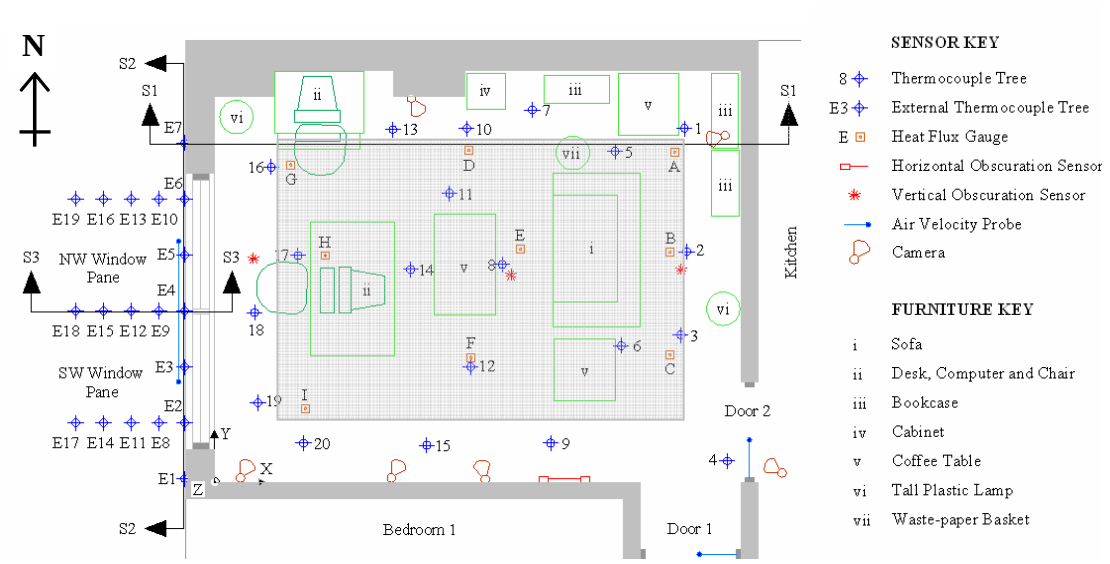

Figure 4.3. Plan view of the general experimental compartment setup showing furniture layout (in green), to scale (*ca.* 1:67). Fire-monitoring sensor locations (*N.B.* some sensors were exclusive to Test One) are also indicated. A section S1-S1 running East-West through the compartment is shown. Sections S2-S2 and S3-S3 represent elevations at different angles through the external sensors. The shaded region indicates the area of the ceiling corresponding to heat flux data. The global coordinate system origin is also shown (at floor level) in the SW corner.

While the main source of fuel was a two-seat sofa consisting of mainly flexible, combustion modified polyurethane foam upholstered with fire-retardant fabric, the compartments also contained: two office work desks (a work table and a tiered computer desk) with desktop computers, each with its own foam-padded office chair; three tall wooden bookcases; a short plastic cabinet; three wooden coffee tables; a range of paper items and two tall plastic lamps. The bookcases were fully-laden with books, video tapes, paper-filled cardboard files, and several other plastic items, as was the small cabinet. The bookcase closest to the sofa also had two plastic containers holding thin cardboard boxes full of polystyrene pellets. Beneath the central computer work table there were two plastic boxes filled with newspapers and magazines. The location of most of these items is shown in Figure 4.3. Further details of the dimensions and mass of furniture can be found in Appendix B.

Other minor living room and office items were included to give the impression of a realistic compartment 'in use'. In both cases, a plastic waste-paper basket filled with crumpled newspaper and 300-500 ml of heptane was used as the ignition source. The basket was placed in between the sofa and a bookcase (*cf.* Figure 4.3, Furniture item vii), directly beneath a blanket that was draped over the sofa arm as seen in Figure 4.2 (b). Although slightly different amounts of accelerant were used in both tests and the time delays between pouring the accelerant and igniting the fire also varied, this difference was not significant to the general behaviour over the timescale of the fires. The accelerant contributed only to the momentary ignition of each fire and was fully consumed within seconds, but the slightly different ignition protocol was sufficient to establish the robustness of the ignition conditions for this fire scenario, by comparison of the characteristics of both tests during the initial fire growth stage [106].

4.2.3 Instrumentation and Data Acquisition

4.2.3.1. Internal Compartment Fire-Monitoring Sensors

In both Test One and Test Two a variety of sensors were set up to monitor the fire. Twenty thermocouple trees held 12 thermocouples (K-type extension) each. These trees were distributed throughout the compartment as shown in Figure 4.3, with a further five small thermocouple trees placed along the window sill. Nine thin-skin calorimeters were used to measure the heat flux incident on the compartment ceiling, the locations of which are also shown in Figure 4.3. A further set of these heat flux gauges were mounted on the partition wall shared with the kitchen (20 in Test One, 9 in Test Two). Eight lasers used to measure smoke obscuration were set in emitter-receiver pairs, such that five were horizontally aligned and three were vertically aligned. Three bi-directional air velocity probes, exclusive to Test One, were placed in both the doorway leading to the flat corridor (Door 1) and in the doorway to the kitchen (Door 2) and a further eight probes were placed outside the compartment window. The specific location of each sensor can be found in Appendix C. Both Figure 4.3 and Figure 4.4 show the layout of some of these fire sensors relative to the furniture distribution.

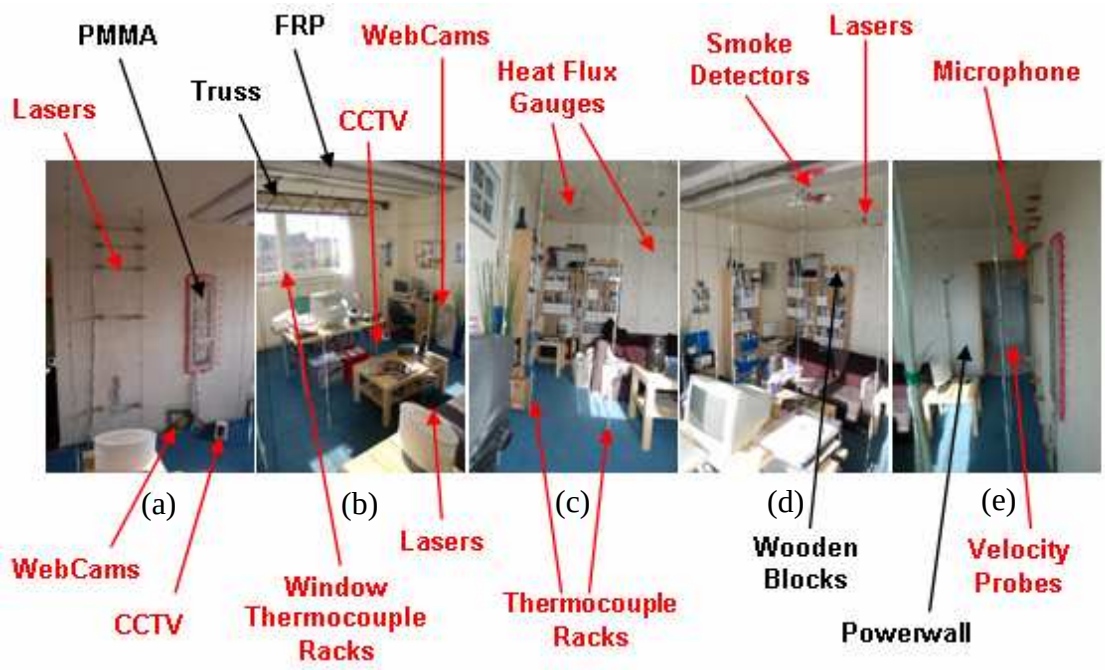

Figure 4.4. Photographs of the experimental setup in Test One, taken from different angles around the compartment, in the respective directions of: (a) S from the East wall; (b) NW from Door 1; (c) E along the North wall from the NW corner; (d) NE from the SW corner; and E along the South wall from the SW corner. The red labels indicate the main types of sensors and the black labels indicate independent demonstrations included in Test One

All sensors were connected to a set of central data loggers recording at an average frequency of 0.5 Hz. These were housed in a separate flat, adjacent to the kitchen (*cf.* Figure 4.1) and protected from the fire by a broad structural wall. Several network-type cameras were also used to monitor the fire growth and all data collected was time stamped, both camera and data logger clocks having been synchronised prior to ignition. This data was streamed live to a remote 'command and control' room setup outside the building. Similarly, several early warning fire alarm systems and additional CCTV cameras were installed in all rooms in the flat and their performance was also monitored live in the remote 'command and control' centre.

4.2.3.2. External Fire-Monitoring Sensors

Test One was planned to reach post-flashover conditions hence additional fire-monitoring sensors were installed outside the main experimental compartment window, running along the west non-combustible façade. These sensors included: a set of 19 thermocouple trees holding 8 thermocouples (K-type extension) each; 20 thin-skin calorimeters to measure heat flux incident on the external façade above the

window; 3 network cameras mounted at 3rd-5th floor level, filming the external flaming from different angles and 3 meter rulers (with 100mm markings) were placed perpendicular to the façade to aid measurement of the key external flame dimensions.

The external sensors were rather more evenly spaced out than those within the internal compartment. The external thermocouple trees were arranged to measure 3-D temperature distribution of the external flames expected to emerge from the post-flashover fire compartment. The trees were aligned in a grid providing regular measurements across the window width at approximately 0.5 m spacings in the row closest to the façade (7 trees) and in others (3 trees) at 1 m spacing, outwards away from the window in five rows spaced at 0.25 m and in height with varied spacing. The plan layout of the regularly aligned external thermocouple trees can be seen in Figure 4.3. In height, the thermocouples were aligned to provide a higher density of sensors close to the window such that the spacing between thermocouples increases with height, ranging from about 0.3 m below the window soffit to about 0.3m below the soffit of the 5th floor window one floor above. A photograph of the westward façade shows the general arrangement of the external thermocouple trees in Figure 4.5 where the layout of the other external sensors can also be seen. Detailed sensor coordinates can be found in Appendix C.

The external heat flux gauges were mounted on the westward façade above the 4th floor compartment window. A main vertical strip of 12 gauges ran centrally from just above the soffit of the main compartment window, up the façade, to near the soffit of the 5th floor window above. Two additional horizontally oriented heat gauge strips allowed for a measure of the heat flux distribution across the width of the windows. One strip of 5 gauges was aligned just across the top of the compartment window soffit, with its central gauge shared with the bottom gauge of the vertical strip. The other horizontal strip of 5 gauges ran across the 5th floor window, again sharing its central gauge with the vertical strip. The gauges were mounted into 10 mm thick plasterboard, which in places was itself mounted on a further 10 mm thick plasterboard sheet, then fixed to the façade, nevertheless for the purposes of data analysis, in terms of scale they can be considered to have been flush-mounted with the façade. In Figure 4.5 these location of these gauges is boxed in red, with the

respective sensor labels illustrated on the left. The detailed coordinates of the heat flux gauge locations can also be found in Appendix C.

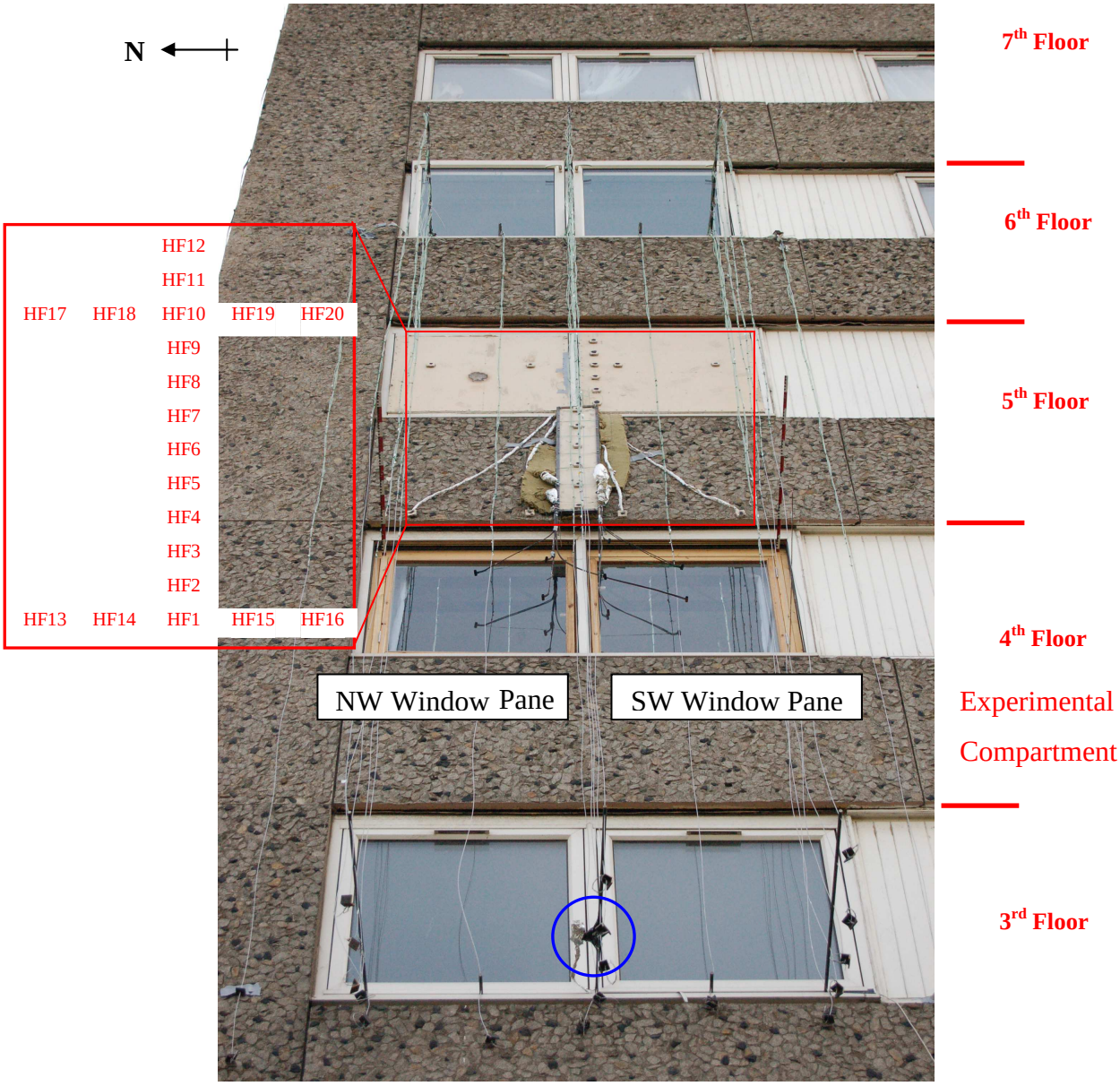

Figure 4.5. Photograph of the elevation of the westward façade showing the layout of the Test One external instrumentation relative to the experimental compartment's wooden-framed window. The area covered by the external heat flux gauges (close to flush-mounted with the façade) is boxed in red with corresponding gauge labels tabulated on the left and the camera at 3rd floor level (oriented upwards) is circled in blue. Markings help identify the different floor levels and the window panes are labelled as 'NW Window Pane' and 'SW Window Pane'.

4.2.3.3. Structural-Monitoring Sensors

The post-flashover conditions expected in Test One made it of interest to include sensors monitoring the structural response. The floor slab above the experimental compartment was heavily instrumented with sensors including 24 thermocouples embedded in the concrete at four different depths and in six different locations, together with 22 strain gauges and nine deflection gauges placed across the top of the slab. Three deflection gauges were also placed in Bedroom-1 to monitor deflections along the height of the partition wall shared with the experimental compartment. In Test One the partition wall shared with the kitchen was also replaced by a lightweight steel frame wall (designed by Powerwall Systems Ltd.) of identical geometry. This wall was rigged with thermocouples and strain gauges in addition to the gauges measuring heat flux incident on its surface, allowing for a detailed study of its performance. A set of six different arrangements of fibre reinforced polymer (FRP) strips embedded in the ceiling was also monitored by thermocouples and strain gauges. Although these same FRP strips were mounted in the ceiling of Test Two, no measurements were taken as they were used for qualitative investigation of their behaviour in fire. Further details of the structural-monitoring sensors can be found in studies that analyse the affect of Test One on the near-field structure [107-110].

4.2.4 Ventilation

The ventilation parameters are of paramount importance as they were not identical in the two tests. In Test One, the initial ventilation conditions were set to favour fire growth to post-flashover conditions, with the window panes in the main compartment left closed but its doors both left open. It is worthy of note that the existing double-glazed window was replaced by a makeshift single-glazed window for the test, the wooden frame of which was unfortunately not well sealed and certainly not air-tight. The kitchen window (~1 m wide by 1 m high) was left partially open, those of Bedroom-2 (a set of window panes with the same dimensions as those in the experimental compartment and a ~0.9 m by 2 m high door) were left completely open and those in Bedroom-1 (same dimensions as those in the experimental compartment) were left closed. While the doors to both bedrooms were left fully open, the front door was only left ajar and the bathroom compartment door was left closed. The bathroom

door was also insulated to seal off the bathroom compartment which housed some of the bi-directional velocity probe pressure transducers. Any changes in ventilation conditions during Test One were naturally fire-induced apart from the north-west window pane in the main experimental compartment which was broken at a pre-specified time.

Conversely, the ventilation conditions in Test Two were purposefully designed to allow for remote control over the main compartment doors and both window panes as well as the main flat door. These windows and doors could be opened and closed via the remote 'command and control' centre allowing for the ventilation conditions to be altered throughout the experiment with the intention of influencing the fire growth. Initially, the main compartment window and its two doors were left closed, as was the flat's front door. All other windows in the flat and the two doors to the bedrooms were left open, with the bathroom door left closed and sealed off as for Test One. The front door was also initially left closed. Additionally, a large hole, approximately 1 m wide by 0.5 m high, at about 1 m from the floor, was bored into the wall separating the main fire compartment from Bedroom-1 as part of the BBC Horizon team requirements. Subsequent changes to the ventilation were remotely controlled from the 'command and control' centre to allow for evacuation of smoke in a bid to reduce the build up of a re-radiating smoke layer, potentially reducing or slowing the fire growth but also in a bid to prolong tenability conditions in the compartment [106].

4.2.5 Data Processing

The sensor data collected during the experiments required some processing before it could be employed in the thorough characterisation of the fires. The data loggers measured only voltage but had in built conversions that allowed for specification of several types of sensors, therefore some of the output data had sensor-relevant units. Hence some of the initial data processing was done automatically.

4.2.5.1. Gas-Phase Temperature

The thermocouple data has been corrected for radiation according to the method described by Welch *et al*. [111], implemented in MatLab® (MatLab R2006, The Mathworks™, MA, U.S.A.). All the internal compartment thermocouple readings are

corrected to 'gas-phase' values with the exception of the uppermost thermocouple in each of the 20 trees (since these were in contact with the ceiling) and all other thermocouples employed in solid-phase temperature measurement. The temperature correction reveals radiation errors to be overall negligible in this case, as the average maximum temperature correction is of the order of ±7 ^{o}C. Some localised corrections are of greater significance, with the maximum correction of 80 ^{o}C occurring during the period of greatest temperature stratification, particularly when the hot layer initially developed. It is of note that most temperature corrections of similar magnitude coincide in time and correspond to thermocouples in the vicinity of the sofa and the central coffee table, as expected as they were among the first items to be alight. Nevertheless the overall corrections due to radiation are significantly low relative to average compartment temperatures. It should be noted that any error arising from the calculation of the average smoke layer extinction coefficient may also contribute towards errors as it was used in these corrections. Corrected gas-phase temperatures are however used throughout the analysis and this process allowed for the identification of a few damaged thermocouples for which substitute values are spatially interpolated from neighbouring thermocouple readings.

4.2.5.2. Properties of the Smoke Layer

The smoke layer evolution in time was characterised in terms of its height and the extinction coefficient. Thermocouple measurements were used to determine the height of the smoke layer over time under the assumption that the hot-cold layer interface is located near the 100°C isotherm (averaged height throughout compartment). This smoke layer height was verified against camera footage.

Laboratory calibration of the laser smoke obscuration sensors allowed for conversion of the raw voltage data into the form of relative power and, as such, percentage obscuration. Together with details of the smoke layer height, this enabled calculation of the equivalent extinction coefficient evolution of the smoke layer over time, following the classical methodology based on the Beer-Lambert Law [21,105,112]. Nevertheless only data from the horizontally-aligned laser smoke obscuration sensors are used for the characterisation of the smoke layer extinction coefficient as the vertically-aligned sensors measurements (in DFT1) were found to be unreliable [113].

Additionally, footage from a network camera stationed at 730 mm from the floor on the north wall opposite the horizontal laser smoke obscuration sensors is used for simple verification of the extinction coefficient calculations. Jin has stated that once a certain object is visually judged to be "*just* no longer visible" due to smoke obscuration, the extinction coefficient of the smoke layer at that time is the quotient of three over the distance to that object [112,114]. The distance to referenced light-reflecting objects in the horizontal line of sight of the footage can be estimated from the scale plan drawings of the furnished compartment (*cf*. Figure 4.3).

4.2.5.3. Incident Heat Flux

The thin-skin calorimeter heat flux gauges used throughout the experiments consist of copper discs embedded in plasterboard which have been calibrated using a radiative panel and a calibrated heat flux meter, in accordance with the theory described by Ingason and Wickstrom [115] and the methods defined in the ASTM standard [116]. All raw heat flux gauge data has been correspondingly post-processed into net incident heat flux values before use in analysis. Further details on the heat flux calibration process highlight the limitations of the gauges employed [105,107].

4.2.5.4. Bi-directional Flow Velocity

The bi-directional velocity probe sensors were linked to pressure transducers which in turn were connected to the data loggers. Conversion of the raw bi-directional velocity probe data has been performed as per literature detailing the calibration of such probes in a wind tunnel at BRE [111,117].

4.2.5.5. Video footage

The video footage obtained throughout the Dalmarnock Fire Tests was streamed directly to the remote 'command and control' centre via a local hub, by passing the data loggers. Hence, no processing is required for the footage to be viewed however image analysis, such as that detailed by Cowlard [118], can yield a more accurate measurement of flame lengths, *etc*. (smoke obscuration permitting) than simple visual estimates.

4.3 Characterisation of Dalmarnock Fire Test One (DFT1)

4.3.1 Major Events Observed

At 12:23:00 a blow torch was used to ignite the contents of the waste-paper basket shown in Figure 4.2 and Figure 4.3 and the fire was allowed to grow unconstrained. Observations indicate the blanket dangling over the waste-paper basket caught fire almost immediately, in turn igniting several cushions with fire spreading swiftly to engulf the polyurethane sofa. Four and a half minutes of sofa burning led to ignition of contents of the bookcase adjacent to the sofa and the waste-paper basket, near the NE corner of the room. Fire progressed up the bookcase followed by a flashover period about 5 min after ignition, when ceiling flames projected into the flat corridor and visibility in the main floor access corridor was suddenly reduced. Simultaneous ignition of paper items in several locations throughout the compartment was also indicative of the flashover period. At this point, the smoke layer quickly descended.

Post flashover the visibility in the compartment was drastically reduced, so camera footage provides little information about the subsequent progression of the fire. Nevertheless the fire burnt steadily for the next eight minutes and black smoke was observed to seep out around the compartment window which was not completely sealed or made air tight. About seven minutes after the onset of flashover the kitchen window shattered, even though it had been left partially open, but the experimental compartment window remained intact. The north-west window pane was manually broken at 12:36:21 (over 13 min after ignition). For a while mostly smoke was seen to billow out with sustained external flaming developing four and a half minutes later, moments after which the second window pane shattered and fell away, providing full ventilation. The fire was allowed to burn freely for a total of 19 min before the fire brigade intervened to extinguish the fire. A summary of the time to key events is provided in
Table 4.2.

Inspection of the aftermath showed mostly only metal components were left intact. A few samples of partially burned books and other partly combusted items were found, but most of the fuel was consumed in the fire, as can be seen in Figure 4.6 which

juxtaposes two images of the east side of the compartment both before and after the fire. All thermocouple trees were found to still be in place hence thermocouple data recorded is assumed to relate back to original spatial coordinates registered.

Major events observed	**Time** (h:m:s)	**Time from ignition** (s)
Growth period		
Ignition	12:23:00	0
Cushions ignite	12:23:09	9
Smoke visible in main corridor	12:26:06	186
Bookcase ignites	12:27:35	275
Flashover period		
Fire engulfs bookcase	12:28:00	300
Flames project to flat corridor ceiling, low visibility in main corridor	12:28:15	315
Ignition of paper lamp and table papers	12:28:23	323
Post-flashover period		
Kitchen Window breakage	12:35:00	720
NW window pane forced breakage	12:36:21	801
Sustained external flaming	12:41:00	1080
SW window pane breakage	12:41:31	1111
Firemen in, begin to extinguish fire	12:42:00	1140
Mostly Smouldering	12:45:00	1320

Table 4.2. List of major events observed via camera footage of the Test One fire. Respective clock time and time elapsed from ignition is given.

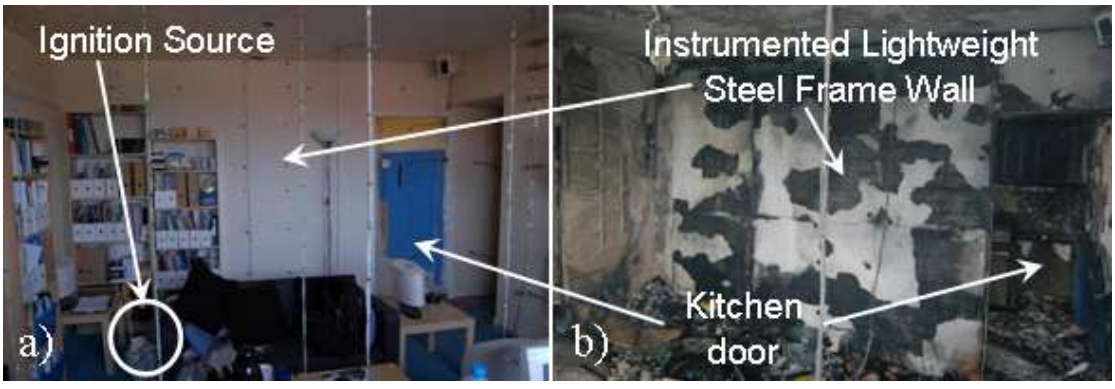

Figure 4.6. Photographs of the half of the Test One compartment (East side) showing the ignition source, bookcases, sofa and other items both: (a) before the fire; and (b) after the fire.

4.3.2 The Internal Compartment Fire (DFT1)

4.3.2.1. Compartment Gas-Phase Temperature (DFT1)

The compartment average gas-phase temperature-time curve, presented in Figure 4.7, shows the general behaviour to match the sequence of major events observed. In order to fully characterise the spatial evolution of the fire, six key time steps have been chosen for comparison of the spatial temperature distribution at consecutive points in time. These time steps and the stages of the fire they represent are described in Table 4.3. The last time step represents the period of peak average compartment temperatures once the first window pane broke and no subsequent time steps are taken as the fire was not allowed to further develop to burn-out, having instead soon been extinguished by fire-brigade intervention.

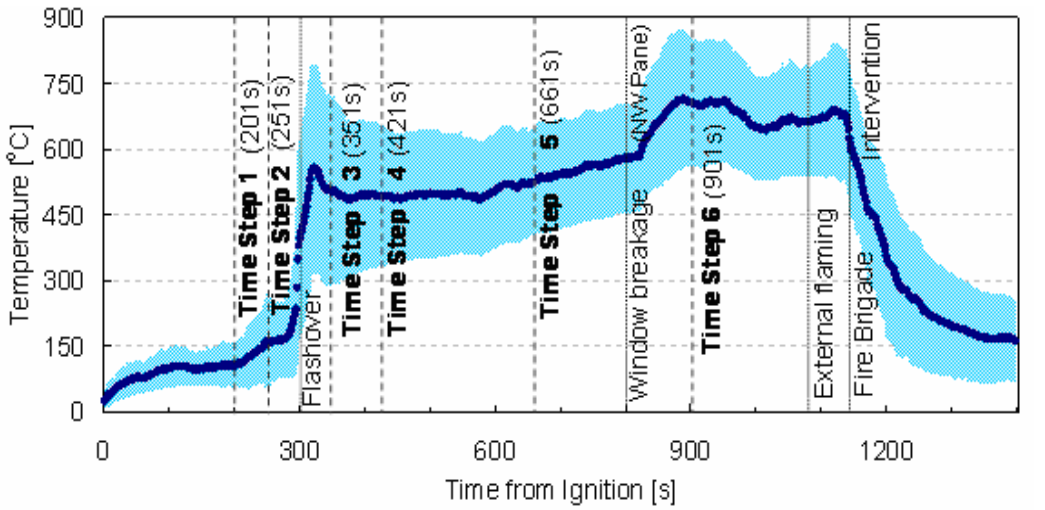

Figure 4.7. Evolution of the average compartment gas-phase temperature. The shaded region indicates the standard deviation of temperature throughout the compartment. Vertical dashed lines indicate Time Steps used for analysis and dotted lines represent time of some major events, as labelled.

Time Step	**Time from Ignition** (s)	**Fire Development Stage**
1	201	Localised sofa fire
2	251	Fire growth significant
3	351	Just after flashover
4	420	Post-flashover steady-state
5	661	Slow temp. rise post-flashover
6	901	Peak temp. after window pane breaks

Table 4.3. Discrete time steps for the comparison of compartment temperature spatial distribution at different stages of the Test One fire.

The spatial gas-phase temperature distribution throughout the compartment has been represented, at each of the time steps identified in Table 4.3, by contour plots created using SigmaPlot® (SigmaPlot 10.0, Systat Software Inc., San Jose, CA). Several vertical sections have been taken through the compartment running both North-South and East-West and contour plots were also made for horizontal sections through the compartment at the 11 different thermocouple heights. Figure 4.8 shows a set of vertical contours taken at different time steps through section S1-S1 (includes data from thermocouple Trees 1, 5, 7, 10, 13 and 16), the location of which is shown in Figure 4.3. Further temperature contours through different sections can be found in Appendix D.

For the vertical sections through the compartment the contour planes comprise data from best-fit lines through the trees such that no tree falls outwith 0.3 m of the section plane, as the thermocouple trees were not arranged in orthogonal lines. Eleven thermocouples between the heights of 0.45-2.40 m are used as the uppermost thermocouple in each tree was in contact with the ceiling and thus is excluded.

Apart from highlighting the spatial temperature variation throughout the compartment, the evolution of the fire can also be inferred from Figure 4.8. Section S1-S1 cuts right through the initial seat of the fire (*cf.* Figure 4.3) and Figure 4.8 (a) and (b) clearly show the temperature rise has a higher gradient locally between Time Steps 1 and 2, suggesting that during this period the fire is still fuel-controlled. The transition to flashover is then evident between Time Steps 2 and 3 (*cf*. Figure 4.8 (b) and (c)) as there is a distinct general rise in temperature, multiple pockets of intensive burning develop and the smoke layer (100 ^{o}C isotherm) descends. While at Time Step 3 the bookcases and a computer station seem to be contributing significantly towards the temperature increase there is a shift towards greater temperature homogeneity seen in Time Step 4 (*cf*. Figure 4.8 (d)). This becomes increasingly evident at Time Step 5 (*cf.* Figure 4.8 (e)), as expected due to the reduced standard deviation evident in Figure 4.7 between Time Steps 4 and 5. Finally Time Step 6 (*cf*. Figure 4.8 (f)) highlights yet another marked increase in general compartment temperature as the air supply is somewhat renewed and partially-combusted fuel is consumed.

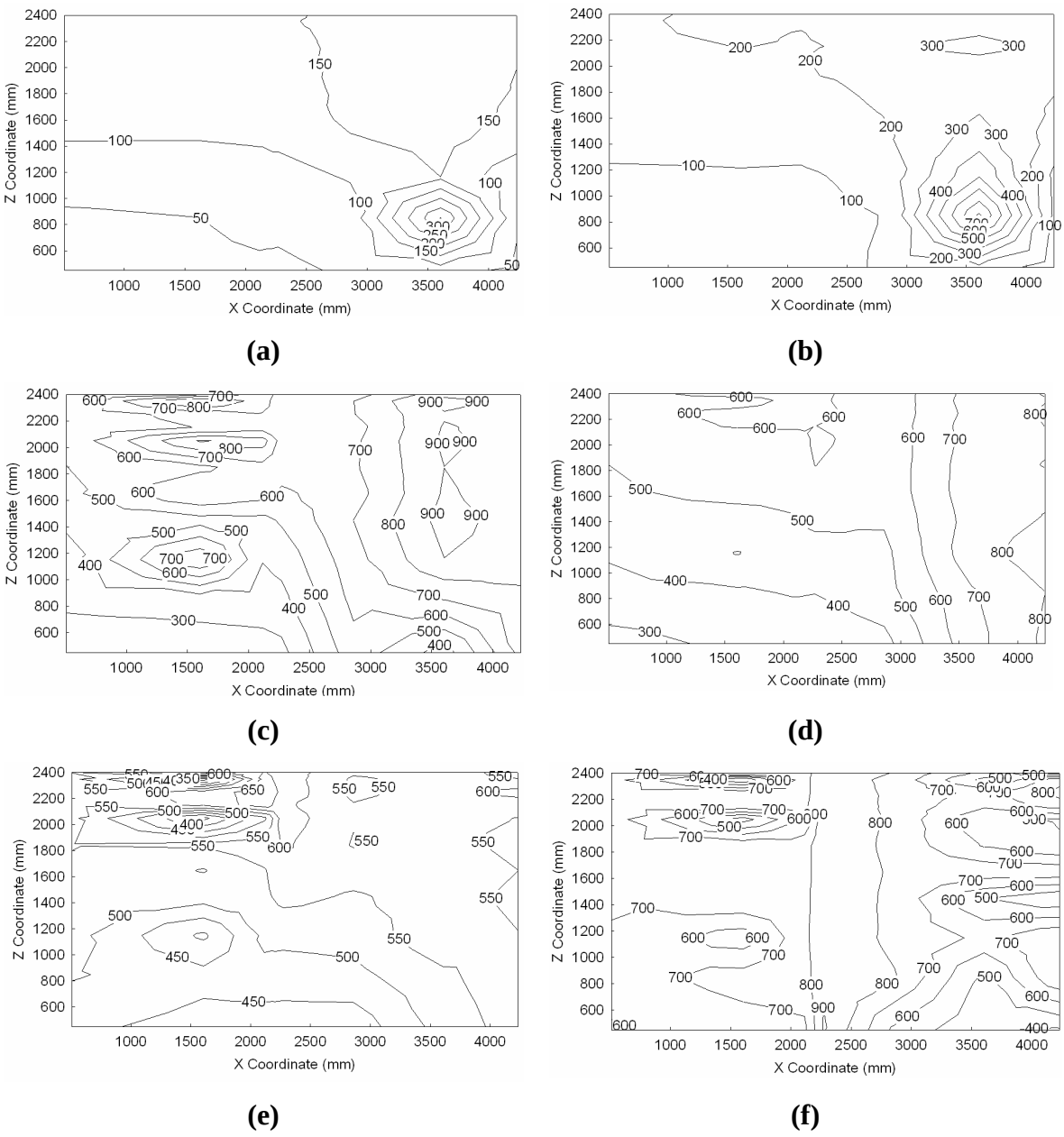

Figure 4.8. Test One gas-phase temperature contours (°C) at a vertical section S1-S1 running East-West through the experimental compartment (*cf*. Figure 4.3). Axes values read distances from the global origin (*cf*. Figure 4.3). The sections were taken at different time steps (time from ignition): (a) Time Step 1 (201s); (b) Time Step 2 (251s); (c) Time Step 3 (351s); (d) Time Step 4 (420s); (e) Time Step 5 (661s); and (f) Time Step 6 (901s).

4.3.2.2. Extinction Coefficient of the Smoke Layer

4.3.2.2.1. Smoke Layer Height

Thermocouple temperature measurements were used to determine the height of the smoke layer over time. 'Height' in this case indicates the vertical distance from the

floor to the base of the smoke layer, assumed to be at a uniform level. Hence the height evolution was taken as an average of the 100 ^{o}C isotherm height at any point in time until the smoke layer descended past the lowermost thermocouples, located at a height of 0.45 m from the floor. The variation of the smoke layer height derived from the 100 ^{o}C isotherm is shown in Figure 4.9. As the thermocouples were only located at discrete heights, the data were interpolated to provide a more detailed evolution of the isotherm.

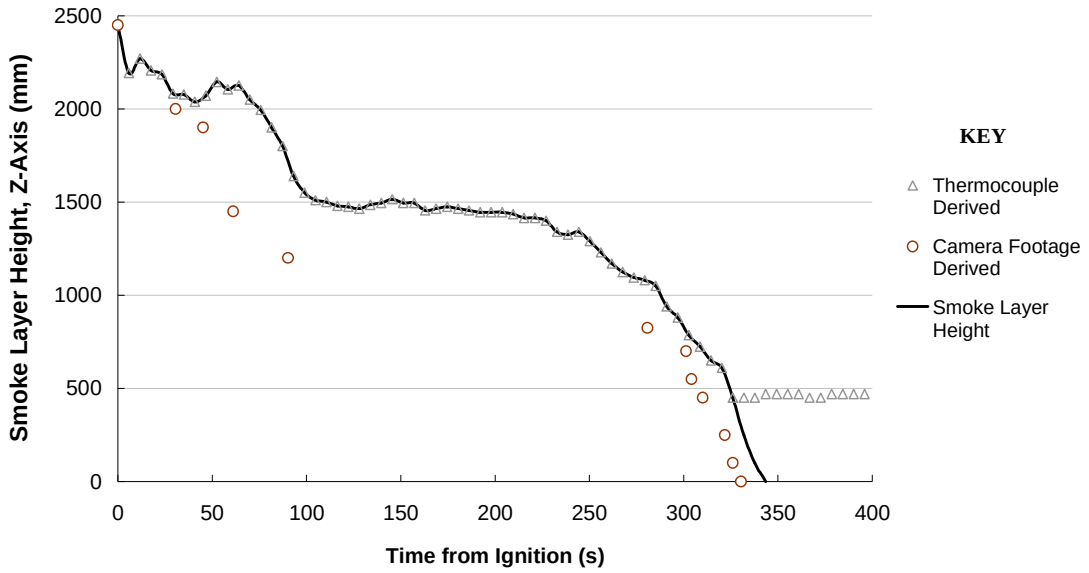

Figure 4.9. Height of the smoke layer boundary within the experimental compartment for Test One, derived from a combination of thermocouple data and visual estimates from camera footage.

Visual estimates from camera footage were used to verify the overall evolution of the smoke layer. The smoke layer height was identified when a visible sustained boundary layer reached the top of objects of known height. While these provide only crude estimates they were found to follow the isotherm data trend, as seen in Figure 4.9, establishing the 100 ^{o}C isotherm as a reasonable criterion for smoke boundary layer identification. Although there is some discrepancy between the data due both to the nature of visual estimates and the turbulent eddy flows that often create a slightly indistinct boundary layer between the evidently smoke-filled and non smoke-filled areas, these estimates provided the best available measure once the smoke layer grew beyond the lowermost thermocouple height. Hence the overall evolution of the smoke layer height shown in Figure 4.9 is derived from a combination of both sources and the smoke layer appears to have filled the compartment soon after flashover.

4.3.2.2.2. *Extinction coefficient*

Processed data from the horizontally aligned laser smoke obscuration sensors gives a measure of the extinction coefficient evolution of the gas-phase at each of the sensor heights, regardless of whether the sensors were engulfed in smoke or outwith the smoke layer. These extinction coefficient evolutions are shown in Figure 4.10.

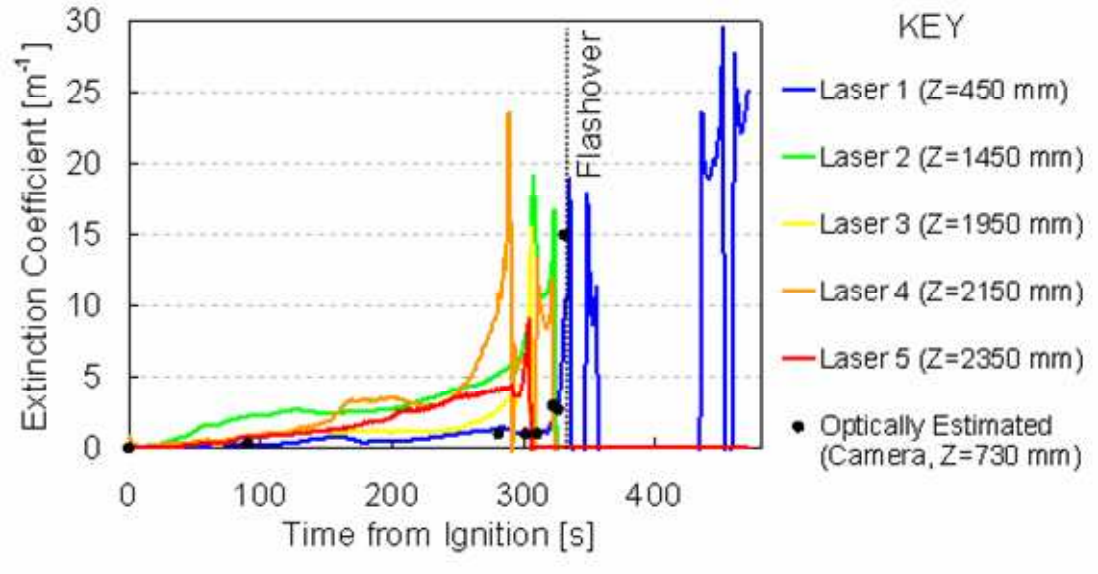

Figure 4.10. Test One evolution of the extinction coefficient of the gas-phase at several different heights.

The various measurements of the extinction coefficient shown in Figure 4.10, together with the evolution of the smoke layer height shown in Figure 4.9, enabled the calculation of a characteristic pre-flashover extinction coefficient of the smoke layer. At any point in time, the extinction coefficient of the smoke layer was established by averaging the data from only the obscuration sensors submerged in the smoke layer. Hence, an evolution of the extinction coefficient is obtained by averaging data from an increased number of sensors as the smoke layer descended over time. This shows a steady rate of increase in the extinction coefficient from 0 m^{-1} to 5 m^{-1} for 300 s from ignition. After the onset of flashover the laser obscuration data are seen to fluctuate erratically, most likely due to heat damage, and therefore are only considered reliable up to this point.

Camera footage was used also used to estimate the extinction coefficient as detailed in Section 4.2.5.2. Although this provides only a crude estimate, the extinction

coefficients derived by employing visual estimates of obstruction of objects at known distances are plotted against the sensor data in Figure 4.10. These optically estimated extinction coefficients show good agreement with the laser-obtained extinction coefficients, inclusive of a data point within the flashover period. In particular the data appears to match that of the lowest set of horizontal laser obscuration sensors (Laser 1), which was located at a similar height as the network camera used.

The optically estimated extinction coefficient is also seen to verify the steep increase in extinction coefficient around the onset of flashover, allowing for the trend to be extrapolated post-flashover as the smoke layer is known to have descended to the floor shortly after 300 s into the fire. In addition, the lowest laser obscuration sensor (Laser 1) output some data around 440-470 s that could be seen to fit such a trend post-flashover. Although its location is thought to have allowed this sensor to last longer than the others the reliability of this information is uncertain, particularly because high extinction coefficients equate to a very low voltage reading in the sensor, so any error become a larger percentage of the weaker signal. Therefore this data set has been used to define a range of bounds for the extinction coefficient beyond flashover. Post-flashover it is assumed the extinction coefficients remain constant. The upper bound stabilisation value estimated is an extinction coefficient of 25 m^{-1}, taking into account the last set of data output by Laser 1. The lower bound stabilisation value is taken at an extinction coefficient of 14 m^{-1} since this is the last value output by several sensors before they were damaged at flashover. These values are assumed to be constant from 400 s onwards and in the absence of adequate data for a better estimate, the extinction coefficient is assumed to grow linearly from 5 m^{-1} at 300 s to the upper or lower bound values at 400 s. Hence, an average extinction coefficient of the smoke layer can be taken as a linear growth from 0-5 m^{-1} between 0-300 s, followed by another period of linear growth from 5-20 m^{-1} between 300-400 s where the value is seen to stabilise at roughly 20 m^{-1} throughout the rest of the fire.

.

While it is appreciated that the laser sensors were only measuring smoke obscuration in one planar location and that the density is likely to have been spatially varied, particularly since the measurements were taken next to a wall (boundary layer), it is also deemed unlikely to have varied significantly given the dimensions of the

compartment and its ventilation conditions. Therefore, throughout the compartment, it is assumed that the extinction coefficient has only a vertical variation.

4.3.2.3. Heat Release Rate

Analysis of velocity probe data allows for an approximate quantification of the fire size in terms of the overall heat release rate (HRR). This provides the essential parameter characterising the fire source.

The evolution of the total heat release rate is derived from bi-directional velocity probe data using the principle of oxygen depletion calorimetry described by Huggett [119]. Since no calorimeter or gas sampling measurements are available, the calculation has been based on the assumption that all oxygen (23% air, by mass) is consumed within the compartment, giving an upper bound estimate of HRR. Therefore this means the calculation of the HRR is only possible for the period when fire flows becomes significantly dominant over ambient flows.

For the majority of the post-flashover period only the six probes located in the two compartment doorways are used for calculation of HRR, as the compartment window panes only broke towards the end of the observed post-flashover fire. The relative location of these probes within the doorways and just outside the window is detailed in Figure 4.11. Although the doorway velocity probe data are very localised and were seen to fluctuate considerably, a number of assumptions allow for an estimate of the magnitude of the characteristic HRR throughout the fire.

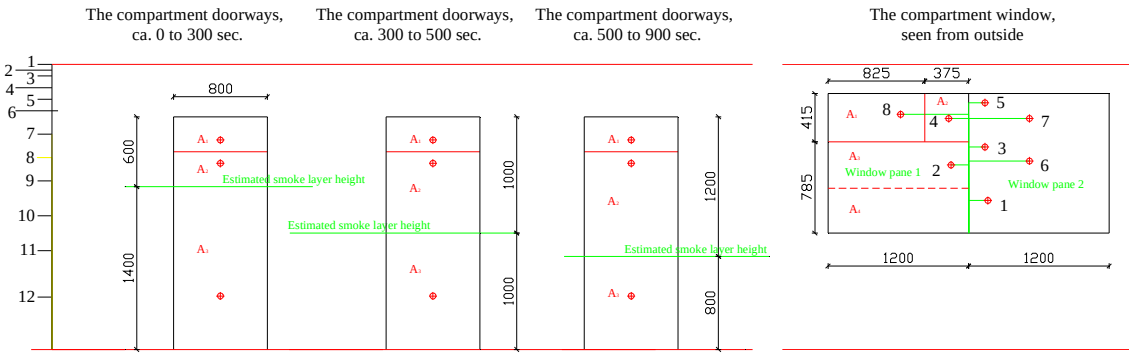

Figure 4.11. Bi-directional velocity flow probes at the doorways and window, labelled with the assumed areas represented by each probe measurement for different periods of Test One. Thermocouple tree heights are labelled to the left, for comparison.

The total gas mass inflow and outflow derived from the velocity probe data, based on the average areas each probe represents at different stages throughout the fire shown in Figure 4.11, are found to be imbalanced, particularly in the early post-flashover period where a deficit of mass inflow is registered. There are a variety of possible reasons for this variation, namely the limited number of probes and the location of these probes. The lowermost probes were at 0.46 m and 0.43 m from the floor in Doors 1 and 2, respectively, and therefore may not have accounted for the majority of the inflow area once the smoke layer descended below this height post-flashover.

Further to the probe heights, the local temperature values used to calculate the gas density surrounding the probes in both doorways are those singly measured by the thermocouples in Tree 4, located in between both doors (*cf*. Figure 4.3). This tree is a horizontal distance of 0.25 m away from the probes in Door 2 and 0.93 m from those in Door 1, with a negligible vertical discrepancy. This means the same local gas density is assumed for probes at similar heights in both doorways, when in reality these were likely to be quite different due to distinct ventilation flows resulting from the flat geometry and relative location of ventilation openings. Hence, an average of both mass inflow and outflow is used to determine the fire HRR, ensuring the mass balance of both. Assuming complete combustion of all oxygen, Huggett's formula [119] can be applied to estimate the heat release rate plotted in Figure 4.12. For the case of Test One, this method is only deemed to be applicable from around the time of Time Step 2 when fire flows became dominant over ambient flows hence the HRR for the initial fire growth period – represented by a dotted line in Figure 4.12 – is only indicative of the approximate HRR expected.

Due to the number of assumptions involved in the assessment of HRR, a check is performed using estimated ventilation factors to compute mass inflow rates for different periods throughout the ventilation-controlled, post-flashover fire. Compartment ventilation factors were calculated for each ventilation condition, in the form of Vent Cases [120]. In Vent Case 1 it is assumed that 30% of the kitchen window area was open and that 50% equivalent (in height reduction) of the flat hallway area was open to simulate the initial ventilation conditions beyond Door 1. Once the kitchen window shattered this was taken into account in the ventilation factor of Vent Case 2. Similarly, when the compartment NW window pane broke (*cf*.

Figure 4.5), this was integrated in the conditions for Vent Case 3. Final Vent Case 4 includes ventilation from both compartment window panes further to the kitchen window and initial conditions. Again implementing the principle of oxygen depletion calorimetry [119] and assuming complete combustion of oxygen to obtain basic HRR values, these cases are plotted against the probe-data derived values in Figure 4.12 and indicate good agreement between both methods. *Ad hoc* laboratory tests, described in Section 4.4.4, were conducted using calorimetry to determine the average heat release rate of replica items of furnishings used in Test One. Data from these tests is also used to verify that the magnitude of the global HRR values is within the expected range.

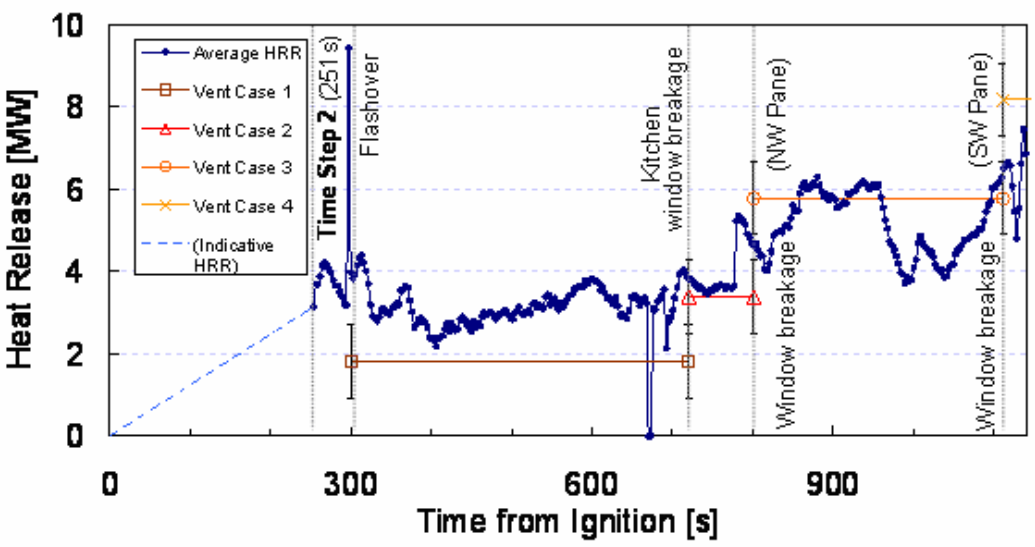

Figure 4.12. Heat release rate of the Test One fire as estimated using the principle of oxygen depletion. Alternative simplified estimates using ventilation factors for the calculation of HRR are shown as Vent Cases (with error bars) corresponding to different ventilation change events. Timing of some major events is represented by vertical dotted lines, as labelled.

The overall heat release rate trend seen in Figure 4.12 corresponds to that of the average compartment temperature in Figure 4.7. The HRR is seen to grow from a quasi-steady-state 3MW fire to a larger ~5MW fire around the time when the first compartment window breaks, accountable also for the distinct increase in average compartment temperatures between Time Steps 5 and 6 seen in Figure 4.7. Although this is a relatively crude measurement of HRR it provides a good indication of the order of magnitude of the fire size throughout Dalmarnock Fire Test One.

4.3.2.4. Heat Flux to the Surroundings

Heat flux measurements have also been used to characterise the fire. Spatial variation of heat flux can lead to varying severity of structural exposure to fire, which will influence the structural response, rendering heat flux an important fire characteristic for structural analysis.

Heat flux gauges located across the compartment ceiling and on the kitchen partition wall were spaced in order to provide a representation of the global distribution of heat flux incident on those surfaces. Contour plots for the net heat flux incident on the compartment ceiling are shown in Figure 4.13 for each key time steps described in Table 4.3, providing a comparison of the heat flux evolution as the fire developed. The approximate area of the ceiling represented by the heat flux measurements is shaded over a plan view of the compartment shown in Figure 4.3.

Patterns of peak net heat flux incident on the ceiling over time, shown in Figure 4.13, correlate to the sharp rises in gas-phase temperature seen in Figure 4.7, particularly the distinct ten fold rise in heat flux to the ceiling between Time Steps 2 and 3 (*cf*. Figure 4.13 (b) and (c)). Similarly, there is a notable increase in global heat flux incident on the ceiling between Time Steps 5 and 6 (*cf*. Figure 4.13 (e) and (f)), corresponding to an average compartment temperature rise once ventilation conditions change. The contour plots also demonstrate a tendency for higher fluxes towards the back of the compartment, over the sofa and heavily fuel-loaded NE corner, particularly as the flaming fire develops between Time Steps 2 and 6 (*cf*. Figure 4.13 (b)-(f)). This illustrates how regular compartment fires can lead to a varying gradient of insult to a single structural component (*i.e.* beams, floor slabs, *etc*.). Similar conclusions can be drawn from contour plots of heat flux incident on the kitchen partition wall in a study detailed by Amundarain [107].

The heat flux data have been used to assess the heat transfer to the respective internal structural components. Together with other the structural-monitoring sensors, this enabled analysis of the behaviour of the structure, under the insult of the Test One fire [107-110].

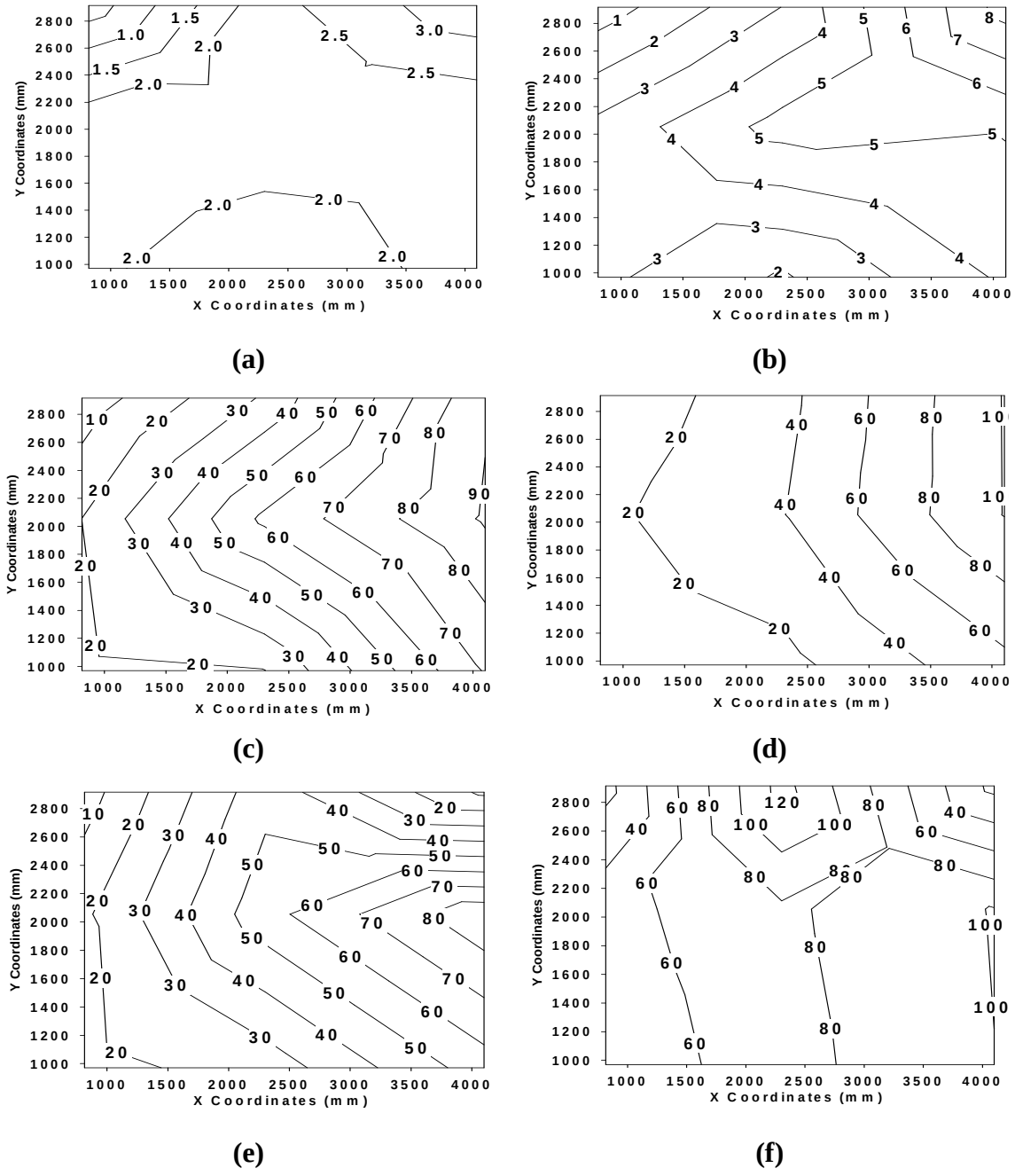

Figure 4.13. Contour plots of heat flux (kW/m^2) incident on the experimental compartment ceiling region corresponding to the shaded area shown in Figure 4.3. Axes values read distances from the global origin (*cf.* Figure 4.3). The contours were taken at different time steps (time from ignition): (a) Time Step 1 (201s); (b) Time Step 2 (251s); (c) Time Step 3 (351s); (d) Time Step 4 (420s); (e) Time Step 5 (661s); and (f) Time Step 6 (901s).

4.3.3 The External Flaming and Resultant Heat Flux

Post-flashover some external flaming was observed once the compartment window panes shattered. Although some smoke was seen to emerge from the vicinity of the window early on, this exhaust seeped mostly through gaps in the poorly sealed window frame while the window panes were still intact. Smoke emerging from the openings in Bedroom-2 was also blown in the direction of the window by wind. The data associated with this early period of smoking is not considered to form part of the characteristic 'external flaming' that ensues during the fully-developed period of a fire, once the compartment window panes break.

4.3.3.1. Major Events Observed

External flaming, constituting both visible flaming and a dense smoke plume of combustion products, occurred only towards the later stages of the fire (after Time Step 5) hence a different time frame of analysis is required than that used for the characterisation of the internal fire. External thermocouple and heat flux data are most significant within the final 5-6 min period of the fire, from about 800 s onwards (*cf.* Table 4.3). This coincides with the (forced) breakage of the compartment NW window pane at 801 s (13 min 21s from ignition), shortly before a large plume of dense combustion and partial-combustion products and intermittent visible flame emerge from the opening. A south wind is seen to tilt the flame and plume northward, wrapping the smoke plume around the NW corner of the building. For the subsequent four and a half minutes both smoke and flame vented from the compartment with varying intensities and often the visible flame was mostly obscured from view as it was surrounded by copious amounts of dense smoke. Although the general tilt of the flame was northward, there were occasions when the local wind direction appeared to die down and gusting saw the plume tilt southward at one point, however these variations were not sustained. The intermittency and length of the visible flame also varied considerably during this period. Combustion of the wooden window frame meant localised flames were observed, however these are not considered as part of the external flaming.

About four and a half minutes after the NW window pane was broken, the visible external flaming became more prominent. The flame depth and flame projection

increased and although part was still intermittent and considerably turbulent a larger portion of persistent flaming was observed. This was sustained for about 30 s before the SW window pane broke (fire-induced), leading to the most pronounced period of external flaming. Flames were seen to emerge from the whole width of the compartment window with a clear area of persistent flaming giving a more distinct outline of the flame shape. Although the brighter area of the flame appeared to have a flame projection of about 0.4-0.5 m (from façade to flame axis), this was surrounded by fainter areas of flame and hot combustion gases such that the flame was not distinctly projecting away from the façade. This flaming was sustained for a further 30 s before the fire brigade intervened to extinguish the fire.

Analysis of some of the external data pre-external flaming allows for an evaluation of the significance of the initial smoke seepage with regards to external heat flux to the façade, compared to that imposed by the latter external flaming. However it is the latter 5-6 min of the fire (13 min 20 s – 19 min from ignition) that are associated with external flaming, only the last minute of which resembles a sustained period of steady-state external flaming.

4.3.3.2. External Gas-Phase Temperature

External thermocouple trees were arranged such that temperature contour plots can be used to map the evolution of the three-dimensional variation of the external flaming. Unlike the internal compartment gas-phase thermocouple data, the external thermocouple temperature measurements have not been corrected for radiation errors as application of the correction methodology in external flows requires a good knowledge of the local velocity fields [111]. Despite the deployment of velocity probes in the main window opening there are several other external influences on the local flows which are difficult to quantify. The exit velocity of the flame was then affected by considerable swirling of the highly turbulent plume as it vented away from the opening. The velocity of the gases surrounding the thermocouples was further affected by the external environmental conditions and local air entrainment. Although the overall affect of the south wind saw the flame tilt mostly to northward, there were periods of varied wind velocity and gusting that also affected local velocities. The significance of these external influences is evident from the effect they have on the

plume geometry, exemplified in the two images of the plume (seen from below) shown in Figure 4.14, taken 12 s apart. Hence the level of accuracy involved in estimating the evolution of local flow renders the thermocouple temperature corrections unjustified. In any case, the thermocouple radiation error is not expected to be large. Therefore external thermocouple measurements have been assumed to correspond to gas-phase temperatures for the purposes of this analysis.

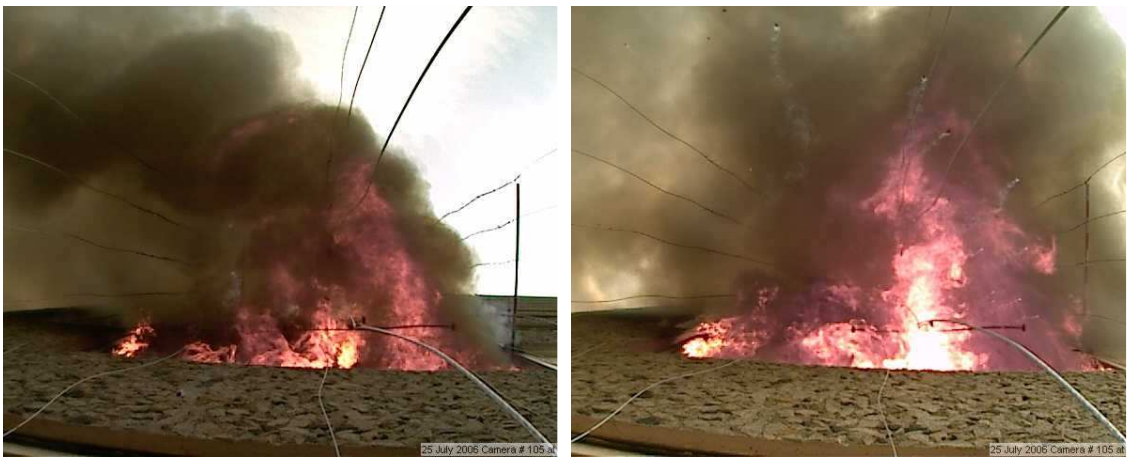

(a) **(b)**

Figure 4.14. Two plan view images of the flames emerging from the Test One experimental compartment window, 12 s apart. The images were obtained from camera footage taken at 3rd floor level looking up at the external flaming (*cf*. Figure 4.5). The extent of change in local velocities is highlight with: (a) a distinct south wind (1116s after ignition at 12:41:36); and (b) flow velocities dominant over lighter wind (1128s after ignition at 12:41:48).

During the initial growth stage of the fire the external temperatures remained mostly at ambient, with the exception of localised temperature rise in the vicinity of the window soffit, close to the gaps through which some smoke and hot gases seeped. At flashover a temperature rise is noted in all external temperature measurements with post-flashover temperatures ranging from just over ambient to about 240 ^{o}C prior to the breakage of the NW window pane. Again, the higher temperatures were registered in the vicinity of the window soffit where smoke was seen to emerge. Following breakage of the first window pane most thermocouples in the NW half of the arrangement registered a further significant increase in temperature, such that temperatures at up to 1 m above the window soffit ranged from 300-750 ^{o}C. Nevertheless temperatures in the SW half of the arrangement remained relatively unaffected until the SW window pane shattered and temperatures quickly soared, with

those close to the window soffit peaking at 860 ^{o}C. The temperature evolution at soffit level outside the centre of the NW window pane, close to the façade, is plotted in Figure 4.15, together with other temperature measurements from the thermocouples in external Tree 5 (*cf.* Figure 4.3), the heights of which are given in the key relative to the window soffit. Similar temperature evolutions are provided in Figure 4.16 for measurements from thermocouples vertically aligned just outside the centre of the SW window pane for comparison.

The temperature measurements obtained allow for a 3-D representation of the plume evolution throughout the duration of the fire, however for the purposes of characterisation of the external flame, the period of sustained external flaming towards the end of the fire is of greatest interest. Since the stage of the fire yielding the highest external temperatures was only allowed to burn for 30 s (after the SW window pane broke), this period is assumed as the best representation of the steady-state external flaming associated with the greatest heat flux insult to the surroundings. Although examination of the combustible contents remaining after the fire was extinguished shows the fire could not have burnt for much longer than a few minutes, the temperature and heat flux trends suggest no signs of imminent decay. Hence had the fire been allowed to develop to burn out, it is likely the conditions seen in the last 30 s of the fire would have been sustained for a few minutes longer. Figure 4.17 shows a set of 2-D temperature contours through sections of the external plume taken instantaneously at 1135s (12:41:55) after ignition and just prior to fire brigade intervention. The frontal elevation shown in Figure 4.17 (a) is taken through the set of trees offset at 0.25 m away from the façade (E8-E10). The lateral elevation in Figure 4.17 (b) is taken perpendicular to the façade along the centreline of the window and Figure 4.17 (c) shows a horizontal cross-section through the plume at window soffit level. These are assumed to provide a general representation of the main characteristics of the steady-state external flame.

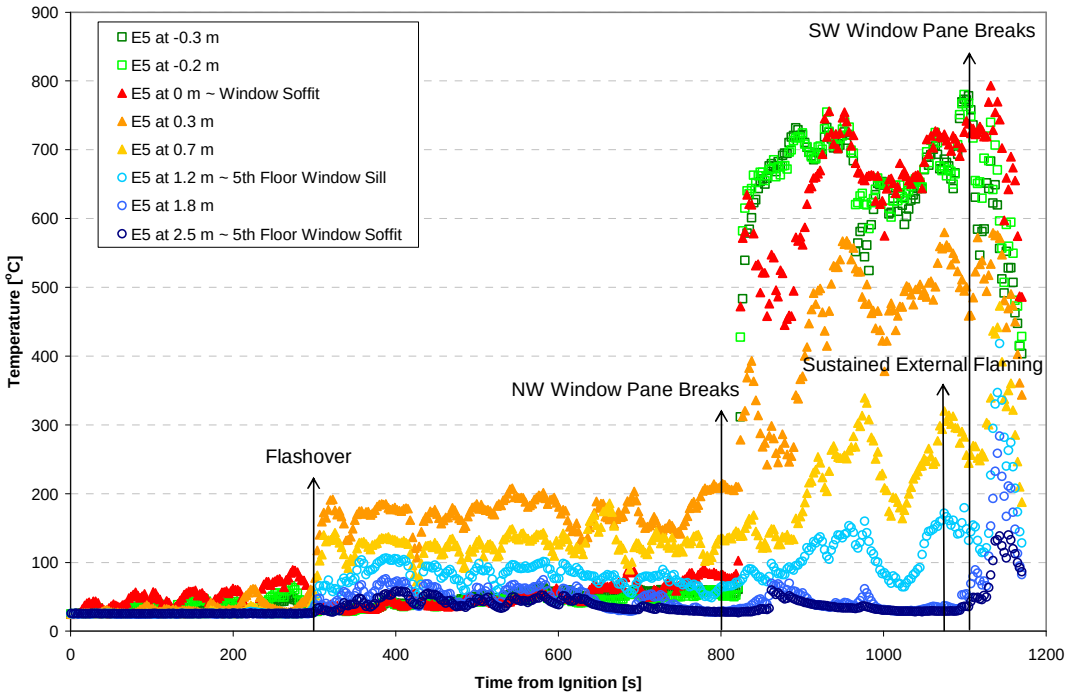

Figure 4.15. Temperature evolution throughout the Test One fire measured by thermocouples in external Tree 5 (E5, *cf.* Figure 4.3), aligned vertically outside the centre of the NW window pane, close to the façade.

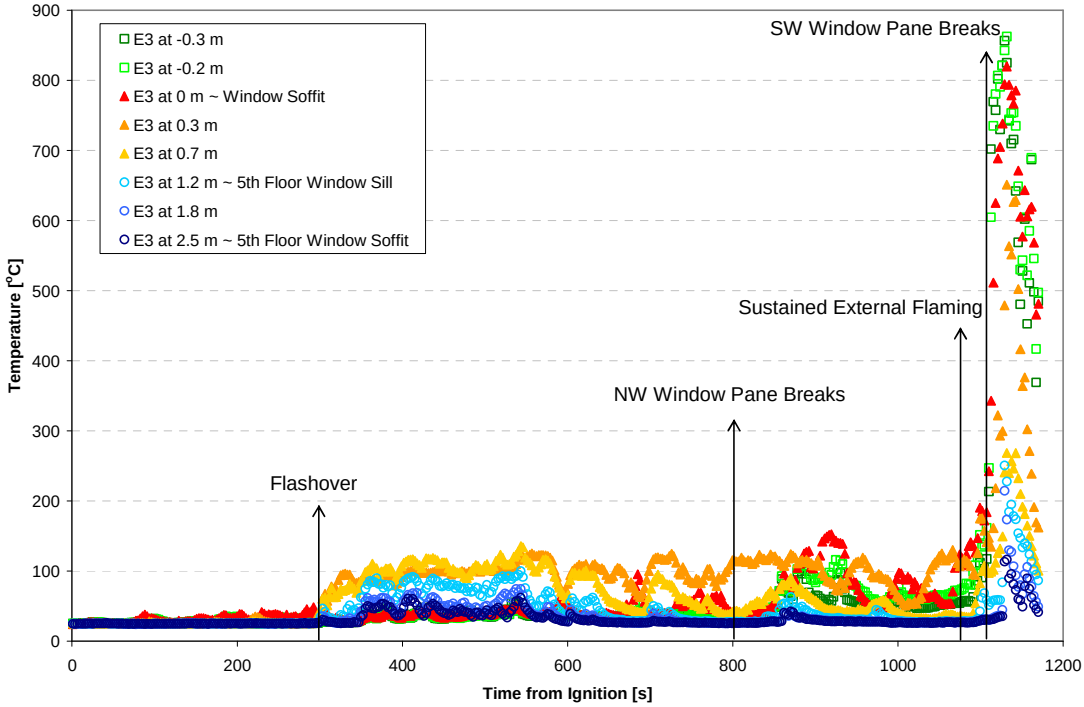

Figure 4.16. Temperature evolution throughout the Test One fire measured by thermocouples in external Tree 3 (E3, *cf.* Figure 4.3), aligned vertically outside the centre of the SW window pane, close to the façade.

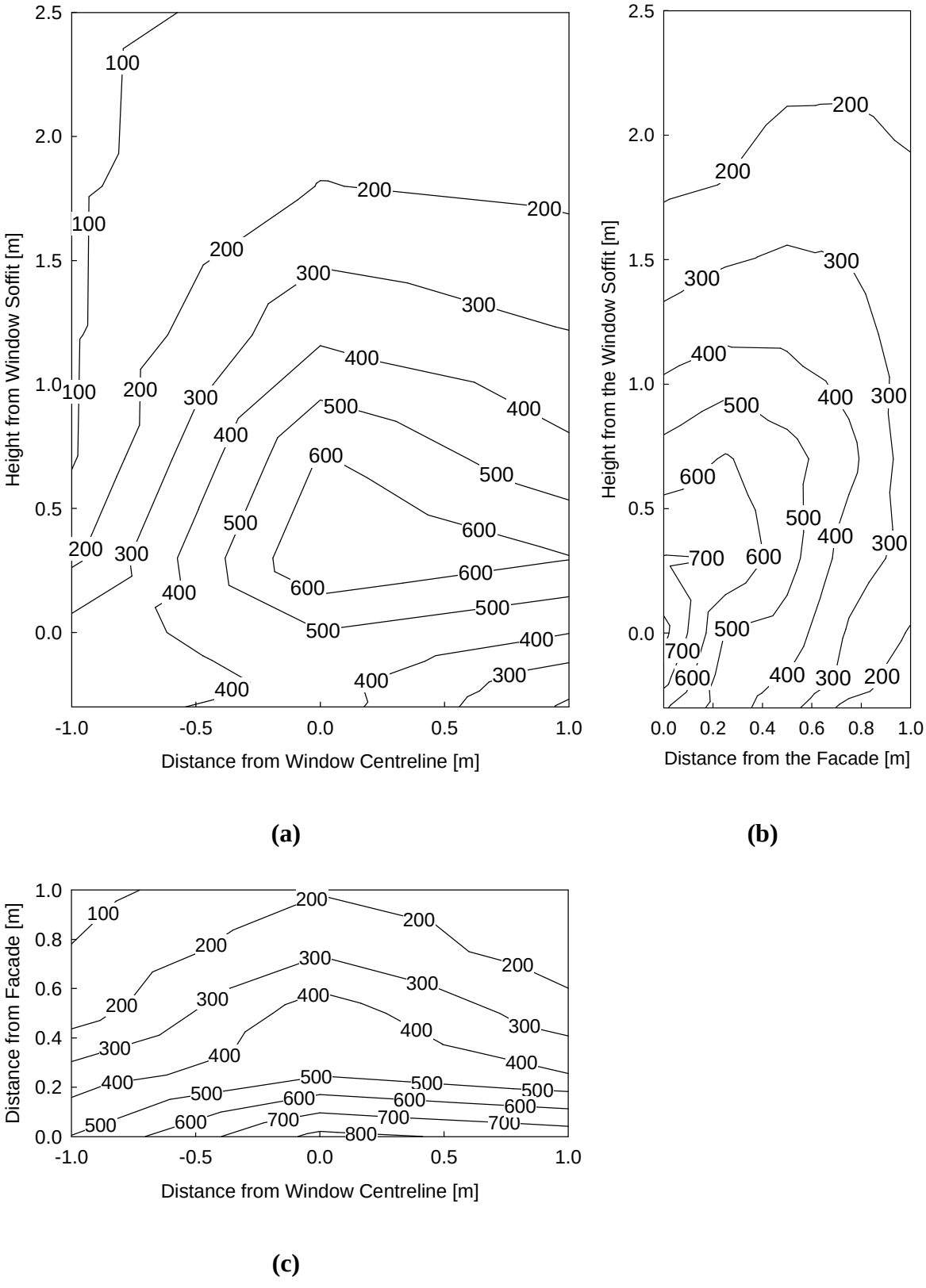

Figure 4.17. Temperature contours (°C) of the external plume during Test One taken 1135 s after ignition (at 12:41:55). The sections represented are: (a) S2-S2, a front elevation; (b) S3-S3, a lateral elevation through the centre of the window; and (c) a horizontal section at window soffit level. Refer to Figure 4.3 for an indication of the section locations relative to a plan view of the compartment.

For the purposes of characterising the flame width, it is worthy of note that temperatures measured by the two thermocouple trees located just over 0.3 m either side of the window did not register temperature as high as those opposite the window, as expected. In fact, temperatures along the height of Tree 1, to the south of the window remained very close to ambient temperature throughout the fire and only once the SW window pane broke did the temperature begin to rise, reaching only a peak of 70 ^{o}C before the fire was extinguished. Those in Tree 7 to the north of the window saw a higher range of temperatures as the wind tilted the plume in its direction. Nevertheless the temperature range seen once the NW window pane broke was 50-440 ^{o}C, with the more elevated temperatures registered between 0.7-1.2 m above the window soffit.

4.3.3.3. External Heat Flux to Façade

Pre-flashover external heat flux gauges all registered an average heat flux of 0.5-1 kW/m^2. This low heat flux was likely due to a combination of exposure to radiation from the sun, exposure to some heat transfer from the limited quantities of smoke and hot gases escaping from the experimental compartment through gaps around the window frame, and also due to experimental errors involved in the gauge calibration process [105]. At flashover a surge in external heat flux is registered by the five gauges aligned across top of the window soffit, with an average momentary peak of 7 kW/m^2. Throughout the post-flashover period prior to breakage of the NW window pane, average heat flux measurements remain at about 0.5-2 kW/m^2 for all gauges other than those just above the soffit which on average registered 3-4 kW/m^2.

Once the NW window pane was breached the heat flux gauges closer to the window soffit registered a steady increase in heat flux, which became most pronounced in the two gauges located just above the soffit along the NW window pane, as expected. Throughout the period of initial intermittent external flaming the heat flux just above the NW half of the soffit fluctuated considerably peaking momentarily at 24 kW/m^2, as seen in Figure 4.18. At the centre of the window arrangement the heat flux peaked at 8 kW/m^2 just above the soffit, decreasing both with height from the window and towards the SW side of the window. Around 1000 s after ignition a general dip in heat flux to the façade is noted to coincide with a dip in external flaming temperatures

shown in Figure 4.15, in turn corresponding to visual records of short period of lesser external exhaust. This is soon followed by a period of pronounced flaming with a greater portion of persistent flaming, in turn corresponding to yet another increase in external temperatures and heat flux to the façade. Throughout the last minute of sustained flaming the overall heat flux to the façade rises considerably, momentarily peaking at 62 kW/m^2, just above the centre of the soffit before the fire is extinguished.

Within the period assumed to be most representative of steady-state external flaming, the heat flux was greatest along the centreline above the window with a peak heat flux of 34 kW/m^2 recorded at 0.85 m above the window and 11 kW/m^2 at 1.35 m above the window. Notably the peak heat flux at 1.1 m above the window centreline was considerably lower than that at 1.35 m. This could have been due to projection and reattachment of the flame or a pocket of trapped air, however the gauge logged only reasonably low values of heat flux throughout so it may have been faulty. Nevertheless the data indicate a higher heat flux would be expected at this portion of the façade had the plume not been significantly deflected by wind as both gauges on the NW pane of the 5th floor window recorded peak heat fluxes of circa 13-14 kW/m^2.

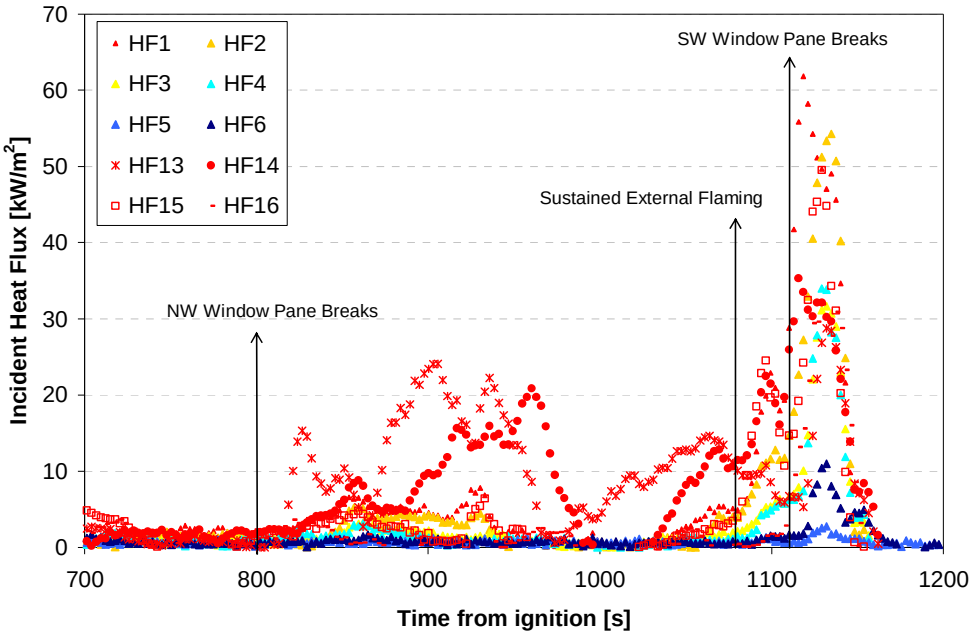

Figure 4.18. Evolution of the heat flux incident on the façade area between the window soffit and the bottom sill of the 5th floor window. This shows only the time period from just prior to the initial window pane breakage to artificial extinction. Refer to Figure 4.5 for relative location of the heat flux gauges. All data in red corresponds to the gauges running just above the window soffit.

4.4 Characterisation of Dalmarnock Fire Test Two (DFT2)

4.4.1 Major Events Observed

Test Two was ignited in the same manner as Test One the following day at 11:54:00. In this case the waste-paper basket contained crumpled newspaper soaked in 300ml of heptane, slightly less accelerant that used in Test One. The time delay between pouring the accelerant and igniting the fire also varied, but this difference is not significant to the general behaviour over the timescale of the fire as the accelerant only contributed to the momentary ignition of each fire and was fully consumed within seconds [106].

As in Test One, the fire quickly spread from the bin to the blanket draped over the side of the sofa and eventually on to sofa cushions. The technician who lit the fire swiftly left the flat and the two doors to the main fire compartment and the front door of the flat were closed via the remote 'command and control' centre outside the building. Since the aim of this test was to achieve smoke evacuation it is interesting to note that the early-warning smoke detection systems activated 12 s post ignition. Shortly thereafter, the both window panes were opened by remote control allowing smoke to vent out. About a minute and a half post ignition, the north end of the sofa was alight. By this stage a clearly perceptible, light grey smoke layer, characteristic of a localised fuel-controlled fire, had formed to a depth below the top of the compartment's door frames. Thus, the door from the main fire compartment to the kitchen was opened to allow smoke to vent out via the kitchen window. This resulted in a visible reduction of the smoke layer within the main compartment. Nevertheless the sofa fire was slowly spreading and three minutes post ignition, all cushions decorating the sofa were alight. The door linking the fire compartment to the corridor was thus opened to allow further smoke evacuation through the rest of the flat, closely followed by the remotely operated opening of the flat's front door to allow further ventilation to the main access corridor. This final alteration of the ventilation conditions occurred four minutes after the ignition of the waste-paper basket [106].

Similar to Test One, the fire spread from the sofa to the bookcase closest to the ignition source and later spread to engulf the whole sofa. Once the bookcase ignited,

with rapid upward flame spread, the smoke layer began to accumulate despite the abundant ventilation. From then on, the growth rate of the fire noticeably increased, with ceiling jet flames seen to travel across the compartment in what appeared to be the beginning of a transition to flashover, away from a fuel-controlled fire [21]. A thicker, darker smoke layer, more indicative of a ventilation-controlled fire was seen to rapidly fill the compartment and the fire brigade intervened to extinguish it, little over five and a half minutes after ignition. Hence, contrary to Test One, the fire was not allowed to reach fully-developed conditions. Details of the precise timing of each of these major events can be found in Table 4.4.

Major events observed	**Time** (h:m:s)	**Time from ignition** (s)
Ignition	11:54:09	0
Blanket ignites	11:54:10	1
Smoke detection systems activate	11:54:21	12
Technician leaves and front door closes	11:54:27	18
Fire compartment door to kitchen is closed	11:54:35	26
Fire compartment door to corridor is closed	11:54:36	27
Both compartment window panes open	11:54:37	28
Front door is fully closed	11:54:44	35
Both window panes are fully open	11:54:53	44
Sofa ignites	11:55:39	90
Smoke accumulation in main compartment	11:55:51	102
Fire compartment door to kitchen is opened	11:55:53	104
Substantial amount of smoke is evacuated	11:56:12	123
Sofa cushions fully burning	11:57:04	175
Fire compartment door to corridor opened	11:57:08	179
Front door is opened	11:58:12	243
Bookcase begins to burn	11:58:37	268
Sofa becomes fully involved in fire	11:59:25	316
First ceiling jet flame occurs	11:59:35	326
Fire Brigade intervention	11:59:41	332

Table 4.4. List of major events observed via camera footage of the Test Two fire. Respective clock time and time elapsed from ignition is given.

Once the fire was fully extinguished the aftermath of the fire was clearly very different to that of Test One. The sofa structure was still considerably intact although a large portion of the polyurethane foam base and back had been consumed. Most items on the bookshelves were heavily singed but not fully consumed, with all bookcases still left standing. Towards the west side of the compartment, the tables and desks also had several singed items but many were left undamaged.

4.4.2 The Internal Compartment Fire (DFT2)

4.4.2.1. Compartment Gas-Phase Temperature (DFT2)

As for Test One, Test Two had a large density of thermocouples measuring gas-phase temperature throughout the compartment. These enable a 3-D evolution of the spatial distribution allowing for detailed characterisation of the temperature gradients throughout the course of the fire. Nevertheless, for the purposes of comparison with the general fire conditions in Test One, the average compartment temperature is used. Gas-phase temperatures were employed by correcting the thermocouple temperatures for radiation errors according to the method described by Welch *et al.* [111]. Nevertheless the overall corrections required were negligible, comparable to the experimental errors inherent in the measurements taken [105,106].

The compartment average gas-phase temperature-time curve, presented in Figure 4.19, shows the general behaviour to match the sequence of major events observed (*cf.* Table 4.4). This is plotted against the standard deviation which gives an indication of the degree of temperature homogeneity throughout the compartment. The first 200s of burning saw fairly low average compartment temperatures associated with a low standard deviation. This is indicative of the small localised fire and the adequate venting of smoke by remote control of the ventilation openings, preventing a distinct temperature rise throughout the compartment. Throughout the growth stage of the fire, the doors and windows were opened when data streamed live to the remote 'command and control' centre indicated the temperatures were beginning to rise. Figure 4.19 shows that these prompt changes in ventilation conditions are in general immediately followed by a slight decrease in rate of average compartment temperature rise. Hence while the fire is confined to a single major fuel source the attempts to limit its growth

through changes in ventilation conditions appear to have a favourable effect. Nevertheless, once the fire spreads to a second major fuel package – in this case the bookcase – the fire experiences a period of rapid growth and becomes unaffected by changes in the environmental conditions. Correspondingly the standard deviation grows as more items in the NE corner become engulfed in flame, in turn leading to the development of the smoke layer and resulting in larger instantaneous temperature gradients generated throughout the compartment.

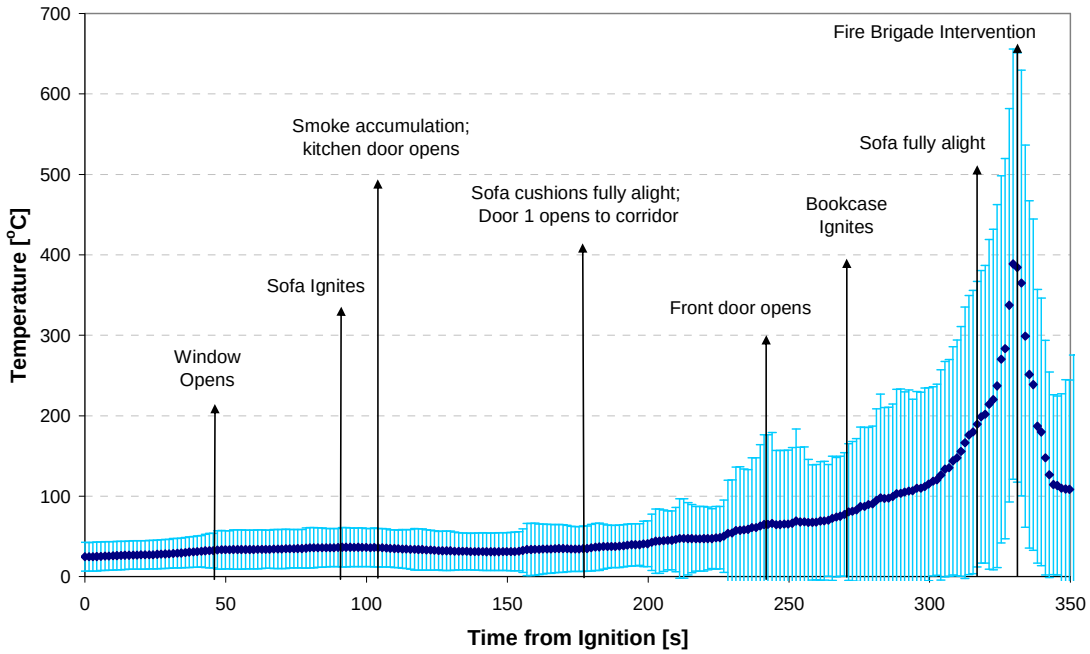

Figure 4.19. Evolution of the average compartment gas-phase temperature. The shaded region indicates the standard deviation of temperature throughout the compartment. Vertical dashed lines indicate Time Steps used for analysis and dotted lines represent time of some major events, as labelled.

As the fire quickly spreads up the bookcase and the conditions in the compartment become increasingly untenable, the radiation from the flames and from the growing and darkening smoke layer contribute towards the pyrolysis of materials which in turn leads to a faster rate of fire spread. This is evident from the global increase in compartment temperatures and in standard deviation. As the average compartment temperature begins to soar, the fire spreads to engulf the rest of the sofa and the onset of flashover becomes inevitable. Five and a half minutes into the fire, the fire brigade intervened and temperatures are seen to drastically decrease.

4.4.2.2. Other Components of the Test Two Fire

Further to characterisation of the compartment temperature evolution, the data collected during Test Two also allows for characterisation of the smoke layer height and its associated extinction coefficient, and for a mapping of the evolution of the heat flux to both the compartment ceiling and the kitchen partition wall. These further components of the fire allow for a global assessment of the efficiency of the test in demonstrating sensor-assisted smoke management, highlighting the potential for sensor-assisted fire-fighting as envisioned by the FireGrid project [24,25]. Nevertheless, for the purposes of this research the characterisation of Test Two is of most interest for highlighting the repeatability and robustness of the test setup. Since Test Two was not allowed to grow to fully ventilation-controlled conditions, no measure of its heat release rate is available. Therefore the evolution of the compartment temperatures provides the best representation of the overall evolution of the fire for the purposes of comparison against Test One. Details of the complete characterisation of Test Two, including temperature contour plots taken through the same S1-S1 section of the compartment as that in the characterisation of Test One, are provided by Cowlard *et al*. [106].

4.4.3 Benchmarking the Dalmarnock Fire Tests

A common problem associated with large-scale (or full-scale) fire tests is the repeatability of the results. Most large-scale tests tend to produce a set of results that will depart from the results of a re-run of the same test. While simple pool fire experiments [21] and *standard* large-scale tests [121] are reasonably repeatable, many *realistic* fire tests do not follow the same trend. In many cases, the variability of the results is associated with ignition conditions and changes in ventilation, relative to the distribution of fuel. Consequently, comparison between deterministic numerical model output (which will always give the same answer for the same input; *e.g*. the Law Model) with *realistic* fire scenarios is generally deemed an unreliable comparison. In these tests repeatability was addressed by varying both the ignition protocol and the ventilation conditions while maintaining the same scenario in terms of fuel distribution. By varying the ignition source and the environmental conditions within reason, a measure of the robustness of the test setup can be established.

Although Test One was a freely growing fire that attained post-flashover conditions and Test Two was curtailed just at the onset of flashover, the similarities in the setup of the two tests render a comparison of the major events during the initial growth period of the two fires useful for assessing the repeatability and hence benchmarking the scenario.

For the ignition protocol, the amount of accelerant used and the time delay between pouring the accelerant and ignition were varied, the range of 'acceptable' variation having been defined from laboratory test results [122]. The impact of this variation on the main timeline of the fire is seen to be minor as the subsequent ignition of items nearby occurs at a comparable time after ignition in both tests. This was ensured by initiating the fire with a well established waste-paper basket fire (in the form of a waste-paper basket with liquid fuel) placed adjacent to a flammable item of furniture which guaranteed a large initiation event regardless of the particular amounts of accelerant. Additionally the main fuel items in the vicinity of the ignition point were arranged in a configuration very similar to the ISO room corner test [121] allowing for entrainment to generally drive the flames towards the heavily fuel laden NE corner. The lack of effect this variability in the ignition protocol has on the subsequent development of the fire demonstrates the procedure is significantly robust.

The potential variability arising from ventilation conditions was addressed as one of the major variables between the setup of Test One and Test Two as discussed in Section 4.2.4. Comparison of the average compartment temperature evolution plotted in Figure 4.20 shows the different ventilation regime adopted in Test Two allowed for average compartment temperatures to remain under 40˚C, which were significantly lower that the > 100˚C average observed in Test One, for the first three minutes of the fire. Together with inducing a reduction in the level of smoke, strategic venting of the early fire allowed for an increase in the duration of tenability of the compartment compared to that of the Test One fire. Despite these differences in environmental conditions, the ignition of the bookcase in both tests occurs within seconds of each other, circa 270 s post ignition. This highlights the robustness of the test with regards to variation in ventilation conditions (pre-flashover). Furthermore, in both cases the ignition of this second major fuel package leads to rapid fire growth, with the

transition to flashover occurring again within a comparable time scale in both tests, as is evident from the peaks in Figure 4.20, despite the earlier lag in average compartment temperatures in Test Two.

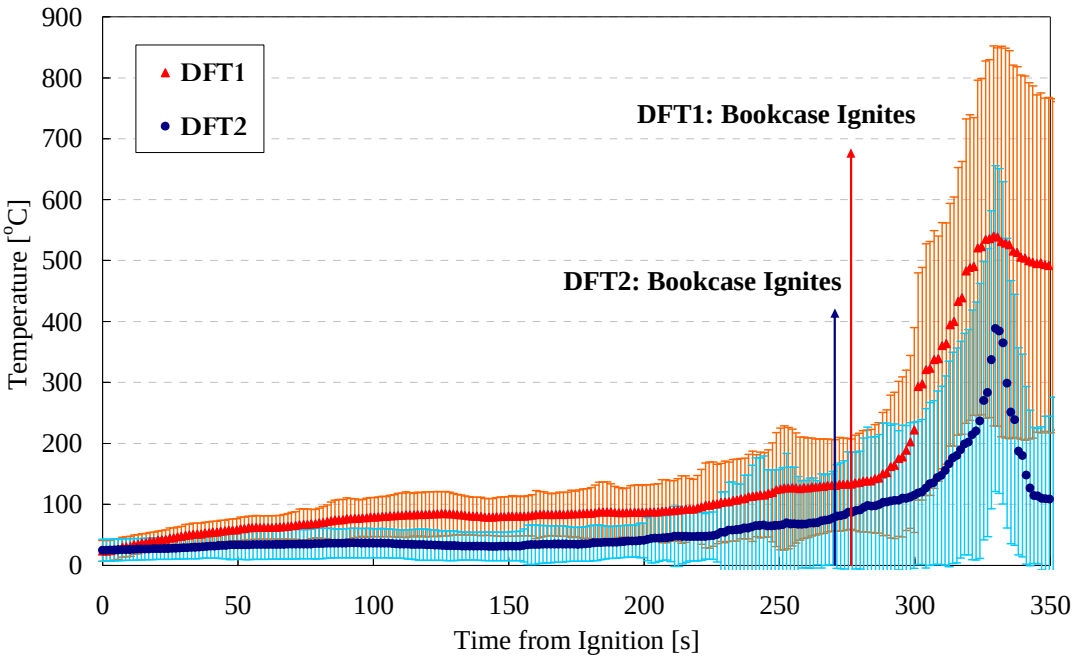

Figure 4.20. Evolution of the average compartment gas-phase temperatures for both Test One and Test Two. In both cases the shaded region indicates the standard deviation of temperature throughout the compartment.

Although the two fires had the potential for significant variation, the correspondence between the timing of major events in both tests illustrates the scenario is robust enough to guarantee a consistent timeline by providing conditions that favour the repeatability of the fire test. While the robustness of the ignition protocol was ensured by initiating the fire with a well-established waste-paper basket fire set directly under a flammable blanket draped over the sofa, the positioning of this same ignition source adjacent to a fuel laden corner was also intended to ensure eventual secondary ignition of the bookcases irrespective of the presence of a smoke layer. This potential ignition of secondary items is discussed in depth by Babrauskas [123].

Hence, provision of a full-scale experimental set up that favours repeatability allows for the benchmarking of a *realistic* fire fuelled by an arrangement of typical furniture rather than standard experimental wooden cribs or pool fires. This provides a vital

contribution to the global attempt to further understand the conditions arising from such regular household or office fires. However most importantly, the benchmarking of this *realistic* scenario renders the comprehensive test data ideally suited for model validation. Note that the use of high-resolution data measurements should be accompanied by the error bars associated with the experimental measurements as derived in detail by Reszka *et al*. [105]. These errors were found to be negligible for the purposes of benchmarking the scenario, compared to the variation in localised corresponding data points between the two tests.

4.4.4 Additional Laboratory Tests

Further to the full-scale Dalmarnock Fire Tests, some additional calorimetry tests were conducted in the laboratory in order to determine the average HRR of specific items of furniture. This enabled further characterisation of the individual properties of some fuel packages. Both large- and small-scale calorimetry tests were conducted for individual replica furniture items and material samples from major furnishings, respectively. The large-scale calorimetry tests were conducted under an exhaust hood, burning a replica of the sofa used in the experimental compartments and a fully-laden bookcase module. Conversely the material samples were tested in the cone calorimeter to determine both their HRR and critical heat flux for the ignition. The data retrieved from these tests is discussed in detail by Steinhaus and Jahn [122].

The HHR measurements obtained in these additional tests have been used to verify that the magnitude of the global HRR evolution, discussed in Section 4.3.2.3, is within the expected range. Together with the information characterising the Dalmarnock Fire Tests, this data set is invaluable for the use of these experiments as a validation tool for computational models [18,19] as it rules out the errors involved in estimating the properties of individual materials for model input.

4.4.5 Dalmarnock Fire Test Data Summary for Comparison with Law Model Output

The benchmarked Dalmarnock Fire Test One provides an ideal scenario for comparison against output from the Law Model. The dimensions of the Dalmarnock

Test compartment are very similar to the approximate dimensions of the compartments most frequently used in the large-scale tests many of the Law Model correlations were validated against, the details of which are discussed in Chapter 3, Section 3.3.1. While the Dalmarnock compartment measures 3.6 m by 4.75 m by 2.45 m high, many of the Law Model correlations derived from tests in compartments of approximate dimensions ~3.6 m by ~4 m by ~2.5 m high. Although Test One did not experience a prolonged period of sustained external flaming, enough data were collected to define quasi-steady-state flame properties and heat flux distribution on the façade and internal fire properties measured can be compared against the various parameters calculated by the Law Model. Additionally, the freely developing fire of Test One is expected to have a had a similar duration to that suggested for design in the Law Model, had it been allowed to develop to burn-out without fire brigade intervention.

The main distinction between the experimental tests the Law Model correlations are based on (and against which they have been validated) and Dalmarnock Fire Test One is the fuel content and fuel distribution. Nevertheless the Law Model was developed to be applied for design and forms the basis of Eurocode standards [2,3], so the *realistic* nature of the scenario setup, with furniture representing a typical household living room and study area, allows for an evaluation of some of the assumptions in the Law Model. The main assumptions challenged by comparison with such a scenario are the Law Model suppositions that a uniformly distributed, wood-equivalent description of fuel provides an appropriate representation of a typical scenario fire. However the detailed resolution of the Dalmarnock data also allows for an evaluation of several other more 'localised' assumptions such as those associated with the temperature distribution within the compartment and the external flame.

In order to compare the Dalmarnock Test One data to output from the Law Model, some of the data have to be processed as they are more refined than the average values used in the model. This data set is summarised below. It is also not clear from the assumptions stated in the Law Model whether the Dalmarnock Test One scenario falls into the *No Through Draught* or the *Through Draught* case as Law refers only to 'windows' as openings. Elsewhere however, the theory refers to openings as both

windows and doors and since additional air is supplied to the compartment through the doors which link to compartments with open windows, it seems reasonable to assume the conditions should be those of a *Through Draught* case. Nevertheless while the door to the kitchen is opposite the window wall it is not clear that the velocity of the wind would be representative of the velocity of any incoming draught, as the kitchen was narrow and the window wall was perpendicular to that of the door. Additionally, the wind was blowing from the South and the kitchen window was to the North, so the effects of the wind on the induced draught are expected to be complex. Since the Dalmarnock scenario appears to lie somewhere between the two draught scenarios, it is prudent to compare the data against Law Model output for both sets of conditions as these should identify the worst-case bounds for design.

4.4.5.1. Geometrical Scenario and Fire Load Data

The main parameters describing the geometrical layout of the Dalmarnock Test One scenario are fixed. These are summarised in Table 4.5 and include the main dimensions of the compartment and those of the window and doors, where door 1 (dr1) denotes the door to the hallway and door 2 (dr2) the door to the kitchen. Table 4.5 also includes the main parameter describing the fire load, L in the Dalmarnock compartment scenario.

The compartment dimensions are as measured however the compartment width is taken as an average width as there were some slight protrusions in the north wall to accommodate structural columns. The fire load, L is estimated from the heat of combustion values obtained for specific furniture items during the additional laboratory experiments, discussed in Section 4.4.4, and other values for common materials are obtained from literature. The mass of most of the large items used in the tests are known and the mass of smaller items are estimated. This is then converted to a wood-equivalent fire load (as required for input in the Law Model). The detailed calculation of the fire load can be found in Appendix E.

Parameter	**Dimension** (m)
W	3.60
D	4.75
H	2.45
w_{win}	2.35
h_{win}	1.18
w_{dr1}	0.85
h_{dr1}	1.98
w_{dr2}	0.90
h_{dr2}	2.00
L (kg)	547

Table 4.5. List of the main parameters characteristic of the Dalmarnock Fire Test One scenario including the geometrical dimensions of the compartment and ventilation openings and the fire load (note different units). These are fixed scenario input parameters.

Parameter	**1 Opening**	**3 Openings**
A_F (m^2)	17.1	17.1
A_T (m^2)	72.3	68.9
A_w (m^2)	2.8	6.3
h_{mo} (m^2)	1.18	1.63
L'' (kg/m^2)	32	32
η ($m^{-0.5}$)	24.0	8.6
ψ (kg/m^2)	38.6	26.4

Table 4.6. List of Dalmarnock Test One intermediate parameters that are calculated as part of the Law Model. The parameters are given for two scenarios: that with 1 opening corresponding to only the window area considered as an opening and that with 3 openings including the window and both doors.

Additional intermediate parameters, calculated from the main parameters listed in Table 4.5 according to the Law Model correlations are given in Chapter 3, Sections 3.2.1 and 3.2.2, are listed in Table 4.6. These highlight the difference in the reciprocal opening factor, η and the modified height of openings, h_{mo} between taking the Dalmarnock scenario as having one single opening only (the window) and having three openings by including the two doors too. Hence the h_{mo} value listed under the

single opening scenario is identical to the window height as it remains unchanged from *h*. The fire load density, L'' is calculated simply by dividing the fire load, L by the total floor area, A_F and the value has an approximate error of ± 2 kg/m^2. While the fire load density of 32 kg/m^2 in the Dalmarnock tests is higher than the 25 kg/m^2 the Law Model suggests for design, it is still within the 20-40 kg/m^2 range used in the CIB experiments which the Law Model correlations are based on [47].

4.4.5.2. Internal Fire and External Flame Data Collected

For the properties of the internal fire and of the external flame, data recorded during the Test One fire has in many cases been averaged in both time and space to provide values comparable to those calculated in the Law Model correlations. A summary of these data is provided in Table 4.7. The fire duration, τ_F is taken from ignition to forced extinction as no better approximation is available for what would have been the burn-out time, although from examination of the remnants of the fire, it is not thought to have had the fuel to burn for much longer.

Parameter	**Average parameter value throughout fully-developed fire *or* throughout external flaming**	**Average parameter value throughout the last minute of external flaming**	**$\pm$ Error**
τ_F (s)	1140	1140	+180
$\dot{m}$ (kg/s)	0.27 (5 MW)	0.38 (7 MW)	*significant*
T_a (^{o}C)	23.5	23.5	0.1
T_f (^{o}C)	625	690	3.8
T_o (^{o}C)	575	745	3.8
l (m)$^\clubsuit$	0.58	0.51	-
T_z (^{o}C)$^\clubsuit$	542	615	3.8
z (m)	0.3	0.7	0.1
x (m)	0.25	0.2	0.1
u (m/s)	-	-	-
Λ(m)*	0.4	0.3	0.1

$^\clubsuit$ The value of T_z is given for a point, l along the 'flame axis' at z = 0.295 m.
* Flame thickness taken as average up the height of the plume to the 540 ^{o}C contour

Table 4.7. List of Dalmarnock Test One parameters describing properties of the internal fire and external flame averaged both over the entire post-flashover period and over the period of sustain external flaming only. The experimental measurement error associated with each value is given as described by Reszka *et al.* for the different instruments at a range of different values [105].

Properties of the fire that evolved over the course of the fire have been averaged over two specific periods. As the Law Model correlations describe properties of a fully-developed fire, select test data were averaged for the period between flashover and extinction (320 s – 1140 s). Within this period, properties pertaining to the external flame were averaged only from the beginning of the external flaming period, when the NW window pane broke, to extinction (801 s – 1140s). However since there was only sustained external flaming for the last minute of the fire or so (1080 s – 1140s), a second set of averaged data values are also provided as representative of this period, in Table 4.7. This enables a more comprehensive set of data for comparison against the Law Model output.

4.4.5.3. External Heat Flux to Façade Data

The external heat flux to the façade once the SW window pane breaks is presented in Table 4.8. This table shows only the variation in heat flux vertically up the façade along the centreline of the window as Law assumes a uniform temperature across the width of the flame, in turn resulting in a uniform horizontal heat flux to the façade engulfed in flame and only very minor variations (due to configuration factor) for the façade in the near-field, not engulfed in flame. Although Figure 4.18 shows there is some variation in the horizontal distribution of heat flux just above the window soffit in Test One, particularly when only one window pane has broken, it also illustrates the variation is most prominent in the vertical direction, as noted in previous experiments conducted by Bullen and Thomas [250] among others (*cf.* Chapter 2).

Since the Law Model is based on the assumption of steady-state conditions (for a worst-case scenario) the heat flux measured in Test One provided for comparison is taken as the average heat flux at each gauge location over the period of sustained external flaming where the heat flux was at its greatest. Hence the averages range from when the SW window pane broke to extinction as the best possible representation of the worst-case heat flux insult to the façade. Although this is not a very prolonged period and steady-state conditions may not have been achieved, it is assumed these conditions would have been at least maintained for a few minutes longer had the fire not been artificially extinguished. In any case, an average is taken over this period of maximum external flaming and the maximum and minimum readings at each gauge height are also listed in Table 4.8, together with the

experimental measurement error as calculated by Reszka *et al*. [105]. It should however be noted that this vertical heat flux distribution is still an underestimate of the potential heat flux to the façade under the Dalmarnock fire scenario due to the tilting of the plume northwards due to the wind, as evidenced from Figure 4.21. The heat flux gauges aligned horizontally along the NW pane of the 5th floor window (HF17 and HF18) registered peak heat fluxes over 1.5 times greater (*cf*. Table 4.8) than that at the same height along the centreline of the window arrangement as they were in general closer to the plume.

Heat Flux Gauge	**Dist. from Window Soffit** (m)	**Av. Heat Flux** (kW/m^2)	**Min. Heat Flux** (kW/m^2)	**Peak Heat Flux** (kW/m^2)	**%Error**
HF1	0.135	52.5	45.7	61.8	10
HF2	0.385	42.3	22.7	54.3	10
HF3	0.635	22.8	7.9	31.6	10
HF4	0.885	22.7	6.7	34.0	10
HF5♣	1.135	1.7	0.6	2.7	*large*
HF6	1.385	6.4	1.6	11.0	*large*
HF7*	1.59	7.5	2.0	12.5	*large*
HF8*	1.79	6.8	2.2	11.0	*large*
HF9*	1.99	5.7	1.6	9.6	*large*
HF10*	2.19	4.9	1.4	8.2	*large*
HF11*	2.39	5.2	1.7	9.1	*large*
HF12*	2.59	4.3	1.3	7.7	*large*
HF13	0.135	18.6	5.3	28.8	10
HF14	0.135	31.1	25.9	35.3	10
HF15	0.135	36.1	19.2	49.5	10
HF16	0.135	25.6	13.1	31.9	10
HF17*	2.19	6.2	2.1	13.9	*large*
HF18*	2.19	7.9	1.9	13.2	*large*
HF19*	2.19	5.1	1.3	9.1	*large*
HF20*	2.19	3.5	0.7	6.8	*large*

♣ This heat flux gauge appears to have been mal-functioning.
* Heat flux gauges mounted on the upper storey window, which is located between 1.5 m and 2.7 m from the fire compartment window soffit.

Table 4.8. Variation of incident heat flux vertically up the façade above the window centreline. Values are averaged over the period of maximum sustained external flaming for each gauge together with the minimum and maximum instantaneous values recorded during this period. The heat flux gauge locations are illustrated in Figure 4.5 and discussed in 4.2.3.2.

Figure 4.21. Photograph of the external façade outside Test One in the aftermath of the fire. A plume smoke record on the façade highlights the general affect of the wind on the plume tilt and shows evidence of a significant plume having emerged from the kitchen window.

4.4.5.4. Discussion of Law Model Assumptions vs. Dalmarnock Data

The validity of several assumptions made in the Law Model can be assessed by comparison with the Test One data. Namely, assuming the fire does not undergo any fire-induced changes in ventilation, other than potentially at flashover, allows for the simplification of the scenario and subsequent assumptions that properties such as the rate of burning are constant throughout the duration of the fire. Nevertheless Figure 4.12 shows there is significant fluctuation in the rate of burning, $\dot{m}$ throughout the fully-developed stage of Test One. Although the minor fluctuations are likely to be associated to experimental error due to the velocity probe setup (*cf.* Section 4.3.2.3) there are distinct changes of the overall rate of burning when ventilation conditions are altered. Although this is expected it shows the assumption of a single value for the rate of burning might not always be a conservative assumption.

Similarly, Law assumes a single compartment gas-phase temperature, T_f can be used to describe the fully-developed fire. Although this is a common assumption, it is often linked to experimental investigation involving only a handful of thermocouples that most often refer only to the hot layer. Nevertheless the dense network of thermocouples placed throughout the Test One compartment provide a much higher resolution of temperature distribution throughout the compartment and even post-

flashover when the smoke layer has descended to floor level, there is evidence that the internal compartment temperature is far from homogenous. As for the burning rate, the temperatures also vary in time throughout the post-flashover fire and this lack of a single temperature representative of the compartment environment is evidently summarised in Figure 4.7. Since the radiation component of the fire contributing to the external heat flux insult is proportional to the fourth power of the compartment temperature, the choice of this single temperature can have a significant effect on the Law Model outcome.

The assumptions regarding the external flame properties are also found to depart from many of the characteristics observed during Test One. Although external flaming was only observed for a fraction of the post-flashover period, preceded mostly by exhaust that appeared to constitute mainly of dense smoke, the area of the window throughout which these emerged varied throughout the test. While only the NW window pane was broken, the smoke and intermittent flaming appeared to emerge on average from roughly less than the top two thirds of the opening, however once the SW window pane broke and sustained external flaming ensued, the neutral axis descended considerably and was seen to fluctuate between the upper two thirds of the opening and the whole window. This could have been due to a change in the main 'venting direction' of the fire, as there was also evidence of a significant smoke plume having emerged from the kitchen window (*cf.* Figure 4.21). Hence, it is unclear whether this behaviour would be assumed to match that expected of *No Through Draught* conditions or that of *Through Draught* conditions. Furthermore, the plume was not seen to significantly project out from the façade as would be assumed under *Through Draught* conditions, even though neither the NW window area on its own nor the whole window area constitute 'narrow' openings. Although this may have been due to the wind, this effect is unaccounted for in the Law Model and the closer the flame is to the façade the higher the heat flux insult. This confirms that the Dalmarnock scenario lies somewhere between both draught cases defined by Law. Hence it would perhaps be prudent in design to suggest calculation of both *No Through Draught* and *Through Draught* conditions for each scenario (when both may be applicable) such that the worst-case can be implemented, since other environmental conditions can affect the notional flame shapes further than assumed by Law.

Other external flame details, such as the assumption the flame bends upwards at 45^{o} under *No Through Draught* conditions appears to be corroborated by camera footage evidence of visible flames during the period of sustained external flaming. Hence the flame thickness at window soffit level (perpendicular to the façade) should equal the depth of the flame as it emerges through the window (*cf*. Chapter 3, Figure 3.2). Nevertheless, assuming the flame edge to be delineated by the 540^{o}C contour, the flame depth inferred from the thermocouple data shows the flame depth to be much smaller than that observed. Using the 540^{o}C isotherm to determine the average flame dimensions is in fact conservative as Law and O'Brien assume the flame temperatures to be uniform through their cross-section hence the flame depth should be taken at the axis temperature as the 540^{o}C isotherm is used only to define decay at the flame tip in the model [1]. Yet even with this conservative assumption the average flame dimensions have been found to be quite small (*cf*. Table 4.7). This could be due to the high smoke concentrations in the external plume as "fuels which generate a lot of smoke will give flames of lower temperature but high emissivity" [21].

With regards to the temperature distribution with the flame, the assumption of a uniform temperature through the cross-section of the flame axis was not verified by the thermocouple measurements. While the temperature distribution along the width of the flame barely varied for the width of the flame (as assumed for a flame the width of the opening), the temperature varied significantly with flame depth, with higher temperatures closer to the façade front as seen in the horizontal section shown in Figure 4.17 (c). Hence, although the flame width assumption appears to match that observed, the flame depth and flame height were in fact quite difficult to determine, due to both the fluctuations in the flame and the lack of a distinct flame axis of reference. This complicates the identification of the variation in flame temperature, T_z however an average was taken from thermocouple points aligned with the centre of the opening (first NW pane, the window centreline) at ~0.295 m from the window soffit, up to about 0.25 m away from the façade which appears be a good approximation of the axis path. This flame temperature is listed in Table 4.7 together with the equivalent distance along the flame axis it is at (according to Law Model theory) such that it can easily be compared against Law Model output. The maximum

external temperatures measured do however mostly coincide with the window soffit, as assumed by Law for the calculation of the temperature at the window, T_o.

In terms of the effect of lateral wind on the emerging flame, Figure 4.14 (a) clearly shows a lateral displacement of the flame face furthest from the façade, as the flame is tilted by a southerly wind, as assumed in the Law Model. The flame does however also appear to tilt with height as can be inferred from Figure 4.21 where the plume appears to have left a smoke record on the façade, clearly at an angle to the vertical. It is unclear whether this behaviour is accounted for in the Law Model however this could effect the heat flux to a structural member located to the side of a window, but outwith the area described by the horizontal tilt of the flame prescribed by Law under the effect of wind. Although several of the Law Model assumptions are seen to depart from the Dalmarnock observations and test data, clear simplifications are required in order to provide an engineering tool of general application.

Chapter 5

Detailed Analysis of the Law Model

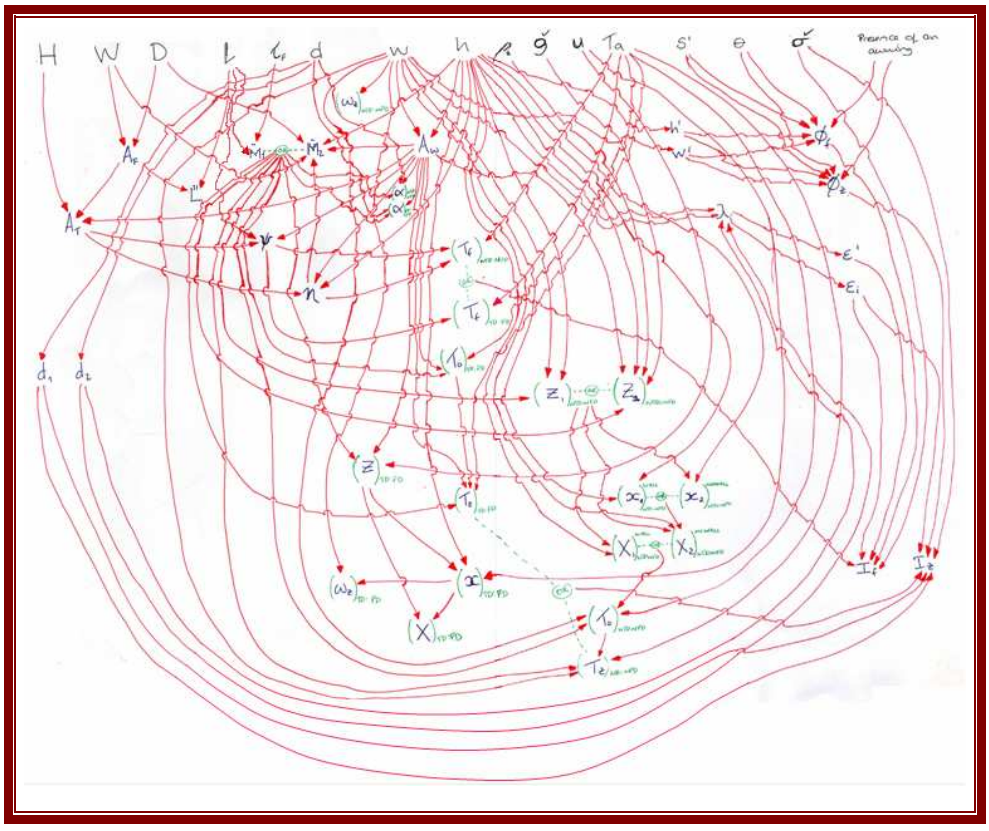

- Diagram summarising the inter-dependencies of parameters used in the Law Model -

It has been several decades since Law and O'Brien [1] formulated the Law Model and evolution in material science has, since then, seen many synthetic materials replace the once mainly wood-based furniture and furnishings used to decorate our homes and offices. Similarly, some traditional construction materials are now often replaced by innovative materials that have better weight-to-strength ratios, are more sustainable or have improved aesthetics, among other properties. Combined with the advances in architecture that have, over the last few decades, driven buildings to much greater heights and allowed for an array of irregular designs, this innovation redefines the 'typical fire scenario' and it is unknown whether this shift has a large effect on the applicability of some of the compartment-fire-based models developed to date. Hence it is a good time to revisit the intricacies of the Law Model and to perhaps re-evaluate the concept and applications of the model as a whole.

5.1 The Objective of the Sensitivity Study

In order to assess the adequacy and general applicability of the Law Model for providing adequate design of external façade components (*i.e.* cladding, window configurations, perimeter structural elements, *etc.*) under *real* fire scenarios it is essential to pinpoint the key parameters that govern the external heat flux output by the model. These parameters are identified by conducting a sensitivity study in which each parameter is individually varied, throughout a range of values that may be expected in standard design. The study is based around a benchmark scenario and the effect of individual parameter variation is evaluated by comparison of the distribution of the heat flux incident on the façade above the compartment opening, as output by the model. The benchmark scenario is taken as that of Dalmarnock Fire Test One (DFT1) as the compartment geometry and its openings are of fairly common dimensions expected in standard design, as is the general fire loading used. The Dalmarnock Fire Test One (DFT1) scenario is found to be an ideal benchmark as the characteristics of the compartment and the fire duration correspond to those in large-scale tests previously used to validate the Law Model (*cf.* Chapter 3, Section 3.3.1), as discussed in Chapter 4, Section 4.4.5. Furthermore thorough measurements of the characteristics of the internal fire, the external flaming and the external heat exposure pertaining to the fully-developed fire are available for comparison with the Law

Model. Nevertheless the characteristics of the fire loading – including fuel type and fuel distribution throughout the compartment – constitute a significant difference from previous tests used for Law Model validation. This renders Dalmarnock Fire Test One more representative of a *realistic* scenario which enables evaluation of the applicability of the Law Model in modern design.

The identification of the key governing parameters in the Law Model may highlight other parameters that make a relatively minor contribution to the model outcome. Given the many assumptions and generalisations inherent in the Law Model, as discussed in detail in Chapter 3, Section 3.4, the relative level of accuracy of the model may not justify the inclusion of such parameters. Hence the overall aim is to devise a simplified analytical expression using the key governing parameters for the prediction of the external heat flux imposed by specific scenarios. While it is possible that, in simplifying the model, some of the intricate detail providing 'resolution' is lost, this should not compromise the overall level of accuracy in the prediction relative to that already inherent in the Law Model and its related assumptions.

5.2 The Sensitivity Study Methodology

The number of parameters and elaborate parameter interdependencies constituting the Law Model render it laborious to run through a single calculation (*i.e.* to determine the heat flux to a single point on the façade or the resultant temperature on a point of an external structural steel member) for a given scenario. Therefore, a computational implementation of the Law Model, *FirExHeat*• was programmed in MatLab (MatLab R2006, The Mathworks™, MA, U.S.A.) in order to facilitate the thorough parameter sensitivity study process. *FirExHeat* includes the assumptions and limitations associated with the Law Model while allowing for variation of all the input parameters, including those that are given nominal values for design in the Law Model, such as ambient temperature, T_a and draught or wind velocity, u. It is programmed to provide the resultant temperature of an external structural steel member – lying either away from the façade, flush against it or even partially embedded within it (*i.e.* respective adjustments were made to the heat flux

• A copy of the *FirExHeat*, the computational implementation of the Law Model, programmed in MatLab, can be found in the CD accompanying this work.

components falling incident in each of the member faces) – or to determine the total heat flux falling incident at any number of points on the façade above a compartment opening. Although for this study, the heat flux to the façade is of greatest interest for the parameter sensitivity study, the capability of *FirExHeat* to determine the temperature of external steel elements was used to ensure the model was adequately programmed by comparison against the several example scenarios given in the Law Model [1].

The Dalmarnock Fire Test One (DFT1) benchmark scenario is first modelled using the known input variables described in Chapter 4. The heat flux is modelled to the same points on the external façade as the location of the gauges measuring external heat flux during the test. Comparison of the modelled and measured heat flux provides an evaluation of the application of the Law Model correlations to a *realistic* scenario, exemplary of a scenario for which the model may typically be used in design. The Dalmarnock scenario is then used as the basis for parameter variation. Each of the main input parameters identified is individually varied as a multiple of its value for the DFT1 scenario, over a given range, and its effect on the output is compared against that of the benchmark. The parameters that, when varied, result in the greatest variation in heat flux to the façade are deemed to be of key importance, particularly if there is a large distinction between the effect some parameters have compared to the effect of others.

The study is based around the heat flux imposed on the façade because it is of particular interest, having further applications than that incident on steelwork at a distance from the façade – although heat flux to such steelwork could similarly have been used. Nevertheless, many of the experiments that eventually led to the development of the Law Model correlations were initially devised to determine the external heat exposure to the façade, due to the risk it posed to external fire spread, as discussed in Chapter 2. This renders it particularly pertinent that heat flux to the façade be used for evaluation of the importance of the individual parameters. Apart from the application of the external heat flux to the façade plane in determining the heat insult to structural steelwork embedded in the façade with an exposed surface – such as a spandrel beam or a perimeter column – it can also be used to determine the potential for fire spread beyond the compartment of origin. Heat flux incident on the

façade could ignite a combustible façade cladding if it reaches its critical heat flux for ignition. Similarly, the heat flux incident on the plane of the façade can be applied to window panes in order to determine a safe inter-storey window separation distance to prevent glass breakage induced by external flaming. This can also be used as a ballpark estimate to determine if typical items in the compartment a floor above the experimental compartment will ignite, given the likely heat insult during a given compartment fire once the upper level compartment window has broken. Hence, it was of interest to set up an array of heat flux gauges on the façade of the Dalmarnock Fire Test One compartment, as discussed in Chapter 4, Section 4.2.3.2, such that experimental data pertaining to a *realistic* scenario would be available for comparison with the model output.

5.3 Dalmarnock Fire Test One as Benchmark Scenario for analysis of the Law Model

In attempting to model the Dalmarnock Fire Test One scenario it became clear that it is not always evident which Law Model specifications should be used to describe a particular scenario. In this case it is unclear whether the Dalmarnock scenario falls into the category of *No Through Draught* or *Through Draught* since the compartment had openings on opposite walls (deemed by Law to result in *Through Draught* conditions), but there did not appear to be a through draught of significant velocity – the kitchen window opening was at a right angle to the kitchen door and compartment window and the wind direction was seen to vary somewhat throughout the test. It is also unclear whether only the window (NW and SW panes) should be accounted for as an opening or whether the doors should also be included as the Law Model makes no direct mention to doors as openings. Although for the purposes of this study it has been assumed that an opening can be defined as either a door or a window, depending on the ventilation conditions of the compartment beyond the door (*cf.* Chapter 3, Section 3.4.2), it is important to evaluate the significance of such interpretations of the Law Model.

Due to the uncertainties in the definition of the model scenario, all potential combinations of cases are modelled and compared against the Dalmarnock data set, allowing for an evaluation of which combination of scenario definitions provide the

best description. Therefore, the Dalmarnock Fire Test One was initially modelled under four different scenario conditions: (a) *No Through Draught* with only window as opening (ND - 1 Opening); (b) *No Through Draught* with the window and both doors defined as openings (ND - 3 Openings); (c) *Through or Forced Draught* with only window as opening (ToFD - 1 Opening); and, (d) *Through or Forced Draught* with the window and both doors defined as openings (ToFD - 3 Openings). Although the Dalmarnock scenario is clearly not under *Forced Draught* conditions, a model scenario with only the compartment window as an opening under *Through or Forced Draught* conditions is included for the purposes of comparison.

The input parameters used in the Law Model calculations were those pertaining to the Dalmarnock scenario as listed in Table 4.5, together with the fire duration and ambient temperature taken from the fire tests data given in Table 4.7. The wind velocity used in the scenario with a *Through or Forced Draught* is taken as 6 m/s as suggested by Law for design, since no better estimate of the wind conditions during the DFT1 tests is available. The heat flux receiver points on the façade to which the model was applied correspond to the respective locations of the 20 heat flux gauges installed in DFT1, illustrated in Chapter 4, Figure 4.5. This enables a direct comparison between the experimental data given in Chapter 4, Table 4.8 and the output of the four potential Law Model cases for the scenario.
Figure 5.1 shows a comparison of the output from all four Law Model cases against the Dalmarnock data for the average heat flux experienced over the period of maximum sustained external flaming (after the SW window pane broke; *cf.*
Table 4.2) at each external gauge location.

Heat flux gauges 1-12 were aligned vertically up the façade along the centreline of the window while gauges 13-14, 15-16 and 17-18, 19-20 were horizontally aligned, two on either side of gauges 1 and 10, respectively (*cf.* Chapter 4, Figure 4.5). What is most evident from
Figure 5.1 is that the modelled heat flux values yielded are not only within the same ballpark figure as those measured but also closely follow the rate of decay measured with vertical distance from the window soffit. While this is a good match, the close correspondence between many of the values is unexpected as the Law Model stipulates many of its assumptions are based on providing a conservative approach

(significant overestimate) such that output is deemed adequate for use in design. In the horizontal direction however the variation in heat flux measured is not reproduced by the modelled heat flux output as the Law Model assumed the flame temperature to remain constant across the flame with, varying only with height. Therefore, it is only outwith the flame height (or when façade is not engulfed in flame) that some variation is seen in the modelled distribution of horizontal heat flux, due to the flame configuration factor. Nevertheless, overall, the variation in measured heat flux is more pronounced in the vertical direction.

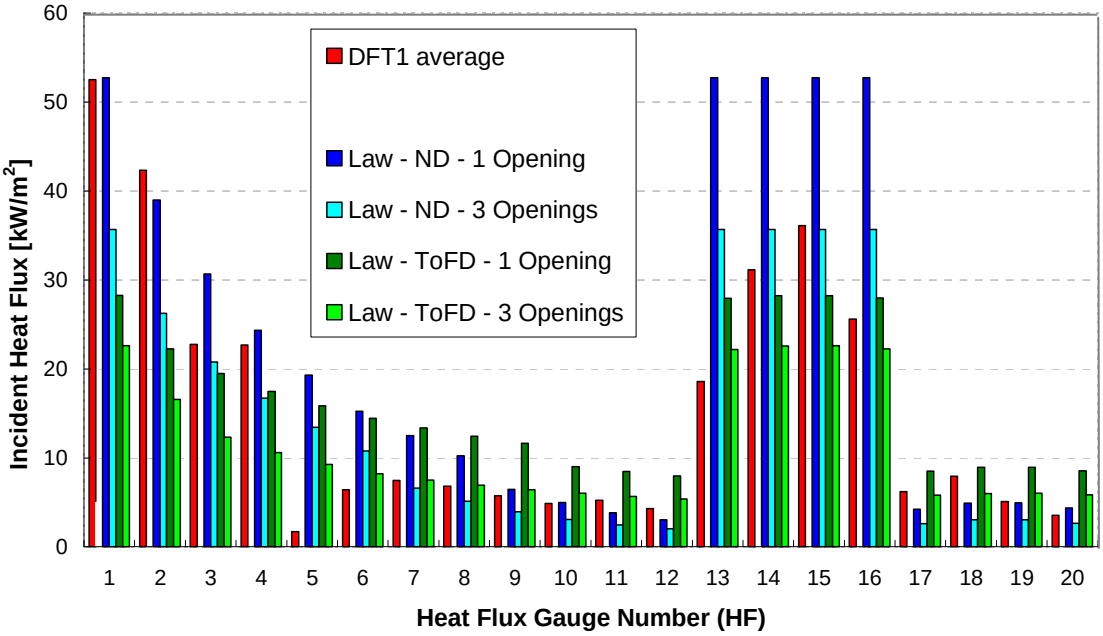

Figure 5.1. Average heat flux to the façade above the compartment window measured during the period of maximum sustained external flaming during Dalmarnock Fire Test One juxtaposed with output from four Law Model computations for cases with a combination of *No Through Draught* and *Through Draught* conditions and one (window) or three (window and 2 doors) openings defined. The heat flux gauge numbers correspond to the gauge locations illustrated in Chapter 4, Figure 4.5. *N.B.* HF5 appears to have been mal-functioning.

On a more detailed level, all Law Model cases appear to underestimate the average heat flux at some point, particularly in the region of higher incident heat flux along the window centreline, in the area just above the soffit. In this region, only the *No Through Draught* scenario with a single opening (ND - 1 Opening) is seen to provide a reasonable heat flux estimate, with all other Law Model cases providing a significant underestimate. While even this model case appears to underestimate the

recorded heat flux ~0.4 m above the window soffit (at HF2), the 3-4 kW/m^2 underestimate is within the error bar associated with the DFT1 heat flux gauge measurements (*cf.* Table 4.8). The heat flux computed by this model case then seems to decay fairly quickly such that further afield, in the vicinity of the window of the compartment above (HF10-20), it considerably underestimates the recorded heat flux. Although the error in the measured data in this region is considerably large, the *Through or Forced Draught* case with 1 opening (ToFD – 1 opening) appears to be the only case that would provide for the heat flux recorded in this area, in a design scenario. Hence none of the Law Model cases would individually have provided a safe estimate of the heat flux incident on the façade along the centreline. Although either side of the centreline the Law Model cases provide better estimates, due to the decay seen in the Dalmarnock data, this is only true of the near-field in the region just above the fire compartment window.

Some of the individual intermediate parameters calculated under each of the four Law Model case scenarios are given in Table 5.1. Comparison of these values with those measured during DFT1, listed in Table 4.7, provides a further insight in to potential limitations inherent in the empirical nature of the model correlations. As it is the overall ability of the Law Model to determine the heat flux incident on the façade that is of most interest to this study, it is not worth delving into a detailed comparison of the individual computed and measured values of these intermediate parameters. Nevertheless it is noteworthy that in several cases the computed intermediate parameters yield very different values to those measured. This is particularly the case in the range of fire and flame temperatures modelled as well as the flame dimensions and projection, where the measured flame dimensions have been obtained from the 540 ^{o}C temperature contour, as stipulated by Law [1,26]. On the other hand, the burning rate of 0.27 kg/s modelled by the *No Through Draught* Law Model case with a single opening (ND – 1 Opening) matches that measured during DFT1 (*cf.* Table 4.7) and this case also provides the best estimate of the high values of heat flux incident on the façade in the near-field to the fire compartment window. Overall, however all cases fare similarly in modelling the *distribution* of heat flux incident on the external façade.

Parameter	**ND – 1 Opening**	**ND – 3 Openings**	**ToFD – 1 Opening**	**ToFD – 3 Openings**
$\dot{m}$ (kg/s)	0.27	0.48	0.48	0.48
T_f (^{o}C)	976	888	968	805
T_o (^{o}C)	1217	1045	762	684
T_z (^{o}C)♣	981	844	762	683
z (m)	1.85	1.55	2.01	0.49
x (m)	0.39	0.39	4.09	2.15
λ (m)	0.79	0.79	1.18	1.18

♣ The value of T_z is given for a point, l along the 'flame axis' at z = 0.295 m.

Table 5.1. List of intermediate parameters describing properties of the internal fire and external flame, calculated under the four different Law Model case scenarios used to describe the DFT1 scenario.

While providing a good estimate of the incident heat flux in the near field is important for design of structural members and for selecting appropriate façade cladding such that its ignition and consequent external façade fire spread can be prevented, the heat flux estimate for the region of the window on the floor above a fire is important to prevent the likelihood of inter-storey fire spread. It should be noted that during DFT1 the external plume was seen to tilt at a distinct angle, away from the window centreline, as noted from the smoke record depicted in Chapter 4, Figure 4.21. It is therefore likely that, had the plume not been tilted, the heat flux incident on the window of the compartment above that of fire origin would have been significantly higher than recorded. While heat flux gauges 17 and 18 (*cf.* Chapter 4, Figure 4.5 for location) appear to have been in the region of the plume at this level (accounting for the higher average heat flux recorded by gauges HF17-18 compared to that of HF10, HF19-20), from Chapter 4, Figure 4.21 the plume axis appears to have been further to the north. Hence it is possible that with no wind the heat flux impingent on this window area could be in the region of 10-20 kW/m^2. Should this be the case, the risk of development of secondary fires would be high as "the approximate radiant heat required for the piloted ignition of a second item varies from 10 to 20 kW/m^2 for easily ignitable items such as thin curtains and loose newsprint to upholstered furniture" [81]. Given the measured DFT1 heat flux constitutes both radiant and

convective components, should the window be open or should it crack due to the fire, this range of would pose a significant risk. Even under the tilted plume the temperatures in the vicinity of the upper window (1.5-2.7 m above the fire compartment window soffit; *cf.* Chapter 4, Figure 4.17) were well above the 50-100 ^{o}C range found to cause glass breakage [124]. The heat flux incident on the window was also within the 4-10 kW/m^2 range noted to break most single-pane window arrangements [125] in other tests. Therefore it is likely the 5th floor window glass would have cracked and broken out had it not been protected by plasterboard and had the period of maximum sustained external flaming not been of relatively short-duration. While this could have led to the ignition of secondary fires in the upper level compartment, depending on the properties of its furnishings, the Law Model does not appear to provide conservative estimates of heat flux in this region for adequate design of the respective façade elements (*i.e.* window arrangements, *etc*.).

Overall the comparison of the Dalmarnock Fire Test data and the Law Model output for the different cases shows that the Law Model does not appear to provide conservatively for design, even though Law classifies most of the assumptions made in the model as conservative in nature [1]. Although the experimental error associated with heat flux gauges, particularly at lower heat fluxes (further away from the window soffit), can be significant (*cf.* Table 4.8), the Dalmarnock data shows a distinct trend in the heat flux measured at the different locations suggesting the data set is robust. In any case, even given the considerable error bar, the Law Model output would not significantly overestimate the heat flux distribution resultant from the DFT1 scenario. Analysis of similar full-scale tests conducted by Klopovic and Turan [79-81] in the late 1990s, where contemporary furniture was likewise used to represent a realistic fire load, also finds measurements of heat flux incident on an external façade are greater than the heat flux described by the Law Model. This discrepancy can potentially be due to the extensive use of non-cellulosic-based fuel in DFT1, which did not feature in the tests used to develop the model correlations (*cf.* Chapter 2) and in most of the larger-scale tests later used for its validation (*cf.* Chapter 3, Section 3.3.1). The Dalmarnock external plume was observed to be large yet to comprise a very small external flame and hence to be very smoky in nature. This type of plume is associated to a large excess fuel factor, f_{ex} which Thomas and Bullen [67] identified as being linked to lower flame temperatures and higher radiant heat flux to the façade.

The flames associated to high concentrations of smoke in the external plume, are known to have higher emissivity [21]. This phenomenon is not accounted for by the Law Model and could potentially also explain the significant underestimate of the steel temperatures of a column [26] used in several of the initial Underwriters' Laboratories tests [62] against which the Law Model correlations were verified [26,46].

Furthermore, it should be noted that the DFT1 compartment described by the Law Model with a single opening (the window; *i.e.* ND – 1 Opening and ToFD – 1 Opening) has a corresponding reciprocal opening factor of 24 $m^{-1/2}$ and that with the three openings (window and 2 doors) has a reciprocal opening factor of 8.6 $m^{-1/2}$. While the cases with the smaller reciprocal opening factor fall well within the range pertaining to tests used to previously validate the Law Model (*cf.* Chapter 3, Section 3.3), the cases with only the window as a single opening result in a reciprocal opening factor that falls in a realm for which the validity of the Law Model correlations has not yet been thoroughly investigated. Nevertheless the DFT1 experimental data and the heat flux distribution described by the four different Law Model cases are in the same ballpark which shows that overall "important parameters have been identified, and a substantial data bank exists from which it is possible to show how these parameters interact" [26] rendering the Law Model useful to establish which of these parameters are of greatest importance. The distinct variation noted in the distribution of heat flux vertically along the façade from the opening soffit compared to that in the horizontal distribution, together with the applications of the heat flux to these different areas renders in design, also renders the vertical distribution most relevant for use in comparing the effect of parameter variation throughout the sensitivity study.

In the meantime, from a design perspective, it should be recommended that a given scenario be modelled according to all potential Law Model cases that may apply, such that the worst-case heat flux to a point of interest can be identified. The worst-case modelled heat flux to a given point should then be applied for design, even if different cases give rise to higher heat fluxes at different points of interest, as seen in Figure 5.1 for the Dalmarnock Fire Test One scenario.

5.4 Variable Parameter Definitions

While implementing the computational version of the Law Model, *FirExHeat*, for the purposes of the sensitivity study, the effect of a number of particulars in the definition of some parameters was investigated. In a number of cases, the definition of certain parameters is ambiguous, and therefore it is prudent to determine whether the adoption of any of the potential definitions would have a significant effect on the model outcome. The parameter definitions investigated include:

- The characteristic length scale, d used in the calculation of the convective heat transfer coefficient, when pertaining to a point receiver on the façade rather than a steel section of discrete dimensions;
- The use of the modified opening height, h_{mo} as opposed to the specific height of a window opening, for determining the characteristic of the flame emerging from the window, when there are several openings of different dimensions;
- The point along the flame at which the flame depth, λ and flame temperature, T_z are taken for use in the calculation of the flame emissivity and the radiative and conductive components of the heat flux incident on a particular point on the façade, when that point is not engulfed in flame.

The effect of the different definitions of each of these parameters was individually investigated, using the Dalmarnock Fire Test One scenario as a benchmark for the evaluation of the effect had on the heat flux distribution vertically up the façade along the window centreline. The definitions found to have a large effect on the outcome heat flux distribution were then compared against the Dalmarnock Fire Tests One data to determine which definition led to more realistic results. Where in the variation in parameter definition was found not to have a significant effect on the outcome heat flux distribution, one of the definitions was chosen and justified. These definitions were incorporated into the *FirExHeat* model and used in the comparison drawn in Section 5.3 as well as the rest of the parameter sensitivity study.

5.4.1 Adjusting the Characteristic Length Scale, *d*

It is not evident how the definition of the characteristic length scale, *d* described in the Law Model [1] and detailed in Chapter 3, Section 3.2.2.1.4 applies to a point on the façade, since it is defined as the average of the two main dimensions of the cross-section of the steel member of interest. Therefore it is important to revisit the function of the characteristic length scale and its use within the heat transfer coefficient. Effectively the convective heat transfer coefficient is a measure of the rate at which heat is transferred convectively across the boundary layer, per degree of temperature difference, between the fluid gases of the plume and the solid point of interest. For the case of flow parallel to a flat plate, the temperature and velocity within the boundary layer vary with the boundary layer thickness, which itself is a function of the length of the solid surface. Similar relationships arise for various combinations of geometry and surface orientation relative to the flow. Hence, the length of the solid surface over which the fluid flows is an important component governing the convective heat transfer coefficient. It is this length that defines the characteristic length scale.

Consider the case of an external spandrel beam outlying from the façade, at a height above the window sill, such that it is in the streamline of plume flow, potentially engulfed in flame. A boundary layer to a point of interest on the beam (mid-point) will form from the leading edge of the beam relative to the flow. In a similar scenario, but with the beam embedded in the façade at a height above the window soffit, such that only one of its surfaces remains exposed and flush with the facade, the first surface the plume will encounter is the façade itself as it exits past the window soffit. Hence, a boundary layer would form over the façade and the exposed surface of the beam would likely be within this boundary layer. In this case, the characteristic length scale should be measured from the leading edge of the boundary layer (*i.e.* from the window soffit to the point of interest on the beam surface). Similarly, should there be an obstruction between the window soffit and the beam face, that protrudes out from the façade further than the boundary layer thickness at that point, a new boundary layer would form with its leading edge at the obstruction, again changing the characteristic length scale pertaining to the beam surface. Therefore, theoretically, the characteristic length scale for a point on the façade should be taken as the vertical distance between the opening soffit and the point itself.

In the case of Dalmarnock Fire Test One, the external heat flux gauges were near to flush-mounted with the external façade. Nevertheless, they were embedded in 5 by 5 cm pieces of plasterboard that were in places 1 cm thick and in others 2 cm thick. Hence, for the purposes of comparison between the definition given in the Law Model and the theoretical definition of the characteristic length scale, the local average dimension of 0.025 m to the point of interest was used as the 'Law Model definition' whereas the vertical distance from the opening soffit to each point of interest was used as the 'Theoretical definition'. The DFT1 scenario was modelled under both *No Through Draught* (1 opening) and *Through or Forced Draught* (3 openings) conditions and the vertical heat flux distribution resultant from both definitions of the characteristic length scale were compared. Figure 5.2 shows the outcome of the two cases under *Through or Forced Draught* conditions. The discrepancy in the heat flux distribution described by the two different characteristic length scale definitions is large, where the distribution described using the Law Model definition is, for the most part, over twice that described using the theoretical definition. The radiative and convective components constituting the total heat flux incident on the façade under both definition cases are also plotted. This illustrates the magnitude of the convective heat flux component in the case described using the Law Model definition, which employs the same, comparably small characteristic length scale throughout all points on the façade. Comparison of both total incident heat flux distribution curves with the vertical distribution of average heat flux measured during the period of maximum sustained external flaming in DFT1 (HF1-9), shows the measured data to match both the decay trend and the ballpark values described by the Theoretical definition far more closely that described by the Law Model definition. Similar trends are found under *No Through Draught* conditions.

Therefore, for calculation of the heat flux to a point on the façade, the characteristic length scale, d is defined in the *FirExHeat* computational implementation of the Law Model using the theoretical definition – the vertical distance from the opening soffit to the point of interest. This affects only the convective heat transfer coefficient and hence the convective heat flux component of the total heat flux incident on the façade. It should however be noted that the characteristic length scale is in the denominator of the Chapter 3, Equations (3.18) and (3.26) describing the convective heat transfer coefficient, α hence as $d \rightarrow 0$, $\alpha \rightarrow \infty$. Therefore for a point of interest on the façade

in the very close vicinity of the opening soffit where the smaller the characteristic length scale is very small, the convective heat transfer coefficient described will be unrealistic and will lead to unrealistic values of heat flux to the façade, with a singularity at the window soffit.

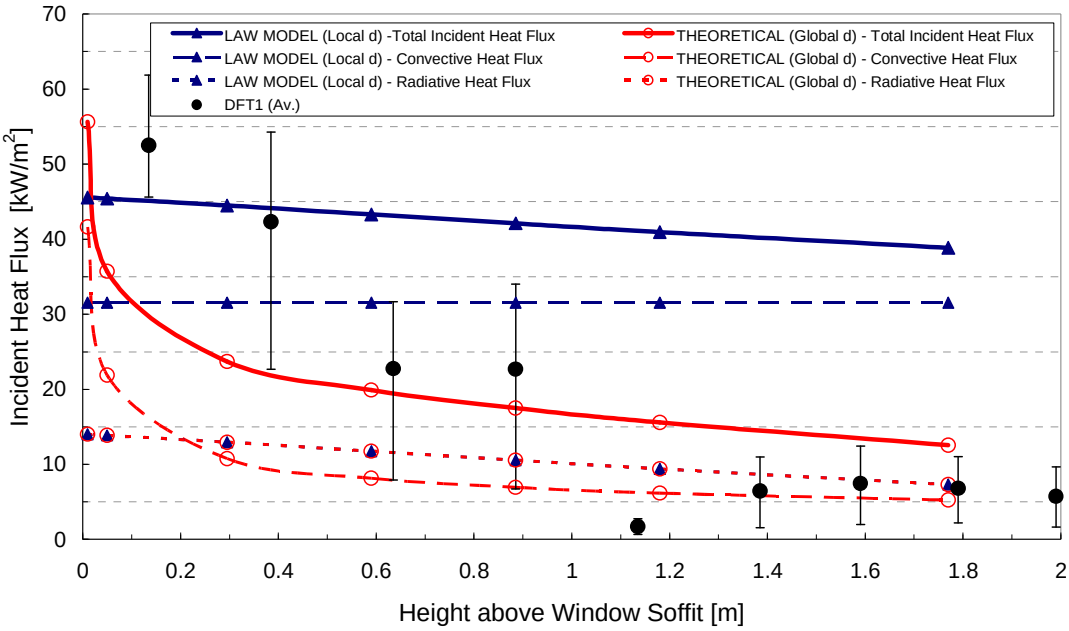

Figure 5.2. Vertical distribution of heat flux incident on the façade resulting from modelling the DFT1 scenario with 3 openings under ToFD conditions, using two different definitions of the characteristic length scale. The respective convective and radiative heat flux components are shown for comparison. The DFT1 data taken as an average over the period of maximum sustained external flaming are shown with error bars accounting for maximum and minimum instantaneous values measured (*cf.* Table 4.8).

5.4.2 Defining the Opening Height to be used in the calculation of Local Flame Conditions

When a scenario has more than one opening, the Law Model takes the openings into account in the form of a single equivalent opening with modified dimensions, as described in Chapter 3, Section 3.2.1 and discussed in Section 3.4.2. It is not clear however, whether the modified opening values should be employed in all equations throughout the model. Therefore, it is of interest to determine the effect of using local opening dimensions versus the modified equivalent opening dimensions to determine the heat flux distribution above the given opening. The definition of the opening height is of particular interest because in scenarios where the compartment openings are of considerably different dimensions, as in DFT1 (both a window and doors), the difference in opening height may be significant depending on the definition used.

In order to evaluate the effect of the opening height definition, the two different cases were compared under both *No Through Draught* and *Through or Forced Draught* conditions, based around the DFT1 benchmark scenario with 3 openings. The window opening height was defined as both the specific height of the window and as the modified height, defined as an area-weight-average of all three openings (the window and two doors), as described in Chapter 3, Section 3.2.1. These definitions were applied in all correlations within the Law Model featuring the opening height.

The vertical distribution of heat flux incident on the façade under *No Through Draught* conditions is shown in Figure 5.3, together with the respective resultant flame height, z for each definition of the opening height. Although the modified window height described a higher overall heat flux along the height of the façade, the difference to that described using the specific window height is negligible, even though the difference between the heights specified was considerable, given the difference between the dimensions of the window and the two doors. The heat flux distribution described by the case where the window opening is specified as the only opening in the compartment is included for the purposes of comparison and is seen to result in a higher overall heat flux than either case with three openings. The respective flame heights are seen to vary accordingly, as expected, as the heat flux distribution is highly dependent on the flame temperature distribution, which in turn is based on the flame height. The average heat flux measured during the period of maximum sustained external flaming during DFT1, together with the maximum and minimum instantaneous values measured at each gauge location (*cf*. Table 4.8), are also plotted in Figure 5.3, providing a ballpark for comparison.

Similarly, Figure 5.4 shows the vertical distribution of heat flux incident on the façade under *Through or Forced Draught* conditions. In this case the specific window height results in a higher overall heat flux distribution than that described using the modified opening height. Nevertheless, once again the discrepancy is not significant and the DFT1 scenario described with only the window as a single opening again results in a higher overall heat flux distribution than both other cases. Since the definition of the opening height used does not appear to have a significant effect on the modelled heat flux, the definition using the area-weight-averaged modified opening height value is maintained in *FirExHeat*, as per the Law Model (*cf*. Chapter 3, Section 3.2.1).

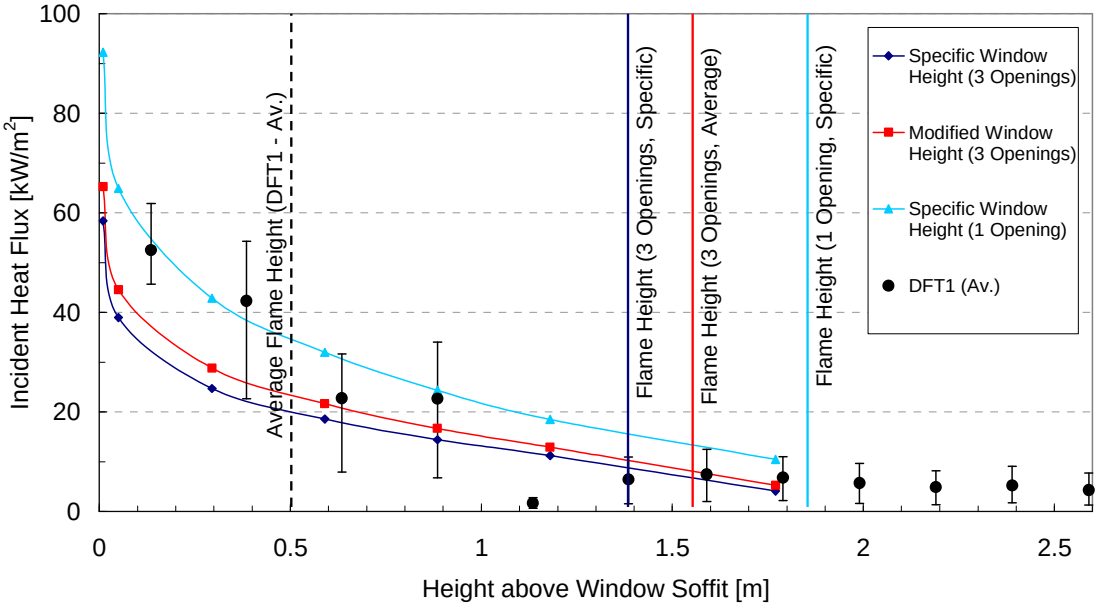

Figure 5.3. Vertical distribution of heat flux incident on the façade resulting from modelling the DFT1 scenario under ND conditions, using two different definitions of the opening height throughout. The respective resultant flame heights, *z* (m) are indicated. The DFT1 data taken as an average over the period of maximum sustained external flaming are shown with error bars accounting for the maximum and minimum instantaneous values measured at each location. The average flame height measured is also indicated.

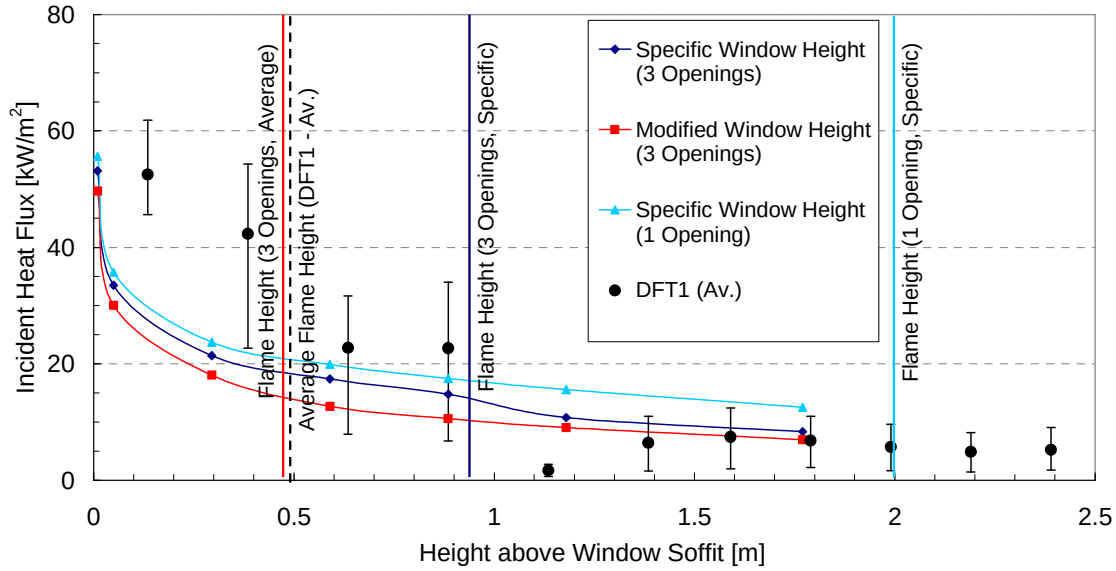

Figure 5.4. Vertical distribution of heat flux incident on the façade resulting from modelling the DFT1 scenario under ToFD conditions, using two different definitions of the opening height throughout. The respective resultant flame heights, *z* (m) are indicated. The DFT1 data taken as an average over the period of maximum sustained external flaming are shown with error bars accounting for the maximum and minimum instantaneous values measured at each location. The average flame height measured is also indicated.

5.4.3 Defining the Flame Thickness and Flame Temperature for a point on the façade not engulfed in flame

When identifying the flame temperature to be used in the Law Model calculations, the point along the flame axis at which to take the flame temperature, T_z and indeed the flame thickness, λ may be apparent when considering a point on the façade engulfed in flame. In this case, the flame temperature is taken as that at the flame axis point, directly opposite the point of interest and its thickness is that perpendicular to the façade. Nevertheless, when the point on the façade is not engulfed in flame, the flame temperature and thickness to be used is not evident. In this case, three potential definitions are considered: the conditions described by the point along the flame axis perpendicular to the opening soffit, defined in the Law Model as a conservative assumption [1]; the average conditions described by the point along the flame axis opposite the opening soffit and by the flame tip, where the temperature is taken as a fourth root of the average of temperatures at both locations taken to the fourth power, as described by Law in a paper describing the development of the Law Model [26]; and, the point along the flame axis where the axis is perpendicular to the element of interest on the façade, as would seem theoretically appropriate. Although the latter involves a little more calculation, it is theoretically the most sound definition.

The effect on the external heat flux distribution had by each of the three potential flame temperature and flame thickness definitions was studied based on the DFT1 scenario under *Through or Forced Draught* conditions, as the flame is expected to project away from the façade, resulting in a façade that is not engulfed by flame. Figure 5.5 shows the heat flux distribution described using each of the flame temperature and flame thickness definitions and the distinction between each is very small. Although taking the flame characteristics pertaining to the height of the window soffit, deemed to be a conservative approach by Law and O'Brien [1], provides the highest heat flux distribution, the comparison shows none of the definitions make a significant difference to the modelled outcome. Since the conservative definition is that least likely to apply to a point on the façade that is not within the near-field of the window soffit, and since the average suggested in Law's description of the development of the model [26] describes the lowest heat flux, the theoretical definition (deemed most appropriate for a point on the façade) is used.

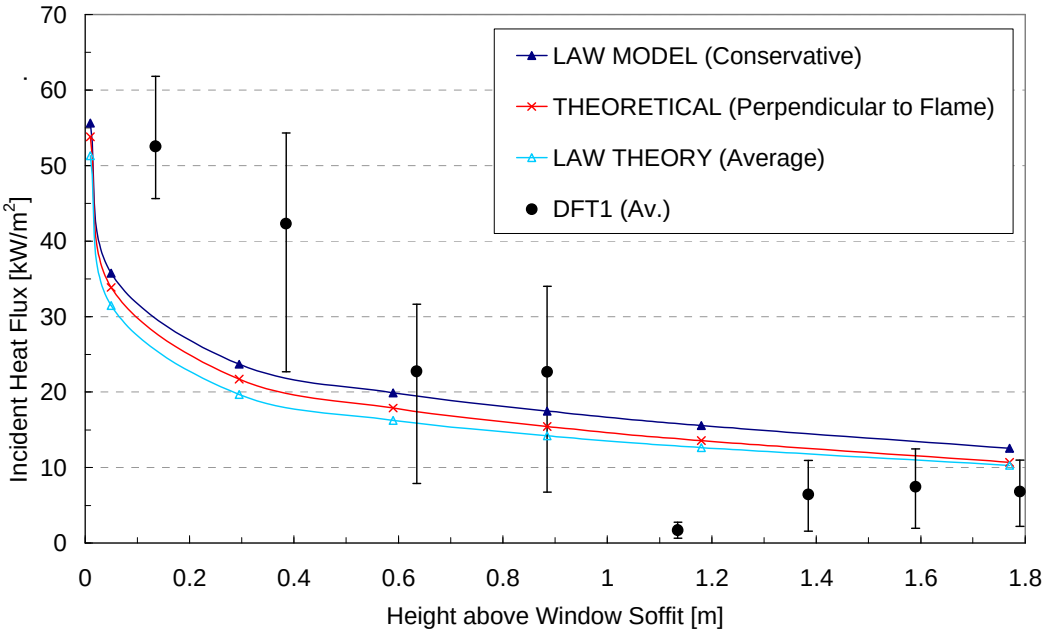

Figure 5.5. Vertical distribution of heat flux incident on the façade resulting from modelling the DFT1 scenario under ToFD conditions, using three different definitions of the flame temperature and thickness. The DFT1 data taken as an average over the period of maximum sustained external flaming are shown with error bars accounting for the maximum and minimum instantaneous values measured.

5.5 Ranges of Variation for Individual Input Parameters

The Law Model has over 14 input parameters. These can be divided into four main categories: *geometric*, *fuel*, *ambient conditions* and *relative*. The *geometric* category includes the three main compartment dimensions (W,D,H), as well as those pertaining to a potential compartment core (C), and the opening dimensions (w, h) of which there can be a number of different ones should the scenario have several openings of different sizes. The *fuel* category involves the fire load (L) (often expressed in terms of fire load density, L'') and fire duration (τ_f) and that of *ambient conditions* includes ambient temperature (T_a) and wind or draught velocity (u). The *relative* category is used to define all other parameters that arise from the relative conditions of the scenario, such as the characteristic length scale (d), the distance between the emitter and receiver (S') and the angle between these (θ) which make up the configuration factors. The dimensions of a potential projection, such as an awning or balcony which may deflect the external flame, are also a potential input parameter as is the plume gas density (ρ) which features in the buoyancy term and is taken as 0.45 kg/m^3 at 540^{o}C throughout the Law Model.

The parameter sensitivity study was undertaken on most of the parameters, with the exception of: the core dimensions (C) because a core does not feature in the DFT1 benchmark scenario and is its effect is thought to be closely linked with that of others in the *geometric* category as it simply alters the A_F, A_T and D/W intermediate parameters; the fire duration (τ_f) which is not directly varied but the effect of its variation is implied in that of the fire load (L) as fire duration only features in rate of burning equations (*cf.* Chapter 3, Equation (3.6) and (3.19)) of which the only other variable is the fire load (L); and the gas density (ρ) which is taken as constant throughout the definitions in the model. Furthermore, the other parameters in the *relative* category (d, S', θ) do not affect the characteristics of the fire and flame development and hence are not *directly* varied, but rather vary as a consequence of the scenario setup.

In using the DFT1 scenario as a benchmark, all the parameters comprising the parameter sensitivity study are systematically varied by increments within a reasonable range, under both *No Through Draught* and *Through or Forced Draught* conditions, in turn. The maximum range studied for each parameter is listed in Table 5.2 and defined as a multiple of the parameter value pertaining to the DFT1 benchmark scenario, covering a variation in values deemed to be expected in standard design scenarios.

Parameter	**Range**	**Lower Bound**	**Upper bound**
Compartment Width (m)	W – 3W	3.6	10.8
Compartment Depth (m)	D – 3D	4.75	14.25
Compartment Height (m)	H – 3H	2.45	7.3
Window Width (m)	0.124w – 1.53w	0.3	3.6
Window Height (m)	0.25h – 2h	0.3	2.36
Fire Load (kg) (density (kg/m^2))	0.1L – 10L	54.72 (3.2)	5472 (320)
Ambient Temperature (^{o}C)	-2.55T_a; 2.55T_a	-60	60
Wind Velocity (m/s)	0.05u-2u	0.3	12

Table 5.2. Law Model input parameters varied during the parameter sensitivity study based around the DFT1 benchmark scenario, detailing the maximum range of values studied.

The main compartment dimensions are varied up to three times the DFT1 dimension each and the window opening is varied from 0.3 m as the smallest dimension to upper bound limits defined by the dimensions of the wall the window sits in. The fire load is varied from a tenth up to ten times that used in DFT1, which is a significant variation allowing for an insight into the effect of the fire load over a range of values that are potentially more realistic than the upper bound defined. The range of ambient temperature is taken to encompass the extremes expected at different locations around the world, such as to establish the significance of the ambient temperature specified for design in regions where the average may vary significantly from the 20^{o}C the Law Model [1] recommends for design. Given that the wind (or draught) velocity during DFT1 is unknown, the value of 6 m/s recommended by the Law Model for design is used for the DFT1 benchmark case and varied from the lowest velocity defining the change from calm to light air (0-1 on the Beaufort scale) to a strong breeze (6 on the Beaufort scale), equating to twice that recommended by Law and O'Brien [1] for design.

For the purposes of the parameter sensitivity study, the DFT1 scenario is defined under *No Through Draught* conditions with only the window as a single opening and under *Through or Forced Draught* conditions with both three openings (under *Through Draught* conditions) and only the window as a single opening (emulating *Forced Draught* conditions). The *No Through Draught* scenario with three openings is not considered, as a compartment with openings on opposite walls would be defined under the Law Model to be under *Through or Forced Draught* conditions, hence such a scenario would not feature in the use of the model for design. In the cases where three openings are defined, only the dimensions of the window are varied, while those of the doors remain as per the DFT1 scenario.

While all parameters listed in Table 5.2 are individually varied, an initial study is conducted to identify the range of reciprocal opening factors, η covered by the range of variation of the window width and height. This places the parameter sensitivity study in context with regards to the range of reciprocal opening factors covered by the large-scale test scenarios against which the Law Model has previously been validated.

5.6 The Effect of the Reciprocal Opening Factor

The systematic variation of the *geometric* parameters results in a range of scenarios with different reciprocal opening factors. Although the variation in compartment dimensions changes the reciprocal opening factor, the relative changes in the opening dimensions are found to cover a larger range. The *Through or Forced Draught* scenarios with three openings are found to cover a 7 $m^{-1/2}$ to 13.5 $m^{-1/2}$ range of the reciprocal opening factor. The variation in window height and width under the *No Through Draught* and *Through or Forced Draught* scenarios with the window as a single opening however, are found to result in a range of reciprocal opening factors from circa 10 $m^{-1/2}$ to 200 $m^{-1/2}$. This range is well above that covered by the large-scale tests previously used to validate the Law Model (henceforth known as the *validated range*), which covered a 5.4 $m^{-1/2}$ and 40.8 $m^{-1/2}$ reciprocal opening factor range over circa 50 tests. Furthermore, as discussed in Chapter 3, Section 3.3.1, the vast majority of these tests fell in the 5.4-18 $m^{-1/2}$ range, therefore a number of the cases considered in the parameter sensitivity study fall outwith the range of scenarios for which the Law Model correlations have been validated.

It is important to note that scenarios with a large reciprocal opening factor (*i.e.* small opening relative to the area of the enclosure walls) under *No Through Draught* may not realistically lead to post-flashover fire conditions and the heat flux incident on the external façade from a fire in such a scenario may be very different from that described by the Law Model. Nevertheless no limitations are imposed on the use of the model for scenarios with reciprocal opening factors that fall outwith the *validated range*. In fact, Law assumes the correlations to generally apply, stating that if "a design approach is adopted, it not only obviates the need for […] *ad hoc* tests, but [the model] also extends to sizes of fire well beyond the limits of size of practical fire tests" [26]. The Eurocode implementation of the Law Model does limit the use of the model specifying that "the size of the fire compartment should not exceed 70 m in length, 18 m in width and 5 m in height" [2] however the parameter values used for the sensitivity study fall well within this range (with the exception of the upper range of compartment height). Therefore it is entirely possible that standard design scenarios for which the Law Model is currently used fall outwith the experimentally

validated reciprocal opening factor range, rendering it essential to investigate the effect of parameter variation for scenarios with a factor that falls outwith this range.

In order to determine the effect of scenarios with a reciprocal opening factor falling outwith the *validated range*, the effect of varying window width, *w* and varying window height, *h* across the ranges given in Table 5.2 on the resultant heat flux under *No Through Draught* conditions are compared, at several different points along the height of the façade. Figure 5.6 and Figure 5.7 respectively show the heat flux incident at a point 0.05 m and a point 1.18 m (*i.e.* the window height, *h* in the DFT1 benchmark scenario) above the window soffit, plotted against the reciprocal opening factor pertaining to the given scenario as the window width and height are varied. For each of the scenarios, the ambient temperature, T_a is *additionally* varied in order that the relative effect of varying these parameters can be evaluated.

In *No Through Draught* conditions the variation of the window width, window height and ambient temperature all appear to have an effect of similar magnitude on the resultant heat flux incident on the façade under the *validated range* of reciprocal opening factors (highlighted in red), as shown in Figure 5.6 and Figure 5.7. Nevertheless, in the case of the window height, the effect of its variation is accentuated with an increase in the reciprocal opening factor, particularly when it is above 20 $m^{-1/2}$. In fact, for values of η > 40 $m^{-1/2}$ the heat flux soars exponentially resulting in unrealistic values of heat flux at 0.05 m from the window soffit, while at 1.18 m above the soffit, it markedly decreases. Conversely the variation in ambient temperature appears to have a negligible effect on the resultant heat flux to the façade throughout, whereas that of varying the window width lies somewhere in between. The same is found for other points on the façade at several distances from the window soffit and in several cases beyond a reciprocal opening factor of 20 $m^{-1/2}$ the modelled heat flux appears to significantly increase, whereas beyond 40 $m^{-1/2}$ the modelled heat flux is often found to be unrealistically high.

A similar comparison was drawn for the scenarios under *Through or Forced Draught* conditions as shown in Figure 5.8 and Figure 5.9, which include data pertaining to both the scenarios with a single opening and those with three (window and 2 doors).

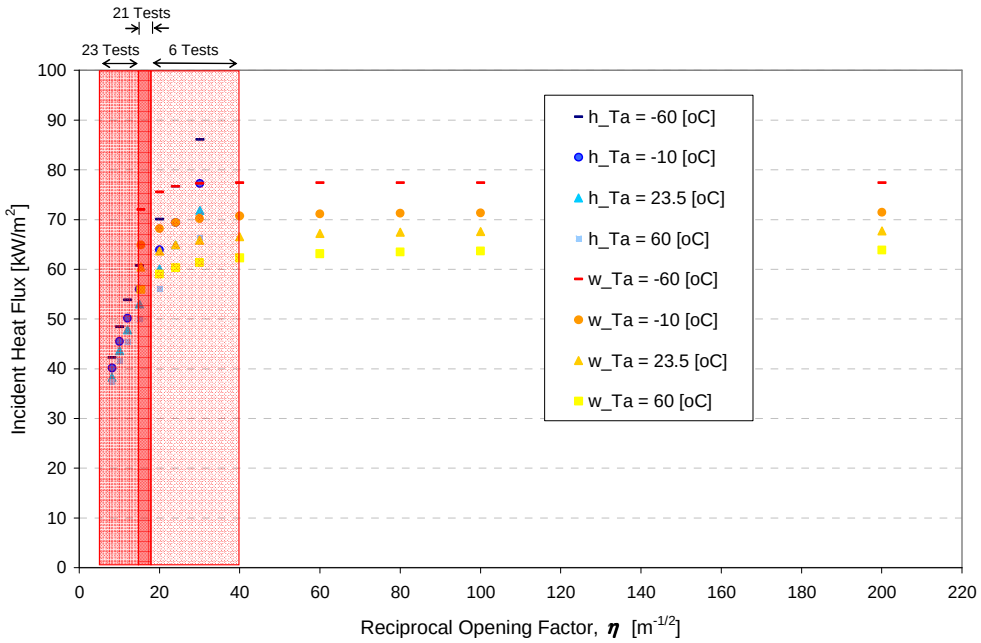

Figure 5.6. Total heat flux incident on the façade, 0.05 m above the opening soffit for a given range of reciprocal opening factors, η pertaining to a number of different scenarios where the window height, h and window width, w where individually varied in *ND* conditions. The ambient temperature, T_a was also additionally varied in each of the scenarios to provide a comparison for the magnitude of effect the parameters have on the resulting heat flux. The areas highlighted in red indicate the reciprocal opening factor range for which the Law Model has been validated via a number of large-scale tests as detailed.

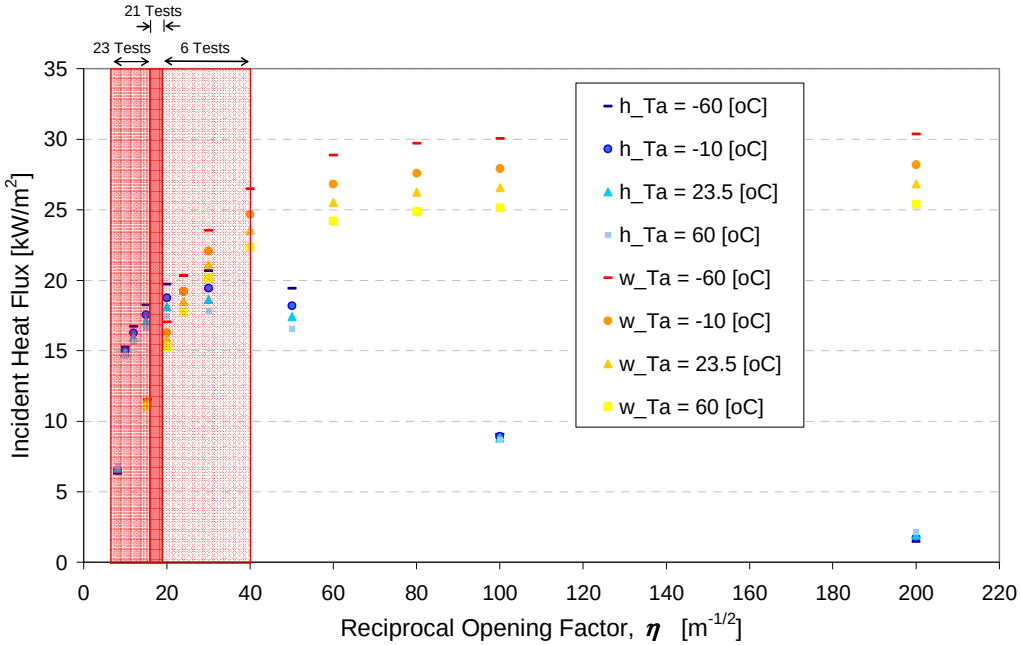

Figure 5.7. Total heat flux incident on the façade, 1.18 m above the opening soffit for a given range of reciprocal opening factors, η pertaining to a number of different scenarios where the window height, h and window width, w where individually varied in *ND* conditions. The ambient temperature, T_a was also additionally varied in each of the scenarios to provide a comparison for the magnitude of effect the parameters have on the resulting heat flux. The areas highlighted in red indicate the reciprocal opening factor range for which the Law Model has been validated via a number of large-scale tests as detailed.

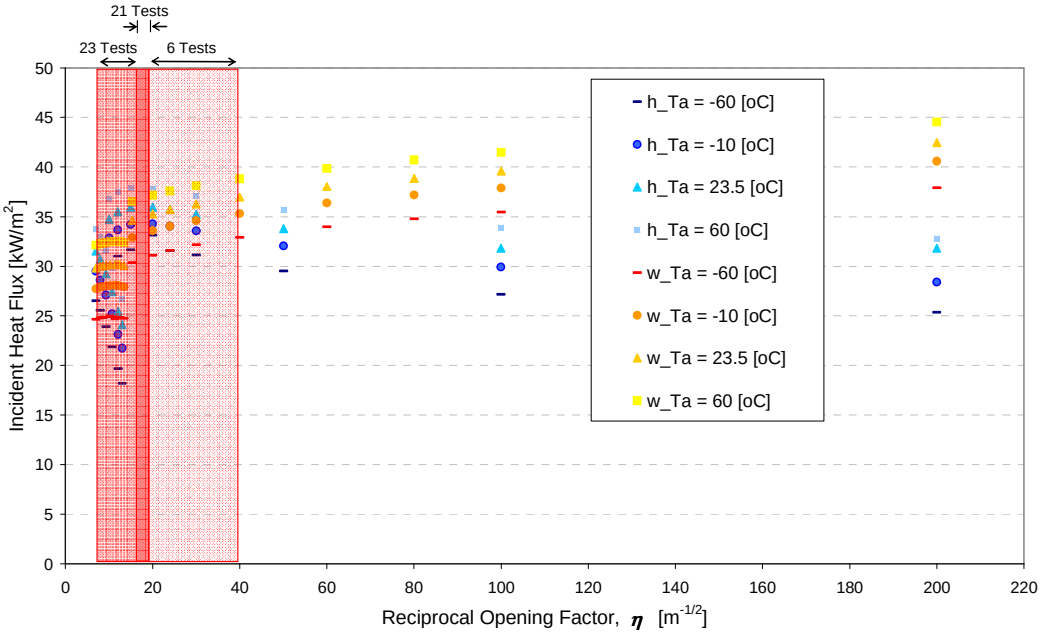

Figure 5.8. Total heat flux incident on the façade, 0.05 m above the opening soffit for a given range of reciprocal opening factors, η pertaining to a number of different scenarios where the window height, h and window width, w where individually varied in *ToFD* conditions. The ambient temperature, T_a was also additionally varied in each of the scenarios to provide a comparison for the magnitude of effect the parameters have on the resulting heat flux. The areas highlighted in red indicate the reciprocal opening factor range for which the Law Model has been validated via a number of large-scale tests as detailed.

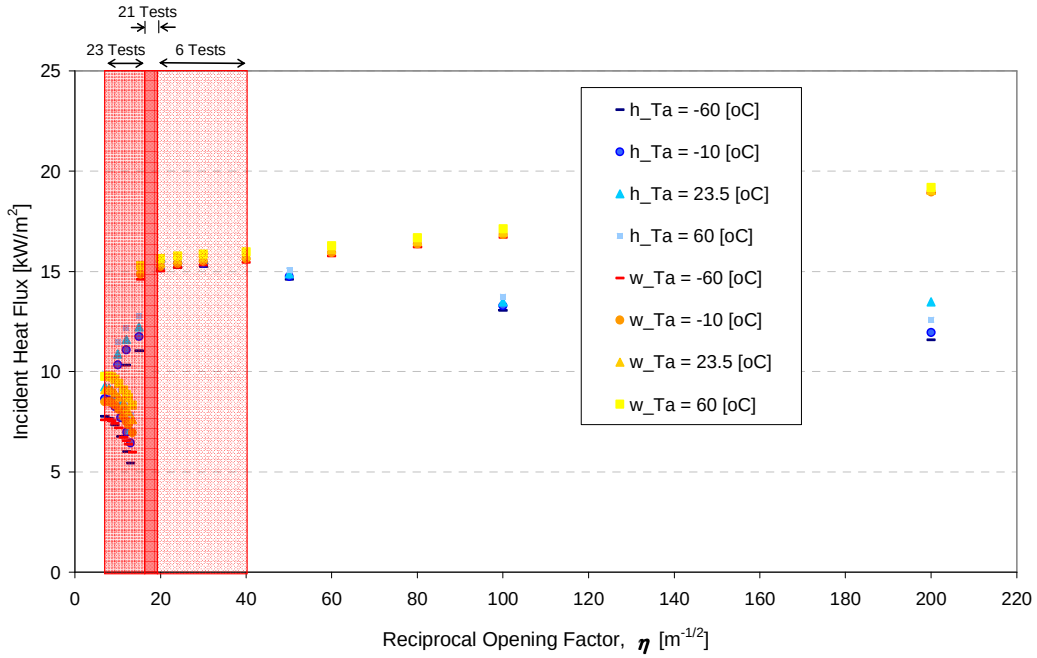

Figure 5.9. Total heat flux incident on the façade, 1.18 m above the opening soffit for a given range of reciprocal opening factors, η pertaining to a number of different scenarios where the window height, h and window width, w where individually varied in *ToFD* conditions. The ambient temperature, T_a was also additionally varied in each of the scenarios to provide a comparison for the magnitude of effect the parameters have on the resulting heat flux. The areas highlighted in red indicate the reciprocal opening factor range for which the Law Model has been validated via a number of large-scale tests as detailed.

In *Through or Forced Draught* conditions the variation of the window width, window height and ambient temperature again all appear to have an effect of similar magnitude on the heat flux incident on the façade under the *validated range* of reciprocal opening factors (highlighted in red), as shown in Figure 5.8 and Figure 5.9. It should be noted that where two distinct patterns of heat flux variation arise from the variation of the window width or window height under the *validated range* of the reciprocal opening factors, these correspond to the scenarios with one and three openings. This is particularly distinct in Figure 5.9. Under the *validated range* the variation in window width results in a cluster of heat flux that decreases from 10 kW/m^2 to 7.5 kW/m^2 (for Ta = 60^oC) associated with low reciprocal opening factors, where the data pertain to scenarios with three openings. The higher heat fluxes around 15-16 kW/m^2 associated with higher values of the reciprocal opening factor pertain to scenarios where there is only a single opening. Nevertheless, within the range of data pertaining to scenarios either with a single opening or with three, the greatest variation in the heat flux pattern is again seen when scenarios have reciprocal opening factors beyond those in the *validated range*, which under *Through or Forced Draught* conditions may realistically have close to free-burning conditions. The same observations are made at other heights along the façade wall and in fact, variation in the window width and window height in scenarios with $\eta > 40$ $m^{-1/2}$ becomes even more noticeable with height from the window soffit. The ambient temperature parameter however appears to make a negligible difference to the resultant heat flux incident on the façade under most conditions.

Overall, analysis of the effect of varying opening dimensions under scenarios with reciprocal opening factors that fall beyond the range for which the Law Model has been validated shows the heat flux output to vary significantly, at times resulting in unrealistic values. This results from the empirical nature of the correlations and from some of the numerical limitations discussed in Chapter 3, Section 3.4.5. Therefore, it appears the Law Model correlations may in fact not be valid for use in scenarios with a reciprocal opening factor greater than that of 40 $m^{-1/2}$. In fact, the limited number of large-scale tests conducted in scenarios where the reciprocal opening factor is greater than circa 20 $m^{-1/2}$ renders it prudent to assume the Law Model is valid only for scenarios within the range of reciprocal opening factors for which there has been thorough large-scale testing. Hence in analysing the detailed parameter sensitivity

study in order to identify the parameters of key importance, it should be kept in mind that the scenarios for which the reciprocal opening factor falls between 5-20 $m^{-1/2}$ are likely to be most useful. In the meantime, it is also important to make-known this limitation such as to prevent the inadequate use of the Law Model, which could result in either over-prediction of the external façade heat flux (costly) or under-prediction which, if consequently used in design, may lead to dangerous situations once there is in fact a fire. For scenarios falling outwith this range of reciprocal opening factors, further large-scale tests should be conducted in order to investigate the effect parameters have on the external heat flux to the façade.

5.7 Independent Parameter Variation

5.7.1 Parameter Variation under No Through Draught (ND)

The parameter sensitivity study is first conducted for scenarios under *No Through Draught* conditions. Dalmarnock Fire Tests One is used as the benchmark scenario with the window as the single opening and the input parameters under the *geometric* category are first varied incrementally, over the range of values listed in Table 5.2. The distribution of resultant heat flux incident on the façade with height from the window soffit is shown in Figures 5.10-5.12 for variation of the compartment width, *W*, depth, *D* and height, *H* respectively. What is immediately striking from the variation of the main compartment dimensions is that they seem to have little effect on the resultant external heat flux distribution on the façade, particularly in the near-field to the window soffit. While in the case of the compartment width and the compartment height there appears to be some variation in the heat flux distribution further afield, at a distance greater than 1 m from the opening soffit, the variation in each case does not appear to be particularly significant. In any case, for variations of the compartment width greater than 1.75*W* (6.3 m), the fire becomes fuel-controlled and the compartment width no longer affects the heat flux to the façade, resulting in an upper bound to the effect of compartment width variation on the heat flux distribution in the far-field. On the other hand, the effect of the compartment depth parameter on the façade heat flux distribution is negligible throughout the range of values studied, which has also been found by others in a thorough computational analysis of the Law Model under *No Through Draught* conditions [126].

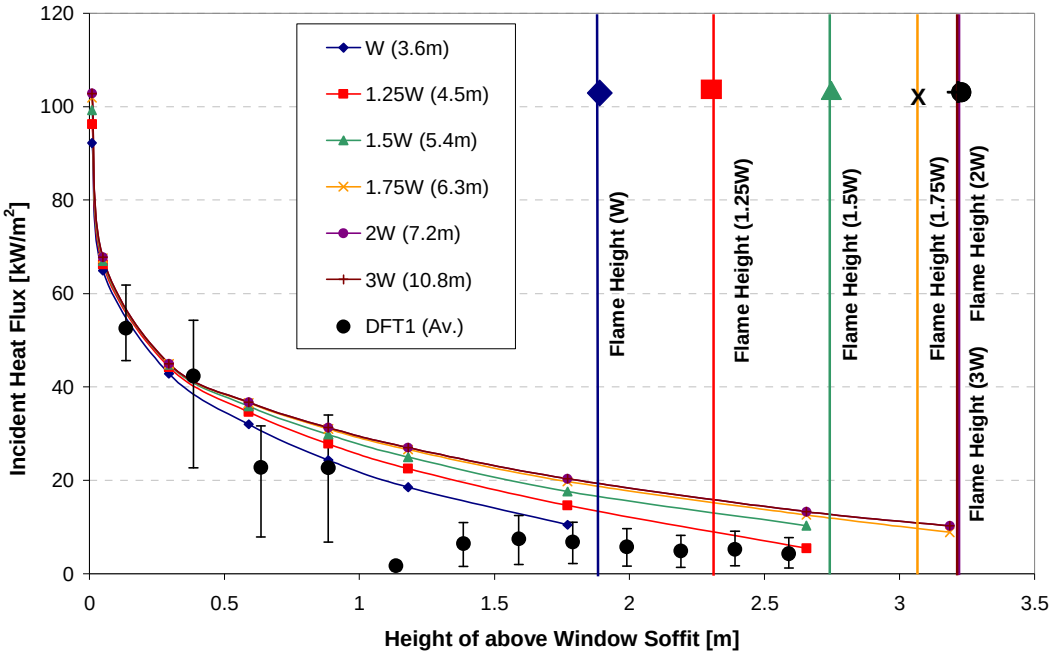

Figure 5.10. Distribution of heat flux incident on the façade as a function of height from the window soffit along its centreline, resulting from several scenarios in which the compartment width, *W* is systematically varied under *No Through Draught* conditions. The respective flame heights are also shown for comparison, as is the average heat flux measured during DFT1 throughout the period of maximum sustained external flaming (error bars indicate max. and min. instantaneous values).

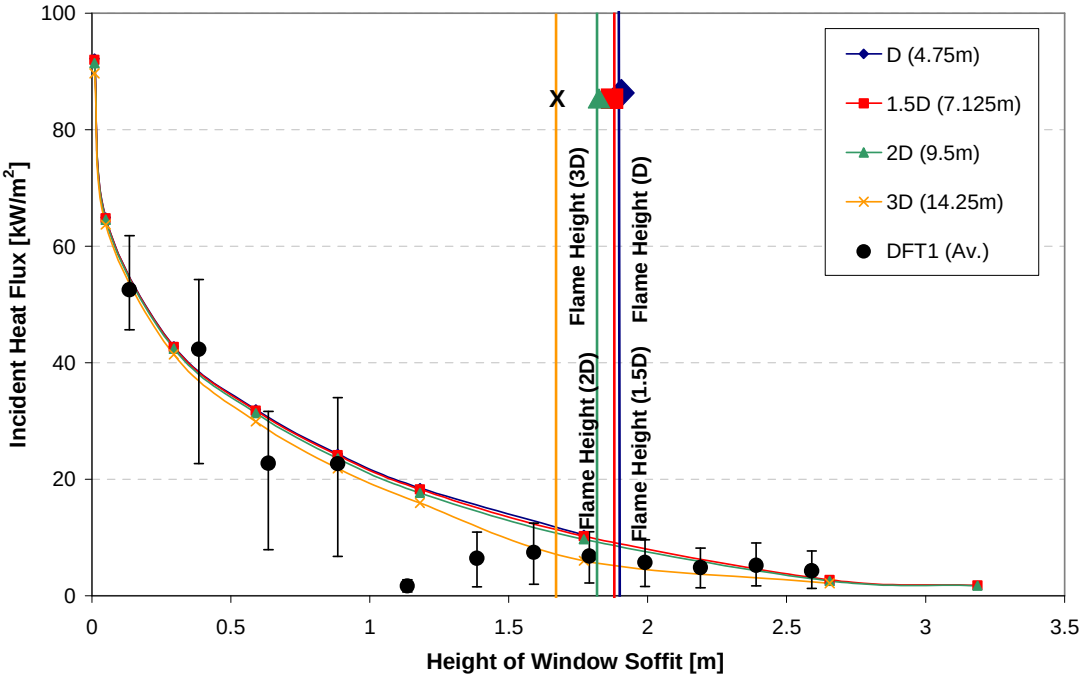

Figure 5.11. Distribution of heat flux incident on the façade as a function of height from the window soffit along its centreline, resulting from several scenarios in which the compartment depth, *D* is systematically varied under *No Through Draught* conditions. The respective flame heights are also shown for comparison, as is the average heat flux measured during DFT1 throughout the period of maximum sustained external flaming (error bars indicate max. and min. instantaneous values).

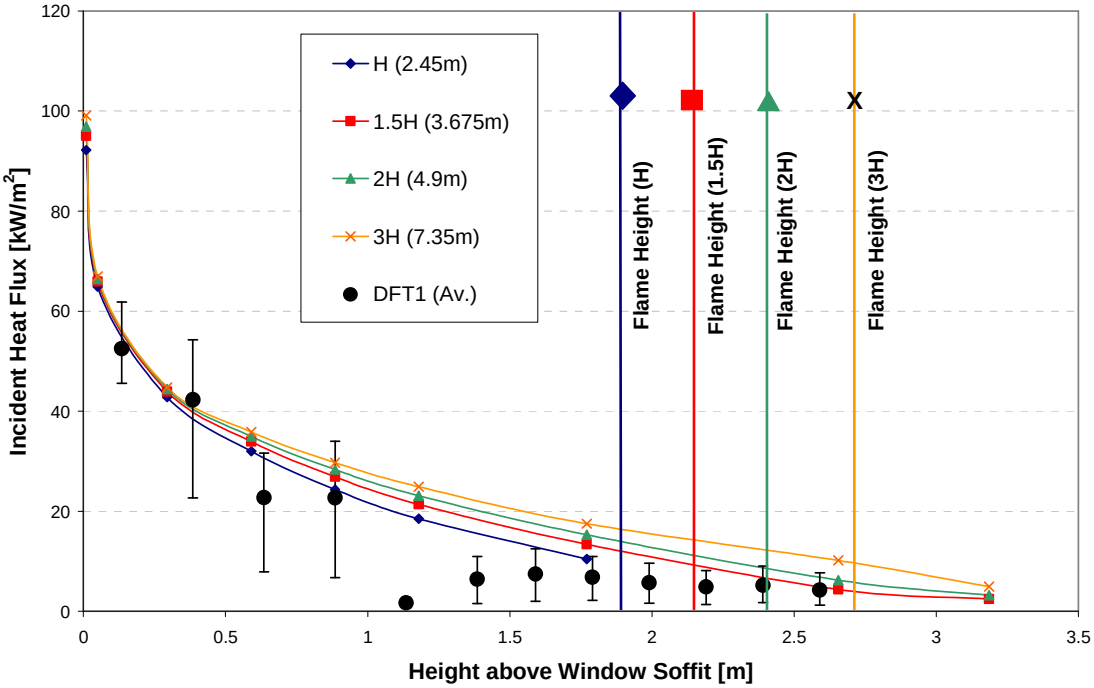

Figure 5.12. Distribution of heat flux incident on the façade as a function of height from the window soffit along its centreline, resulting from several scenarios in which the compartment height, *H* is systematically varied under *No Through Draught* conditions. The respective flame heights are also shown for comparison, as is the average heat flux measured during DFT1 throughout the period of maximum sustained external flaming (error bars indicate max. and min. instantaneous values).

Similarly, the window width, *w* and height, *h* parameters are incrementally varied over the range listed in Table 5.2. In the near-field to the window soffit, variation of the window width, *w* does not appear to have a significant effect on the resultant heat flux to the façade. Further afield, at heights which the heat flux may be of interest for the design of inter-storey compartment window separation and for the prevention of glass cracking, the window width appears to have a more significant affect on the heat flux distribution. Nevertheless, yet again, an upper bound is found in the effect the window width has, as under a certain width the difference in the heat flux distribution described becomes negligible. In any case, all window widths below 0.61*w* (1.43 m) result in scenarios with a reciprocal opening factor over 40 $m^{-1/2}$, describing very low rates of burning and very high external flame heights, and the validity of the Law Model output in this region is unknown.

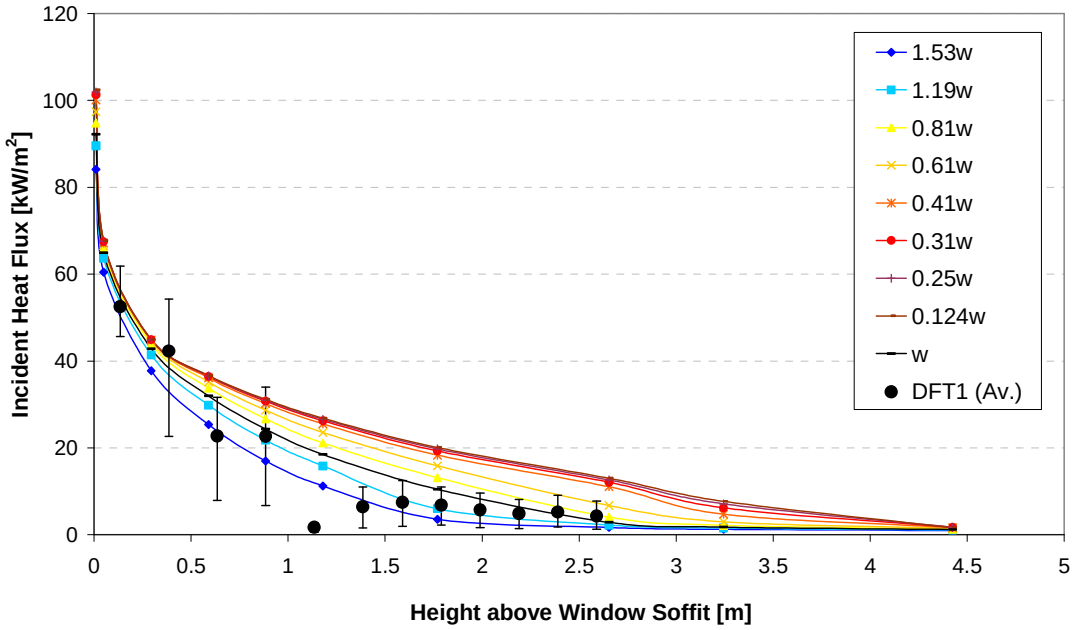

Figure 5.13. Distribution of heat flux incident on the façade as a function of height from the window soffit along its centreline, resulting from several scenarios in which the window width, *w* is systematically varied under *No Through Draught* conditions. The average heat flux measured during DFT1 throughout the period of maximum sustained external flaming is also shown with error bars indicating the maximum and minimum instantaneous values over that period.

The variation of window height, *h* on the other hand, appears to have a larger effect on the near-field heat flux distribution, close to the window soffit and a negligible effect in the far-field. All scenarios investigated with a window height under 0.86*h* (1.02 m) however correspond to compartments with a reciprocal opening factor over 40 $m^{-1/2}$ and the low rates of burning described lead to unrealistically high temperatures at the opening, T_o which in turn affects the flame temperature, T_z and results in unrealistic values of heat flux in the near-field. This occurs due to a numerical discontinuity in the empirical correlations used, as described in Chapter 3, Section 3.4.5. Therefore, within the *validated range* of the Law Model, the overall effect of opening height variation on the heat flux incident on the façade is less pronounced than that seen at the far-field under variation of the window width.

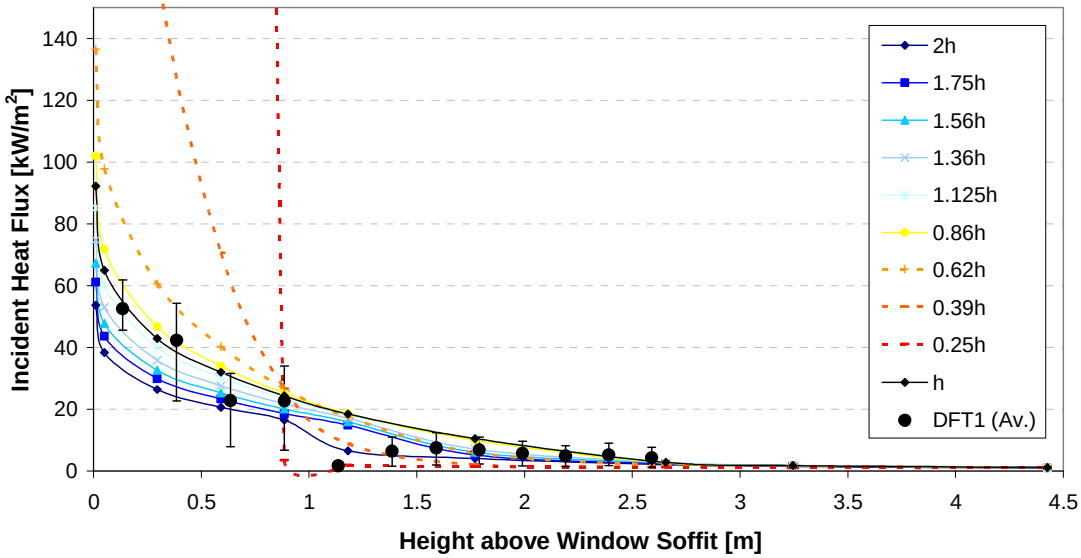

Figure 5.14. Distribution of heat flux incident on the façade as a function of height from the window soffit along its centreline, resulting from several scenarios in which the window height, *h* is systematically varied under *No Through Draught* conditions. Dashed lines correspond to scenarios for which the Law Model output has been found to be unrealistic. The average heat flux measured during DFT1 throughout the period of maximum sustained external flaming is also shown with error bars indicating the maximum and minimum instantaneous values over that period.

In the *fuel* category of parameters, the fire load, L is varied over the range listed in Table 5.2. As the compartment dimensions are fixed at those of the DFT1 scenario, the floor area is constant hence the variation in fire load can also be expressed in terms of variation in fire load density, L'' which is a more common description of the fire load in a given scenario. The fire load parameter is found to have a marked effect on the distribution of heat flux incident on the façade, both in the near- and far-field of the window soffit, as seen from Figure 5.15. Beyond a fire load of 0.57 L (311 kg, or a fire load density, L'' of 18.2 kg/m^2) the fire becomes ventilation controlled and the fire load is found to have no effect on the resultant external heat flux, while for values of low fire load the external heat flux decreases, as expected. Although the Law Model specifies no lower limit of fire load for which it is applicable, the Eurocode implementation of the model specifies it is only applicable for scenarios with a fire load *density* greater than circa 11 kg/m^2 of wood equivalent, as discussed in Chapter 3, Section 3.4.5. While the fire duration has not been varied, it is expected to have a similar effect, as discussed in Section 5.5, where the effect of a longer fire duration would equate to that of a lower fire load and that of a shorter fire to a higher fire load,

as such having a similar effect on the resultant rate of burning under the assumptions made in the Law Model.

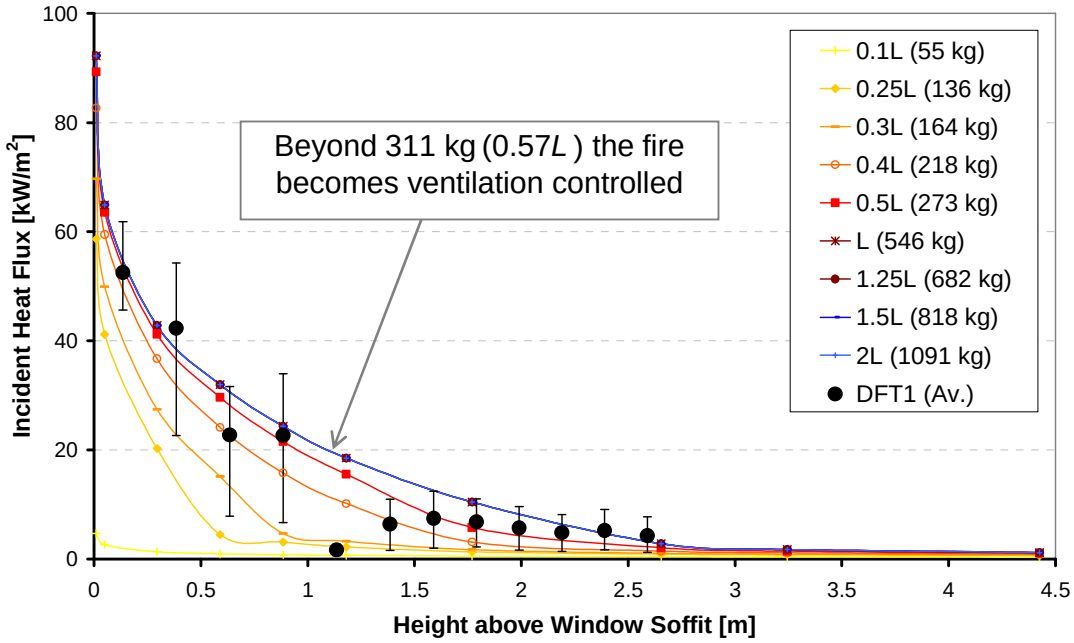

Figure 5.15. Distribution of heat flux incident on the façade as a function of height from the window soffit along its centreline, resulting from several scenarios in which the fire load, *L* is systematically varied under *No Through Draught* conditions. The average heat flux measured during DFT1 throughout the period of maximum sustained external flaming is also shown with error bars indicating the maximum and minimum instantaneous values over that period.

Under *No Through Draught* conditions only the ambient temperature, T_a from the *ambient conditions* category is varied as it is assumed there is no draught flowing through the compartment, hence any wind is deemed to only deflect the external plume sideways but not to affect its characteristic dimensions or temperature distribution. The ambient temperature, varied within the range expected under extreme conditions, is found to have very little effect on the distribution of external heat flux on the façade in the near-field of the opening soffit and no noticeable effect in the far-field, further than 1 m above the opening soffit.

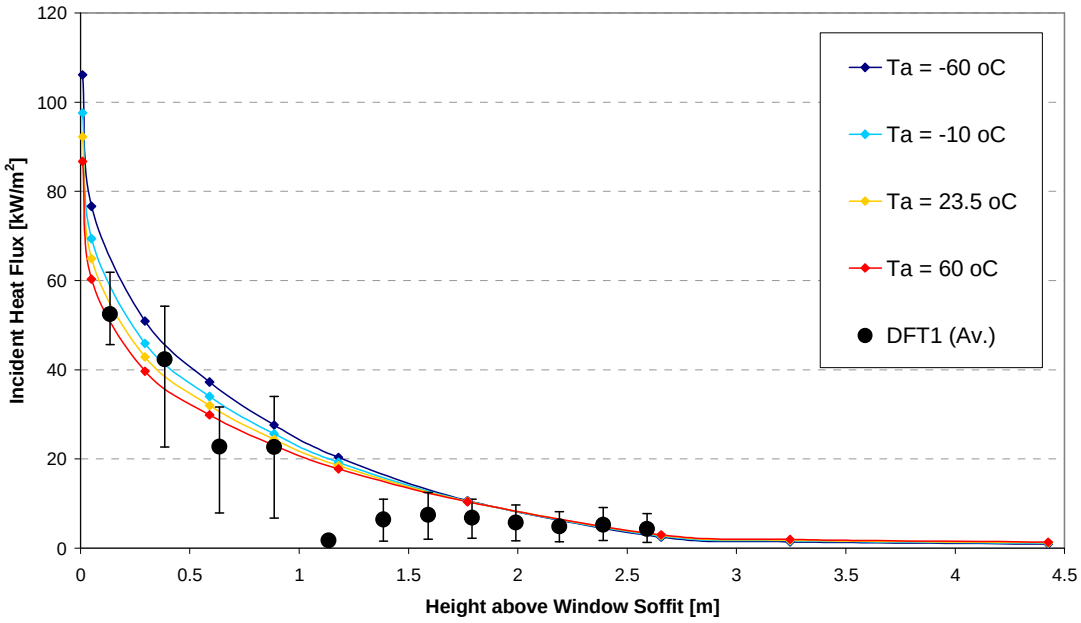

Figure 5.16. Distribution of heat flux incident on the façade as a function of height from the window soffit along its centreline, resulting from several scenarios in which the ambient temperature, T_a is systematically varied under *No Through Draught* conditions. The average heat flux measured during DFT1 throughout the period of maximum sustained external flaming is also shown with error bars indicating the maximum and minimum instantaneous values over that period.

Overall, under *No Through Draught* conditions, the vertical distribution of heat flux along the centreline of the façade from the opening soffit is found to follow the same decay pattern as that measured in Dalmarnock Fire Test One. Although the variation of some parameters is found to alter the heat flux distribution (mostly in either the near-field or far-field to the opening soffit), none seem to do so significantly. Only the fire load parameter is found to have a significant effect on the heat flux distribution both in the near- and far-field of the opening soffit. Even the heat flux distribution described by scenarios where the parameters are varied to the extreme upper or lower bound limits described in Table 5.2, appear to fall within the ballpark range of heat flux measured during DFT1. While there appears to be some variation in the heat flux in the close vicinity of the opening soffit, this heat flux is unlikely to be realistic due to the numerical limitations associated with every small characteristic length scales, as discussed in Section 5.4.1. Nevertheless, at a distance of 0.05 m from the opening soffit, the heat flux described by most scenarios is very similar to that described by the first DFT1 data point, at the same height.

5.7.2 Parameter Variation under Through or Forced Draught (ToFD)

The parameter sensitivity study is similarly carried out around the DFT1 benchmark scenario under *Through or Forced Draught* conditions, including both cases with a single opening (window) and with three openings (window and 2 doors) where appropriate. Variation of the compartment dimensions is seen to have no effect on the resultant heat flux distribution on the façade, with the same distribution described in Figure 5.17, Figure 5.18 and Figure 5.19, where the compartment width, W, compartment depth, D and compartment height, H were respectively varied, in a scenario with three openings. This is expected as under *Through or Forced Draught* conditions the fire is assumed to be under fuel-controlled conditions and the compartment dimension parameters feature only in the form of the compartment scenario parameter, ψ in Chapter 3, Equation (3.20), which describes the compartment fire temperature, T_f. Since the compartment fire temperature affects only the radiative heat transfer component from the internal fire, it has no bearing on the resultant heat flux on the façade wall as it does not 'see' the window. In the near-field the heat flux distribution describes by these scenarios significantly underestimates that measured during DFT1, however in the far-field it described the data measured remarkably well. This was found in an earlier comparison described in Section 5.3. A similar set of curves is found when the compartment dimensions parameters are varied in a scenario with only the window as a single opening under *Through or Forced Draught* conditions. Although the curves describe an overall slightly higher heat flux distribution, varying the compartment dimension parameters again has no effect.

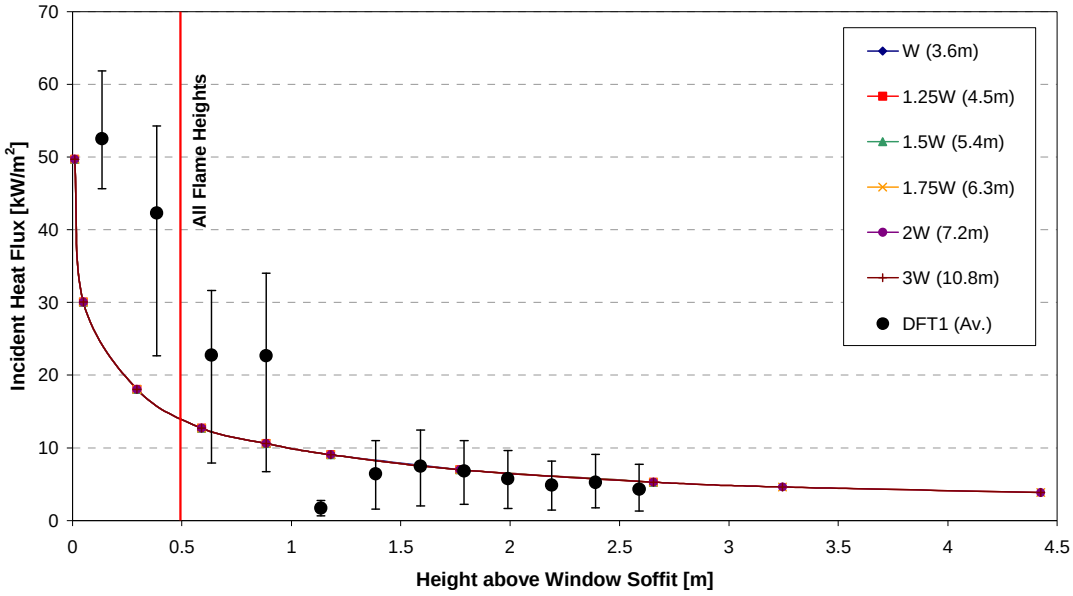

Figure 5.17. Distribution of heat flux incident on the façade as a function of height from the window soffit along its centreline, resulting from several scenarios in which the compartment width, *W* is systematically varied under *Through or Forced Draught* conditions with three openings (window and 2 doors). The respective flame heights are also shown for comparison, as is the average heat flux measured during DFT1 throughout the period of maximum sustained external flaming (error bars indicate max. and min. instantaneous values).

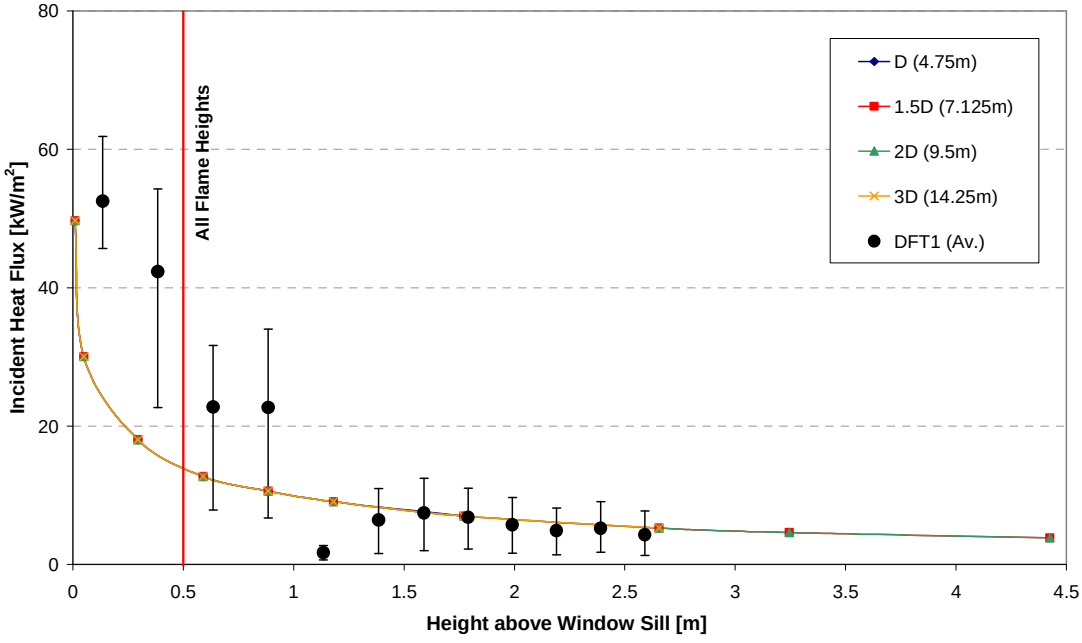

Figure 5.18. Distribution of heat flux incident on the façade as a function of height from the window soffit along its centreline, resulting from several scenarios in which the compartment depth, *D* is systematically varied under *Through or Forced Draught* conditions with three openings (window and 2 doors). The respective flame heights are also shown for comparison, as is the average heat flux measured during DFT1 throughout the period of maximum sustained external flaming (error bars indicate max. and min. instantaneous values).

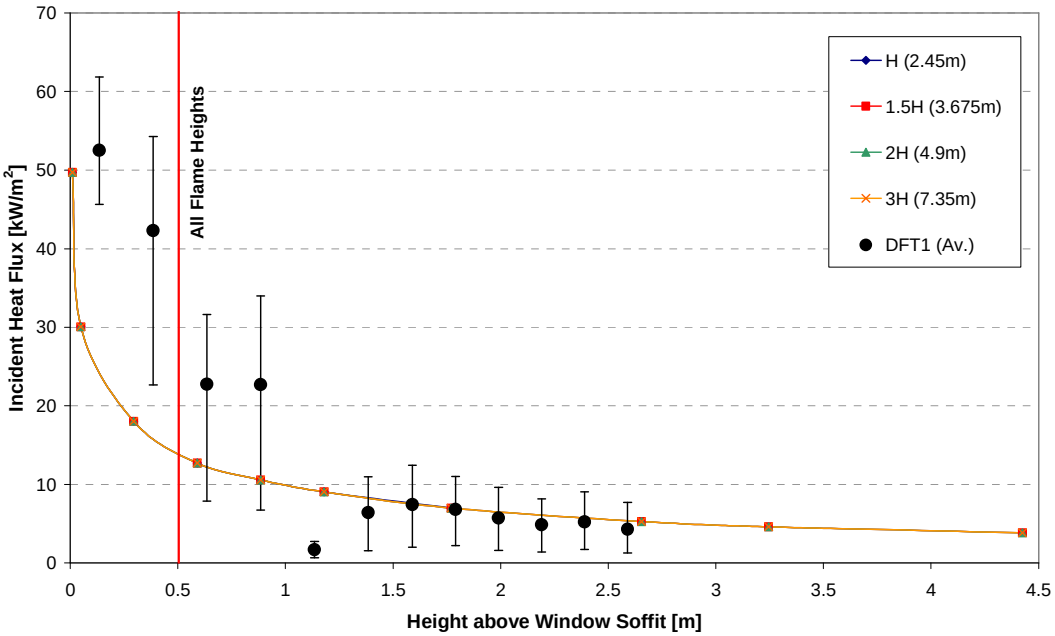

Figure 5.19. Distribution of heat flux incident on the façade as a function of height from the window soffit along its centreline, resulting from several scenarios in which the compartment height, *H* is systematically varied under *Through or Forced Draught* conditions with three openings (window and 2 doors). The respective flame heights are also shown for comparison, as is the average heat flux measured during DFT1 throughout the period of maximum sustained external flaming (error bars indicate max. and min. instantaneous values).

Varying the width of the compartment window across the range listed in Table 5.2, under *Through or Forced Draught* conditions in scenarios both with a single opening (window) and with three openings (window and 2 doors), shows the window width to have very limited effect on the distribution of heat flux incident on the façade, as seen in Figure 5.20. While once again the scenarios with a single opening (larger η) describe an overall higher distribution of heat flux than those with three openings, there is negligible difference in the distribution resulting from variation of the window width in each of the two sets of opening cases. Even between the two sets of cases, the difference in the heat flux described is not large. In the near-field, both sets of curves underestimate the recorded heat flux significantly, while in the far-field the scenarios with a single opening over-estimate the DFT1 data. Similarly, variation of the window height under *Through or Forced Draught* conditions appears to have little effect on the resultant façade heat flux distribution described. Figure 5.21 shows very little difference between the heat flux described with variation of window width under both opening scenarios and the difference between the two sets of scenarios is even less in this case than that of window width variation.

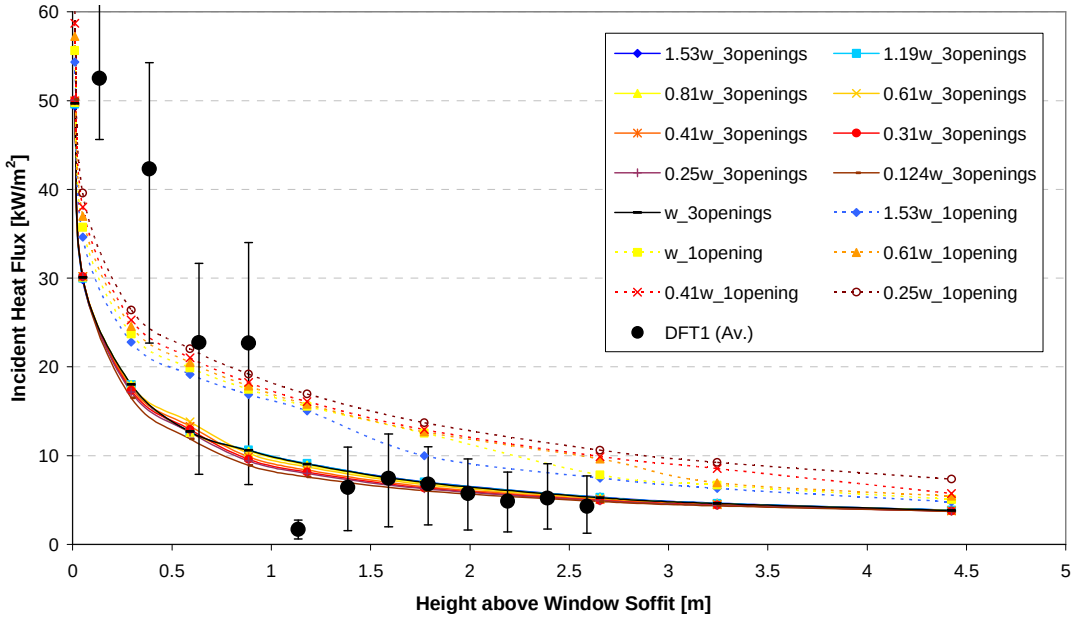

Figure 5.20. Distribution of heat flux incident on the façade as a function of height from the window soffit along its centreline, resulting from several scenarios in which the window width, *w* is systematically varied under *Through or Forced Draught* conditions with both a single opening (window) and three openings (window and 2 doors). The average heat flux measured during DFT1 throughout the period of maximum sustained external flaming is also shown with error bars indicating the maximum and minimum instantaneous values over that period.

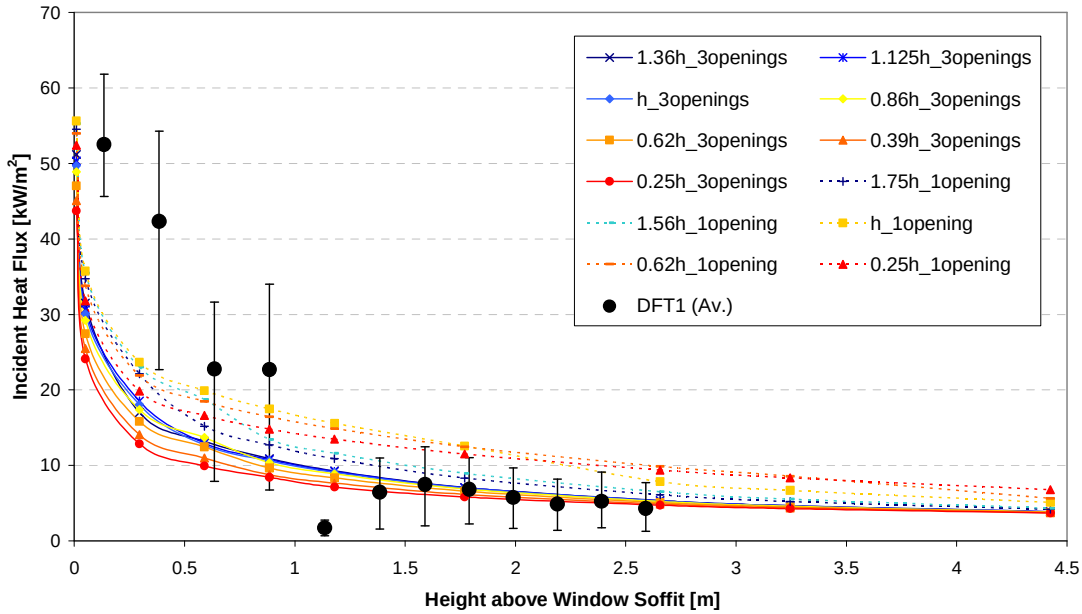

Figure 5.21. Distribution of heat flux incident on the façade as a function of height from the window soffit along its centreline, resulting from several scenarios in which the window height, *h* is systematically varied under *Through or Forced Draught* conditions with both a single opening (window) and three openings (window and 2 doors). The average heat flux measured during DFT1 throughout the period of maximum sustained external flaming is also shown with error bars indicating the maximum and minimum instantaneous values over that period.

Under *Through or Forced Draught* conditions, the fire load parameter, L is again the sole parameter from the *fuel* category that is varied, as variation in the fire duration is implied in its results as previously discussed. The fire load parameter is often expressed in terms of fire load density, L'' and since the compartment dimensions are maintained equal to those in the DFT1 benchmark scenario while the fire load is varied, the fire load density varies correspondingly. Figure 5.22 show the heat flux distribution on the façade resulting from variation of the fire load parameter for scenarios with the window as a single opening. Similarly, Figure 5.23 shows the heat flux distribution resulting from variation of the fire load in scenarios with three openings (window and 2 doors). In both cases the fire load is seen to have an important effect on the heat flux distribution described, in both the near- and far-field to the window soffit. Although 10L (5457 kg, or a fire load density, L'' of 319 kg/m^2) is perhaps unrealistically high, even given the properties of modern furnishings, there is no upper bound to the effect this parameter can have as it directly affects the rate of burning under the assumptions given in the Law Model, in the case of *Through or Forced Draught*. In turn, the rate of burning features in most of the equations that determine the temperature at the window and the characteristics of the external flame, as well as the convective heat transfer coefficient, therefore it is directly related to the resultant heat flux incident on the façade.

In the case of scenarios with just a single opening, values of fire load studied below that of 0.4L (218 kg or a fire load density, L'' of 12.8 kg/m^2) are found to lead to negative flame heights due to very low values of burning rate that feature in Chapter 3, Equation (3.21). This limitation of the Law Model has been discussed in Chapter 3, Section 3.4.5. The same occurs in the scenarios with three openings however the unrealistic, negative values of flame height arise from scenarios with a fire load under that of the DFT1 benchmark, L (546 kg, or a fire load density, L'' of 32 kg/m^2). While it is unknown whether the Law Model correlations are valid for the range of fire load studied, or even for part of the range, this variable appears to be that which has the largest effect on the overall resultant heat flux incident on the façade so far. Nevertheless, as previously seen under *Through or Forced Draught* conditions, even scenarios with a very high fire load – that result in the highest distribution of heat flux – are seen to underestimate the heat flux measured in the near-field of the window soffit during DFT1.

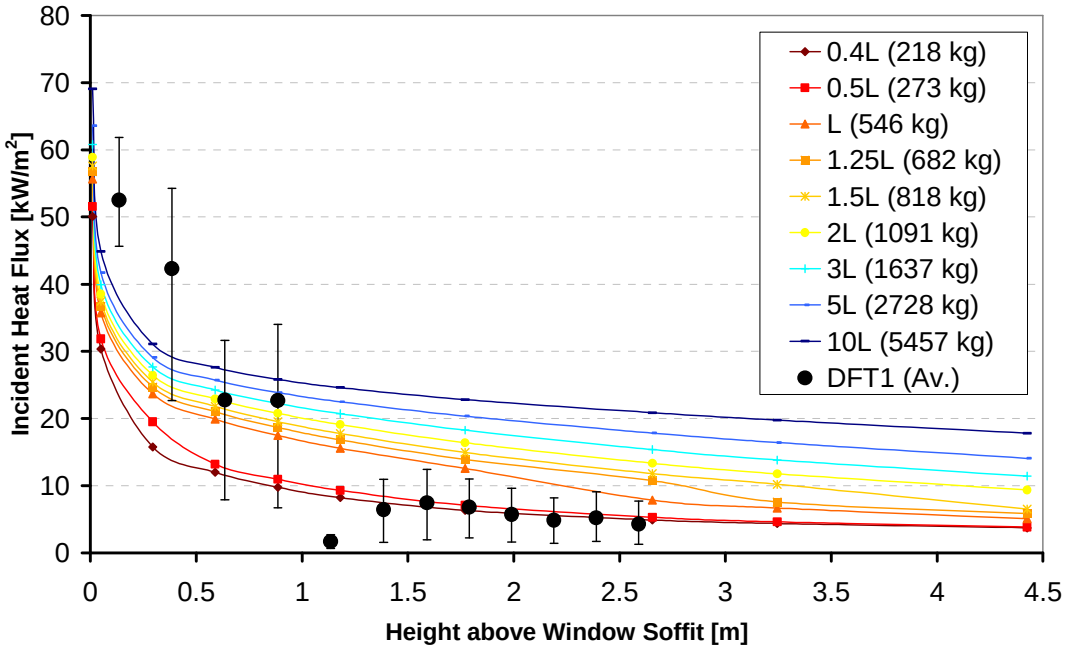

Figure 5.22. Distribution of heat flux incident on the façade as a function of height from the window soffit along its centreline, resulting from several scenarios in which the fire load, *L* is systematically varied under *Through or Forced Draught* conditions with a single opening (window). The average heat flux measured during DFT1 throughout the period of maximum sustained external flaming is also shown with error bars indicating the maximum and minimum instantaneous values over that period.

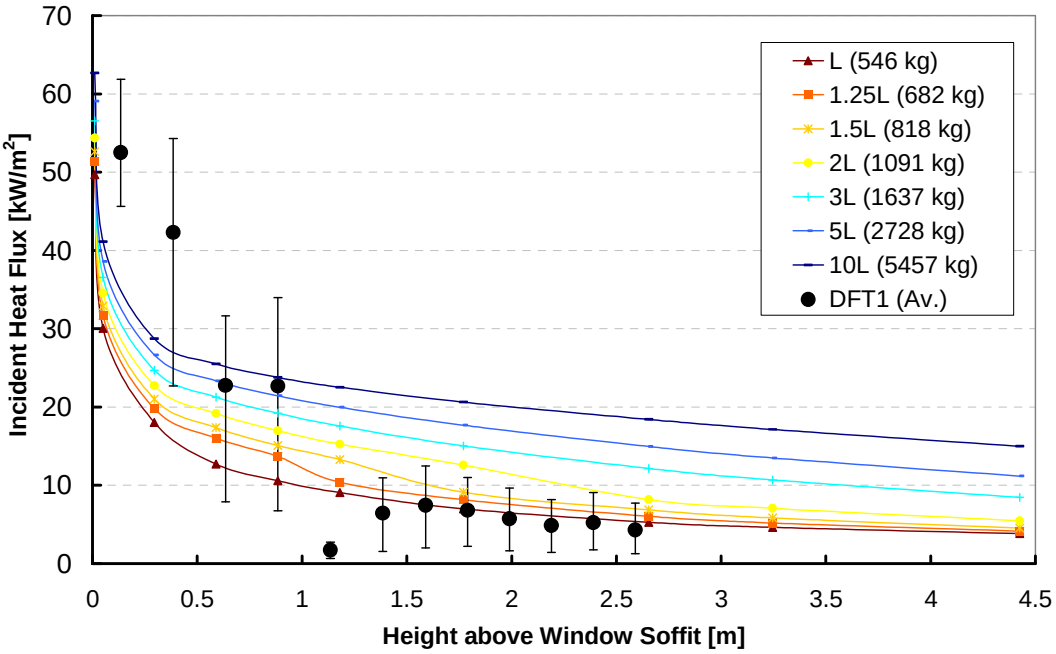

Figure 5.23. Distribution of heat flux incident on the façade as a function of height from the window soffit along its centreline, resulting from several scenarios in which the fire load, *L* is systematically varied under *Through or Forced Draught* conditions with three openings (window and 2 doors). The average heat flux measured during DFT1 throughout the period of maximum sustained external flaming is also shown with error bars indicating the maximum and minimum instantaneous values over that period.

From the *ambient conditions* category of parameters, both the effect of varying the ambient temperature, T_a and that of varying the wind or draught velocity, u are explored under *Through or Forced Draught* conditions. The distribution of façade heat flux resulting from the variation in ambient temperature shown in Figure 5.24 again reveals the ambient temperature to have negligible effect, both in the near- and far-field of the window soffit, particularly in scenarios with a single opening but also in those with three.

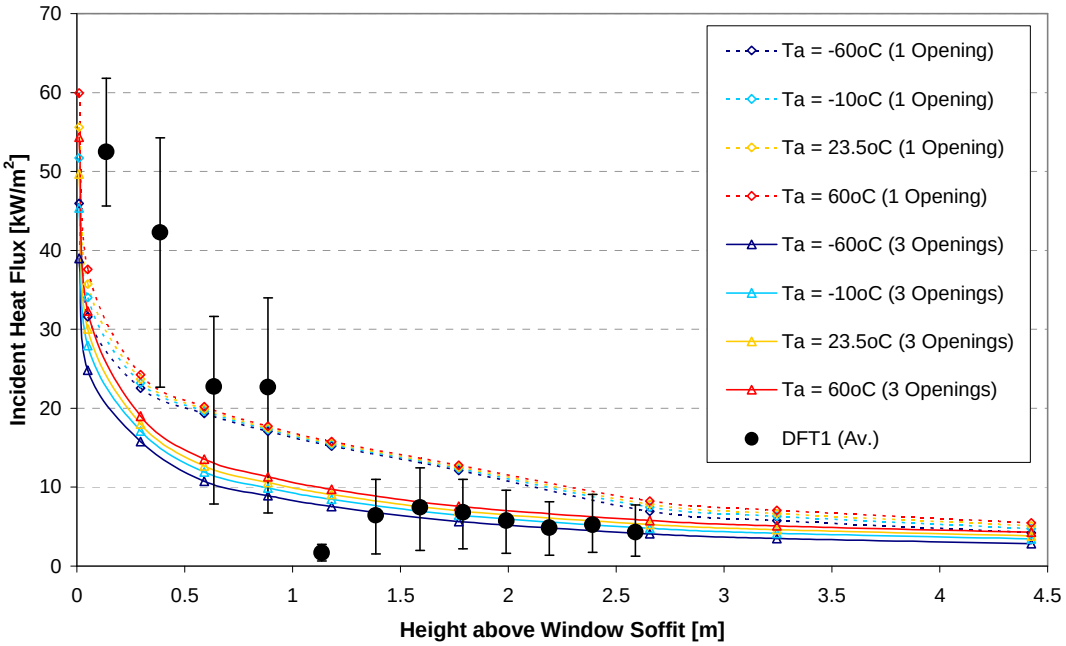

Figure 5.24. Distribution of heat flux incident on the façade as a function of height from the window soffit along its centreline, resulting from several scenarios in which the ambient temperature, T_a is systematically varied under *Through or Forced Draught* conditions with both a single opening (window) and three openings (window and 2 doors). The average heat flux measured during DFT1 throughout the period of maximum sustained external flaming is also shown with error bars indicating the maximum and minimum instantaneous values over that period.

The wind or draught parameter, u is varied over a large range of conditions from very light air to a string breeze, as listed in Table 5.2. Figure 5.25 shows the distribution of heat flux incident on the façade to be highly sensitive to variation in the wind velocity over the range explored, however closer inspection shows that for velocities smaller than 0.25u (1.5 m/s) the temperature at the plane of the opening, T_o increases significantly, eventually reaching unrealistic values, and the flame heights described are also unrealistically high. This is perhaps expected as under *Through or Forced Draught* conditions in the Law Model the wind has the effect of increasing the

horizontal external flame projections, therefore for very low wind velocities the flame becomes increasingly closer to the façade and it is likely that the correlations are no longer valid for very low wind velocities. Such scenarios are likely to be more closely described by the *No Through Draught* scenario correlations. For wind velocities higher than 0.25*u* (1.5 m/s), the heat flux distribution described by further changes in the wind velocity is very similar hence, in fact, the wind velocity is found to have a negligible effect. For wind velocities equal to or greater than 2*u* (12 m/s) the correlations become invalid as the flame height described becomes negative. This is again due to the empirical nature of the correlation describing flame height, as discussed in Chapter 3, Section 3.4.5. Therefore, while the actual wind velocity during the Dalmarnock Fire Test One benchmark scenario case is unknown, it has been shown not to matter as whatever the value it is likely to have had a negligible effect on the outcome heat flux distribution on the façade, according to the Law Model correlations.

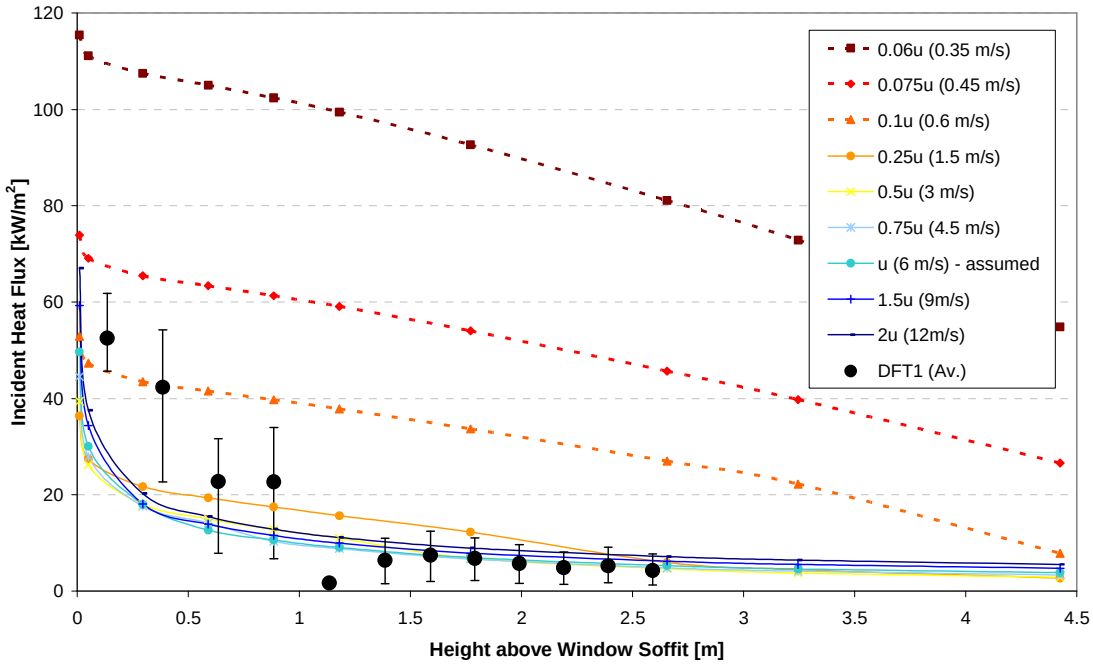

Figure 5.25. Distribution of heat flux incident on the façade as a function of height from the window soffit along its centreline, resulting from several scenarios in which the wind or draught velocity, *u* is systematically varied under *Through or Forced Draught* conditions with three openings (window and 2 doors). Dashed lines correspond to scenarios for which the Law Model output has been found to be unrealistic. The average heat flux measured during DFT1 throughout the period of maximum sustained external flaming is also shown with error bars indicating the maximum and minimum instantaneous values over that period.

Overall the parameter sensitivity study under *Through or Forced Draught* conditions shows that the distribution of heat flux on the façade wall does not appear to be significantly sensitive to many parameters. In most cases there does appear to be some discrepancy in the heat flux described by scenarios with three openings and opposed to that with a single opening. *Through Draught* conditions, by definition, pertain to compartments with more than one opening however *Forced Draught* conditions may apply in compartments with a single opening. Since the Law Model adopts modified opening dimensions that describe a single opening of some equivalence to the multiple openings, it is theoretically possible to describe a scenario more than one opening on opposite walls that results in the same reciprocal opening factor as that described by the DFT1 scenario with a single opening. Hence, while in theory if the size of both the window and doors in the DFT1 scenario are made small enough and of the adequate aspect ratio dimensions, the heat flux distribution described under the "single opening" cases could be reproduce by a compartment under *Through Draught* conditions. Nevertheless, the openings in this case would be rather small and fuel-controlled conditions assumed inside the compartment would perhaps not realistically be achieved. Therefore, the heat flux distributions described by the DFT1 scenarios with three openings are more likely to result from scenarios under *Through Draught* conditions whereas the higher heat flux distributions described throughout under the DFT1 scenario with only a single opening is likely only to pertain to scenarios where there is a *Forced Draught*.

5.8 Identification of key parameters

The sensitivity of the distribution of external heat flux along the height of the façade to many of the Law Model root parameters is surprisingly low. From the extensive parameter study discussed in Section 5.7 the fire load parameter appears to be the only parameter that has a significant effect on the overall distribution of the heat flux both in the near- and far-field from the opening soffit under scenarios where the rate of burning is described as fuel-controlled. The effect of this parameter on the internal compartment fire temperature could already be noted from a plot of the data pertaining to the large-scale tests used to validate the Law Model, shown in the Chapter 3, Figure 3.7. While the suggested correlations for the internal compartment

fire temperature where then adjusted accordingly such as to feature the fire load parameter (in the form of the compartment scenario parameter, ψ), the full effect of the fire load parameter on the characteristics of the external flame was perhaps not considered in detail. Nevertheless, for the case of *No Through Draught* conditions where the scenario is ventilation controlled, no parameter appears to have a significant effect on the outcome of the heat flux to the façade. In any case, in order to compare the relative effect of varying each parameter the highest heat flux distribution resulting from the variation of each individual parameter explored (or defined by highest heat flux distribution pertaining to realistic conditions) is plotted in Figure 5.26 for those pertaining to *No Through Draught* conditions and in Figure 5.27 for those pertaining to *Through or Forced Draught* conditions. It is of greatest interest to explore the upper bound of heat flux described as it is most conservative to account for this in design, particularly if the parameters have no significant effect such that the lower bound heat flux distribution described will not differ greatly from that described by the upper bound curve.

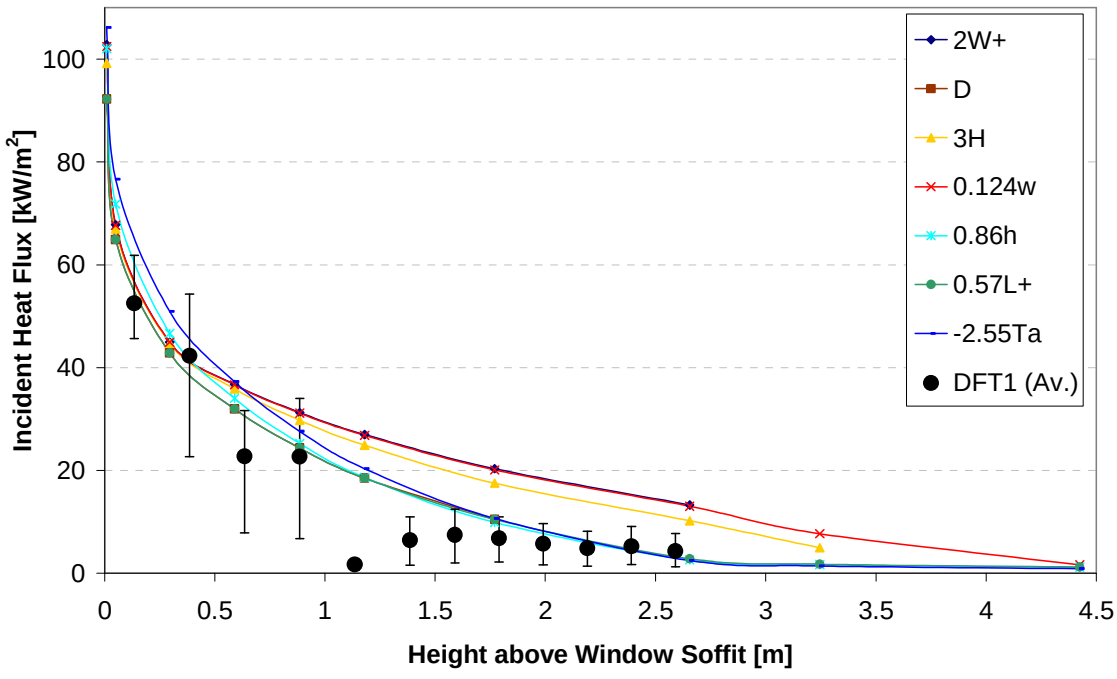

Figure 5.26. Vertical distribution of heat flux to the façade along the window centreline, pertaining to the highest distribution of heat flux described during the variation of single parameters under the *No Through Draught* scenario. The average heat flux measured during DFT1 throughout the period of maximum sustained external flaming is plotted for comparison with error bars indicating the maximum and minimum instantaneous values over that period.

Under *No Through Draught* conditions the following describe the conditions under which a maximum distribution of heat flux on the façade results for each of the parameters varied:

- Compartment width, W: becomes fuel-controlled just under $2W$ so any wider compartments yield the same heat flux distribution;
- Compartment depth, D: any variation has a negligible effect;
- Compartment height, H: does not have a significant effect but will become higher with increased height; nevertheless Law Model correlations not validated for compartments with heights much greater than $3H$, so this is taken as the upper bound;
- Window width, w: a narrow opening produces flames that project further but also a lot higher, therefore the narrowest opening explored, $0.124w$ yields the highest heat flux distribution; this equates to a width of under 0.3 m creating an opening aspect ratio outwith that covered by experimental validation of the Law Model;
- Window height, h: a height of $0.86h$ results in the highest distribution of heat flux, whereas shorter openings lead to unrealistically high values of temperature at the plane of the opening, T_o.
- Fire load, L: once the fire becomes ventilation controlled at $0.57L$ an increase in fire load will not result in a higher heat flux distribution;
- Ambient temperature, T_a: the lowest value of ambient temperature explored, $-2.55T_a$ leads to the highest external heat flux due to an increase in the temperature difference term, θ_f; any lower would be unrealistic as this already describes extreme conditions.

Hence, the comparison of the highest distribution of heat flux described by each of the parameter variations under *No Through Draught* conditions, shown in Figure 5.26, indicates that none of the root parameters appear to have a significant effect on the resultant heat flux incident on the façade. Nevertheless, it is found in Section 5.7.1 that for scenarios under *No Through Draught* fuel-controlled conditions, the fire load parameter has a significant effect on the overall distribution of heat flux to the façade which is in any case lower than that described by the $0.57L$.

Similarly, under *Through or Forced Draught* conditions the following describe the conditions under which a maximum distribution of heat flux on the façade results for each of the parameters varied:

- Compartment width, W: any variation has a negligible effect;
- Compartment depth, D: any variation has a negligible effect;
- Compartment height, H: any variation has a negligible effect;
- Window width, w: produces the highest heat flux distribution at its widest, when it is limited only by the width of the wall at $1.53w$;
- Window height, h: a height of $0.86h$ results in the highest distribution of heat flux, whereas shorter openings lead to unrealistically high values of temperature at the plane of the opening, T_o.
- Fire load, L: the maximum fire load explored, $10L$ results in the highest distribution of heat flux which would continue to increase with higher values of fire load; since $10L$ is perhaps an unrealistic upper bound value, $2L$ is also plotted for comparison;
- Ambient temperature, T_a: in this case the highest value of ambient temperature explored, $2.55T_a$ leads to the highest external heat flux; any higher would be unrealistic as this already describes extreme conditions.
- Wind or draught velocity, u: within the range of wind velocities explored that result in realistic conditions, the highest wind velocity, $1.5u$ results in the highest distribution of heat flux to the façade; any higher leads to a negative flame height which is unrealistic.

The comparison of the highest distribution of heat flux described by each of the parameter variations under *Through or Forced Draught* conditions, shown in Figure 5.26, indicates that most upper bound heat flux distribution curves by each of the root parameters of the root parameters are incredibly similar, with the exception of that described by the fire load parameter. While the heat flux distribution described by the upper bound variation of the fire load parameter is perhaps unrealistic, even a two fold increase in the fire load from that of the benchmark DFT1 case appears to have a significant effect. Hence, under *Through or Forced Draught* conditions, it appears

that the fire load parameter is the sole root parameter to have a significant effect on the distribution of heat flux incident on the façade wall.

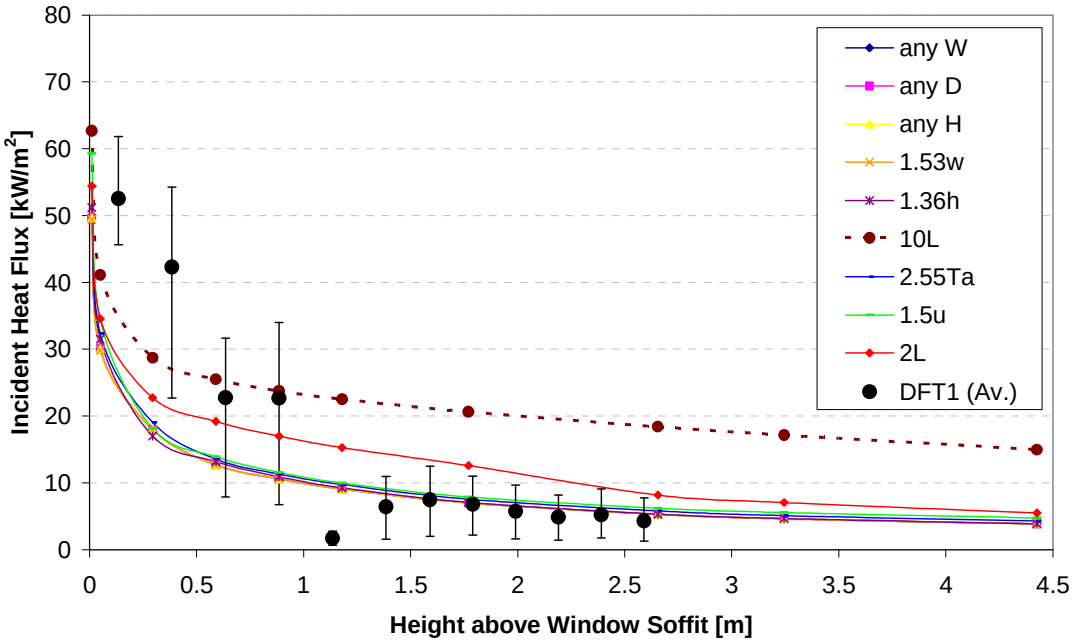

Figure 5.27. Vertical distribution of heat flux to the façade along the window centreline, pertaining to the highest distribution of heat flux described during the variation of single parameters under the *Through or Forced Draught* scenario. The average heat flux measured during DFT1 throughout the period of maximum sustained external flaming is plotted for comparison with error bars indicating the maximum and minimum instantaneous values over that period.

The overall distinct sensitivity of the Law Model to fire load compared to that of all other input parameters renders it unnecessary to explore the effect of combined parameter variation as these will likely again be dwarfed by the marked effect had by the fire load. Given the importance of this parameter it would be prudent to further explore the number of assumptions surrounding its use within the model. In fact, the fire load affects only the rate of burning, $\dot{m}$ intermediate parameter which subsequently features in many of the Law Model correlations. Since the rate of burning is described by the fire load, L divided by the fire duration, τ_F (*cf.* Chapter 3, Equations (3.6) and (3.19)) the fire duration is also thought to potentially have a big effect on the resultant external heat flux to the façade. The fire duration is not independently varied in the parameter sensitivity study because of its close link to the fire load parameter in terms of its use within the Law Model correlations. Therefore, assumptions surrounding the uniform burning rate within the compartment, the assumption that the fire load is uniformly distributed throughout the compartment and

the assumption that the Law Model correlations still hold for non-cellulosic fuels as long as they are represented by a wood-equivalent should all be revisited to explore whether they obfuscate other parameters that may be of importance in describing the resultant heat flux to the façade.

The findings from this parameter sensitivity study are most relevant to the use of the Law Model correlations (with the adaptations detailed in Section 5.4) in determining the heat flux to the plane of the building façade. While the fire load has been identified as the key parameter influencing the external heat flux in this case, the effect of the Law Model input parameters on the radiative heat flux from the internal fire has not been studied. This heat transfer component does not affect the total heat flux incident on the plane of the façade however it will feature in the heat flux falling incident on an external structural member lying outwith the building façade if it is within 'view' of a compartment opening. Therefore, while it is thought the fire load parameter will still have a significant influence, further study is necessary to identify the relative sensitivity of the incident heat flux to other Law Model input parameters for the case of an external structural element lying outwith the façade.

Chapter 6

Simplified Model Proposed

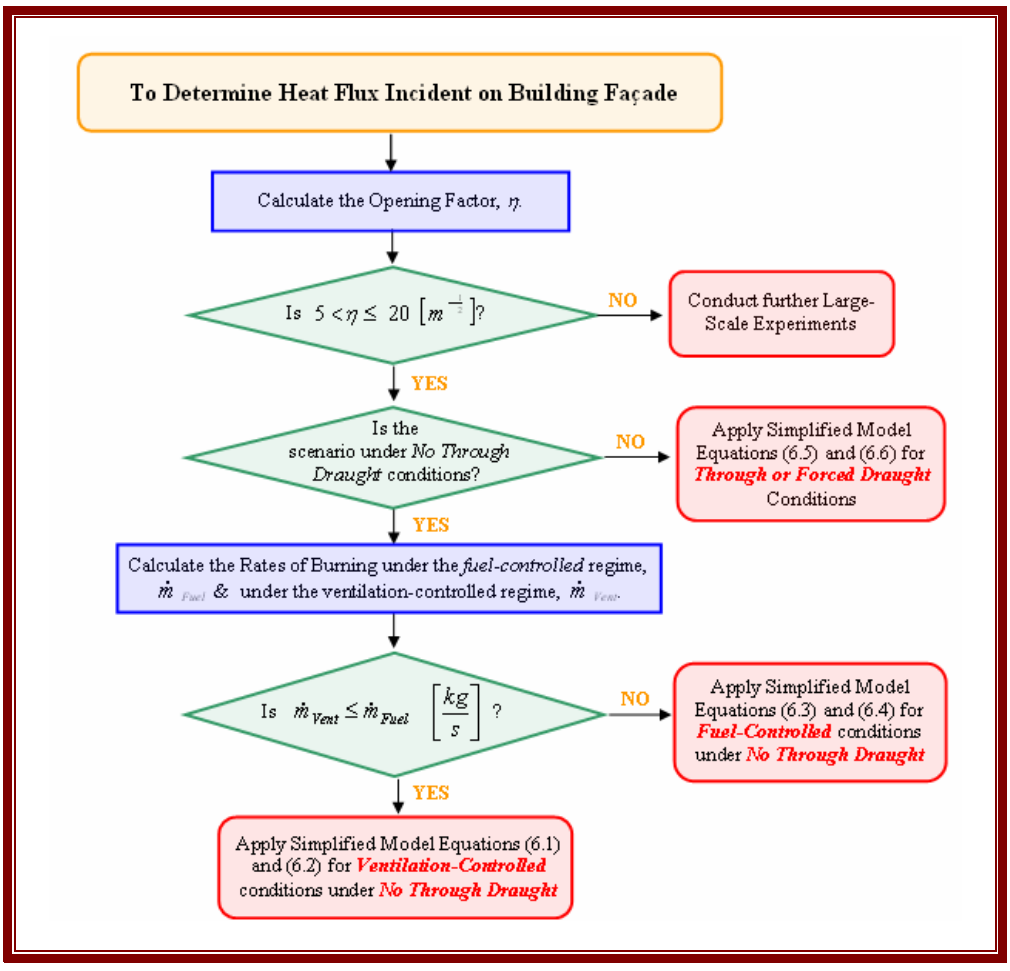

- Steps for implementing the Simplified Model Proposed -

A detailed analysis of the Law Model has shown the fire load parameter is of key importance in determining the heat flux incident on the external façade, its influence dominant over that of other parameters featured in the correlations. Although the analysis has also highlighted several limitations in the application of the Law Model, it is still the most comprehensive model available for estimating the heat flux to the external façade in the event of a compartment fire. Hence, it is beneficial to incorporate the findings into a simplified model with clear bounds of applicability. This will enable use of the model by a greater number of people in the field while ensuring it is not applied to scenarios for which it is not valid.

The laborious nature of the Law Model calculation method, which features numerous correlations with a high degree of parameter interactivity, appears to be unnecessary as it provides little resolution to the model outcome. Hence, a simplified method should feature the key parameter found to be of importance while minor variation to the model output arising from the influence of other parameters can be accounted for using adequate error bars. The level of accuracy of the simplified model will not differ from that in the Law Model since it is merely a simplification of the Law Model, so any measures of accuracy inherent in the Law Model and its assumptions will be carried through. Nevertheless the loss of accuracy of the Law Model associated to its numerical limitations, mostly due to the empirical nature of the correlations as discussed in Chapter 3, Section 3.4.5, will not feature in a simplified model which specifies clear bounds of applicability. Any loss of resolution resulting from grouping most of the parameters into error bars is within the level of accuracy of the model, however the error bars can be used to account for other characteristics that have since been found to be of some importance, such as the type of fire load (*i.e.* non-cellulosic, *etc*.). Hence, the simplified model could be used to obtain a ballpark estimate of the magnitude of the heat flux distribution on the façade and although conservative error bars are recommended (with regards to the Law Model output), engineering judgement can be used to justify any further modification to the error bars to be applied, depending on the scenario and on the respective use of the model output.

6.1 Simplification Approach

Analysis of the scenarios which lead to the highest distribution of heat flux resulting from the individual variation of each input parameter, under both *No Through Draught* and *Through or Forced Draught* conditions, allows for the development of a simplified model. Under *No Through Draught* conditions Figure 5.26 provides a comparison of the output from these scenarios where the façade heat flux distribution is seen to be mostly independent of parameter variation, under ventilation-controlled conditions. On the other hand, Figure 5.15 shows that under fuel-controlled conditions the heat flux distribution is markedly dependent on the fire load parameter. Similarly, the fire load is found to be the parameter that has the largest effect on the distribution of heat flux to the façade under *Through or Forced Draught* conditions, as seen in Figure 5.22 and Figure 5.23. Its distinct influence relative to variation in other parameters is evident in Figure 5.27. Nevertheless, the parameter sensitivity study described in Chapter 5 covers a wide range of variation in each of the individual parameters (*cf*. Table 5.2) which at times is found to result in unrealistic output from the Law Model and in other cases the scenarios described have reciprocal opening factors, η that fall outwith the range for which the Law Model has been validated. In creating a simplified model with clear bounds of applicability, it is therefore desirable that only output pertaining to scenarios for which the Law Model has been validated is considered for the development of new correlations.

The Law Model was validated against several large-scale tests, most of which fell within a narrow range of the reciprocal opening factor as described in Chapter 3, Section 3.3.1. While a range of 5-40 $m^{-1/2}$ was covered by these tests, only six tests fell into the 20-40 $m^{-1/2}$ range. Given that there has been very limited validation of the model within this range and that the effect of some parameters is found to become slightly more pronounced in scenarios with a reciprocal opening factor greater than 20 $m^{-1/2}$ (*cf*. Figure 5.6 for example), it is prudent to assume the Law Model is valid only for scenarios with a reciprocal opening factor between 5-20 $m^{-1/2}$, for which there has been thorough testing. Under such scenarios regressional analysis is used to determine the functions that best-fit the heat flux distribution under each of the draught cases. Where there is a discrepancy between the Law Model data and new functions, this is accounted for with the provision of appropriate error bars.

6.2 The No Through Draught (ND) Case

6.2.1 Ventilation-Controlled (ND)

In identifying the key parameters in the Law Model, a graph is plotted to compare the highest distribution of heat flux resultant from the variation of each individual parameter under *No Through Draught* conditions (*cf.* Figure 5.26). Under ventilation-controlled conditions no parameter is found to have a significant influence over the distribution of heat flux on the façade. In order to determine a simplified correlation for the external heat flux distribution under these conditions, the data shown in Figure 6.1 are used, where the highest heat flux distributions described pertain to scenarios with a reciprocal opening factor under 20 $m^{-1/2}$. Since the *geometric* parameters describing the DFT1 benchmark scenario under *No Through Draught* conditions (window as single opening) represent a reciprocal opening factor of 24 $m^{-1/2}$ (*cf.* Table 4.6), the highest heat flux described under variation of the fire load, L and ambient temperature, T_a parameters corresponds to scenarios with an opening of 3 m by 1.5 m, such that the corresponding reciprocal opening factor is under 20 $m^{-1/2}$.

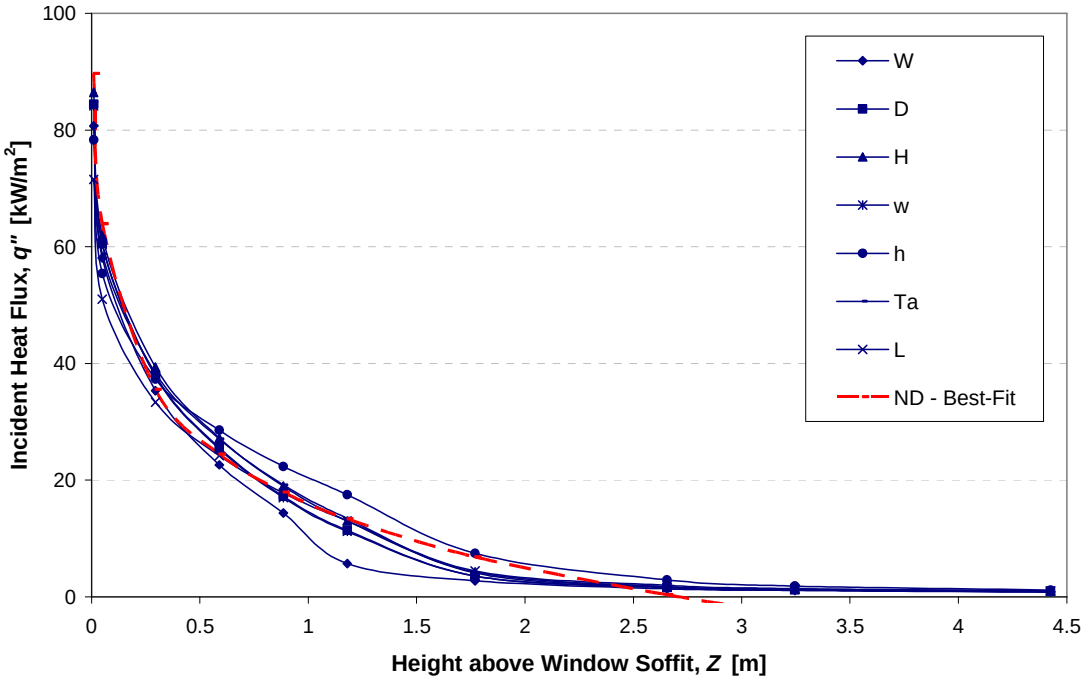

Figure 6.1. Vertical distribution of heat flux incident on the façade pertaining to the highest distribution of heat flux described by the variation of each individual parameter under the *No Through Draught* case for scenarios with a reciprocal opening factor between 5-20 $m^{-1/2}$. The red dashed line represents a best-fit function taken through the data.

A best-fit function taken through the upper bound description of heat flux distribution under the variation of all variables, shown as a red dashed line in Figure 6.1, is proposed for use in describing the heat flux distribution under *No Through Draught* ventilation-controlled conditions in a simplified model. This can be described as:

$$\forall\ 0.05 \le Z < e \qquad \dot{q}'' = 16\left(1 - Ln(Z)\right) \qquad \pm 10 \quad \left[\frac{kW}{m^2}\right] \qquad \textbf{(6.1)}$$

$$\forall\ Z \ge e \qquad \dot{q}'' = 0 \qquad \left[\frac{kW}{m^2}\right] \qquad \textbf{(6.2)}$$

where Z (m) is the height above the opening soffit and $\dot{q}''$ (kW/m^2) is the heat flux incident on the façade. A conservative error bar of $\pm$ 10 kW/m^2 is advised for the use of the model in design, accounting for any potential minor influence of *geometric* or *ambient conditions* parameter variation. Beyond a height of about 2.5 m from the opening soffit, the heat flux described by the Law Model output is seen to be negligible in terms of its application for design of façade cladding, window placement and structural perimeter members, therefore the heat flux distribution defined by the Simplified Model is conservatively limited at a height of about 2.7 m above the opening soffit. Similarly, the validity of the proposed equations in the very close vicinity of the opening soffit unclear due to the unrealistically high values of heat flux described by the Law Model in this region, resulting from limitations associated with the small characteristic length scales as described in Section 5.4.1. Therefore use of the proposed function is limited to heights above 0.05 m from the opening soffit.

6.2.2 Fuel-Controlled (ND)

The parameter sensitivity study showed that scenarios under *No Through Draught* fuel-controlled conditions are highly sensitive to the fire load parameter. Taking into account scenarios with a reciprocal opening factor between 5-20 m$^{-1/2}$ Figure 6.2 shows the heat flux distribution described under several different fire loads. The maximum heat flux distribution curves described by the variation of other variables are shown for comparison (in navy blue). These describe the upper bound limit to the heat flux distribution as they pertain to ventilation-controlled scenarios, nevertheless

they serve to highlight the difference in the model sensitivity to all other parameters compared to the sensitivity to the fire load. Lines of best-fit through the data for different fire load cases are shown as dashed.

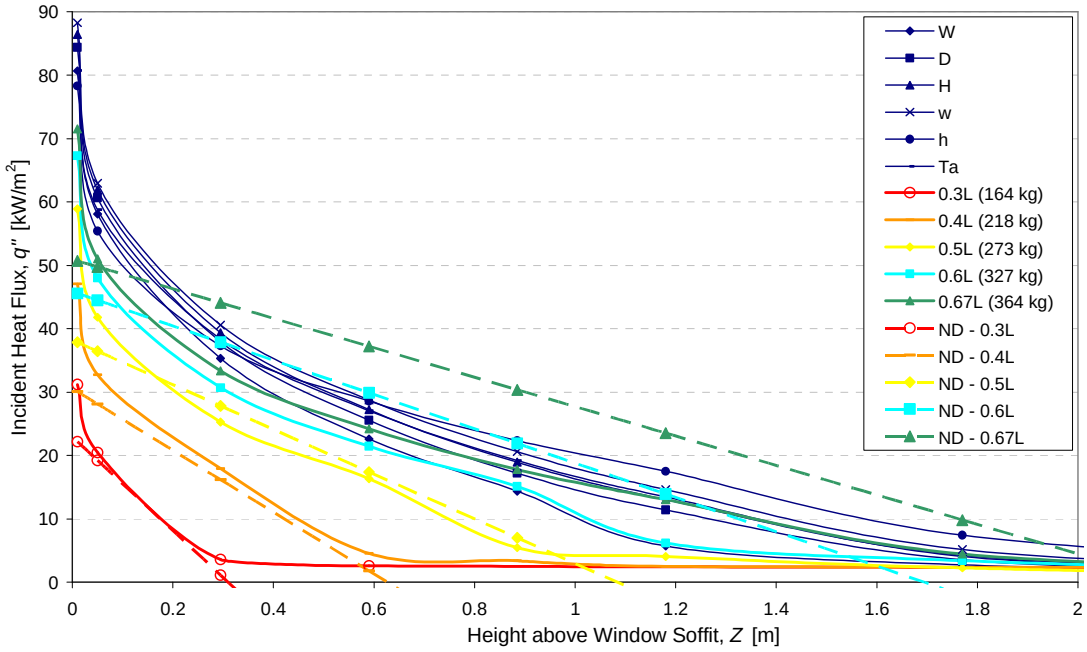

Figure 6.2. Vertical distribution of heat flux incident on the façade pertaining to scenarios with different fire loads under *No Through Draught* fuel-controlled conditions for scenarios with a reciprocal opening factor between 5-20 $m^{-1/2}$. The heat flux distribution resulting from parameter variation under ventilation-controlled conditions is also shown for comparison. The dashed lines represent the best-fit functions taken through the data.

The proposed function describing the distribution of heat flux incident on the façade under *No Through Draught* fuel-controlled conditions is also described as a set of two equations:

$$\forall\ 0.05 \le Z < 1.67\times10^{-6}\ L^{\,2.45} \qquad \dot{q}'' = 0.14\,L - \left(\frac{1.2\times10^{5}\ Z}{L^{\,1.45}}\right) \pm 5 \quad \left[\frac{kW}{m^2}\right] \qquad \textbf{(6.3)}$$

$$\forall\ Z \ge 1.67\times10^{-6}\ L^{\,2.45} \qquad \dot{q}'' = 0 \quad \left[\frac{kW}{m^2}\right] \qquad \textbf{(6.4)}$$

where Z (m) is the height above the opening soffit, L (kg) is the fire load and $\dot{q}''$ (kW/m^2) is the heat flux incident on the façade. Under each fire load case, the heat flux described is found to become negligible above a certain height, such that it would be unlikely to adversely affect window glass, cladding or structural elements. This is accounted for in the proposed equations. While the error bar suggested is most appropriate for low values of fire load, its application throughout will result only in a conservative solution. In the near-field to the opening soffit, the proposed function again underestimates the heat flux described by the Law Model, which in turn becomes unrealistic in this regions where the characteristic length scale is small (*cf.* 5.4.1), hence it is deemed as valid only for locations on the façade further than 0.05 m from the opening soffit.

6.3 The Through or Forced Draught (ToFD) Case

For the case of *Through or Forced Draught* conditions, the regression of the distribution of heat flux under variation of the fire load parameter is based on the cases studied where there are three openings in the DFT1 compartment (*cf.* Chapter 5, Figure 5.23) and hence a reciprocal opening factor of 8.6 $m^{-1/2}$ which is in the 5-20 $m^{-1/2}$ validated range. Figure 6.3 shows the heat flux distribution described both by the Law Model and by a simplified function proposed under a variety of different fire loads. While at a distance from the opening soffit the heat flux described by the proposed function tends to slightly over-estimate the heat flux described by the Law Model, Figure 6.4 shows that in the very near-field to the opening soffit the heat flux described by the Law Model is underestimated by the proposed function. While the level of validity of the Law Model in the very near-field to the opening soffit is unclear due to the numerical problems associated with small characteristic length scales (*cf.* Section 5.4.1), it is prudent to define a limit to the validity of the proposed function in terms of height above the opening soffit. Therefore, as for the previous correlations, the proposed function is conservatively specified as valid only for heights greater than 0.05 m above an opening soffit as it can be seen from Figure 6.4 that above this point, the proposed function provides a conservative estimate of the heat flux distribution.

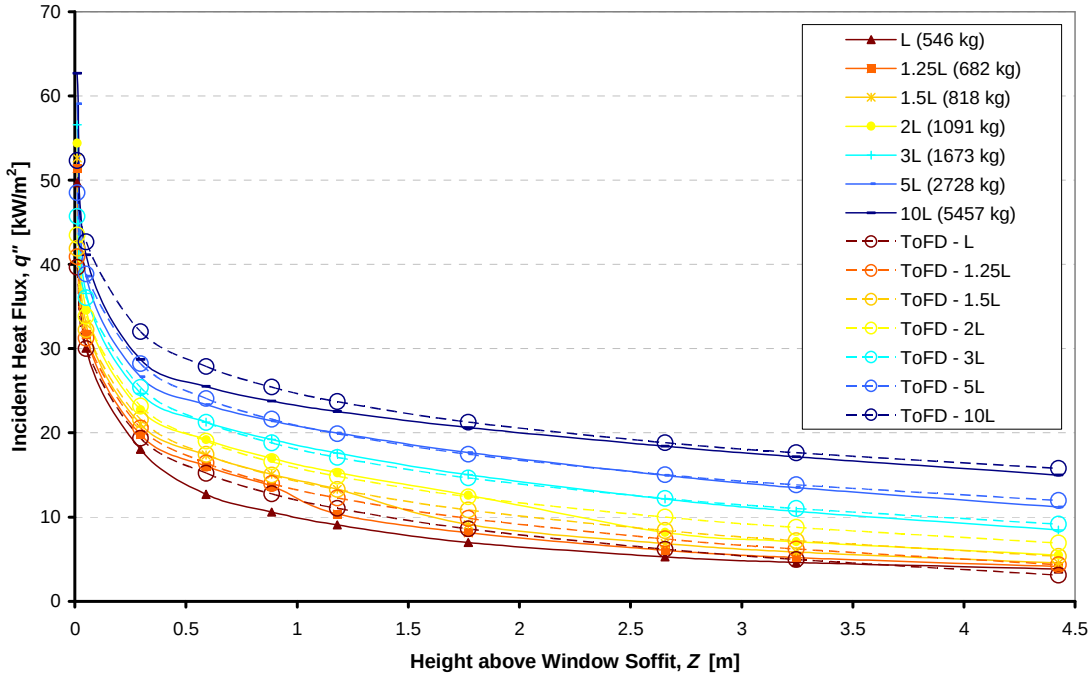

Figure 6.3. Vertical distribution of heat flux incident on the façade pertaining to scenarios with different fire loads under *Through or Forced Draught* conditions for scenarios with a reciprocal opening factor between 5-20 $m^{-1/2}$. The dashed lines represent the best-fit functions taken through the data.

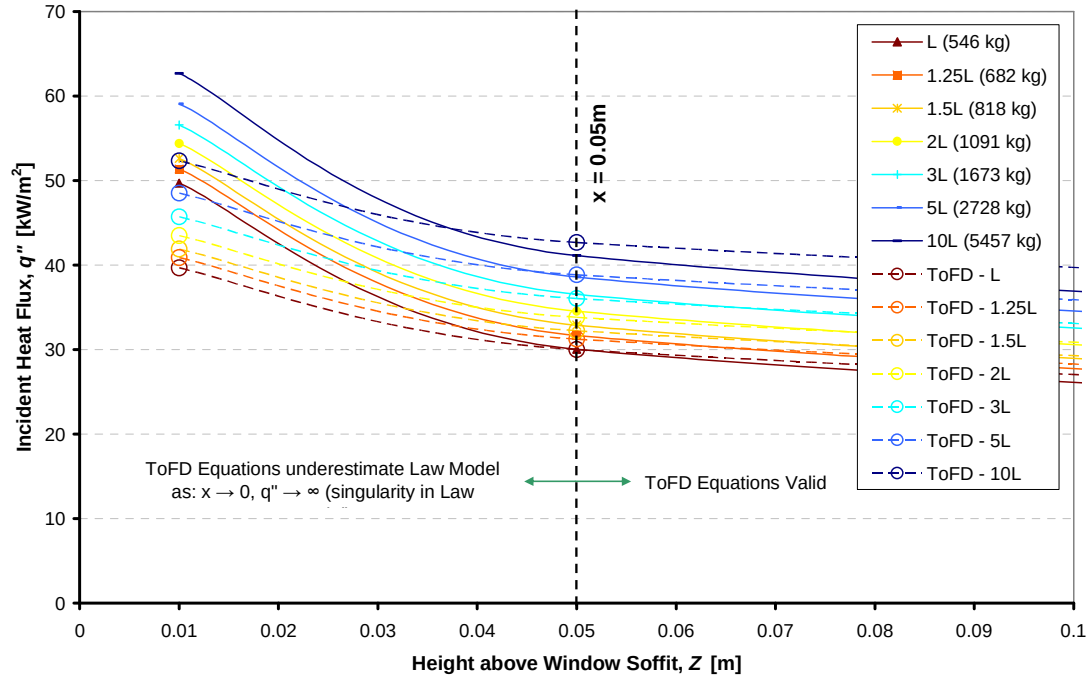

Figure 6.4. Vertical distribution of heat flux incident on the façade pertaining to scenarios with different fire loads under *Through or Forced Draught* conditions for scenarios with a reciprocal opening factor between 5-20 $m^{-1/2}$, in the near-field to the opening soffit. The dashed lines represent the best-fit functions taken through the data.

The proposed function describing the distribution of heat flux incident on the façade under *Through or Forced Draught* conditions is described as a set of two equations:

$$\forall\ 0.05 \le Z < \left(\frac{L^{5.5}}{1.6\times10^{7}\,e^{7}}\right)^{\frac{1}{6}} \approx 0.02\,L^{0.92} \qquad \dot{q}'' = Ln\left(\frac{L^{5.5}}{1.6\times10^{7}\,Z^{6}}\right) - 7 \quad \pm 2^{*}\left[\frac{kW}{m^{2}}\right] \qquad \textbf{(6.5)}$$

$$\forall\ Z \ge 0.02\,L^{0.92} \qquad \dot{q}'' = 0 \qquad \left[\frac{kW}{m^{2}}\right] \qquad \textbf{(6.6)}$$

*Note the error can be up to ± 8 kW/m^2 when the height of openings within the compartment varies significantly.

where Z (m) is the height above the opening soffit, L (kg) is the fire load and $\dot{q}''$ (kW/m^2) is the heat flux incident on the façade. While the suggested error bar is appropriate for scenarios with a reasonably low reciprocal opening factor, it can be adjusted for scenarios with larger reciprocal opening factors. Analysis of the correspondence between the suggested function and the heat flux distribution described by the Law Model in the case of only a single compartment opening (*cf.* Chapter 5, Figure 5.22) shows a ± 8 kW/m^2 error bar would suffice. Since such a scenario has a reciprocal opening factor outwith that of the validate range, ± 8 kW/m^2 is deemed as an upper bound error bar.

6.4 Applying the Simplified Model to DFT1

The Simplified Model describes the potential distribution of heat flux on the façade above a compartment opening under three potential draught and burning rate cases. The Simplified Model equations described in Sections 6.2 and 6.3 are used to determine the heat flux distribution for the Dalmarnock Fire Test One scenario, where the fire load is described as 546 kg (equivalent to a fire load density of 32 kg/m^2 in this case). Figure 6.5 shows the heat flux distribution described by the Simplified Model for all potential conditions compared to the average heat flux measured during the DFT1 period of maximum sustained external flaming. The respective recommended error bars are represented by the shaded areas.

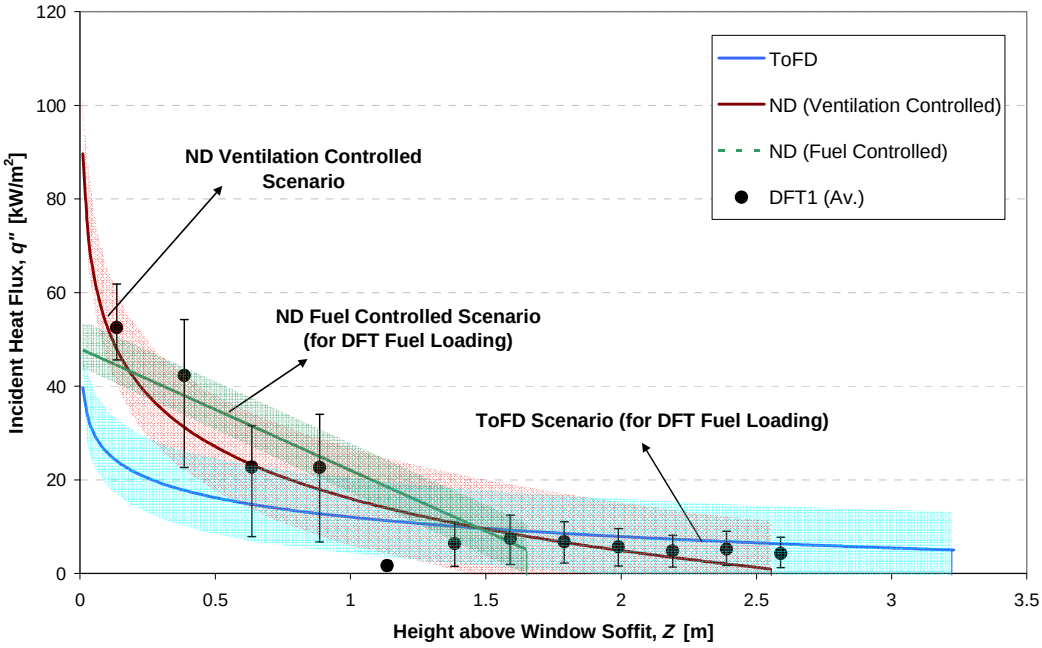

Figure 6.5. Vertical distribution of heat flux on the façade described by the proposed functions for three different draught and burning scenarios, where the *No Through Draught* fuel-controlled and the *Through or Forced Draught* scenarios are described using a fire load of 546kg. The average heat flux measured during DFT1 throughout the period of maximum sustained external flaming is plotted for comparison with error bars indicating the max. and min. instantaneous values over that period.

Comparison of the heat flux distributions described by the Simplified Model and those measured during DFT1 shows the model to account for the average measured heat flux, if all potential draught and burning rate scenarios are taken into account, much as was found with the Law Model output as described in Chapter 5, Section 5.3. The error bars recommended in the Simplified Model however account for higher heat flux than that in the Law Model which did underestimate the heat flux falling incident on at least one point on the façade during DFT1. It should however be noted that the peak instantaneous heat flux measurements recorded during DFT1 are in places higher than that estimated by the Simplified Model. While such peaks in heat flux tend to be momentary and hence not provide enough heat transfer over their short duration to adversely effect the components of the façade, this average heat flux measured is in places *just* accounted for by the Simplified Model whereas for use in design, the estimate should be conservative. Therefore, while the recommended error bars encompass the potential variability due to variation in other parameters in the Law Model found to have lesser influence, for scenarios that differ significantly from the assumptions made in the Law Model (*i.e.* different fuel type, as is the case for DFT1), a different error bar should be used and adequately justified.

6.5 How to use the Simplified Model

This Simplified Model is appropriate only for scenarios that fall within the 5-20 $m^{-1/2}$ range of the reciprocal opening factor, η, hence this is the first check necessary for any given scenario of interest before the rest of the model can be implemented. The reciprocal opening factor is defined in Chapter 3, Equation (3.4). It should then be determined if the scenario of interest is clearly under *No Through Draught* conditions or under *Through or Forced Draught* conditions, according to the Law Model definitions described in Chapter 3, Section 3.2.2. If the scenario of interest is clearly under *Through or Forced Draught* conditions, Equations (6.5) and (6.6) should be applied to determine the heat flux incident on the point (or points) of interest on the façade plane, where the fire load is defined in terms of its wood-equivalent. Should the scenario be found to clearly be under *No Through Draught* conditions, it is necessary to determine whether a fire would be ventilation- or fuel-controlled depending on the potential rate of burning, as per the method used in the Law Model, described in Chapter 3, Section 3.2.2.1.1. The rate of burning, $\dot{m}$ in both cases is described by Chapter 3, Equations (3.6) and (3.7) and the *actual* burning conditions within the compartment for a given scenario are described by the conditions that correspond to the lower of the two values. Hence, depending on the burning conditions in the scenario of interest, Equations (6.1) and (6.2) should be applied if the scenario is ventilation-controlled and Equations (6.3) and (6.4) should be applied if it is fuel-controlled. In the latter case, case should be taken to define the fire load in terms of its wood-equivalent. This method is best summarised in the form or a flow chart, depicted in Figure 6.6.

If the scenario of interest does not distinctly fall into either of the draught conditions, it is prudent to apply all conditions described by the Simplified Model to the points of interest on the façade and, in the case of design, to account for the worst-case heat flux potentially incident at each point. While the *No Through Draught* case under fuel-controlled conditions may not realistically lead to significant external flaming, it is merely used to define a lower burning rate and the correlations derive from tests Yokoi conducted (*cf.* Chapter 2) where the temperature was measured in the external plume. Although the characteristics (*i.e.* emissivity) of a hot external plume may

differ from those of external flames, a plume is still likely to impose a heat flux on the external façade, hence this scenario is still of interest.

For the case of scenarios that fall outwith the reciprocal opening factor range for which the model has been validated, further experimental tests need to be conducted in order to determine the relative effect of each parameter.

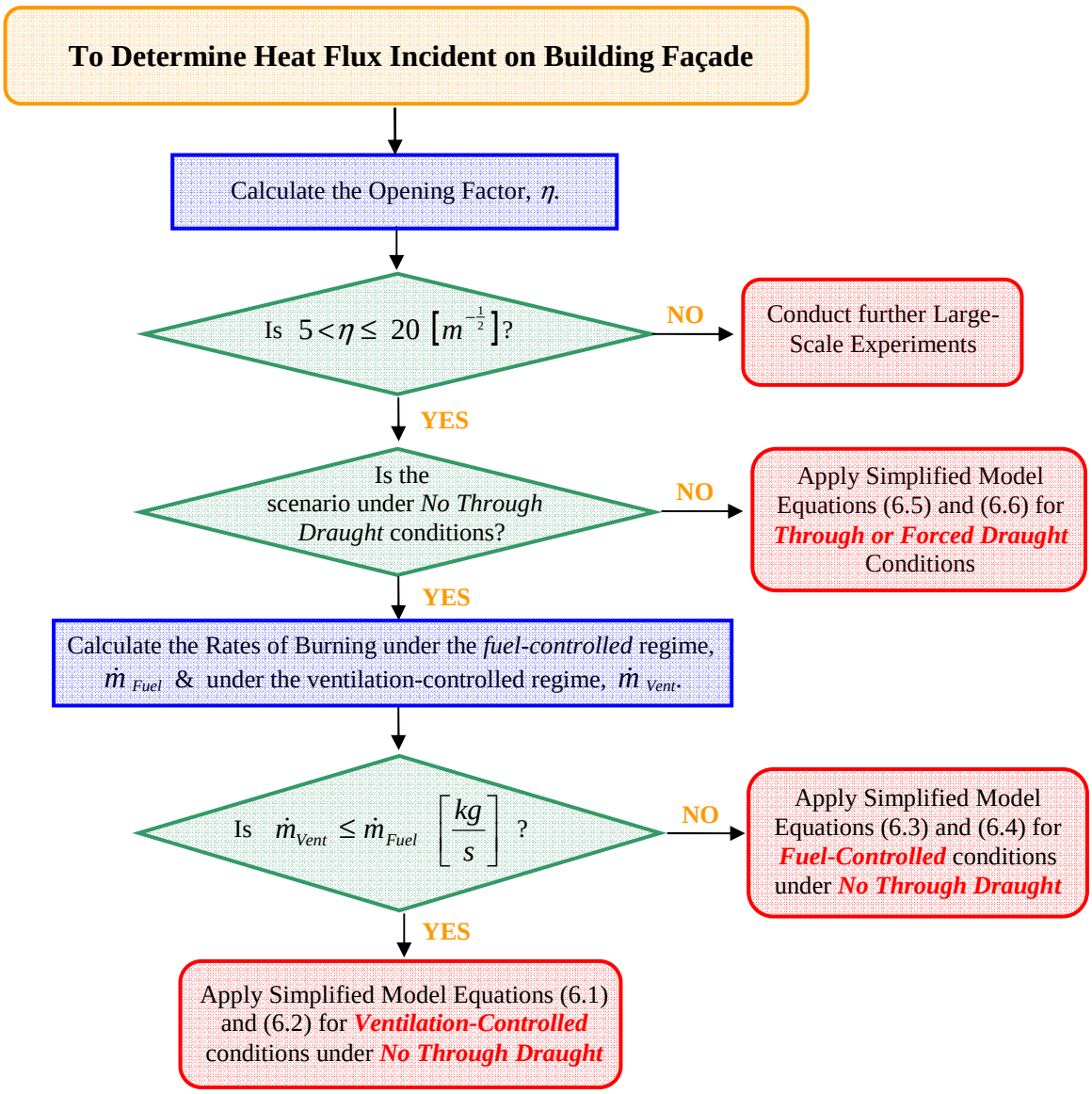

Figure 6.6. Flow chart describing the method by which the Simplified Model should be implemented.

The error bars recommended for use with the Simplified Model equations are adjustable depending on the characteristics of the scenario for which the model is to be applied. Although the model is theoretically applicable to any scenario that falls within the limits defined, modified error bars should be used for scenarios with characteristics that differ greatly from the tests from which the Law Model correlations were empirically derived. This is particularly the case for characteristics associated with the fire load, as the effect of variations in the type of fire load, the fire load distribution within the compartment and the fire load surface area, *etc*. has not yet been thoroughly investigated. Should a scenario involve fuel that is mostly non-cellulosic, a higher upper-bound error bar should be applied to all scenarios and justification for this alteration should be provided by the model user. Similarly, the Law Model correlations have been validated by tests that had a fire duration, τ_F of close to 20 min. Although the fire duration is taken into account in defining the rate of burning in the cases under *No Through Draught* fuel-controlled and *Through or Forced Draught* conditions, it is unknown whether the heat flux described by the model would be representative of that resulting from a high intensity-short duration fire, for example. The propensity for such a fire is linked to characteristics of the fire load and larger error bars should again be applied in this case.

The Simplified Model is applicable for determining the heat flux to the façade above 0.05 m from the soffit of a compartment opening. For the first 0.05 m of the façade it is recommended that the heat flux is taken as that described by the model at 0.05 m plus an upper error bar to be applied to that value. The heat flux distribution described as a function of height from the opening soffit derives from the worst-case heat flux which occurs opposite the external flame axis, described as the centreline above the opening for the case of no external deflection by wind. The heat flux described by the Simplified Model can therefore be applied to any point above the opening soffit and even if this is not at the opening centreline, the model will conservatively predict the heat flux. Similarly, should the scenario be affected by an external wind that may deflect the external flame, the heat flux described by the Simplified Model to any point on the façade is a conservative estimate as lateral deflection of the flame will only lead to a lower heat flux at any given point, assuming the Law Model assumption that the lateral wind has no other effect other than changing the relative orientation of the external flame. The effect of flame deflection by an external protrusion such as a

balcony or an awning is also not taken into account in the Simplified Model, however since such an obstruction will only result in flame deflection away from the façade, the heat flux described by the model to any given point will again be a conservative estimate of the actual heat flux in such a scenario.

In practice it is likely the Simplified Model will be used to define the heat flux incident on different regions of the façade, such as to select cladding with an appropriate critical heat flux for ignition and to design upper-storey window arrangements that are unlikely to crack and fall out under the heat flux incident in the case of a fire in the compartment below, or even to decide on an inter-storey height to be used between openings. In these cases, the highest heat flux incident on that region should be applied (*i.e.* corresponding to the lowest height). For the case of the close near-field to the opening soffit, it may be economic to apply a single strip of a different material to the first 0.05 m with a higher critical heat flux for ignition than that of the rest of the façade cladding material (*i.e*. such as a opening headstone), if the heat flux to that region is significantly higher than that incident further afield.

6.6 Comparison of Simplified Model with other Experimental Data

Apart from the Dalmarnock Fire Tests, the only other full-scale experimental tests conducted using a realistic fire load and fire load layout (*i.e*. modern furniture) where external heat flux measurements to the external façade were recorded, are those conducted by Klopovic and Turan in the late 1990s [80,81]. Eight tests were conducted however the external heat flux measurements recorded for six of the tests are most pertinent for comparison against the Simplified Method. The tests were conducted in a 3.6 by 5.3 m (by 2.4 m high) compartment with a 2.4 m by 1.5 m window (and in some cases a 0.8 m by 2 m back door). The fire load consisted of furniture resembling a living room type layout, with a 3-seat polyurethane foam sofa, two similar armchairs, two bookcases laden mostly with books, and two wooden coffee tables. The large sofa was positioned just in front of the compartment window and in each case the fire was igniting using a small wood crib placed on the centre of this sofa. Four of the tests were conducted under what is defined by the Law Model as *Through or Forced Draught* conditions where a door was left open on a wall opposite

that of the window. Nevertheless, it is worth noting that this door led into a long internal building corridor and the ambient conditions are reported to have been 'still' during these six tests, with average external wind speeds recorded falling between circa 1-2 m/s. The remaining two tests were conducted under *No Through Draught* conditions where only the window was open. Under these test conditions, "the presence of flames beyond the opening prior to flashover" was reported and attributed to the proximity of the 3-seat sofa (and ignition source) to the compartment window [80]. Further characteristics of each of the fire tests are summarised in Table 6.1 and the tests are noted to have been of relatively short duration.

Test	**Fire Load** (kg)	**Ventilation Conditions**	**Fire Duration** (s)
Klop1	445	ToFD – door and window	480
Klop2	536	ToFD – door and window	300
Klop5	539	ToFD – door and window	360
Klop8	544	ToFD – door and window	420
Klop4	541	ND - window	480
Klop7	534	ND - window	360

Table 6.1. Characteristics of some of the full-scale fire tests conducted by Klopovic and Turan [80]. The fire load is stated in its wood-equivalent.

In applying the Simplified Model to each of these test scenarios, it was found that the tests under *Through or Forced Draught* conditions correspond to scenarios with a reciprocal opening factor, η of 22-27 $m^{-1/2}$ and those under *No Through Draught* conditions to a reciprocal opening factor, η of circa 32 $m^{-1/2}$. Therefore all tests are outwith the range of applicability of the Simplified Model, nevertheless since they are within the 20-40 $m^{-1/2}$ range for which data from a limited number of large-scale tests has been previously compared against the Law Model (*cf*. Chapter 3, Section 3.3.1) and since there are no other more adequate data for comparison, the Simplified Model is applied to each scenario. According to the respective burning rate calculations for each of the *No Through Draught* test scenarios, both scenarios are expected to be under ventilation-controlled conditions. Due to the ventilation conditions surrounding the *Through or Forced Draught* tests, where there appears to be a very limited through draught and the external flame is expected to have little horizontal projection,

for this case the Simplified Model is applied under both *Through or Forced Draught* and *No Through Draught* (ventilation-controlled) scenarios for comparison. During the tests the incident heat flux was only recorded to a small number of points on the façade. A comparison of the test data and the heat flux distributions described by the Simplified Model for the respective scenarios is shown in Figure 6.7.

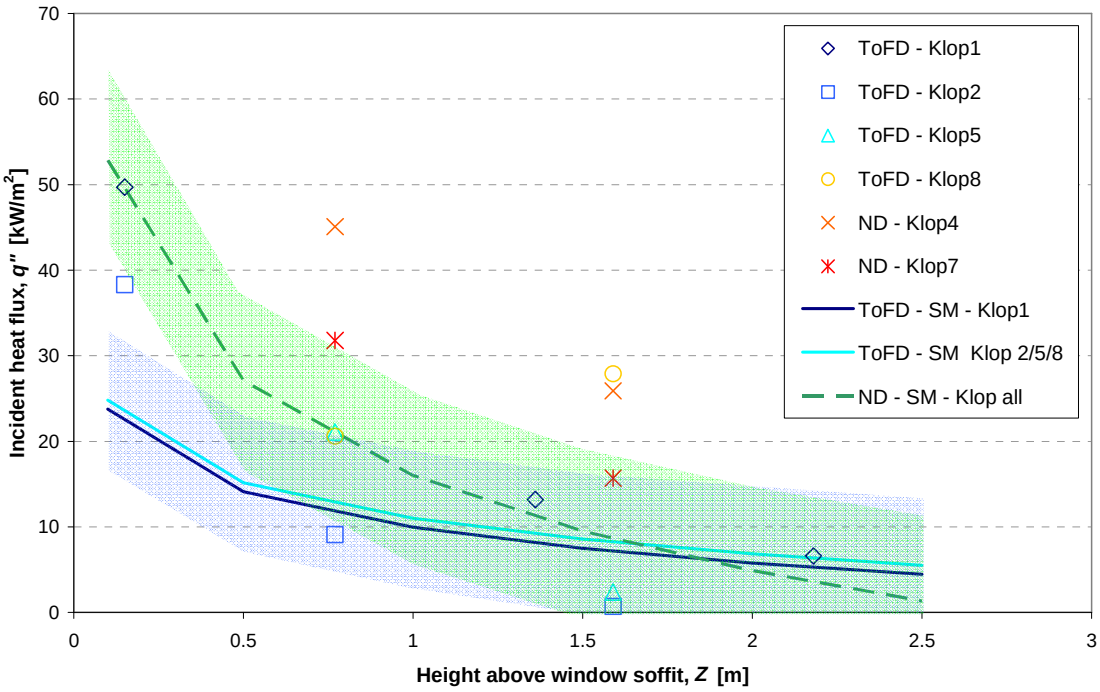

Figure 6.7. Heat flux measured at different heights during a series of tests conducted by Klopovic and Turan [80,81], together with the heat flux distribution described by the Simplified Model for the given tests scenarios. The shaded area represents the error bars associated to the respective Simplified Model heat flux distributions described.

In the case of the tests under *Through or Forced Draught* conditions, the *Through or Forced Draught* Simplified Model predictions are seen to significantly underestimate the recorded heat flux in the near-field to the window soffit which lies above the range accounted for by the suggested error bars. Further afield (> 0.5 m from the opening soffit) the same Simplified Model correlations fare fairly well, although one data point (corresponding to ToFD – Klop8) is still underestimated by the model. Judging by the fact the heat flux incident at this latter point is higher than that measured closer to the window soffit during this test, it may be that some errors are associated with this measurement. The *No Through Draught* heat flux distribution described by the Simplified Model however appears to provide good estimates for these same near-

field measurements. Although the Simplified Model is not directly applicable to these scenarios (due to their reciprocal opening factor), it appears that these scenarios are closer to *No Through Draught* conditions than those resulting from a distinct through draught. The tests scenarios under *No Through Draught* conditions, on the other hand, result in heat flux measurements distinctly greater than those predicted by the Simplified Model *No Through Draught* (ventilation-controlled) case. Although again the Simplified Model is not directly applicable to these test scenarios, in this case the large discrepancy is likely to be additionally due to specific characteristics of the test conditions. The heat flux data reported for these tests is distinctively high and likely to have resulted from the external flaming observed during the tests while the fires were still free-burning, pre-flashover. This external flaming – thought to have originated from the proximity of the sofa (and ignition source) to the compartment window – is not taken into account in the Law Model and is certainly not represented by the correlations for scenarios under *No Through Draught* ventilation-controlled conditions.

While the test scenarios compared are not directly applicable to the Simplified Model (due to their reciprocal opening factors) the large discrepancy between the measured heat flux and that predicted by the Simplified Model is likely to be due to differences related to the fire load parameter which are not accounted for in the Law Model, and as a result are also not accounted for in the Simplified Model. The conditions inside the fire compartments appeared not to present uniform burning, particularly during the initial stages of the *No Through Draught* condition tests and localised pockets of burning may result in burning rates different to those previously correlated for the models. The fires were also of relatively short duration as they were extinguished once the period of sustained external flaming was seen to die down, however in most cases there was still some fuel left, so the burning rate appears not to have been uniform throughout the short duration of the fire. These results further highlight the need to thoroughly investigate the effect of the type of: fire load (perhaps along the lines of the research into the excess fuel factor described in Chapter 2, Section 2.2.2.2); the fuel distribution throughout the compartment (which is rarely homogenous as assumed); localised pockets of burning and non-uniform rates of burning; and high intensity-short duration fires, among other potential parameters associated to the fire load. An earlier comparison of the Law Model against the

external flame temperature measurements taken during a series of full-scale tests conducted at Lehrte in Germany in 1978, many of which had furniture as fire loading, already indicated the fire load parameter may be of importance. The study, conducted by Law, reported that “there is considerable scatter, but it has not been possible so far to find any specific variation with such factors as the wind speed and direction or with fire load” [98].

Chapter 7

Exploring Further Parameters

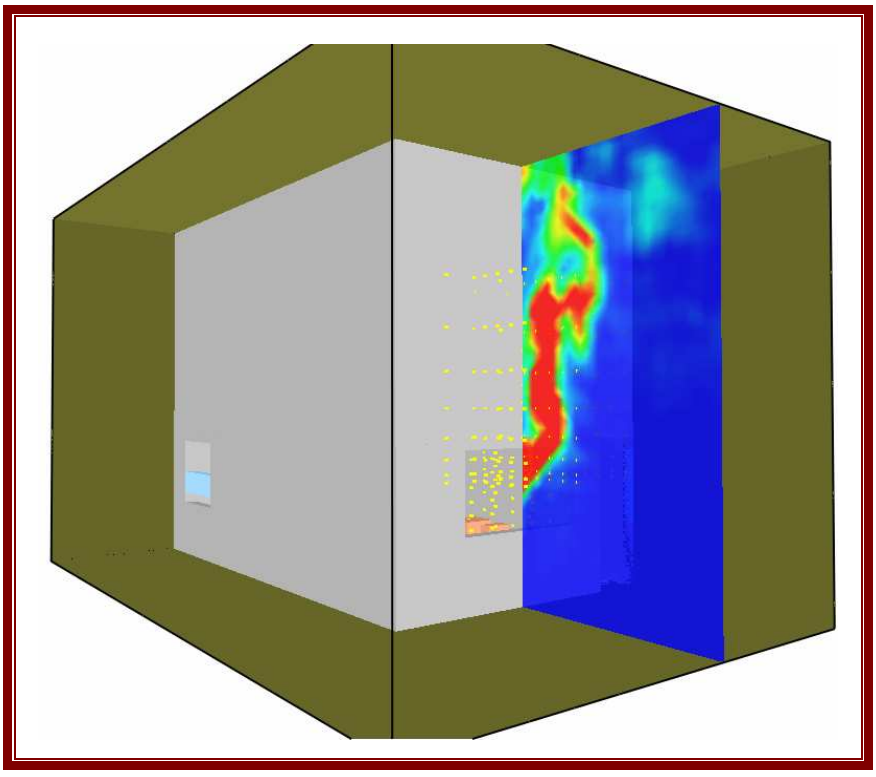

- External plume temperature contours (vertical section through the window centreline) extracted from a computational simulation (FDS) of Dalmarnock Fire Test One -

A detailed analysis of the Law Model identifies fire load as the key parameter of importance in determining the heat flux to the façade during a given compartment fire scenario. A Simplified Model is therefore proposed, incorporating these findings. The proposed model provides a faster, more straightforward method of obtaining an estimate of the distribution of heat flux to the façade than that of the more convoluted Law Model. Its imposed limits of applicability also ensure it is not applied for scenarios outwith its validity. Nevertheless, comparison of the model predictions against data pertaining to *realistic* compartment fire scenarios indicates there may be further parameters that influence the external heat flux that have not been adequately investigated. The models are found to underestimate heat flux incident on the façade in the near-field to the soffit of the compartment opening, often where it is at its highest. While the Simplified Model allows for versatile error bars to be applied to the heat flux distribution described by the model for scenarios that are found to differ significantly from the assumptions inherent in the model's development, it is of interest to investigate the influence of parameters surrounding the characteristics of the fire load such that the model and its given error bars can be further refined.

In order to determine the effect of compartment fire parameters on the consequent compartment fire, it is customary to resort to computational modelling when there is thorough experimental data for a scenario that can be used as a benchmark, as it is more affordable than resorting to extensive experimental testing. The benchmark scenario is usually modelled using Computational Fluid Dynamics (CFD) and the model output is compared against the experimental data. Disparity between the model prediction and the experimental measurements is common so the model input parameter values for which there is some uncertainty are usually adjusted in order to ensure reasonable agreement between the model output and the experimental measurements. It should be ensured, however, that the adjusted parameter values are realistic. The parameters of interest can then be systematically varied in a series of computational simulations such as to analyse its effect on the output of interest. Using Dalmarnock Fire Test One as a benchmark scenario, computational fluid dynamics analysis is undertaken to investigate the effect of varying the fire load distribution within the compartment as a uniform rate of burning over the entire compartment floor area is one of the main assumptions surrounding the use of the fire load parameter in the Law Model correlations.

7.1 The Objective of using Computational Modelling

The Law Model, like most compartment fire models, assumes the fire load is uniformly distributed throughout a compartment (in terms of fire load density) and that it burns uniformly, with a steady burning rate, over the duration of the fire. This assumption allows for a simple fire load, or fire load density, to be used in correlations that describe the overall behaviour of a compartment fire for a given scenario, facilitating the comparison of data from different scenarios. It appears to be an appropriate assumption for design given that the fire load and its location within a compartment can change over the lifetime of a building. Nevertheless comparison of the models against data pertaining to *realistic* scenarios, such as those of Dalmarnock Fire Test One [105,113] and the tests conducted by Klopovic and Turan [80,81], show the models underestimate the external heat flux falling incident on the façade. Therefore it is important to reassess the importance of the assumptions surrounding 'uniformly burning fire load' assumption.

In order to encapsulate the intricacy of the fire load characteristics in a *realistic* scenario, it is important to conduct the computational analysis using *realistic* fuel packages, such as diverse items of furniture, as used in DFT1 and the Klopovic and Turan tests. Realistic fire load differs from a uniform fire load such as liquid fuel or wood cribs, in that diverse furniture can have: different chemical compositions; a correspondingly different heat of combustion and critical heat flux for ignition for different items or even parts of items; different rates of burning and resultant emissivity of combustion products; different surface areas; varying height of fuel bed; different surface orientation, *etc*. Hence while a localised pool fire with a prescribed heat release rate (HRR) could be used in the computational study, to systematically change the fire load distribution by moving the pool around the compartment floor for different simulations, this would only analyse the effect of *one* of the potential parameters associated with the assumptions surrounding the fire load parameter. Therefore several assumptions would be necessary to use a pool fire scenario and benchmark it against the realistic DFT1 scenario data. Furthermore such a study would not enable a systematic analysis of all the other characteristics associated with a *realistic* fire load whereas the use of several different items of furniture allows for each of the individual characteristic parameters of interest to be individually varied.

Several of the characteristics associated with the fire load parameter have already been found to have an effect on the resultant characteristics of an enclosure fire. Thermoplastics, for example, tend to burn as pools under post-flashover conditions which may lead to a higher surface area of burning (which is simply assumed to be equal to that of the floor area), in turn affecting the rate of burning when a wood-equivalent fire load is assumed [21]. The combustion of hydrocarbon polymers requires more air than that of cellulosic fuels which can result in very different rates of soot production, in turn affecting the emissivity of the fire and flames [21]. Bullen and Thomas [67] have defined a parameter to represent some of these properties in the form of an excess fuel factor, f_{ex} and it has been found to affect the external heat flux however it does not feature in the Law Model definition of fire load the properties of which are generalised by using a wood-equivalent fire load. Desanghere [126] conducted a computational study to determine the effect of the excess fuel factor (in the form of a global equivalence ratio) on the characteristics of external flames by running the same model scenario with two different types of fuel (wood and ethylene which have different stoichiometric burning ratios) and again showed the excess fuel factor to have a considerable effect. Although the latter study also investigated the effect of fuel location within the compartment, it was conducted solely using a single type of fuel represented by a burning area with a prescribed heat release rate.

Therefore, as an initial study, it would be ideal to investigate the effect of the location of the fire load within the compartment on the resultant external heat flux incident on the façade, using the Dalmarnock Fire Test One scenario as a benchmark case since the fire load distribution is not uniform throughout the compartment and the shape and composition of each fuel package is different. Nevertheless, it is generally accepted that CFD models are not yet suitable for detailed modelling of *realistic* compartment fires under a ventilation-controlled regime [18,127]. *Quantitatively*, under the ventilation-controlled regime, computational models tend to over-predict the combustion that takes place at the compartment openings which in turn affects the modelled heat flux to the façade. Since the models are based on stoichiometric burning ratios and the heat release rate is artificially prescribed, often the air within the model compartment becomes vitiated and fuel volatiles that may in reality burn within the compartment, are transported to the openings in the model. Hence, in the

model, a greater portion of the reaction takes place outside the compartment openings, where there is a surplus supply of air, compared to that in real fires. Computation fluid dynamics model are however reasonably adequate at providing a reliable representation of the transportation of combustion products and partial-combustion products. While in practice this may *quantitatively* result in an over-prediction of external heat flux to the façade, *qualitatively* the *comparative* distribution of the transport of fuel to each of the compartment openings is of interest as it may demonstrate that the fuel location relative to the openings may have an effect on the resultant external heat flux. Hence this study is conducted to determine the *qualitative* rather than *quantitative* effects effect of varying characteristics of the fire load.

7.2 The Scenarios Modelled

For the purpose of demonstrating the potential effect of variation in the location of realistic fire load on the resultant heat flux to the external structural façade, three main scenarios are modelled using Fire Dynamics Simulator (FDS) [127] – although other fire-related CFD software (*e.g.* SOFIE) could also have been used. Dalmarnock Fire Test One is used as the base scenario (FDS_Case1) and the fuel properties prescribed are obtained from the additional laboratory experiments used to characterise items of the Dalmarnock scenario fuel, as discussed in Chapter 4, Section 4.4.4, together with properties obtained from the available literature for mainstream materials. Among the properties assigned to each of the items of furniture are the density, heat of combustion, heat of gasification and ignition temperature. Most of the main furniture items are described with approximate dimensions adjusted to fit the grid-mesh resolution used (0.1 by 0.1 by 0.1 m) and for the base scenario (FDS_Case1), the items are located as per DFT1 (*cf.* Chapter 4, Figure 4.3), as shown in Figure 7.1. The prescribed areas of heat release rate match those observed during the initial stages of fire growth of DFT1, as described in Chapter 4, Section 4.3.1. The heat release rate of the waste-paper basket and blanket are prescribed as per the HRR measured in laboratory tests [122] and the data collected during a sofa calorimetry burn is also used to specify the HRR for a specified burning area on a portion of the sofa. The bookcase closest to the ignition source is also given a pre-specified HRR, obtained from laboratory calorimetry tests that included both the bookcase and its contents [122]. The surface areas with specific HRR are seen in yellow in Figure 7.1. The

initial ventilation conditions are specified as per the DFT1 scenario however to reduce the computational requirements of the model, the flat is truncated mid-way through the hallway and the ventilation conditions at the door to the hallway (Door 1) are approximated by modelling an open-ended corridor at a right angle to the door (*cf.* Figure 7.1). The compartment window panes and part of the kitchen window are removed at pre-specified times as per observations of DFT1 and the prescribed computational domain provides 1.6 m outside the compartment such as not to interfere with the buoyant external flow. The fire duration is set at 1200s, just a minute over the period of 'free-burning' of DFT1 when it was actively extinguished (*i.e.* by fire-fighters rather than burn-out). Apart from internal and external thermocouple point measurements of gas-phase temperature, the model fire scenario is also resolved for a number of cold surface temperatures located in the same positions on the external façade as those in Dalmarnock Fire Test One (*cf.* Chapter 4, Figure 4.5), from which incident heat flux is inferred.

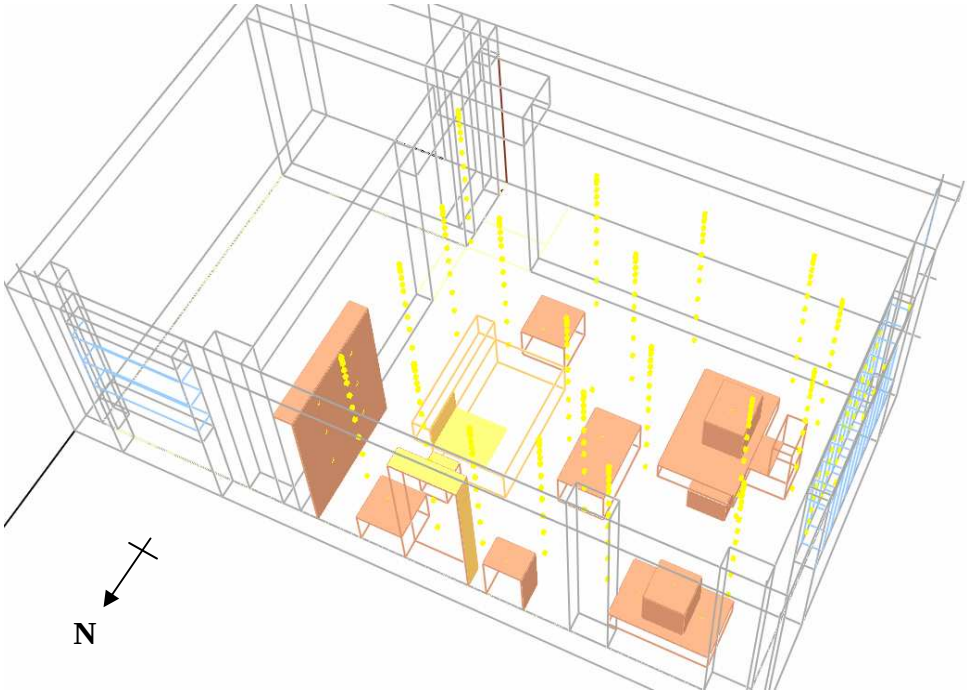

Figure 7.1. FDS model outline of the Dalmarnock Fire Test One compartment and layout of the furniture items as per the DFT1 scenario (FDS_Case1). Yellow surfaces denote areas with a pre-specified HRR and yellow dots represent thermocouple point measurements. *See* Chapter 4, Figure 4.3 for comparative layout of furniture items during DFT1.

The simulated scenario differs drastically from the fire evolution observed during Dalmarnock Test One as many of the modelled items never ignite. While some disparity was expected, due to previous results from a number of related studies [18,19], the internal compartment temperature evolution described is significantly low compared to that measured in DFT1 and the critical temperatures for ignition of most of the items are never attained. Several input parameters of which the values are uncertain were varied however further iterations of the model simulation did not yield a closer match to the DFT1 fire evolution. If the ignition temperature of each item were instead inferred from the model simulated compartment temperature conditions at the time when ignition is *known* to have occurred during DFT1 rather than as a physical material property, in theory all the items could be made to ignite at the same time as experimentally observed. Nevertheless this would require many iterations of the simulation in order to determine the resultant compartment fire temperature in the vicinity of the *next* item to ignite once the *previous* item to ignite is burning. This process would have been laborious and very computationally intensive.

One such study has been conducted by Jahn *et al*. [19] in an attempt to adjust the input parameters such as to model *just* the pre-flashover stage of DFT1 using FDS. It was shown that even if the input is optimised to allow for a better match between certain output values from the fire model and those of the experimental data, the discrepancy between other aspects of the output and experimental data will remain, particularly (but not solely) at a localised level where the difference is often considerable. This was similarly found in a round-robin study conducted by Rein *et al*. [18]. Had such an intensive study been conducted it is likely that the required input parameters for the model to result in a façade heat flux distribution comparable to that of DFT1 would have been physically unrealistic. Hence, it would then have been of questionable value to conduct subsequent simulations based on the variation of these input parameters in order to evaluate the resultant effect on the heat flux incident on the façade. Therefore, no further alterations were made to the base scenario (FDS_Case1) model and the characteristics of the items of fuel specified were left as originally specified (*i.e*. the properties obtained from a combination of experimental tests and the literature), allowing only for a *qualitative* comparison of the external heat flux resulting from variation of the fire load location in each the scenario.

The second scenario considered (FDS_Case2) is identical to the first, except the furniture has been transposed to one half of the compartment, between the NE corner and the doors to the hallway and kitchen, as illustrated in Figure 7.2. The third scenario (FDS_Case3) is also based on the first but in this case all the furniture has been moved to the other half of the compartment such that it runs along the base of the window with shelves and work desks either side, as shown in Figure 7.3. Such scenarios could be representative of temporary uses of offices or household rooms (*i.e.* where the furniture is stacked up) however in these cases none of the flammable material surfaces are in direct contact. While it is unlikely that FDS is able to simulate the complex conditions involved when items of furniture are found closely together – particularly in the vertical direction – the purpose of maintaining the DFT1 scenario furniture is part of the *qualitative* study such as to remove any assumptions linked to using 'equivalent' descriptions of fuel. Nevertheless the errors involved in the *quantitative* prediction of the resultant external heat flux – due to the limitations inherent in the modelling tool – renders limited use in conducting simulations for further combinations of DFT1 furniture distribution.

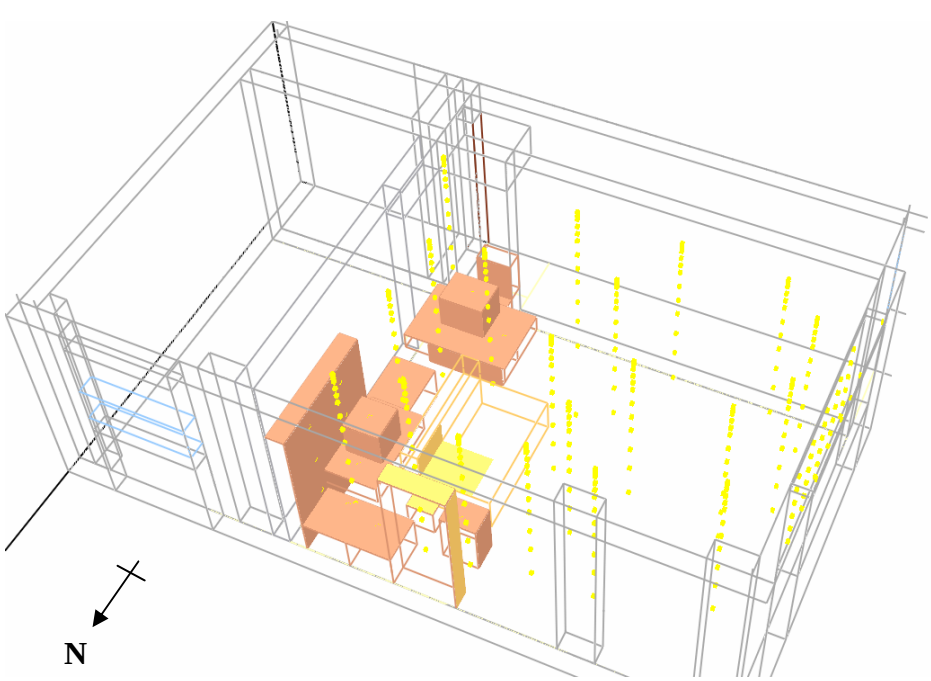

Figure 7.2. FDS model outline of the Dalmarnock Fire Test One compartment and layout of the DFT1 furniture items all stacked in the East half of the compartment, between the NE corner and both doors (FDS_Case2). Yellow surfaces denote areas with a pre-specified HRR and yellow dots represent thermocouple point measurements. *See* Chapter 4, Figure 4.3 for comparative layout of furniture items during DFT1.

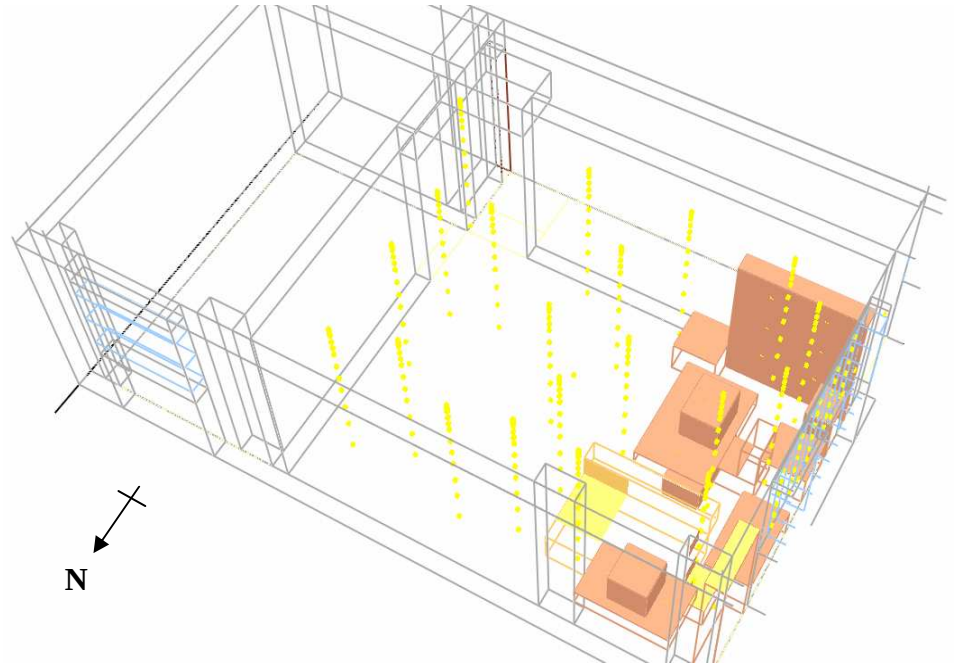

Figure 7.3. FDS model outline of the Dalmarnock Fire Test One compartment and layout of the DFT1 furniture items all stacked by the window area (FDS_Case3). Yellow surfaces denote areas with a pre-specified HRR and yellow dots represent thermocouple point measurements. *See* Chapter 4, Figure 4.3 for comparative layout of furniture items during DFT1.

7.3 Analysis of CFD output

Although the thermocouples were specified both inside and outside the compartment in the same locations as those employed during DFT1, these measurements were only used in initial attempts to adjust the model input parameters such as to improve the correspondence between the modelled output and the measured data. The simulated heat flux incident on the external façade above the compartment window was used for comparison between the FDS_Case1 output values and the Dalmarnock Fire Test One data, for ballpark gauging the internal fire represented by the models. During the course of the fire only a second bookcase ignited further to the items with a prescribed HRR, hence the simulated external heat flux, taken from the model – as both an average and an instantaneous peak value within the same time-frame as DFT1 – was very low by comparison. Nevertheless, the pattern in the heat flux distribution was similar to that measured during DFT1 and the standard deviation between the peak heat flux and the average heat flux over the last minute of burning in the modelled

scenario appears to be proportional to that measured during DFT1. Therefore, in essence, the simulated scenario represents burning conditions under a much lower fire load than the DFT1 scenario due to the limited number of items that ignite in the simulated internal compartment fire. In any case, given the *qualitative* nature of the study, the comparison of heat flux output by the three model cases shown in Figure 7.4 enables an evaluation of whether the fire load location is expected to influence the distribution of heat flux to the external façade.

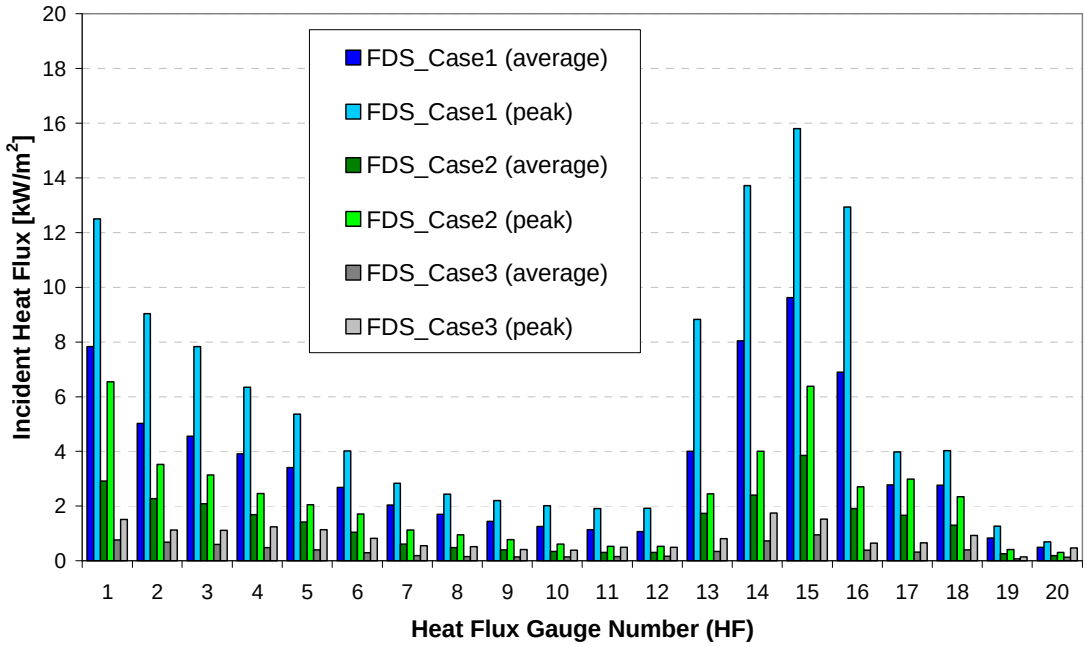

Figure 7.4. Distribution of average and instantaneous peak heat flux to the façade above the compartment opening output by three different cases modelled using FDS where the fire load location was varied. The heat flux gauge numbers correspond to the gauge locations illustrated in Chapter 4, Figure 4.5.

The external heat flux resulting from FDS_Case2 and FDS_Case3 are comparably evaluated against the outcome of FDS_Case1. The cases in which the furniture is concentrated in either the East or West side of the compartment appear to indicate considerably lower heat flux to the façade than those output by the scenario with a more even fuel distribution, as per DFT1. This is expected even though the furniture items with a prescribed HRR are in the same location in FDS_Case1 and FDS_Case2, because of differences in air entrainment between fuel items and in the ignition sequence of secondary items. Some of the fuel items are packed very closely together, within only a single grid-cell spacing in places, such as to limit air entrainment as in practise the surfaces of stacked furniture would be in very close contact, limiting the

fuel surface area. Such narrow spacing between fuel items is also likely to affect the simulated interaction between burning items. Nevertheless, when the case with all the furniture towards the back of the compartment (FDS_Case2) is compared against that with the furniture close to the window (FDS_Case3) a significant difference in the output heat flux is also observed, regardless of the fact that the items are closely packed together. While in practise fuel items close to the compartment window (open supply of air) are likely to result in higher external heat exposure (as found by Desanghere [126], albeit in a compartment with the window as a single opening), in this case the FDS_Case2 scenario, with the items towards the back of the compartment, resulted in higher external heat flux by comparison. Whereas some external flaming may have been expected due to the proximity of the furniture to the window (as recorded in some of the Klopovic and Turan tests [80,81], albeit under *No Through Draught* conditions, *cf.* Chapter 6, Section 6.6) in the FDS_Case3 scenario, the items with a prescribed HRR were located both to the side of the window and a way back from the window, so this was not the case. It is thought the difference in the heat flux distribution output from both the second and third scenarios could be due to air entrainment through the doors and through the closely packed fuel items in the second scenario (FDS_Case2) as opposed to the third scenario (FDS_Case3) where the furniture items were all either below or to the side of the compartment window. Therefore, *qualitatively* this study can be assumed to demonstrate that the distribution and location of the fuel relative to the openings may have a significant effect on the resultant external heat flux nevertheless further experimental research is necessary to investigate and *quantify* what that effect may be.

7.4 Contribution from CFD Modelling

The development of CFD modelling tools is not yet at a stage that allows for adequate simulation of complex ventilation-controlled scenarios [127], nevertheless in the absence of comprehensive physical data, this tool allows for *qualitative* assessment of parameters that may influence the internal fire development and the consequent external heat flux. While it is likely that the *quantitative* output from these models is unrealistic, it is also possible that the relative magnitude of the output for each of the three cases is not accurate. Therefore, this comparative study has demonstrated solely that some of the assumptions inherent in the definition of the fire load used in the Law

Model (and its implementation in the model in the assumption of a uniform rate of burning) may mask other parameters of potential importance in determining the resultant external heat flux, as well as the overall burning regime, both within and external to the compartment. Nevertheless the limitations associated with current CFD modelling of *realistic* post-flashover fire compartments, in terms of producing *quantitative* output adequate for scenario comparison, render it of limited use to extend this study to subsequent scenarios where the effect of varying other characteristics of the fire load is simulated and compared.

Thus, the most important conclusion drawn from the computational modelling study is that the numerical tools available are not yet elaborate enough to allow for a systematic study of all the characteristics of the fire load and their respective effect on the resultant external heat exposure (and internal fire development), and that therefore it is essential to resort to a series of comprehensive experimental tests. Given the importance of the fire load parameter in the determining the distribution of heat flux to the façade in the Law Model, a thorough experimental investigation of these fire-load-related parameters is the most appropriate way to establish *why* there is a discrepancy between the prediction of current analytical models and the external heat flux measured during *realistic* fire scenarios, and to quantify it by linking it to the contributing parameters.

Chapter 8

Conclusions, Applications and Further Work

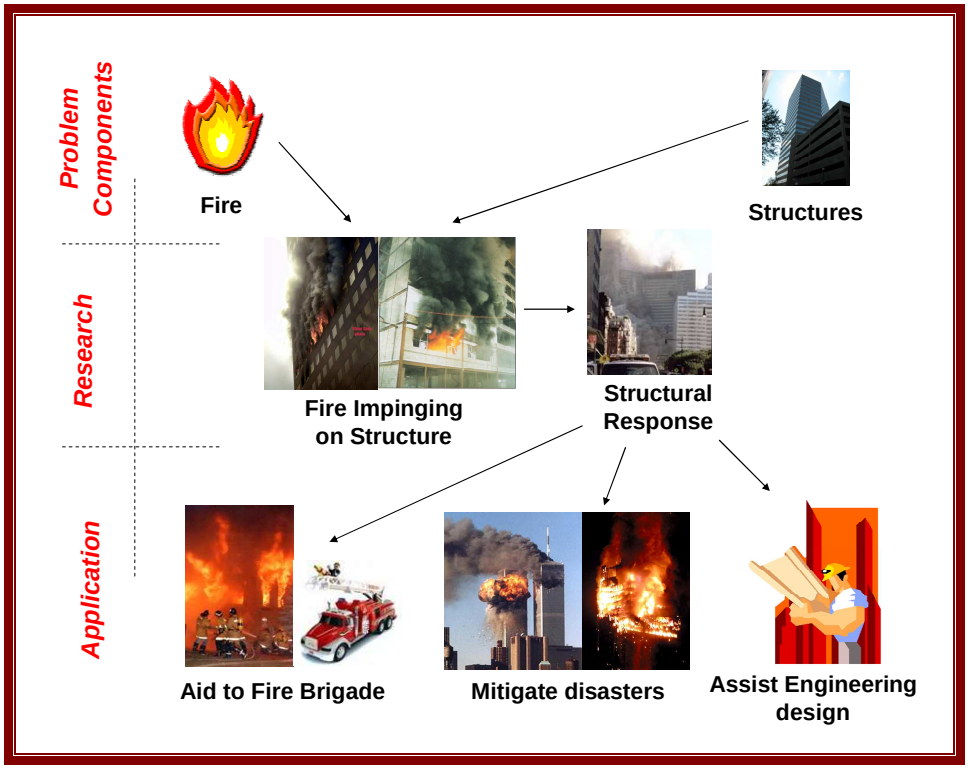

- Schematic of General Problem, Research and Application Context of the work -

Recent advances in the field of architecture, civil engineering and material science have changed buildings and their use, rendering it necessary to re-evaluate our understanding of the characteristics of a compartment fire. In terms of external fire spread, the Law Model is still the most comprehensive analytical model available to describe the external heat exposure resulting from compartment fires, however it was empirically derived in the 1970s. Since then the concept of a standard compartment (*i.e*. furnishings materials, structural materials, geometry and size of compartment and openings, *etc*.) has changed considerably.

8.1 Conclusions

In developing the Law Model, Law and O'Brien envisioned that "as more use is made of the method it is likely that more straightforward rules will be worked out" [1]. While advances in computational capacity have enabled a thorough analysis of the Law Model, it has also been adequate to assess the model's applicability to modern, *realistic* scenarios. A detailed parameter sensitivity study conducted on the model, with regards to the resultant heat flux incident on the building façade above the compartment opening (incorporating some slight model adaptations as discussed in Chapter 5, Section 5.4), highlights the influence of the fire load parameter as dominant over that of other parameters used to describe the scenario. Moreover, although the Law Model is based on a number of correlations with intricate inter-dependencies linking several parameters characteristic of a compartment fire scenario, the resultant external heat flux incident on the façade appears to be relatively insensitive to reasonable variations in parameters other than that of the fire load. The study also identifies several limits of applicability of the Law Model that arise from the empirical nature of the model correlations, as detailed in Chapter 3, Section 3.4. If these limits are not imposed, the Law Model can yield non-physical or unrealistic properties of either gas-phase temperature or external flame dimensions and projection, under a combination of parameters that can easily fall within the range of parameter values expected in a scenario for standard compartment design. Consequently, this can result in an unrealistic estimate of the heat flux incident on the façade.

A review of the literature concerning the large-scale experiments against which the Law Model has previously been validated (*cf.* Chapter 3, Section 3.3) shows the scenarios tested lie only within a narrow range of the reciprocal opening factor, with the majority of experiments falling within the 5-20 $m^{-1/2}$ range [26]. Due to the empirical nature of many of these experimentally derived correlations, it is often the application of the Law Model outwith this range that leads to unrealistic output values. However non-physical values also arise from the numerical limitations inherent in some of the equations used, where singularities (points of discontinuity) can occur again within a reasonable combination of ranges that could correspond to a typical scenario encountered in design. Therefore, it is prudent to limit the applicability of the Law Model to scenarios that fall within this range of reciprocal opening factor, before further tests are conducted to evaluate the model's validity outwith this range. It is recommended that the identified limits of applicability of the Law Model be brought to the attention of those who use Eurocode 1 – Annex B [2], an adaptation of the Law Model used in structural-fire design standards.

The general distribution of heat flux incident on the façade (varying with height above the compartment opening soffit) described by the Law Model, appears to be distinctive for the scenarios under *No Through Draught* and *Through or Forced Draught* conditions, as well as for *fuel-controlled* and *ventilation-controlled* fires under a *No Through Draught* scenario. Together with the dominance of the fire load parameter over that of other compartment fire parameters defined in the Law Model, in terms of the influence had on the heat flux to the façade, this indicates the Law Model is unnecessarily convoluted. Therefore a Simplified Model is proposed, whereby the heat flux incident on the plane of the façade under each of the draught and rate of burning conditions is defined by a single correlation. The correlation proposed for the distribution of heat flux to the façade under a '*No Through Draught - ventilation-controlled*' scenario is simply a function of height from the opening soffit and for the cases of '*No Through Draught - fuel-controlled*' or '*Through or Forced Draught*' conditions the correlations are also a function of the compartment fire load. The proposed expressions are specified with recommended error bars that account for the smaller potential variations in the resultant heat flux incident on the façade due to all other input compartment fire parameters.

While the effects of wind are not directly considered, the simplified expressions have been derived for heat flux incident on the façade along the window centreline which provides a worst-case estimate of heat flux distribution compared to the heat flux incident either side of the centreline, above the compartment window. This is due to the properties of external flames which appear to have a fairly even temperature distribution along their width, with any variation usually peaking along it axis. Hence, whether the façade is engulfed in flame (under *No Through Draught* conditions) or whether it projects from the wall (under *Through or Forced Draught* conditions) the combination of temperature distribution within the flame and the configuration factor result in higher heat flux incident along the window centreline under still conditions. Since the heat flux decays with height along the centreline, any angle tilting of the plume due to wind should result in a lower heat flux incident on the façade at any specific height above the opening soffit, compared to that calculated at the same height along the centreline. The same applies for scenarios with a horizontal projection (*i.e*. an awning, balcony, *etc*.) which are assumed to deflect the external plume outwards but not to affect the flame length or its temperature distribution, therefore resulting in a lower heat flux to the façade at any given point that that described by scenario without a projection. Hence, for any case, the centreline heat flux distribution should provide a conservative estimate provided the error bars are appropriately applied.

The Simplified Model proposed consists of a handful of simple steps to determine whether the model is applicable to a specific scenario and which of the three main expressions should be used, as summarised in the flow chart shown in Chapter 6, Figure 6.6. Since the Simplified Model is based on the Law Model, its limitations still apply hence it should also only be used within the 5-20 $m^{-1/2}$ range of reciprocal opening factors. The error associated with the simplified expressions is within the same range of error expected from implementation of the Law Model, however the error bars provided with each of the expressions can be altered depending on the particulars of the scenario and the level of associated risk, provided the choice of error margin to be applied is justified by the design engineer. Furthermore the Simplified Model does not provide estimates for the heat flux incident on the first 5 cm above the

opening soffit – the region where the highest incident heat flux is expected – due to a numerical limitation inherent in the Law Model adaptation associated with infinitely large convective heat transfer coefficients that result from the use of small characteristic length scales. While it is suggested that heat flux incident over this area not be taken as any less than that incident at 5 cm above the window soffit, since it does not constitute part of the Simplified Model, the upper error bar to be applied to that ballpark estimate is left up to the user's discretion.

8.2 Applications of the Simplified Model Proposed

The proposed Simplified Model provides an estimate of the heat flux incident on an external façade above the opening of a compartment under situation of fire, comparable in use to the output of the Law Model however much simpler and quicker to implement. Furthermore the Simplified Model imposes clear limits of applicability in order to avoid implementation of the model in scenarios outwith its validity.

Comparison of Law Model output based on a modern, *realistic* scenario, with data measured during Dalmarnock Fire Test One (DFT1) – a comprehensively instrumented full-scale fire test with verified levels of repeatability – shows a very good agreement between the trends describing the distribution of heat flux incident on the façade as a function of height from the opening soffit. While the ballpark values output by the model are comparable with those measured, the Law Model does not conservatively estimate the heat flux as expected given it is supposedly based on several 'conservative' assumptions. In places, however, the incident heat flux measured is higher that any of those calculated by the Law Model, under different sets of scenario draught and burning rate conditions. The same is found when the Law Model is applied to another modern, *realistic* scenario and compared against the data reported by Klopovic and Turan [80,81], yet with a larger discrepancy between the model output and the test data. Hence, when applied to modern, *realistic* scenarios, the Law Model is perhaps no longer conservative as is implied in the supporting literature [1,26]. Nevertheless, in the Simplified Model the discrepancy can easily be accounted for by the error bars applied. While it appears the discrepancy is related to the characteristics of the fire load used (*i.e.* not solely cellulosic as in previous large-

scale tests used to validate the Law Model, not uniformly distributed throughout the compartment, *etc*.) the particular reason for the discrepancy is not yet known. Once further experimental investigation identifies further parameters of importance that may account for this discrepancy, they can be taken into account at the design engineer's discretion by adjusting the error bars accordingly.

It is of additional interest to note that, in the comparison of the Law Model with the DFT1 experimental data, the heat flux incident in the near-field of the window is best matched by one of the Law Model draught scenario conditions while further afield, in the potential vicinity of windows from upper compartments, a different draught condition provides a better match for the experimental data. Hence, in terms of design, it may be prudent to determine the heat flux resultant from all potential draught and rate of burning conditions that may apply, given that the exact compartment conditions in the event of a fire may be unknown – as a compartment may have doors on a wall opposite a window (*i.e*. *Through Draught* condition usually assumed), but the doors may be closed at the time of the fire (*i.e*. resulting in *No Through Draught* conditions). Therefore, at any point of interest on the façade above an opening, the highest incident heat flux resulting from all potential cases should be applied, such as to ensure worst-case conditions are accounted for in both the near- and far-field areas. This should particularly be applied if an element of high sensitivity to incident heat flux lies within the height from the opening soffit for which the Simplified Model describes a heat flux under any of the three scenarios.

The simple nature of Simplified Model tool renders it easily applicable to any scenario within the range of its limits of applicability regardless of the characteristic parameters that describe the fire compartment such as its key *geometric* dimensions, those of its openings, and *ambient conditions* such as ambient temperature and through wind (*i.e***.** a *Through Draught*) or even the velocity of an imposed *Forced Draught*. The distribution of heat flux incident on the façade plane can be applied as a boundary condition for design of several components of the façade. For the design of structural steel elements embedded in the façade with one face left exposed, flush with the surface – such as perimeter columns or spandrel beams – this boundary condition could be used to determine the resultant temperature gradients within the

element. In turn the resultant thermal stresses induced in the member could be evaluated for different end-restraint conditions at the member connections, taking into account the support conditions provided by the rest of the façade.

An estimate of the typical incident heat flux in the event of a compartment fire could also aid in the design of cladding materials such as to ensure the critical heat flux for ignition of the cladding material is higher than that predicted by the model, at any given location where the cladding is to be applied. Hence, different cladding materials can be provided in bands, should it be economical to provide a strip of material with a higher critical heat flux for ignition in the near-field of the opening (*i.e*. a headstone, *etc*.) rather than throughout the whole of the façade. Such provision could help prevent fire spread up the external façade which has been noted in several cases to contribute to the severity of large tall-building fires (*cf*. Chapter 2). As previously discussed, although the heat flux described by the Simplified Model pertains to the distribution along the centreline of the opening under still conditions, it should account for a worst-case scenario and any cladding selected should not be adversely affected by flames tilting due to lateral wind.

Similarly, the Simplified Model can also be applied to glass windows in upper-level compartments that are in the plane of the façade, in order to establish whether they are likely to crack or shatter under the imposed incident heat flux resulting from a compartment fire below. Glass breakage can increase the risk of secondary ignition in upper-level compartments hence the tool can be used to specify adequate vertical spacing of window arrangements or the provision of adequate glazing systems. Should the window be at an angle from the fire compartment window (*i.e*. rather than directly above it) the incident heat flux can also be calculated using trigonometry to identify the distance from the upper corner of the compartment window closet to the second window, to the closest point on that window pane. This length should then be input into the relevant Simplified Model expression in order to quantify the expected heat flux incident on a point of equivalent vertical distance above the compartment fire opening. The conditions at that point should provide a conservative estimate of the heat flux incident on the window of interest, which would be at its highest only when there is a lateral wind tilting the external plume in its direction.

For all these example applications the model can not only be used in design but also as a simple tool for design *approval* as the expressions are simple and quick to apply, as opposed to the numerous calculations and scenario checks required for the implementation of the Law Model. The quick computational time of the model also renders it beneficial for use in emergency fire situations, particularly those of building-integrated emergency response, such as that envisioned by the FireGrid project [24,25]. In such a system the integrated building sensors could be used to determine the ventilation (draught) conditions of the compartment during the fire (*i.e.* doors and windows open or closed) in order to provide pertinent and potentially dynamic (should the conditions change) predictions of the estimated external heat flux. The model could also be employed to predict the thermal boundary condition applied to the external face of steelwork embedded in the façade such that its expected behaviour under insult from the specified fire conditions could then be predicted using finite element analysis. As for design, it could also be used to define the likelihood of external fire spread or secondary ignition due to shattering of windows above the fire compartment if the properties of the cladding materials and window glass (and their relative distance from a given fire compartment opening soffit) is pre-recorded in the systems' building information database.

While these are some examples of practical application of the model they are not exhaustive as the incident heat flux can be applied to any element on the plane of the façade as an external boundary condition (*i.e.* in structural terms: a fire load), provided the scenario falls within the limits of applicability of the model. Nevertheless it should be noted that, in emergency situations if the fire does spread to an upper floor, the model can no longer be used as flames emerging from openings on multiple floors often merge to some extent and this effect is unaccounted for in the Law Model and in the Simplified Model proposed.

8.3 Recommendations for Further Work

Although the Simplified Model provides a concise representation of the heat flux incident on the façade and has clearly defined limits of applicability, it is still

fundamentally based on many of the same assumptions (and associated limiting conditions) inherent in the array of experimental tests the Law Model from which the correlations derive and against which they were initially validated (c*f.* Chapter 2, Section 2.2 and Chapter 3, Section 3.3, respectively). While the extent to which departure from these assumptions is expected to affect the Simplified Model correlations is unknown, it is recommended that further extensive experimental research be carried out such that for all cases outwith the limits of applicability of the model an estimate can also be made.

Apart from the limits of the general assumptions in the Law Model, the discrepancy noted between the Law Model output and the measurements from full-scale experimental tests pertaining to a *realistic* scenario implies that perhaps not all the compartment fire parameters that have a significant effect on the resultant heat flux incident on the external façade have yet been identified, in particular those related to the characteristics of the fire load parameter. Given the dominant influence of the fire load on the resultant external heat flux it is recommended that the assumptions surrounding the use of this parameter be investigated foremost. A computational fluid dynamics study of the comparative effect of varying fire load location for otherwise identical scenarios provides an initial *qualitative* indication that the assumptions inherent in the definition of the fire load (and its use in the assumption of a homogenous compartment burning rate) may have a bearing on the resultant external heat flux incident on the façade. Nevertheless, limitations in the current capabilities of computational fluid dynamics tools in simulating the complex properties of *realistic* compartment fire scenarios under ventilation-controlled conditions render further computational investigation the *quantitative* importance of characteristics surrounding the fire load parameter of limited value. Therefore it is highly recommended that a comprehensive series of experiments be conducted in order to determine the effect of the characteristics of the fire load that may constitute other parameters of importance in terms of the resultant external heat exposure, such as: the relative location of different components of the fire load; the material properties of the fire load and the resultant emissivity of combustion products; the effect of having fire load items (or parts of items) with a different heat of combustion and critical heat flux for ignition;

localised rates of burning; different surface areas of the fire load; different surface orientation; varying height of the fuel bed, *etc*.

Subsequently, the relative importance of any further parameters identified will determine whether the Simplified Model needs to be revisited or whether the importance of these parameters can simply be incorporated into better estimates of the error bars for a given scenario. Then, should a parameter such as the fire load location – which is potentially variable from that specified in the design phase of a building throughout its lifetime – be found to be of considerable importance, an inter-active system such as that proposed by FireGrid could employ sensor-assisted input information to provide time-variable predictions pertinent to the particular characteristics of the fire scenario in a given emergency situation.

References

1 Law, M. and O'Brien, T. (1989), Fire safety of bare external structural steel, The Steel Construction Institute, SCI Publication 009, U.K. ISBN: 0 86200 026 2.

2 BSI (2002), Eurocode 1: Actions on structures – Part 1-2: General actions – Actions on structures exposed to fire, *British Standards*, U.K. BS EN 1991-1-2:2002.

3 BSI (2005), Eurocode 3: Design of steel structures – Part 1-2: General rules – Structural fire design, *British Standards*, U.K. BS EN 1993-1-2:2005.

4 Balter, M. (2004), Earliest signs of human-controlled fire uncovered in Israel, *Science* 304 (5671), pp.663 – 665.

5 Plato (*ca*. 360 BC) Timaeus, translated by W.R.M. Lamb in Plato in Twelve Volumes (9), Cambridge, MA, Harvard University Press; London, William Heinemann Ltd.

6 Richardson, J.K., (Ed.) (2003), History of Fire Protection Engineering, National Fire Protection Association, Inc., Massachusetts, USA.

7 Emmons, H.W. (1984), The further history of fire science, *Combustion Science and Technology* 40, pp.167-174. Gordon and Breach Science Publishers.

8 Cote, A.E. (2008), History of fire protection engineering, *Fire Protection Engineering* (10 Year magazine), Fall of 2008, Society of Fire Protection Engineers, U.S.A., pp.28-36.

9 Beyler, C. (1999), Guest editorial: Professor Howard Emmons 1912-1998, *Fire Technology* 35 (1), pp.1-3.

10 Rothermel, R.C. (1990), Modeling fire behavior, International Conference on Forest Fire Research, Coimbra, Portugal.

11 Trouvé A. (2007), Challenges in CFD modeling of large-scale pool fires, Proceedings of Advanced Research Workshop on Fire Computer Modeling, (Ed.) J. A. Capote Abreu, GIDAI, Univ. Cantabria, Santander, Spain, pp.1-14.

12 Hollis, L. (1876), Ye Firemen of 1776 (*Watercolor Painting*), Photographed by Library of Congress Prints and Photographs Division, Washington, DC 20540 USA. Digital ID: () cph 3a10844 http://hdl.loc.gov/loc.pnp/cph.3a10844 [accessed 04/02/2010]. Reproduction Number: LC-USZ62-8228 (b&w film copy neg.).

13 BBC (2007), Skyscraper Fire Fighters (documentary), BBC Horizon, U.K. www.bbc.co.uk/sn/tvradio/programmes/horizon/broadband/tx/firegrid/ [accessed 16/09/2009]

14 McAllister, T., Barnett, J., Gross, J., Hamburger, R., Magnusson, J. (2002), World Trade Center building performance study: data collection, preliminary observations and recommendations, Chapter 1: Introduction, Technical Report FEMA 403, Federal Emergency Management Agency, Washington, D.C., U.S.A.

15 Usmani, A.S., Chung, Y.C. and Torero, J.L. (2003), How did the WTC towers collapse: a new theory, *Fire Safety Journal* 38 (6), pp.501-533.

16 Quintiere, J.G. (1989), Scaling applications in fire research, *Fire Safety Journal* 15 (1), pp.3-29.

17 Ma, T.G. and Quintiere, J.G. (2003), Numerical simulation of axi-symmetric fire plumes: accuracy and limitations, *Fire Safety Journal* 38 (5), pp.467-492.

18 Rein, G., Torero, J.L., Wolfram, J., Stern-Gottfried, J., Ryder, N.L., Desanghere, S., Lázaro, M., Mowrer, F., Coles, A., Joyeux, D., Alvear, D., Capote, J.A., Jowsey, A., Abecassis-Empis, C. and Reszka, P. (2009), Round-robin study of a priori modelling predictions of the Dalmarnock Fire Test One, *Fire Safety Journal* 44 (4), pp.590-602

19 Jahn, W., Rein, G. and Torero, J.L. (2007), Posteriori modelling of Fire Test One, Chapter 11, The Dalmarnock Fire Tests: Experiments and Modelling, (Eds.) Rein, G., Abecassis

Empis, C. and Carvel, R., School of Engineering and Electronics, The University of Edinburgh, U.K. ISBN 978-0-9557497-0-4.

20 Fernandez-Pello, A.C. (1994), The solid phase, Chapter 2, Combustion Fundamentals of Fire, (Ed.) G. Cox, Academic Press, pp.31-100.

21 Drysdale, D. (1998), An Introduction to Fire Dynamics, 2nd Edition, John Wiley & Sons, U.K. ISBN: 0-471-97291-6.

22 NFPA (2003), Fire Protection Handbook, 19th Edition, National Fire Protection Association, U.S.A.

23 BSI (2001), Application of fire safety engineering principles to the design of buildings – Code of Practice, *British Standards*, U.K. BS 7974:2001.

24 Cowlard, A., Jahn, W., Abecassis-Empis, C., Rein, G. and Torero, J.L. (2010), Sensor assisted fire fighting, *Fire Technology*, 46 (3), pp.719-741.

25 Upadhyay, R., Pringle, G., Beckett, G., Potter, S., Han, L., Welch, S., Usmani, A. and Torero, J. (2009), An architecture for an integrated fire emergency response system for the built environment, *Fire Safety Science* 9, pp.427-438.

26 Law, M. (1978), Fire safety of external building elements – The design approach, *Engineering Journal*, Second Quarter, pp.59-74, American Institute of Steel Construction (AISC), U.S.A.

27 Law, M. (1981), Designing fire safety for steel – recent work, ASCE Spring Convention, American Society of Civil Engineers, U.S.A.

28 Tonkelaar, E. den (2003), Prediction of the effect of breaking windows in a double skin façade as a result of fire, Eighth International IBPSA Conference, Eindhoven, Netherlands.

29 Colwell, S. and Martin, B. (2003), Fire performance of external thermal insulation for walls of multi-storey buildings, BR 135, Building Research Establishment (BRE), U.K. ISBN 1-86081-622-3.

30 Read, R. E. H. (1991), External fire spread: building separation and boundary distances, BR187, Building Research Establishment (BRE), U.K.

31 Johnson, C. and Tarlin, E. (1974), Incêndio (film), National Fire Protection Association and the National Bureau of Standards, U.S. Department of Commerce.

32 Routley, J., Jennings, C. and Chubb, M. (1991) High-rise office building fire, One Meridian Plaza, Philadelphia, Penn., February 23, 1991, United States Fire Administration, Technical Report Series, Report 049, FEMA, U.S.A.

33 Kenichi, I. and Sekizawa, A. (2005), Collapse mechanism of the Windsor building by fire in Madrid and the plan for its demolition process, International Workshop on Emergency Response and Rescue 2005, Taiwan.

34 Jacobs, A. (2009), Fire ravages renowned building in Beijing, *The New York Times* (Feb. 10th 2009), New York Edition, U.S.A.

35 Soares, G. (2010), Incêndio danifica hotel de 25 milhões, *Diário de Notícias* (10th March 2010), Portugal.

36 Cunha, S. (2010), Braga: Incêndio destrói parte da fachada de hotel, *Correio da Manhã* (9th March 2010), Portugal.

37 Cooke, G. (2009), Andraus high-rise, São Paulo, Brazil, February 1972 (presentation), Fire Safety Consultant London 2009, http://www.cookeonfire.com/pdfs/Andraus%20pdf.pdf [03/02/2010]

38 Tavares, R. M. (2008), Prescriptive codes vs. performance-based codes: Which one is the best fire safety code for the Brazilian context?, *Safety Science Monitor* 12 (1), Australia.

39 Beitel, J. and Iwankiw, N. (2002), Analysis of needs and existing capabilities for full-scale fire resistance testing, NIST GCR 02-843, National Institute of Standards and Technology, U.S.A.

40 Demers, D. P. (1981), Hotel fire, Las Vegas, NV, February 10, 1981, NFPA Fire Investigation, National Fire Protection Association, Quincy, MA, U.S.A.

41 O'Connor, D. J. (2008), Building façade or fire safety façade?, CTBUH 8th World Congress, Dubai.

42 Knight, K. (2009), Report to the Secretary of State by the Chief Fire and Rescue Adviser on the emerging issues arising from the fatal fire at Lakanal House, Camberwell on 3 July 2009, communities and Local Government, London, UK. ISBN 978-1-4098-1175-8.

43 Ingberg, S. H. (1928), Test of the severity of building fires, *National Fire Protection Association Quarterly*, 22 (1), pp.43-61.

44 Fujita, K. (1958), Characteristics of fire inside a non-combustible room and prevention of fire damage, Report 2 (2), Japanese Ministry of Construction, Building Research Institute, Tokyo, Japan.

45 Kawagoe, K. (1958), Fire behaviour in rooms, Report 27, Building Research Institute, Tokyo, Japan.

46 Thomas, P.H. and Law, M. (1972), The projection of flames from burning buildings, FRN 921, Fire Research Station, Borehamwood, U.K.

47 Thomas, P.H. and Heselden, A.J.M. (1972), Fully-developed fires in single compartments – A co-operative research programme of the Conseil International du Bâtiment, CIB Report No.20, FRN 923, Fire Research Station, Borehamwood, U.K.

48 Thomas, P.H. (1974), Fires in model rooms: CIB research programmes, Building Research Establishment Current Paper CP32/74, BRR, Borehamwood, U.K.

49 Magnusson, S.E. and Thelandersson, S. (1970), Temperature-time curves of complete process of fire development. Theoretical study of wood fuel fires in enclosed spaces, Acta Polytechnica Scandinavia, *Civil Engineering and Building Construction Series 65*, Stockholm, Sweden.

50 Babrauskas, V. and Williamson, R.B. (1978), Post-flashover compartment fires: Basis of a theoretical model, *Fire and Materials* 2 (2), pp.39-53.

51 Babrauskas, V. (1981), A closed-form approximation for post-flashover compartment fire temperatures, *Fire Safety Journal* 4, pp.63-73.

52 Yokoi, S. (1960), Study on the prevention of fire-spread caused by hot upward current, Building Research Institute, Report No. 34, Tokyo, Japan.

53 Webster, C.T. and Raftery, M.M. (1959), The burning of fires in rooms – Part II, FRN 401, Joint Fire Research Organization, Borehamwood, U.K.

54 Webster, C.T., Raftery, M.M., and Smith, P.G. (1961), The burning of fires in rooms – Part III, FRN 474, Joint Fire Research Organization, Borehamwood, U.K.

55 Webster, C.T. and Smith, P.G. (1964), The burning of well-ventilated compartment fires – Part IV brick compartment, 2.4 m (8 ft) cube, FRN 578, Joint Fire Research Organization, Borehamwood, U.K.

56 Thomas, P. H. (1961), On the heights of buoyant flames, FRN 489, Fire Research Station, Borehamwood, U.K.

57 Seigel, L.G. (1969), The projection of flames from burning buildings, *Fire Technology* 5 (1), pp.43-51.

58 Heselden, A.J.M., Smith, P.G. and Theobald, C.R. (1966), Fires in a large compartment containing structural steelwork – Detailed measurements of fire behaviour, FRN 646, Fire Research Station, Borehamwood, U.K.

59 Gross, D. (1967), Field burnout tests of apartment dwelling units, *Building Science Series* 10, National Bureau of Standards, Sept. 29.

60 Underwriters Laboratories, Inc. (1970), Fire test of Walt Disney World unitized guest room, report for United States Steel Corporation, Underwriters Laboratories, Inc., July 1, Illinois, U.S.A.

61 Butcher, E.G., Chitty, T.B. and Ashton, L.A. (1966), The temperature attained by steel in building fires, *Fire Research Technical Paper 15*, HMSO, London, U.K.

62 Underwriters Laboratories, Inc. (1975), Fire severity at the exterior of a burning building, American Iron and Steel Institute, April 3, Washington, D.C., U.S.A.

63 Stromdahl, I. (1972), The Tranas Fire Tests – Field studies of heat radiation from fires in a timber structure, National Swedish Institute for Building Research, Document D3, Stockholm, Sweden.

64 Kordina, K. (1978), Brandversuche Lehrte - Schriftenreihe "Bau und Wohnforschung" des Bundesministers für Raumordnung, Bauwesen und Städtebau, Bonn, Germany.

65 Buchanan, A.H. (2002), Structural Design for Fire Safety, John Wiley & Sons, U.K. ISBN: 0-471-89060-X.

66 Thomas, P.H. (1963), The size of flames from natural fires, *Symposium (International) on Combustion 9 (1)*, pp.844-859.

67 Bullen, M.L. and Thomas, P.H. (1979), Compartment fires with non-cellulosic fuels, Proceedings of the 17th Symposium (International) on Combustion 17 (1), pp.1139-1148, The Combustion Institute, U.S.A.

68 Bohm, B. and Rasmussen, B.M. (1987), The development of a small-scale fire compartment in order to determine thermal exposure inside and outside buildings, *Fire Safety Journal* 12 (2), pp.103-108.

69 Oleszkiewicz, I. (1989), Heat transfer from a window fire plume to a building façade, HTD 123, ASME Collected papers on Heat Transfer, Book No. H00526, pp.163-170.

70 Oleszkiewicz, I. (1990), Fire exposure to exterior walls and flame spread on combustible cladding, *Fire Technology 26*, pp.357-375.

71 Oleszkiewicz, I. (1991), Vertical separation of windows using spandrel walls and horizontal projections, *Fire Technology 27*, pp.334-340.

72 Gottuk, D.T., Roby, R.J. and Beyler, C.L. (1992), A study of carbon monoxide and smoke yields from compartment fires with external burning, Symposium (International) on Combustion 24 (1), pp.1729-1735.

73 Ohmiya, Y., Yusa, S., Suzuki, J.I., Koshikawa, K. and Delichatsios, M.A. (2003), Aerodynamics of fully involved enclosure fires having external flames, Proceedings of the Fourth International Seminar on Fire and Explosion Hazards, University of Ulster, Belfast, U.K.

74 Ohmiya, Y., Tanaka, T. and Wakamatsu, T. (1998), A room fire model for predicting fire spread by external flames, *Fire Science and Technology* 18 (1), pp.11-21.

75 Ohmiya, Y., Hori, Y., Sagimori, K. and Wakamatsu, T. (2000), Predictive method for properties of flame ejected from an opening incorporating excess fuel, Proceedings of the Fourth Asia-Oceania Symposium on Fire Science and Technology, pp. 375-386.

76 Lee, Y.-P., Delichatsios, M.A. and Silcock, G.W.H. (2007), Heat fluxes and flame heights in façades from fires in enclosures of varying geometry, Proceedings of the Combustion Institute 31 (2), pp.2521-2528.

77 Lee, Y.-P. (2006), Heat fluxes and flame heights in external façades from enclosure fires, Ph.D. Thesis, The University of Ulster, Belfast, U.K.

78 Goble, K. (2007), Height of flames projecting from compartment openings, Masters Thesis, The University of Canterbury, Christchurch, New Zealand.

79 Klopovic, S. and Turan, Ö.F. (1998), Flames venting externally during full-scale flashover fires: Two sample ventilation cases, *Fire Safety Journal* 31 (2), pp.117-142.

80 Klopovic, S. and Turan, Ö.F. (2001) A comprehensive study of externally venting flames – Part I: External plume characteristics for through-draught and no-through-draught ventilation conditions and repeatability, *Fire Safety Journal* 36 (2), pp.99-133.

81 Klopovic, S. and Turan, Ö.F. (2001), A comprehensive study of externally venting flames – Part II: Plume envelope and centre-line temperature comparisons, secondary fires, wind effects and smoke management system, *Fire Safety Journal* 36 (2), pp.135-172.

82 Suzuki, T., Sekizawa, A., Satoh, H., Yamada, T., Yanai, E., Kurioka, H. and Kimura, Y. (1999), An experimental study of ejected flames of a high-rise building Part I, National Research Institute of Fire and Disaster No.88, Japan, pp.51-63.

83 Takahashi, K., Suzuki, T., Yamada, T., Yanai, E., Sekizawa, A., Kurioka, H. and Satoh, H. (2001), Flame configuration derived from video camera picture – An experimental study of ejected flames of a high-rise building Part II, National Research Institute of Fire and Disaster No.91, Japan, pp.48-58.

84 Yamada, T., Takahashi, K., Yanai, E., Suziki, T., Sekizawa, A., Satoh, H. and Kurioka, H. (2001), Heat flux to surface walls above fire floor level – An experimental study of ejected flames of a high-rise building Part III, National Research Institute of Fire and Disaster No.88, Japan, pp.59-68.

85 Hakkarainen, T. and Oksanen, T. (2002), Fire safety assessment of wooden façades, *Fire and Materials* 26, pp.7-27.

86 Sugawa, O., Momita, D. and Takahashi, W. (1996), Flow behaviour of ejected fire flame/plume from an opening effected by external side wind, Proceedings of the 5th International Syposium on Fire Safety Science, pp.249-260.

87 ARUP, Innovator's hall of fame, Short biography of "Margaret Law",

http://info.arup.com/arup/feature.cfm?pageid=8984 [accessed 05/03/09]

88 Incropera, F.P. and DeWitt, D.P. (2002), Fundamentals of Mass and Heat Transfer, Fifth Edition, John Wiley & Sons, Inc., U.S.A. ISBN: 0-471-38650-2.

89 Arnault, P., Ehm, H. and Kruppa, J. (1973), Rapport experimental sur les essays avec des feux naturels executes dans la petite installation, CECM 3/73-11-F, CTICM, Puteaux, France.

90 Howell, J.R. (1982), A catalog of radiation heat transfer configuration factors, 3rd Edition, The University of Texas at Austin, Austin, Texas, U.S.A. http://www.engr.uky.edu/rtl/Catalog/ [accessed 07/09/2008]

91 McGuire, J.H. (1952), The calculation of heat transfer by radiation, FRN 20, Fire Research Station, Borehamwood, U.K.

92 BSI (1972), BS476: Part 20: 1987 – Fire tests on building materials and structures: Methods for determination of the fire resistance of elements of construction (general principles), *British Standards*, U.K.

93 BSI (1972), BS476: Part 21: 1987 – Fire tests on building materials and structures: Methods for determination of the fire resistance of load bearing elements of construction, *British Standards*, U.K.

94 BRE Global (2005), Requirements, tests and methods of assessment of passive fire protection systems for structural steelwork, Fire Loss Prevention Standard, 1107: Issue 1.1: 16/09/05, BRE Global Limited, U.K.

95 BSI (1972), BS476: Part 8: 1972 - Fire tests on building materials and structures: Test methods and criteria for the fire resistance of elements of building construction, *British Standards*, U.K.

96 Seigel, L.G. (1970), Fire test of an exposed steel spandrel girder, *Materials Research and Standards*, MTRSA 10 (2), pp.10-13.

97 Arnault, P., Ehm, H. and Kruppa, J. (1974), Evolution des temperatures dans des poteaux exterieurs soumis a des incendices, CECM 3-74/7F, CTICM, Puteaux, France.

98 Law, M. (1981/2), Notes on the external fire exposure measured at Lehrte, *Fire Safety Journal* 4 (4), pp.243-246, Elsevier Science, U.K.

99 Ashton, L.A. and Malhotra, H.L. (1960), External walls on buildings, I – The protection of openings against spread of fire from storey to storey, FRN 836, Borehamwood, U.K.

100 Moulen, A.W. (1971), Horizontal projections in the prevention of spread of fire from storey to storey, Report TR52/75/397, Commonwealth Experimental Building Station, Australia.

101 Harmathy, T.Z. (1979), Design to cope with fully developed compartment fires, in Design of Buildings for Fire Safety, (Eds.) E.E. Smith and T.Z. Harmathy, American Society for Testing and Materials, STP 685, pp.198-276.

102 Becker, R. (2002), Structural behaviour of simple steel structures with non-uniform longitudinal temperature distributions under fire conditions, *Fire Safety Journal* 37 (5), pp.495-515.

103 Gillie, M., Usmani, A.S. and Rotter, J.M. (2002), A structural analysis of the Cardington British Steel Corner Test, *Journal of Construction Steel Research* 58 (4), pp.427-442.

104 Welch, S. and Lennon, T. (2001), Comments on Eurocode 1 – Actions on structures, Part 1-2: General actions – actions on structures exposed to fire, Amended FINAL DRAFT (Stage 34), 24 August 2001, BRE, U.K.

105 Reszka, P., Abecassis Empis, C., Biteau, H., Cowlard, A., Steinhaus, T., Fletcher, I.A., Fuentes, A., Gillie, M. and Welch, S. (2007), Experimental layout and building description, Chapter 2, The Dalmarnock Fire Tests: Experiments and Modelling, (Eds.) Rein, G., Abecassis Empis, C. and Carvel, R., School of Engineering and Electronics, The University of Edinburgh, U.K. ISBN 978-0-9557497-0-4.

106 Cowlard, A., Steinhaus, T., Abecassis Empis, C. and Torero, J.L. (2007), Test Two: The 'Controlled fire', Chapter 4, The Dalmarnock Fire Tests: Experiments and Modelling, (Eds.) Rein, G., Abecassis Empis, C. and Carvel, R., School of Engineering and Electronics, The University of Edinburgh, U.K. ISBN 978-0-9557497-0-4.

107 Amundarain, A.A, Torero, J.L., Usmani, A., Al-Remal, A.M. (2007), Assessment of the thermal efficiency, structure and fire resistance of lightweight building systems for optimised design, PhD Thesis, School of Engineering, The University of Edinburgh, U.K. http://hdl.handle.net/1842/2128 [accessed 01/04/2008].

108 Jowsey, A., Torero, J.L., and Lane, B. (2007), Heat transfer to the structure during the Fire, Chapter 7, The Dalmarnock Fire Tests: Experiments and Modelling, (Eds.) Rein, G., Abecassis Empis, C. and Carvel, R., School of Engineering and Electronics, The University of Edinburgh, U.K. ISBN 978-0-9557497-0-4.

109 Gillie, M. and Stratford, T. (2007), Behaviour of the structure during the fire, Chapter 8, The Dalmarnock Fire Tests: Experiments and Modelling, (Eds.) Rein, G., Abecassis Empis, C. and Carvel, R., School of Engineering and Electronics, The University of Edinburgh, U.K. ISBN 978-0-9557497-0-4.

110 Stratford, T., Gillie, M. and Chen, J-F. (2007), The performance of fibre reinforced polymer strengthening in the fire, Chapter 9, The Dalmarnock Fire Tests: Experiments and Modelling, (Eds.) Rein, G., Abecassis Empis, C. and Carvel, R., School of Engineering and Electronics, The University of Edinburgh, U.K. ISBN 978-0-9557497-0-4.

111 Welch, S., Jowsey, A., Deeny, S., Morgan, R. and Torero, J.L. (2007), BRE large compartment fire tests – characterising post-flashover fires for model validation, *Fire Safety Journal* 42 (8), pp.548-567. doi:10.1016/j.firesaf.2007.04.002.

112 Jin, T. (2008), Visibility and human behaviour in fire smoke, The SFPE Handbook of Fire Protection Engineering, 4th Edition, (Eds.) P.J. DiNenno *et al.*, National Fire Protection Association, Massachusetts, U.S.A., pp. 2-54 – 2-66.

113 Abecassis Empis, C., Cowlard, A., Welch, S. and Torero, J.L. (2007), Test One: The 'Uncontrolled' fire, Chapter 3, The Dalmarnock Fire Tests: Experiments and Modelling, (Eds.) Rein, G., Abecassis Empis, C. and Carvel, R., School of Engineering and Electronics, The University of Edinburgh, U.K. ISBN 978-0-9557497-0-4.

114 Mulholland, G.W. (2002), Smoke production and properties, The SFPE Handbook of Fire Protection Engineering, 3rd Edition, (Eds.) P.J. DiNenno *et al.*, National Fire Protection Association, Massachusetts, U.S.A, pp. 2-291 – 2-302.

115 Ingason, H. and Wickstrom, U. (2007), Measuring incident radiant heat flux using the plate thermometer, *Fire Safety Journal* 42 (2), pp.161-166.

116 ASTM (2005), ASTM E459 – 05: Standard test method for measuring heat transfer rate using a thin-skin calorimeter, ASTM International, U.S.A. DOI: 10.1520/E0459-05.

117 McCaffrey, B.J., Heskestad, G. (1979), A robust bidirectional low-velocity probe for flame and fire application, *Combustion and Flame* 26 (1), pp.125-127.

118 Cowlard, A. (2009), Sensor and model integration for the rapid prediction of concurrent flow flame spread, PhD Thesis, School of Engineering, The University of Edinburgh, U.K. http://hdl.handle.net/1842/2753 [accessed 18/09/2009].

119 Huggett, C. (1980), Estimation of rate of heat release by means of oxygen consumption measurements, *Fire and Materials* 4, pp.61-65.

120 Kawagoe, K. and Sekine, T. (1963), Estimation of fire temperature-time curve in rooms, BRI Occasional Report 11, Building Research Institute, Tokyo, Japan.

121 BSI (1993), BS 476: Part 33: 1993 (ISO 9705:1993) - Fire tests on building materials and structures: full-scale room test for surface products, *British Standards*, U.K.

122 Steinhaus, T. and Jahn W. (2007), Laboratory experiments and their application, Chapter 6, The Dalmarnock Fire Tests: Experiments and Modelling, (Eds.) Rein, G., Abecassis Empis, C. and Carvel, R., School of Engineering and Electronics, The University of Edinburgh, U.K. ISBN 978-0-9557497-0-4.

123 Babrauskas, V. (1981), Will the second item ignite?, National Bureau of Standards, Gaithersburg, MD, U.S.A. NBSIR 81-2271.

124 Joshi, A. and Pagni, P.J. (1990), Thermal analysis of effect of a compartment fire on window glass, *Fire Research and Safety*, 11th Joint Panel Meeting, (Eds.) Jason, N. H., Cramer, D. M., , Berkeley, CA, pp. 233-252.

125 Mowrer, F.W. (1997), Window breakage induced by exterior fires, Proceedings of the 2nd International Conference on Fire Research and Engineering (ICFRE2), NIST and SFPE sponsored, Gaithersburg, MD, U.S.A.

126 Desanghere, S. (2007), Development of a simplified model aimed at predicting external members heating conditions, Interflam 2007 – Proceedings of the Eleventh International Conference (2), Interscience Communications, London, UK., pp. 955-966.

127 McGrattan, KB. & Forney, G. Fire Dynamics Simulator (Version 4) User's Guide, NIST Special Publication 1019, National Institute of Standards and Technology, Gaithersburg, MD, USA, 2006.

Appendix A : Detailed Measurements of the Experimental Compartment used in Dalmarnock Fire Test One and Test Two

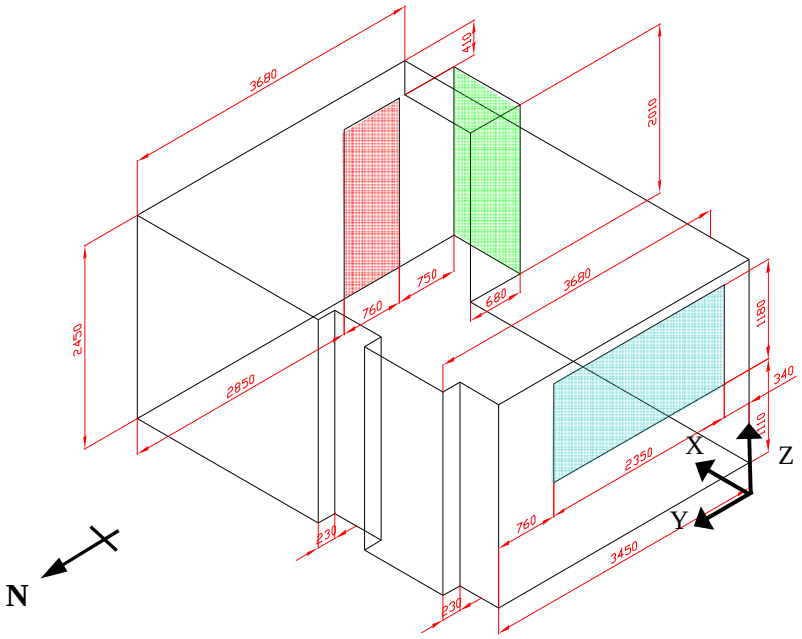

Figure A.1. The main experimental compartment viewed from the NW. The window is shaded in blue, the door to the kitchen in pink and the door to the hallway in green. All dimensions are labelled in mm and the Global Coordinate System origin is shown.

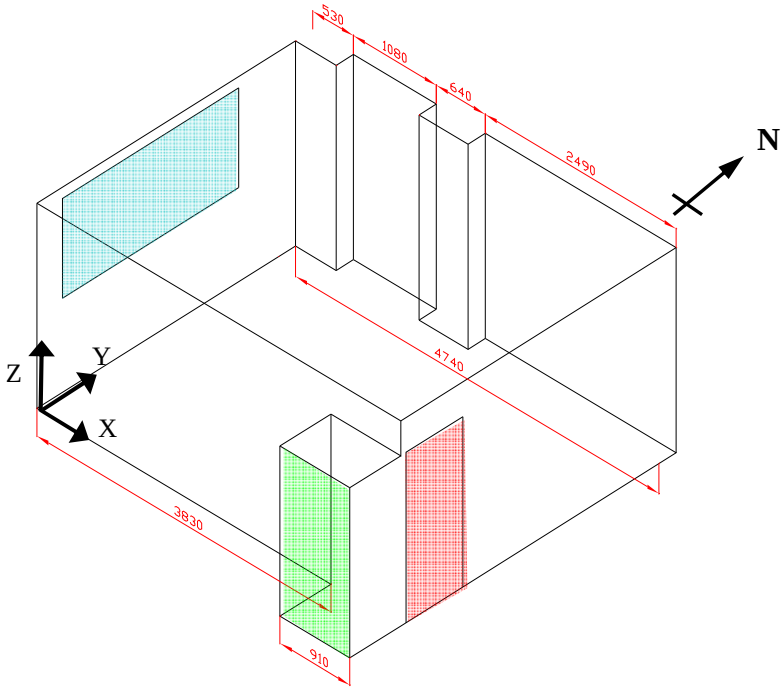

Figure A.2. The main experimental compartment viewed from the SE. The window is shaded in blue, the door to the kitchen in pink and the door to the hallway in green. All dimensions are labelled in mm.

Appendix B : Details of the Main Items of Furniture (Fire Load) used in the Dalmarnock Fire Tests

Sofa

This is one of the main furniture items in the experimental compartment and was amongst the first items to ignite. It is labelled as item (i) in Chapter 4, Figure 4.3 which shows the location of the sofa relative to other items in the compartment.

Figure B.1. Sofa.

Width (mm)	**Depth** (mm)	**Height** (mm)	**Seat Depth** (mm)	**Seat Height** (mm)
1370	780	720	550	390

Table B.1. The main dimensions of the sofa.

Total Mass

34 kg

Materials

Frame: Particleboard.

Back rest and seat cushions: Polyurethane foam 32 kg/m^3 and Polyester filling.

Cover: 100 % cotton. According to the manufacturer, the cover and filling material are cigarette and match resistant.

Desks

The two desks in the experimental compartments used in the Dalmarnock Fire Tests include a regular work table, shown in Figure B.2, and a tiered computer desk, shown in Figure B.3. These are labelled in Chapter 4, Figure 4.3 as part of items (ii), where the work table (Figure B.2) is in front of the compartment window and the tiered computer desk (Figure B.3) is placed against the north wall. Their main dimensions are listed in Table B.2 together with their respective mass. These desks were laden with typical office materials such as a large computer monitor (not flat-screen), a keyboard, mouse, a telephone (on the work table in Figure B.2), plastic trays and paper storage, among other minor office paraphernalia, as can be seen in the figures.

Figure B.2. Work table.

Figure B.3. Tiered computer desk.

Name	**Width** (mm)	**Length** (mm)	**Height** (mm)	**Mass** (kg)
Work table	775	1200	730	8.5
Computer Desk	550	800	730	25.5

Table B.2. The main dimensions and mass of the work table (shown in Figure B.2) and the tiered computer desk (shown in Figure B.3).

Materials

Work Table: Particleboard and metal legs

Tiered Computer Desk: Particleboard.

Chair

Both the table and desk had swivel chairs as illustrated in Chapter 4, Figure 4.3 (next to the table and desk with desktop computers), also labelled as part of items (ii). The main dimensions of the chair components are listed in Table B.3.

Figure B.4. Swivel Chair

Chair Part	**Width** (mm)	**Length** (mm)	**Thickness** (mm)
Seat	400	400	50
Back Rest	400	300	50 (average)

Table B.3. The main dimensions of different parts of the swivel chair.

Materials

Seat and back and arm rests: Polystyrene and polyurethane

Legs: Metal

Total Mass

15 kg

Bookcases

The bookcases in the NE corner of the compartment are represented in Chapter 4, Figure 4.3 as furniture items (iii). These bookcases were fully-laden with books, files, magazines, video tapes and other common office or living room items as depicted in the sample bookcase shown in Figure B.5. One of the bookcases was taller and slightly wider than the other two however they were generally very similar as were the contents placed on the shelves. Both sets of the dimensions are listed in Table B.4, together with the mass of each (un-laden) bookcase. Figure B.5 also depicts the waste-paper basket used, corresponding to item (vii) in Chapter 4, Figure 4.3.

Figure B.5. An example of the typically fuel-laden bookcases used.

Name	**Width** (mm)	**Depth** (mm)	**Height** (mm)	**Total Mass** (kg)
Bookcase	590	250	1710	19.5
Tall Bookcase	670	240	1940	21.3

Table B.4. The main dimensions and mass of the different (un-laden) bookcases.

Materials

Bookcases (only): Particleboard and acrylic paint.

Cabinet

A small plastic storage cabinet was used in the Dalmarnock Fire Tests, labelled in Chapter 4, Figure 4.3 as item (iv). It was full of office items such as cardboard boxes and video tapes. The cabinet, shown in Figure B.6, is composed of polypropylene plastic.

Figure B.6. Plastic storage cabinet

Name	**Width** (mm)	**Depth** (mm)	**Height** (mm)	**Total Mass** (kg)
Cabinet	350	320	610	2.7

Table B.5. The main dimensions and mass of the plastic cabinet.

Coffee Tables

There were three coffee tables, one larger (depicted in Figure B.7) than the other two (depicted in Figure B.8). They are labelled as items (v) in Chapter 4, Figure 4.3 and their main dimensions and mass are listed in Table B.6. The larger table, located in the centre of the compartment, has a lower tier with some magazines. The two smaller tables had paper lamps and were located one on either side of the sofa.

Figure B.7. Large coffee table

Figure B.8. Coffee table

Name	**Width** (mm)	**Depth** (mm)	**Height** (mm)	**Total Mass** (kg)
Large coffee table	900	550	450	10.5
Coffee table	550	550	450	4.4

Table B.6. The main dimensions and mass of the coffee tables.

Materials

All coffee tables: Particleboard and acrylic paint.

Tall Floor Lamps

There were two tall floor lamps identical to that shown in Figure B.9. Their location is shown in Chapter 4, Figure 4.3 where they are labelled as item (vi). The lamps are 1740 mm tall and the lamp shade is 300 mm in diameter and 100 mm high.

Figure B.9. Tall floor lamps

Materials

Shade: Polypropylene plastic

Stand and base: Steel

Total Mass

7 kg

Plastic Magazine Box

Under the work table, near the window, there were two plastic boxes full of mostly magazines and some newspaper, as seen in Figure B.10.

Figure B.10. Plastic magazine box

Materials

Box: Polypropylene plastic

Contents: Paper and cardboard

Total Mass

Box: 1 kg

Contents: 42 kg

Appendix C : Tables of Coordinates for Relevant Sensor Locations for Dalmarnock Fire Test One

The data presented in several figures correspond to sensor measurements taken at specific locations. The location of the sensors is defined relative to a global coordinate system, the origin of which is at floor level in the SW corner of the Dalmarnock Fire Test One experimental compartment, as indicated in Chapter 4, Figure 4.3. Coordinates for fire-monitoring sensors relevant to the data presented are grouped into sets of sensors and listed in several tables below.

Internal Compartment Sensors

Tree	X (mm)	Y (mm)
1	4230	3160
2	4250	2060
3	4195	1315
4	4615	190
5	3605	2955
6	3660	1220
7	2860	3325
8	2590	1945
9	3025	350
10	2270	3160
11	2115	2580
12	2305	1030
13	1605	3150
14	1765	1900
15	1910	330
16	510	2815
17	750	2025
18	360	1515
19	390	710
20	800	350

(a)

Name	Z (mm)
TC1	2450
TC2	2400
TC3	2350
TC4	2250
TC5	2150
TC6	2050
TC7	1850
TC8	1650
TC9	1450
TC10	1150
TC11	850
TC12	450

(b)

Table C.1. Internal compartment thermocouple coordinates where: (a) shows the tree location; and (b) the height of thermocouples on each tree.

Name	X (mm)	Y (mm)	Z (mm)
Laser 1	3300	0	2350
Laser 2	3300	0	2150
Laser 3	3300	0	1950
Laser 4	3300	0	1450
Laser 5	3300	0	450

Table C.2. Coordinates for laser receivers for horizontally aligned sensors measuring smoke obscuration.

Name	X (mm)	Y (mm)	Z (mm)
Door 1 – A1	4270	-680	1810
Door 1 – A2	4270	-680	1610
Door 1 – A3	4270	-680	460
Door 2 – A1	4740	400	1890
Door 2 – A2	4740	400	1750
Door 2 – A3	4740	400	430
Window – 1	-300	1350	1390
Window – 2	-300	1795	1695
Window – 3	-300	1375	1850
Window - 4	-300	1685	2095
Window - 5	-300	1375	2230
Window - 6	-300	995	1730
Window - 7	-300	995	2095
Window - 8	-300	2095	2130

Table C.3. Coordinates for the bi-directional air velocity probes located in both the doorways and window.

Name	X (mm)	Y (mm)	Z (mm)
HF A	4140	2950	2440
HF B	4100	2055	2440
HF C	4100	1140	2440
HF D	2290	2965	2440
HF E	2755	2080	2440
HF F	2310	1115	2440
HF G	685	2835	2440
HF H	995	2025	2440
HF I	815	660	2400

Table C.4. Coordinates for the heat flux gauges mounted on the compartment ceiling.

External Sensors

Tree	X (mm)	Y (mm)
E1	-270	30
E2	-270	530
E3	-270	1030
E4	-270	1530
E5	-270	2030
E6	-270	2530
E7	-270	3030
E8	-500	530
E9	-500	1530
E10	-500	2530
E11	-750	530
E12	-750	1530
E13	-750	2530
E14	-1000	530
E15	-1000	1530
E16	-1000	2530
E17	-1250	530
E18	-1250	1530
E19	-1250	2530

(a)

Name	Z (mm)
ETC1	1880
ETC2	1980
ETC3	2180
ETC4	2480
ETC5	2880
ETC6	3380
ETC7	3980
ETC8	4680

(b)

Table C.5. External thermocouple coordinates where: (a) shows the tree location; and (b) the height of thermocouples on each tree.

Name	X (mm)	Y (mm)	Z (mm)
HF 1	-320	1540	2455
HF 2	-320	1540	2705
HF 3	-320	1540	2955
HF 4	-320	1540	3205
HF 5	-320	1540	3455
HF 6	-320	1540	3705
HF 7	-240	1460	3910
HF 8	-240	1460	4110
HF 9	-240	1460	4310
HF 10	-240	1460	4510
HF 11	-240	1460	4710
HF 12	-240	1460	4910
HF 13	-280	2515	2455
HF 14	-280	1815	2455
HF 15	-280	1265	2455
HF 16	-280	565	2455
HF 17	-240	2450	4510
HF 18	-240	1820	4510
HF 19	-240	1260	4510
HF 20	-240	630	4510

Table C.6. Coordinates for the external heat flux gauges mounted on the façade.

Appendix D : Gas-phase temperature contour plots for different sections through the experimental compartment and outside its window, at discrete time steps, for DFT1

The density of thermocouple sensors used in the Dalmarnock Fire Tests provides a high resolution of the evolution of temperature distribution during the tests, both inside the main compartment and outside the compartment window. A sample of the data is shown in a series of sections taken both through the compartment and the external plume at different time steps that correspond to different stages of the fire.

Internal Temperature Contours

For the internal compartment temperature, several sections are taken North-South (NS) and East-West (EW) through the compartment as well as horizontally (HOR) at each thermocouple height (except for the uppermost thermocouple in each tree, TC1 which was in contact with the ceiling). For the vertical planes (the NS and EW series) the thermocouple trees were not always aligned, so a best-fit plane through several trees has been taken in each case, where no thermocouple tree lies further than 0.3 m from the plane taken. This may result in a slightly steeper representation of temperature gradients in the plane of the sections, in places where one of the X- or Y-coordinates of two trees is similar, such as is the case with the Y-coordinate of Trees 10 and 13. Nevertheless, overall the vertical sections provide a good representation of the temperature through different sections of the compartment. The location of these sections is illustrated in Figure D.1. The compartment temperature evolution at each of these section locations is shown in six Time Steps that represent different stages of the fire, as described in Chapter 4, Table 4.3. Refer to Chapter 4, Figure 4.7 to see where these Time Steps fall in relation to the evolution of the average compartment temperature. Figures D.2 – D.6 show the NS series, Figures D.7 – D.10 show the EW series, and Figures D.11 – D.21 show the HOR series which is numbered, in order, from the highest thermocouples to those closest to the floor. The data are presented relative to the Global Coordinate System the origin of which is located at floor level in the SW corner as shown in Figure D.1.

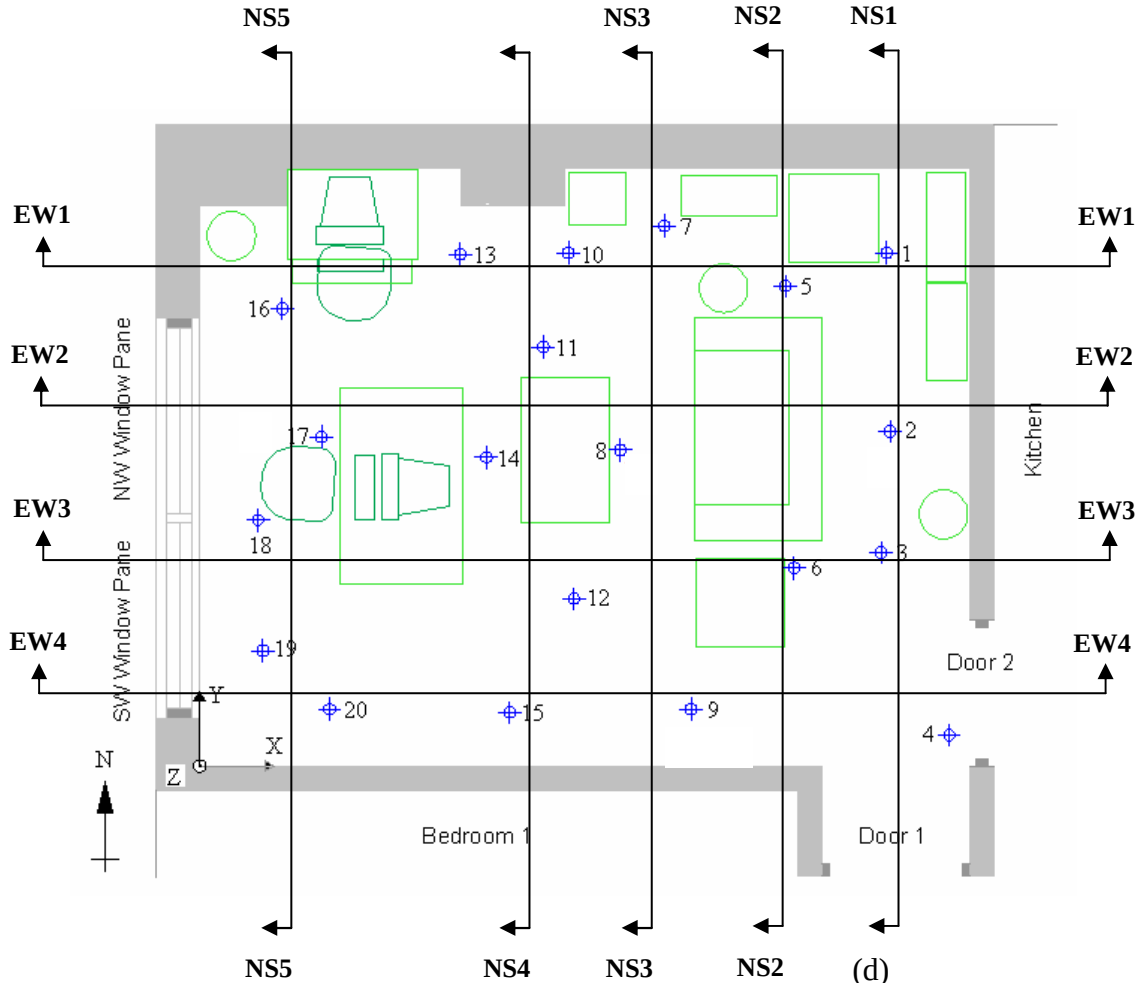

Figure D.1. Plan view of the Dalmarnock Fire Test One compartment showing the furniture (fire load; *cf.* Chapter 4, Figure 4.3 for the furniture item key) layout relative to the window and doors. Thermocouple trees are labelled as are the vertical sections taken through the compartment. The global coordinate system origin is shown in the SW corner, at floor level.

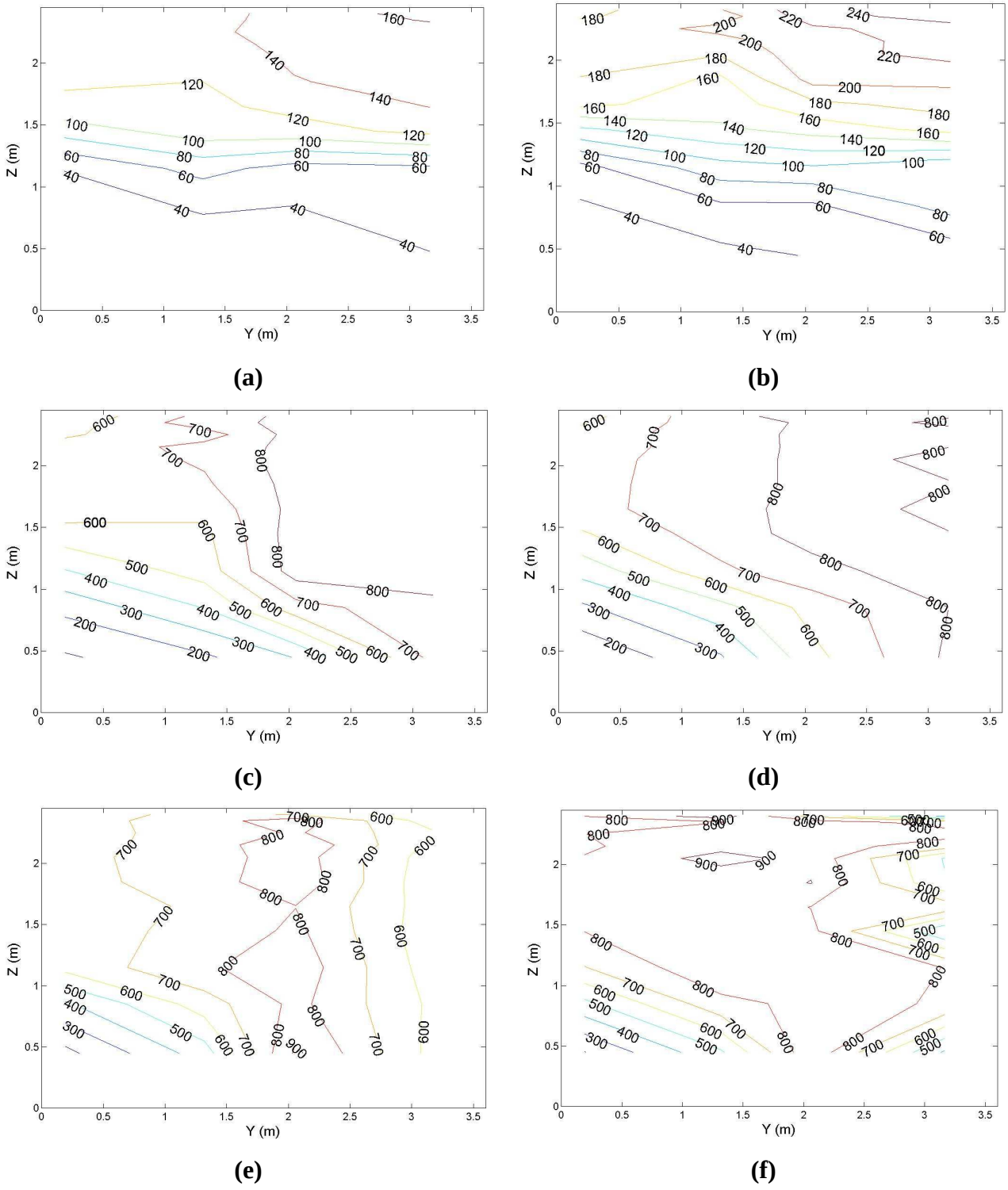

Figure D.2. The evolution of temperature contours through section NS1 (*cf*. Figure D.1) which is defined by the plane at X = 4.32 m, at Time Steps: (a) 201 s; (b) 251 s; (c) 351 s; (d) 420 s; (e) 661 s; and, (f) 901 s from ignition of Dalmarnock Fire Test One.

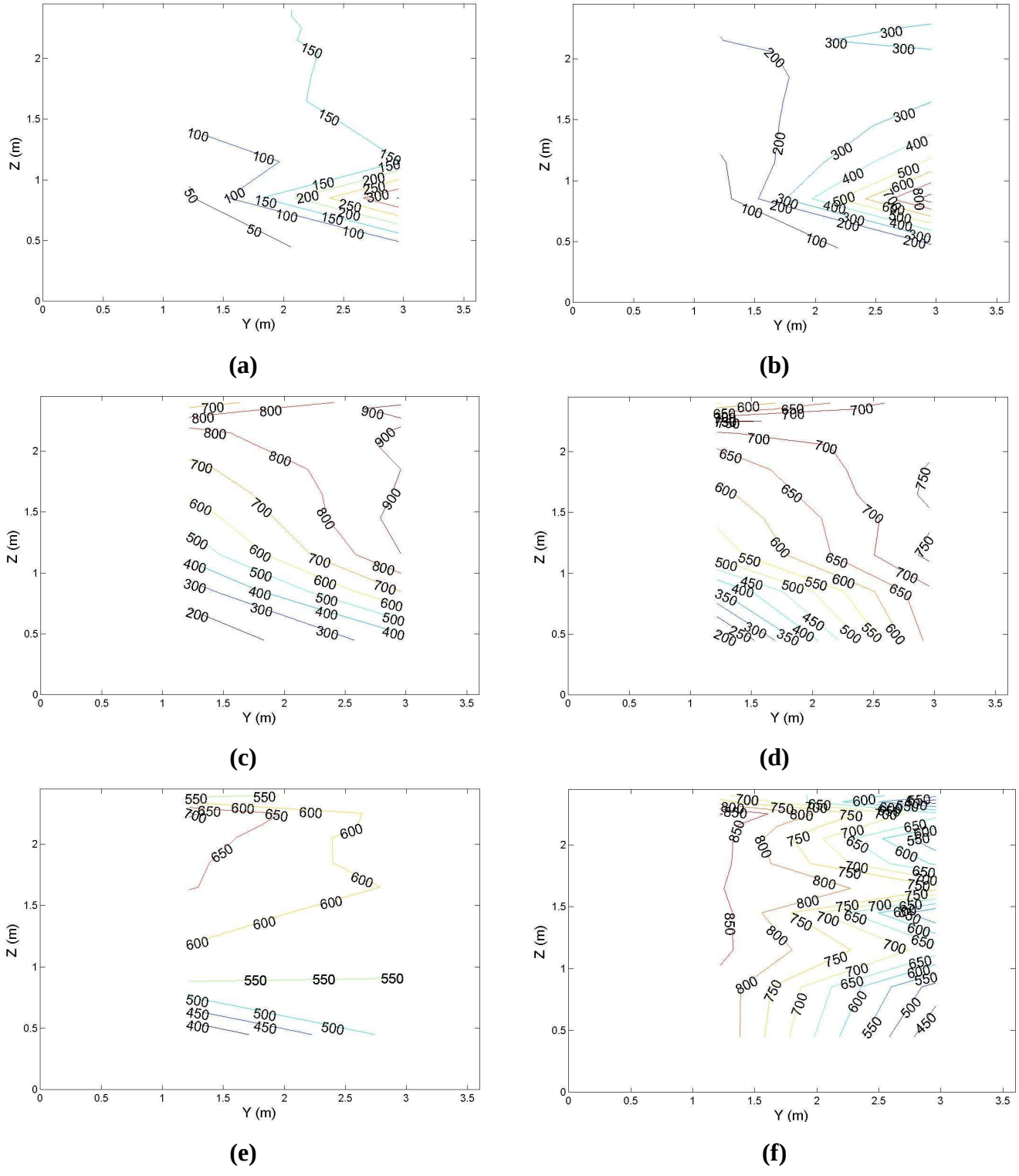

Figure D.3. The evolution of temperature contours through section NS2 (*cf*. Figure D.1) which is defined by the plane at X = 3.63 m, at Time Steps: (a) 201 s; (b) 251 s; (c) 351 s; (d) 420 s; (e) 661 s; and, (f) 901 s from ignition of Dalmarnock Fire Test One.

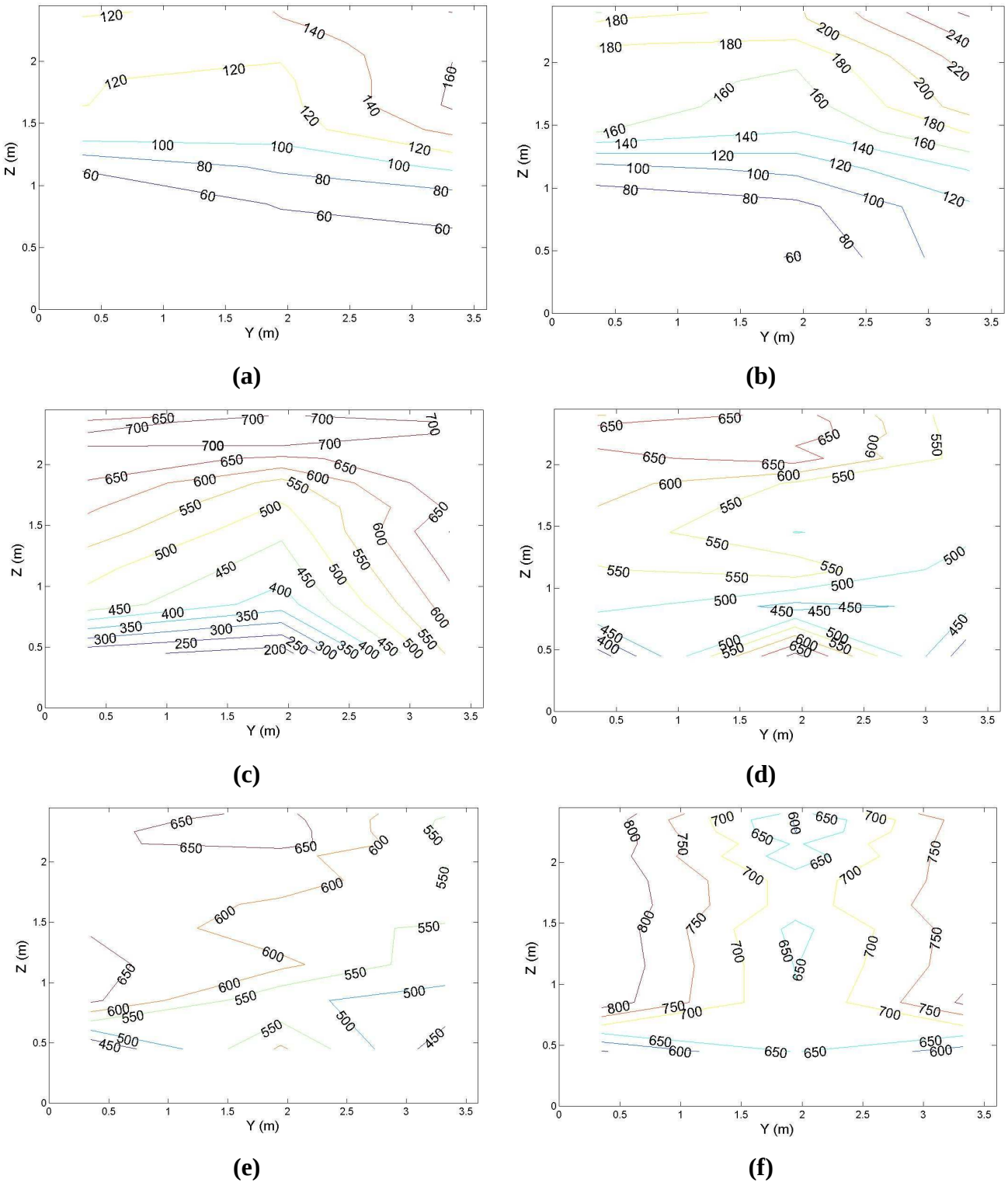

Figure D.4. The evolution of temperature contours through section NS3 (*cf*. Figure D.1) which is defined by the plane at X = 2.83 m, at Time Steps: (a) 201 s; (b) 251 s; (c) 351 s; (d) 420 s; (e) 661 s; and, (f) 901 s from ignition of Dalmarnock Fire Test One.

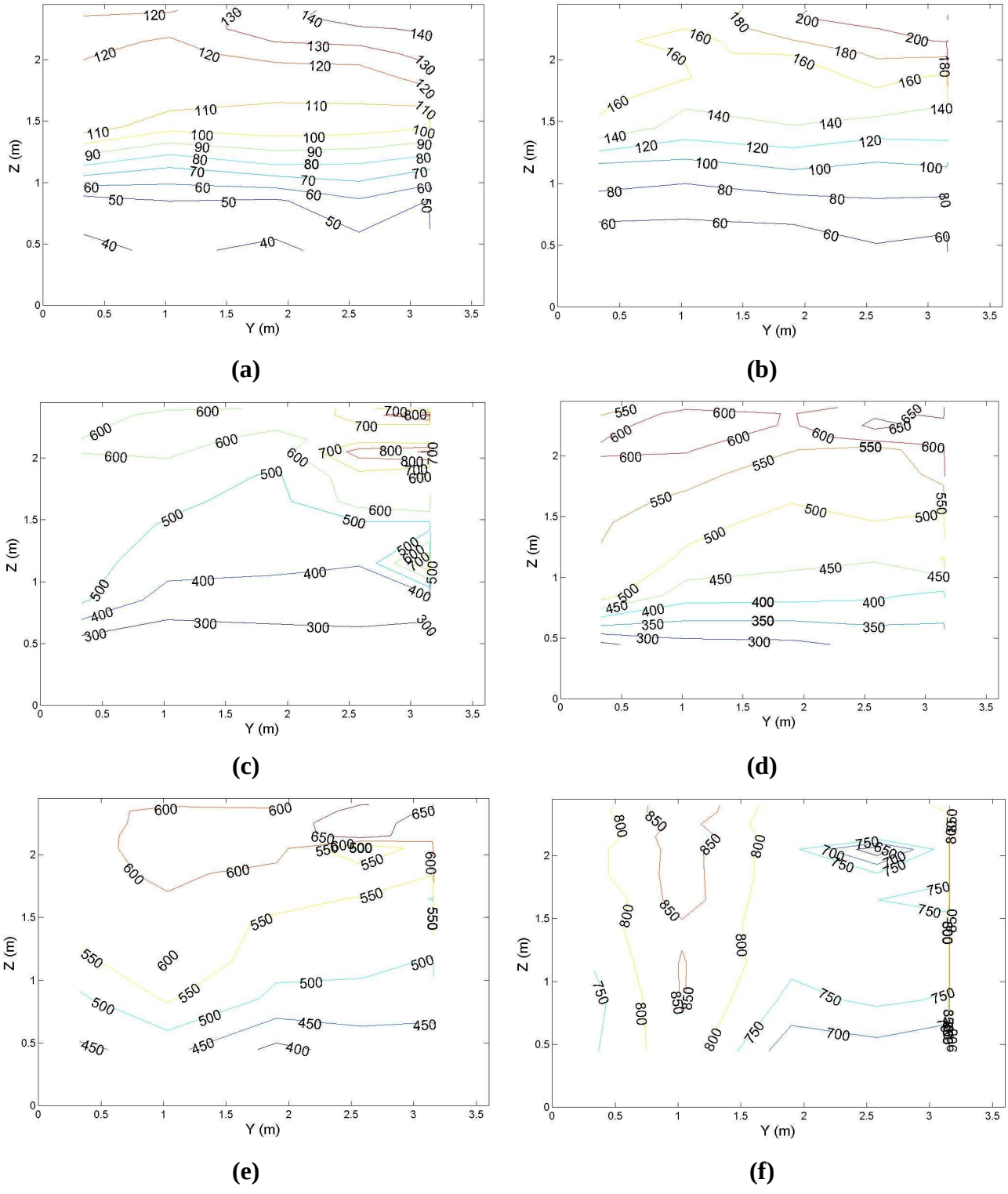

Figure D.5. The evolution of temperature contours through section NS4 (*cf*. Figure D.1) which is defined by the plane at X = 2.00 m, at Time Steps: (a) 201 s; (b) 251 s; (c) 351 s; (d) 420 s; (e) 661 s; and, (f) 901 s from ignition of Dalmarnock Fire Test One.

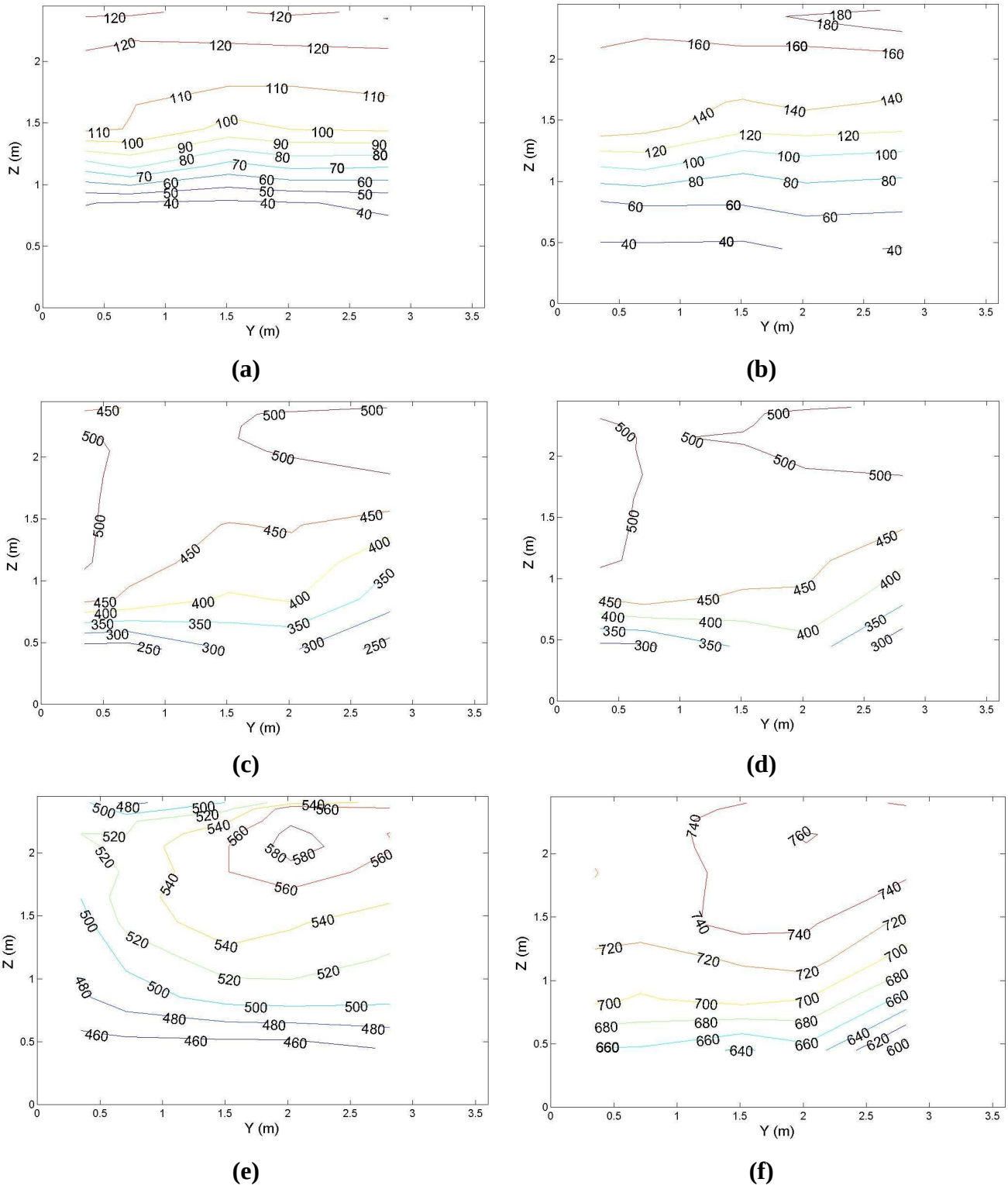

Figure D.6. The evolution of temperature contours through section NS5 (*cf*. Figure D.1) which is defined by the plane at X = 0.56 m, at Time Steps: (a) 201 s; (b) 251 s; (c) 351 s; (d) 420 s; (e) 661 s; and, (f) 901 s from ignition of Dalmarnock Fire Test One.

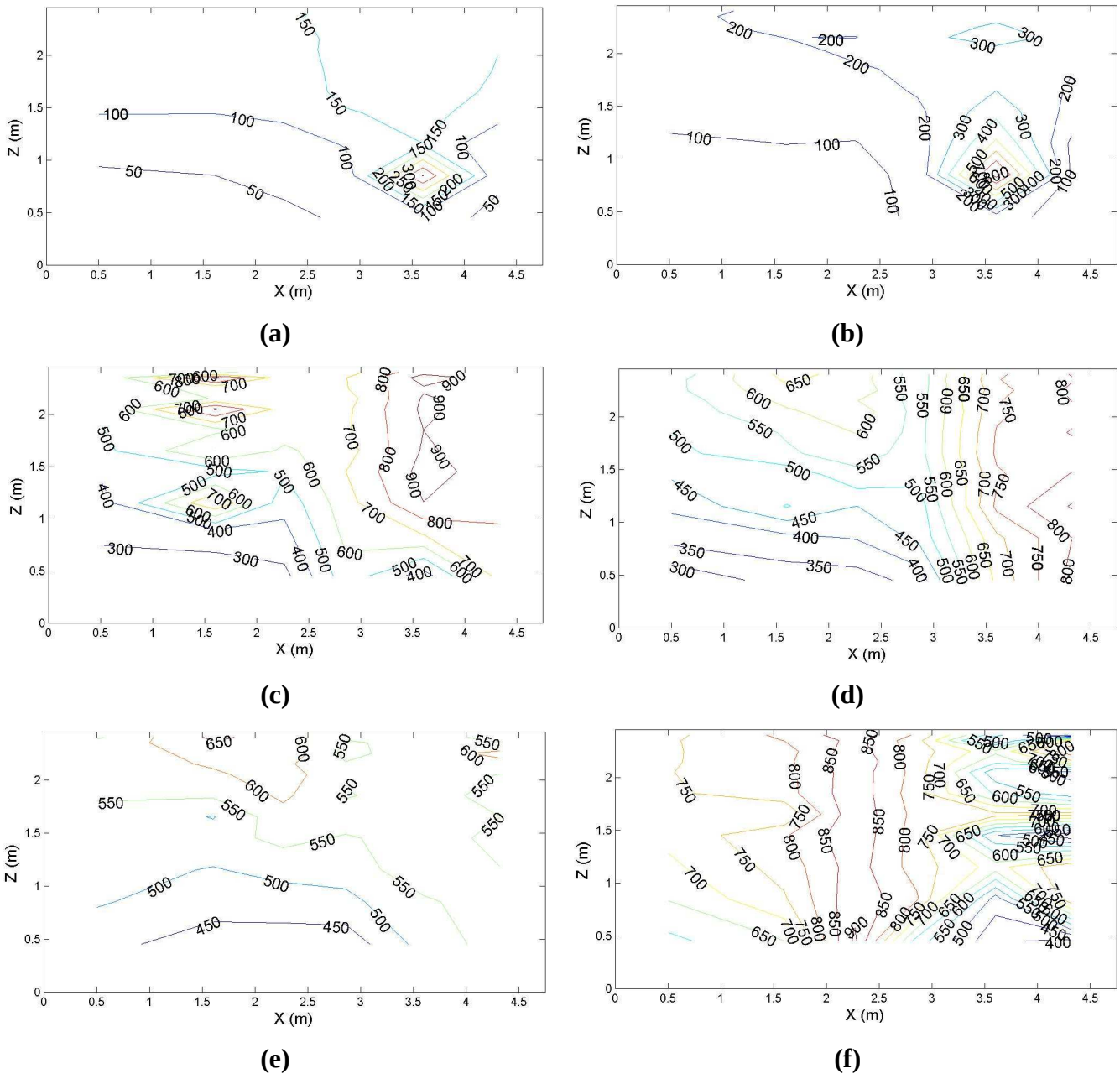

Figure D.7. The evolution of temperature contours through section EW1 (*cf*. Figure D.1) which is defined by the plane at Y = 3.09 m, at Time Steps: (a) 201 s; (b) 251 s; (c) 351 s; (d) 420 s; (e) 661 s; and, (f) 901 s from ignition of Dalmarnock Fire Test One.

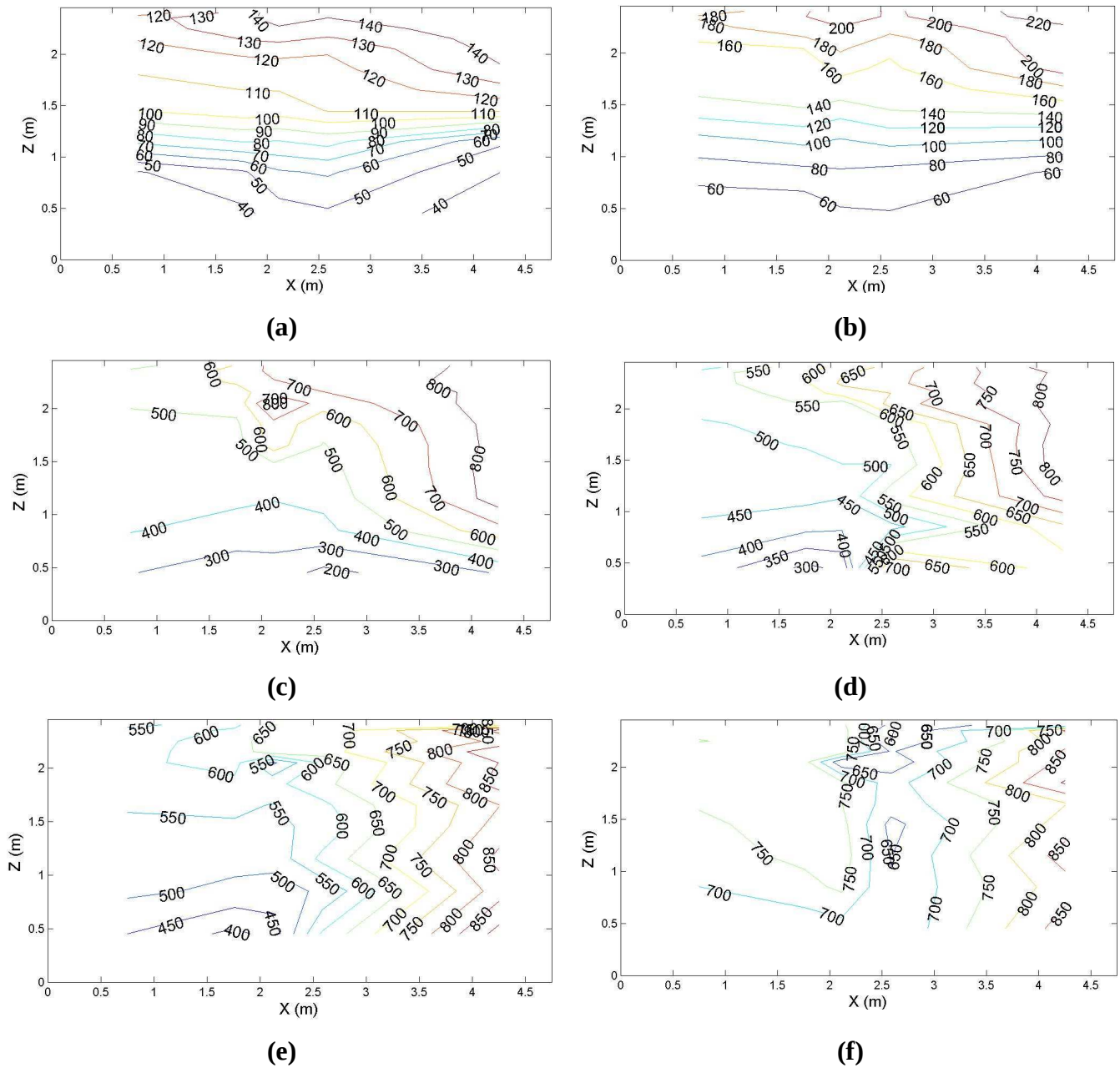

Figure D.8. The evolution of temperature contours through section EW2 (*cf.* Figure D.1) which is defined by the plane at Y = 2.10 m, at Time Steps: (a) 201 s; (b) 251 s; (c) 351 s; (d) 420 s; (e) 661 s; and, (f) 901 s from ignition of Dalmarnock Fire Test One.

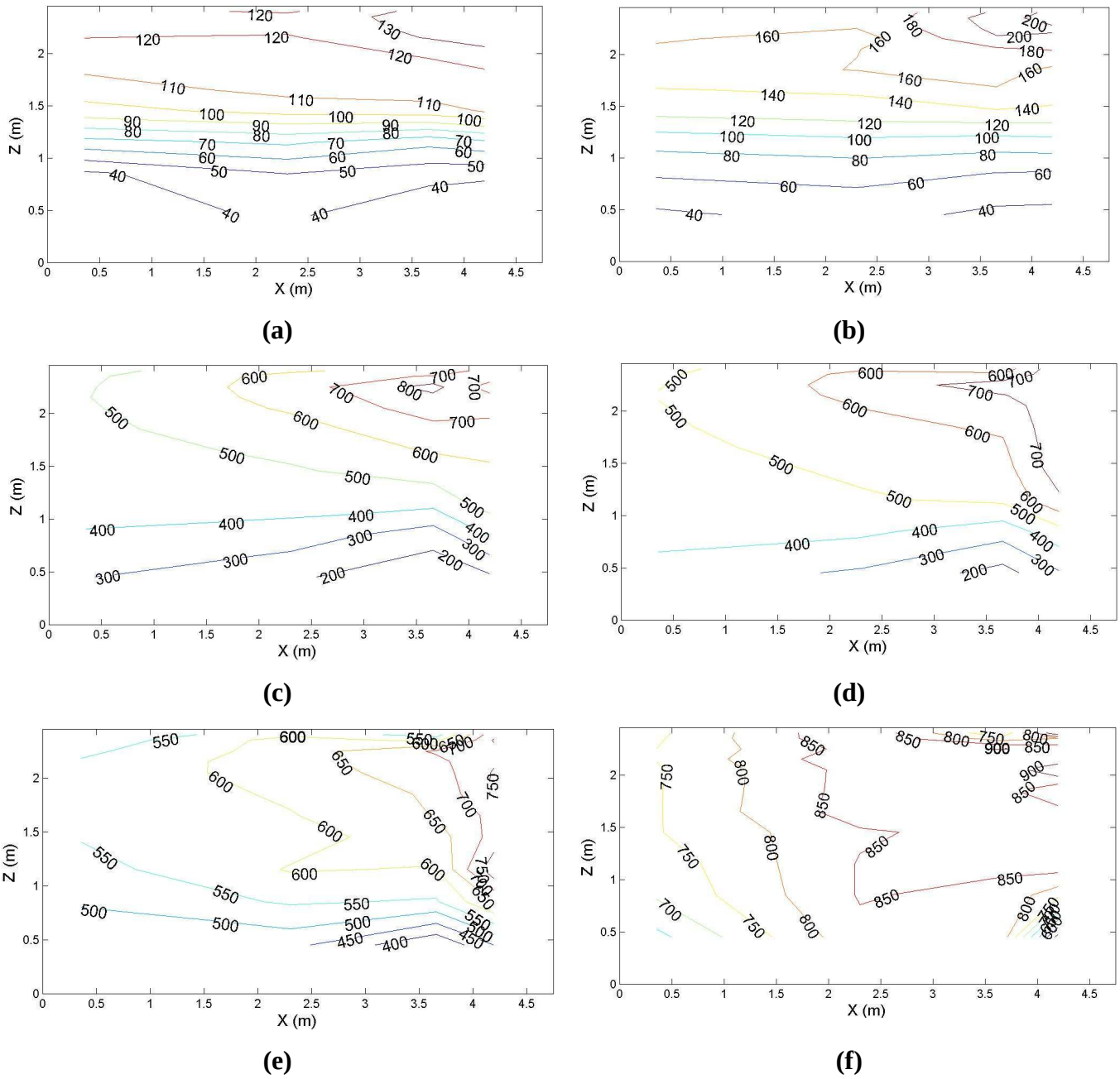

Figure D.9. The evolution of temperature contours through section EW3 (*cf.* Figure D.1) which is defined by the plane at Y = 1.27 m, at Time Steps: (a) 201 s; (b) 251 s; (c) 351 s; (d) 420 s; (e) 661 s; and, (f) 901 s from ignition of Dalmarnock Fire Test One.

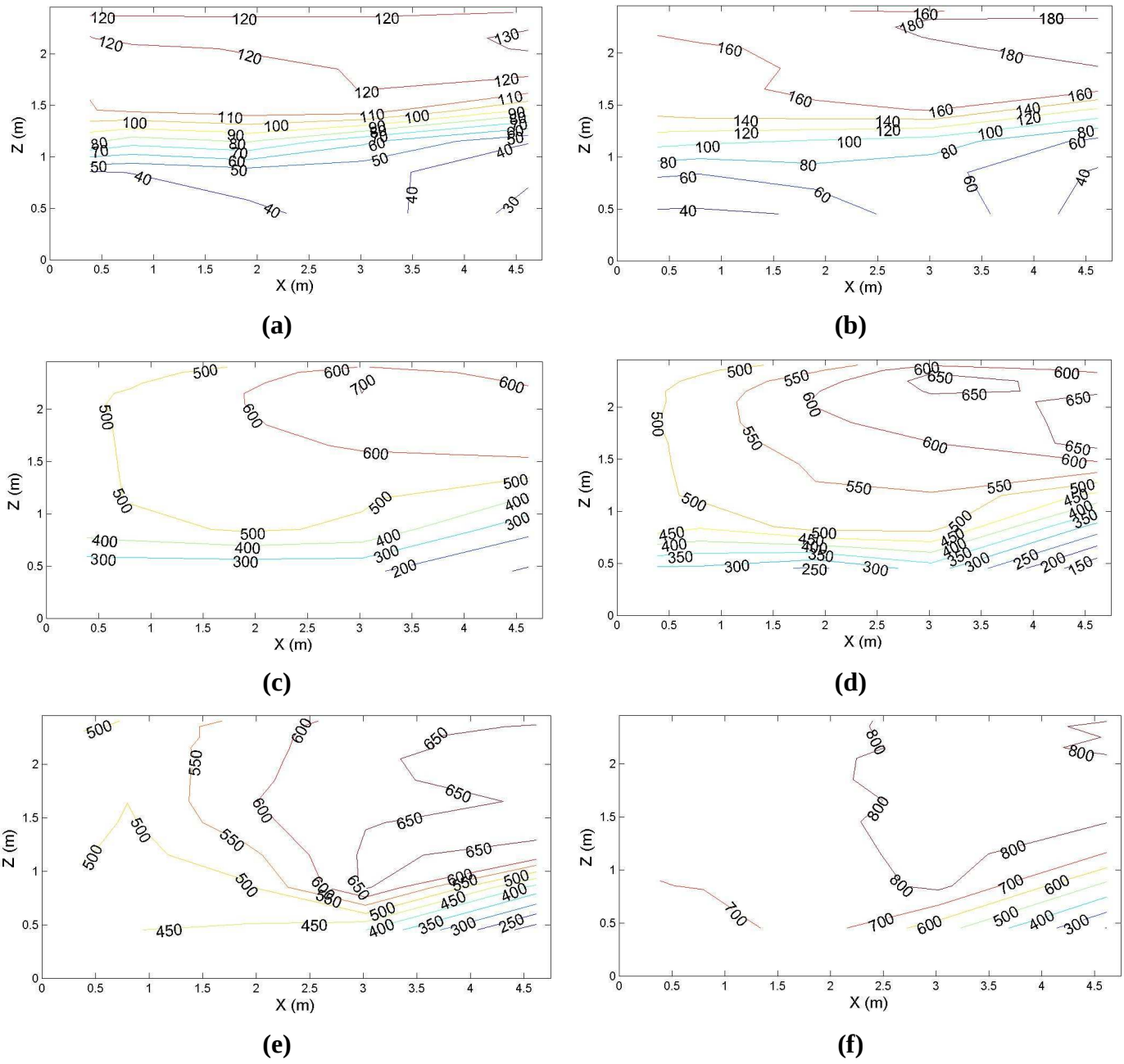

Figure D.10. The evolution of temperature contours through section EW4 (*cf*. Figure D.1) which is defined by the plane at Y = 0.39 m, at Time Steps: (a) 201 s; (b) 251 s; (c) 351 s; (d) 420 s; (e) 661 s; and, (f) 901 s from ignition of Dalmarnock Fire Test One.

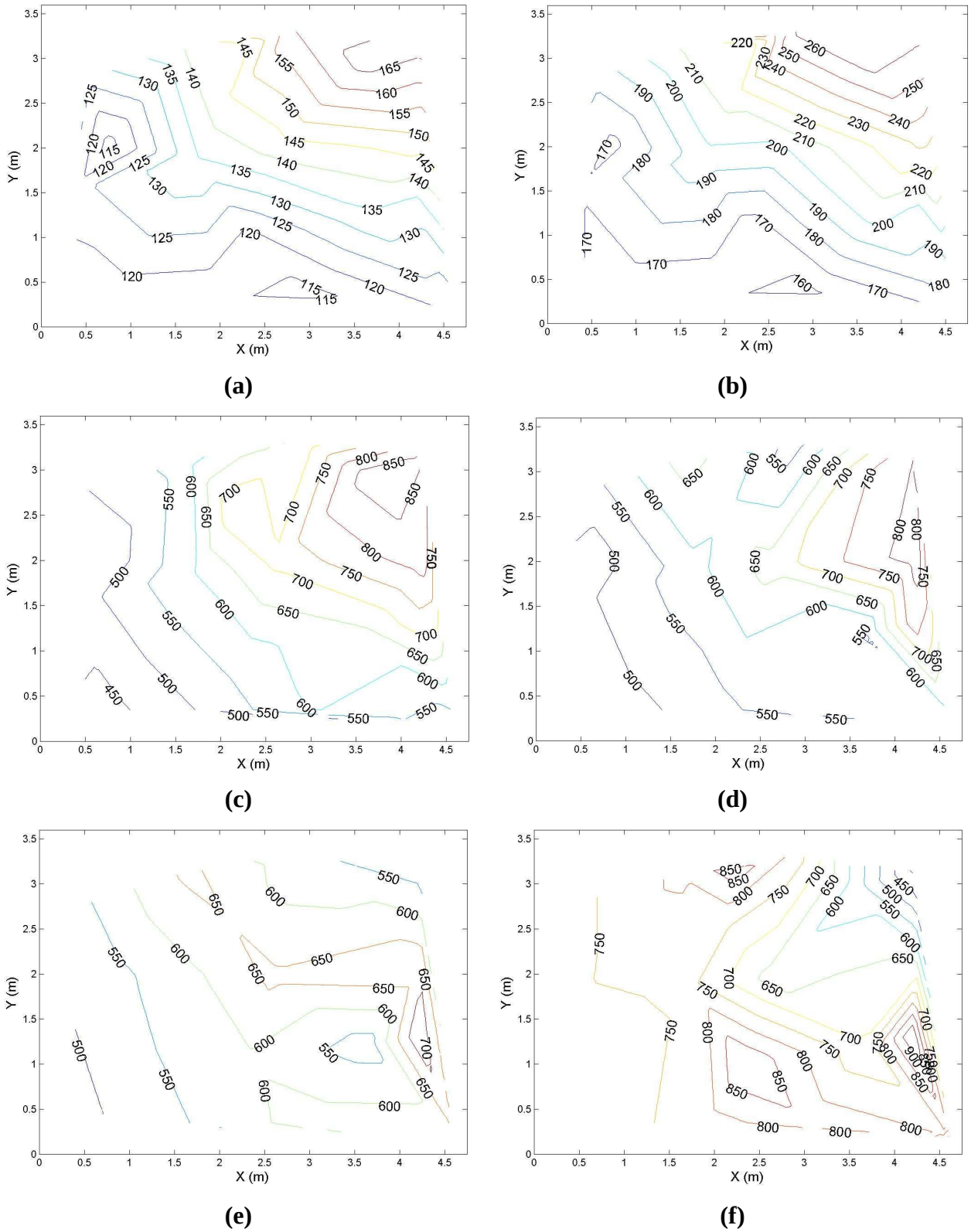

Figure D.11. The evolution of temperature contours through section HOR1 which is defined by the horizontal plane at Z = 2.40 m, at Time Steps: (a) 201 s; (b) 251 s; (c) 351 s; (d) 420 s; (e) 661 s; and, (f) 901 s from ignition of Dalmarnock Fire Test One.

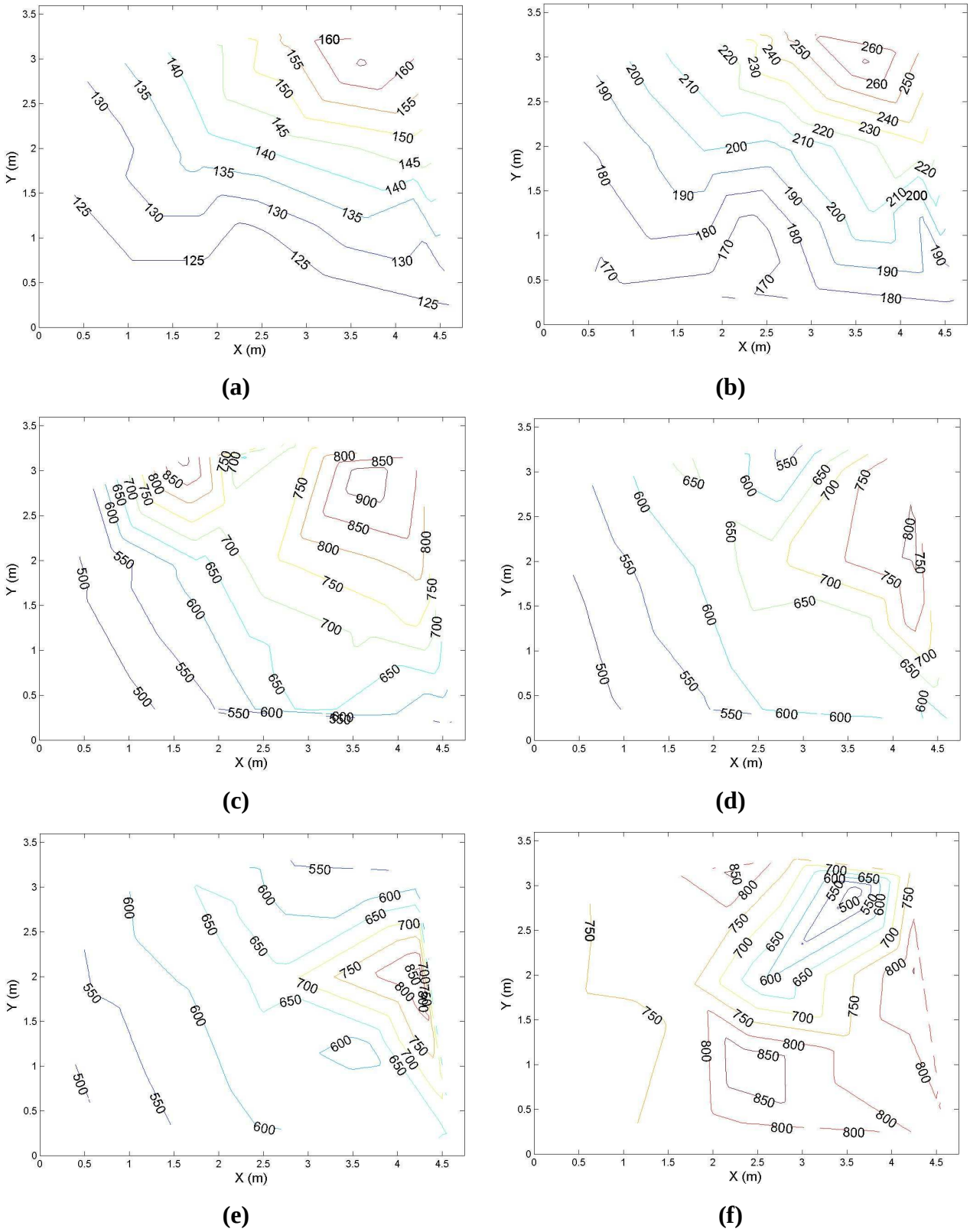

Figure D.12. The evolution of temperature contours through section HOR2 which is defined by the horizontal plane at Z = 2.35 m, at Time Steps: (a) 201 s; (b) 251 s; (c) 351 s; (d) 420 s; (e) 661 s; and, (f) 901 s from ignition of Dalmarnock Fire Test One.

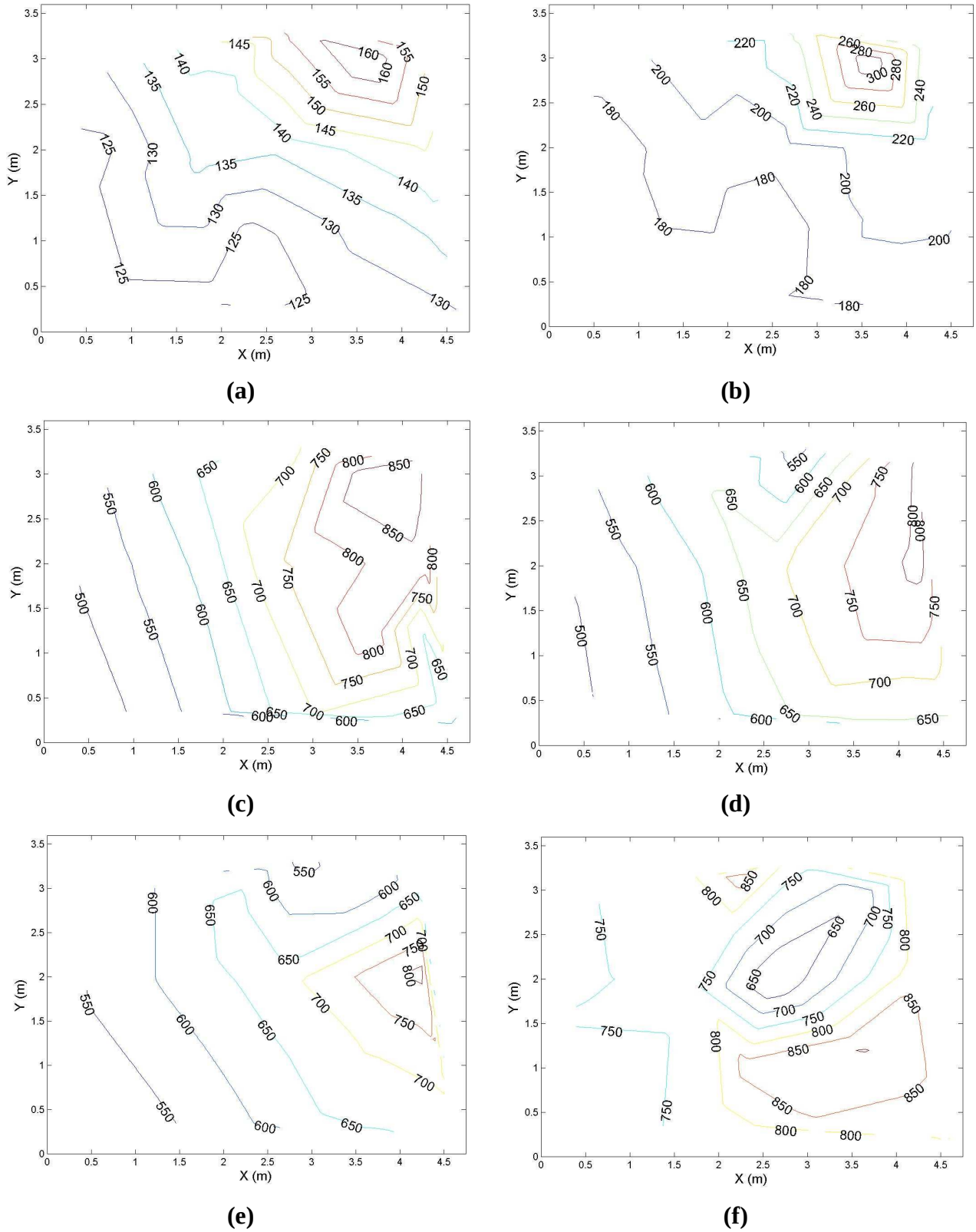

Figure D.13. The evolution of temperature contours through section HOR3 which is defined by the horizontal plane at Z = 2.25 m, at Time Steps: (a) 201 s; (b) 251 s; (c) 351 s; (d) 420 s; (e) 661 s; and, (f) 901 s from ignition of Dalmarnock Fire Test One.

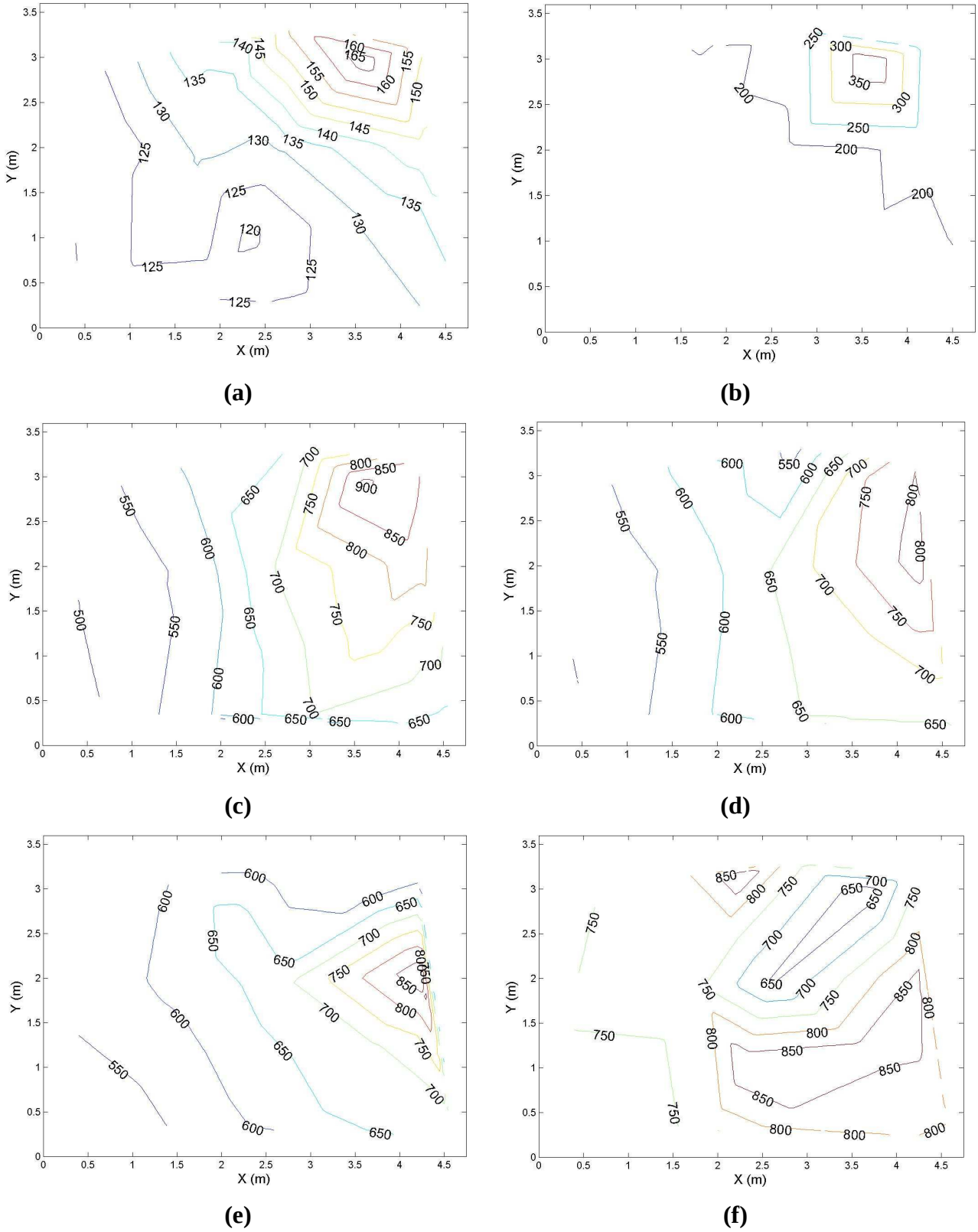

Figure D.14. The evolution of temperature contours through section HOR4 which is defined by the horizontal plane at Z = 2.15 m, at Time Steps: (a) 201 s; (b) 251 s; (c) 351 s; (d) 420 s; (e) 661 s; and, (f) 901 s from ignition of Dalmarnock Fire Test One.

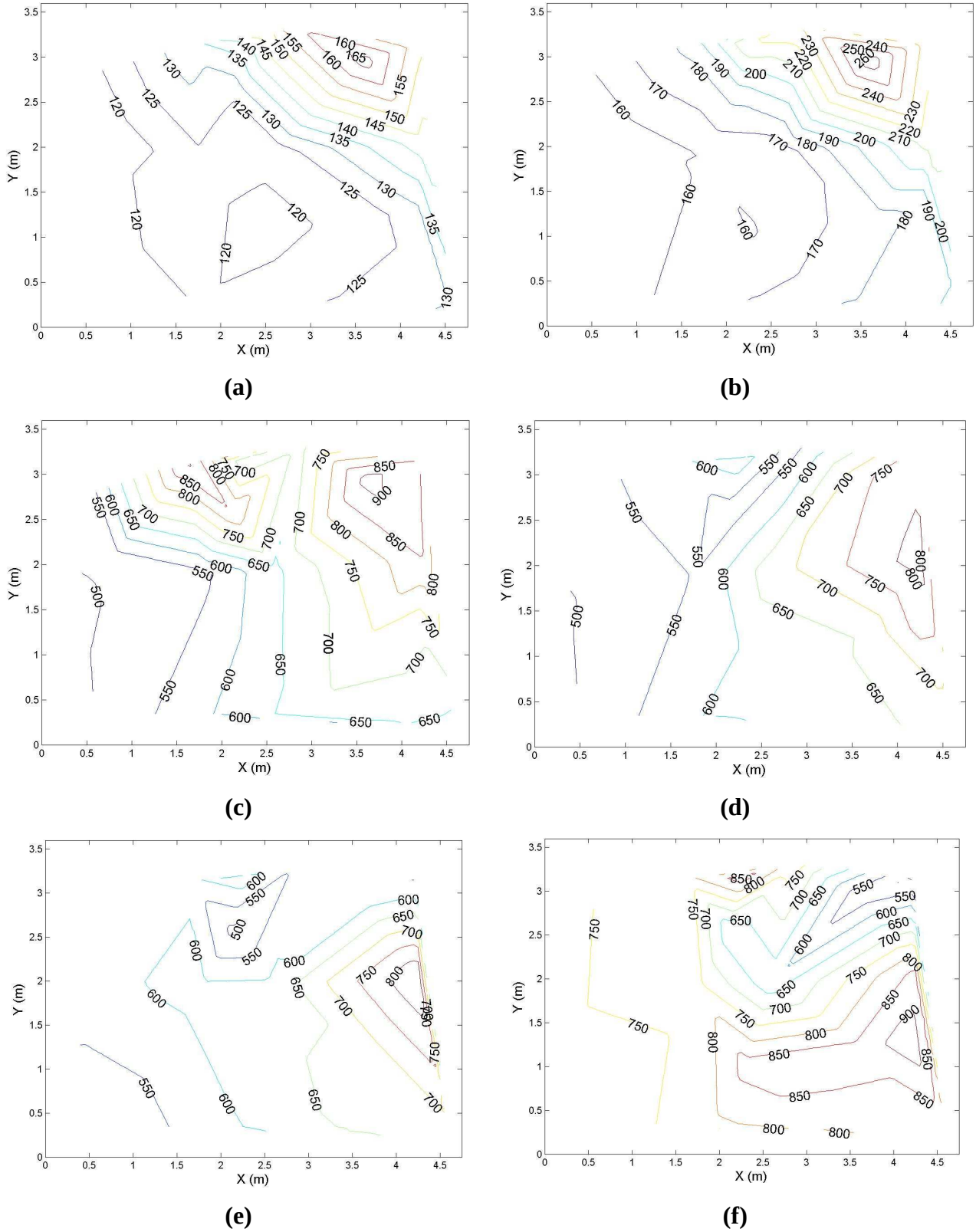

Figure D.15. The evolution of temperature contours through section HOR5 which is defined by the horizontal plane at Z = 2.05 m, at Time Steps: (a) 201 s; (b) 251 s; (c) 351 s; (d) 420 s; (e) 661 s; and, (f) 901 s from ignition of Dalmarnock Fire Test One.

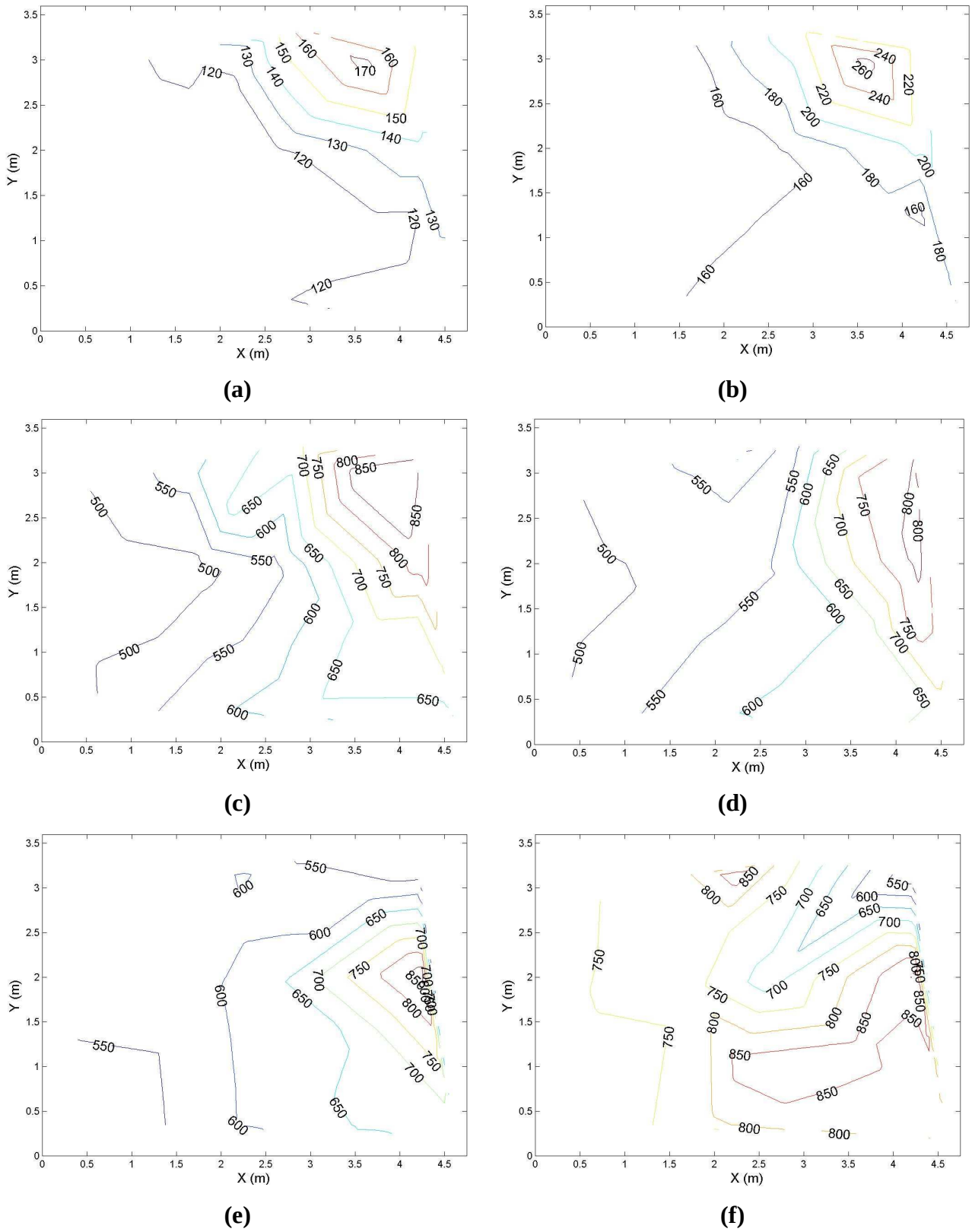

Figure D.16. The evolution of temperature contours through section HOR6 which is defined by the horizontal plane at Z = 1.85 m, at Time Steps: (a) 201 s; (b) 251 s; (c) 351 s; (d) 420 s; (e) 661 s; and, (f) 901 s from ignition of Dalmarnock Fire Test One.

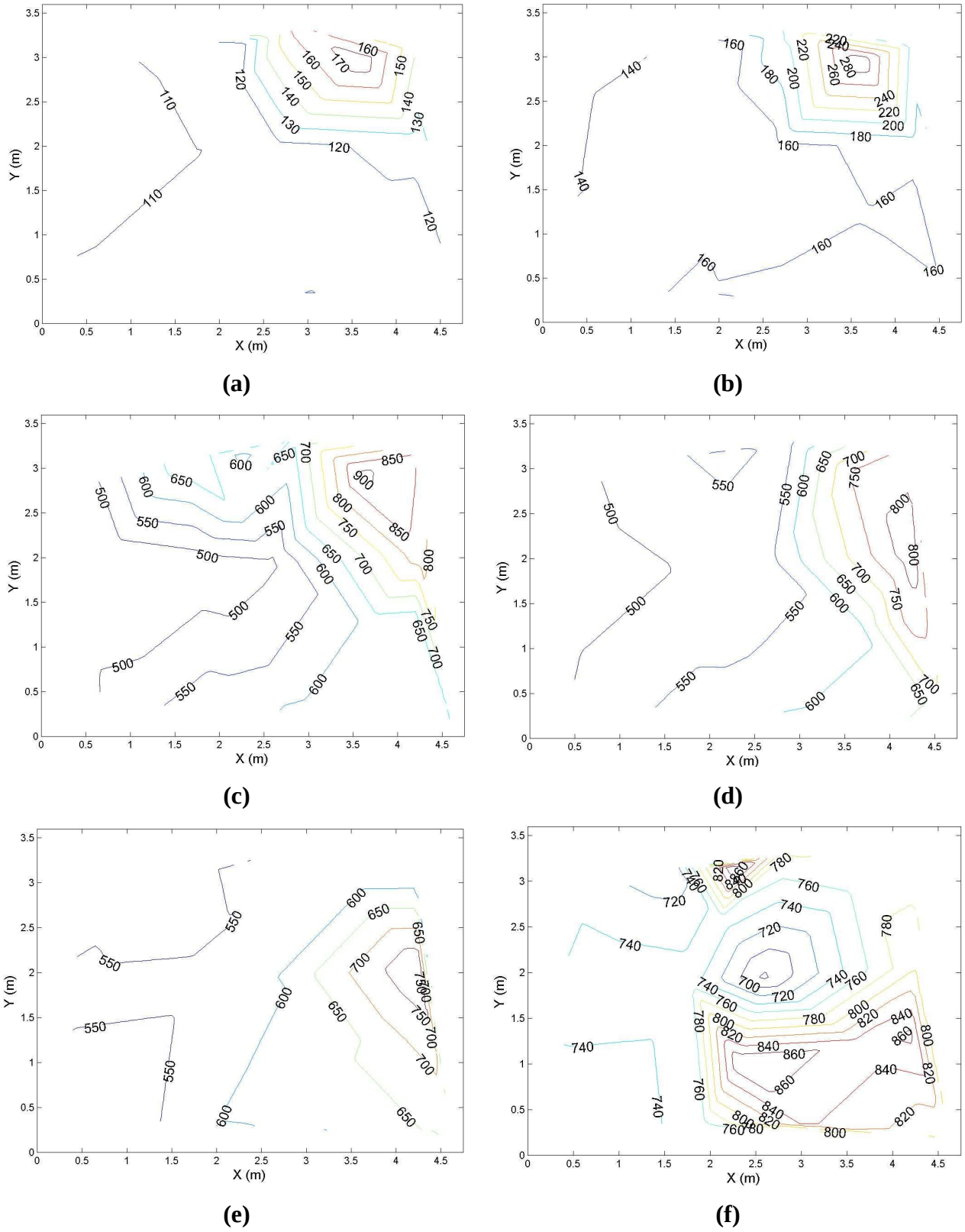

Figure D.17. The evolution of temperature contours through section HOR7 which is defined by the horizontal plane at Z = 1.65 m, at Time Steps: (a) 201 s; (b) 251 s; (c) 351 s; (d) 420 s; (e) 661 s; and, (f) 901 s from ignition of Dalmarnock Fire Test One.

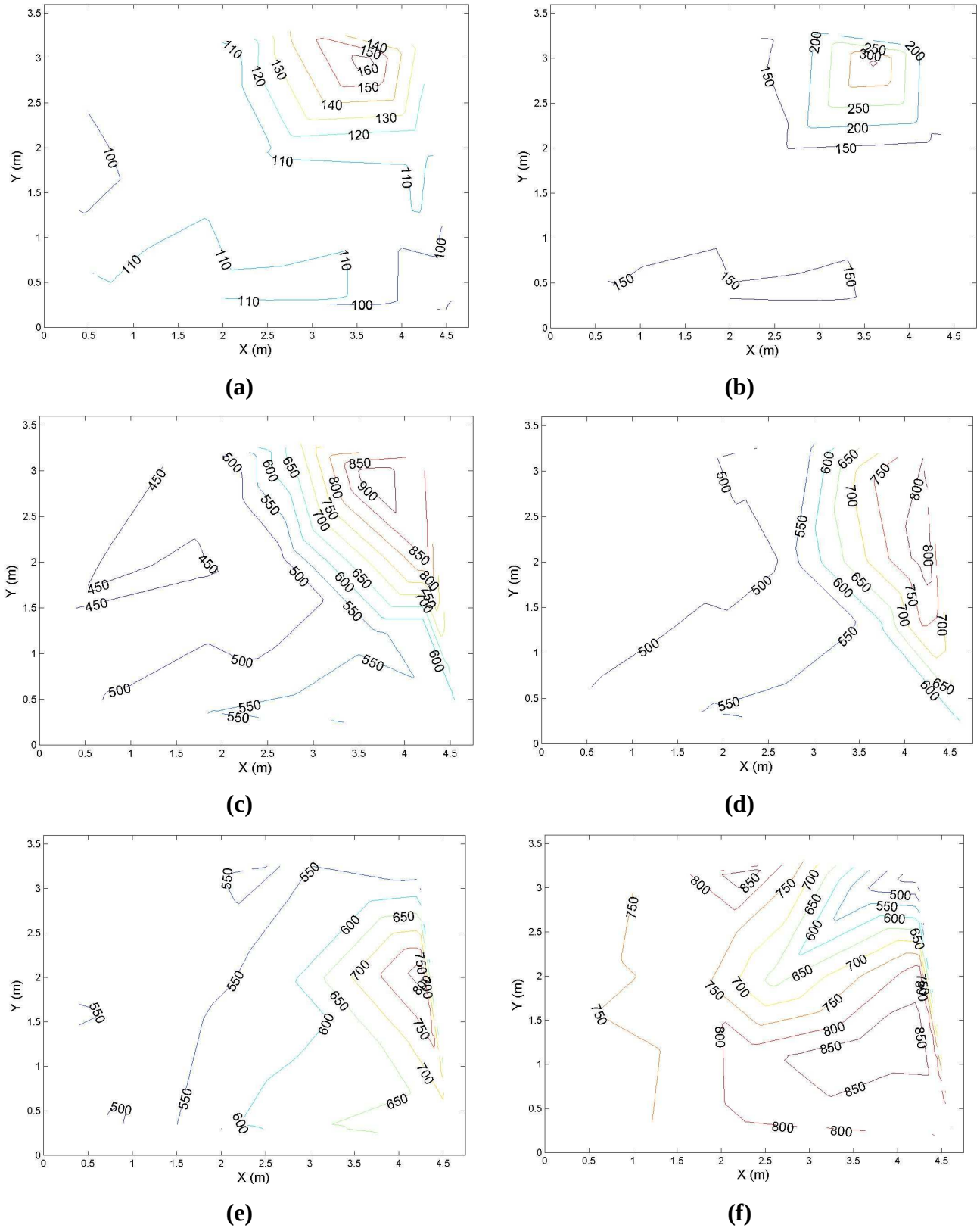

Figure D.18. The evolution of temperature contours through section HOR8 which is defined by the horizontal plane at Z = 1.45 m, at Time Steps: (a) 201 s; (b) 251 s; (c) 351 s; (d) 420 s; (e) 661 s; and, (f) 901 s from ignition of Dalmarnock Fire Test One.

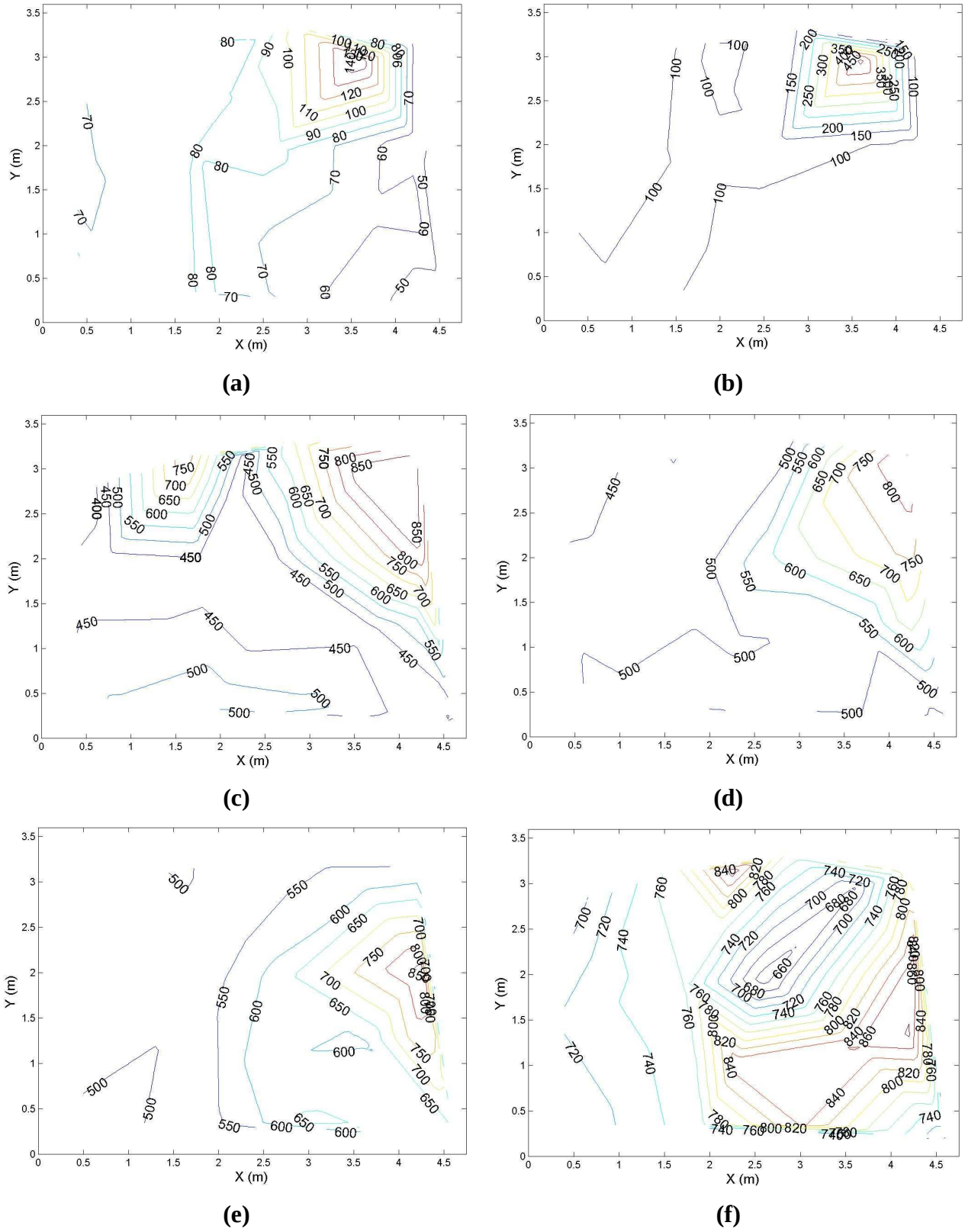

Figure D.19. The evolution of temperature contours through section HOR9 which is defined by the horizontal plane at Z = 1.15 m, at Time Steps: (a) 201 s; (b) 251 s; (c) 351 s; (d) 420 s; (e) 661 s; and, (f) 901 s from ignition of Dalmarnock Fire Test One.

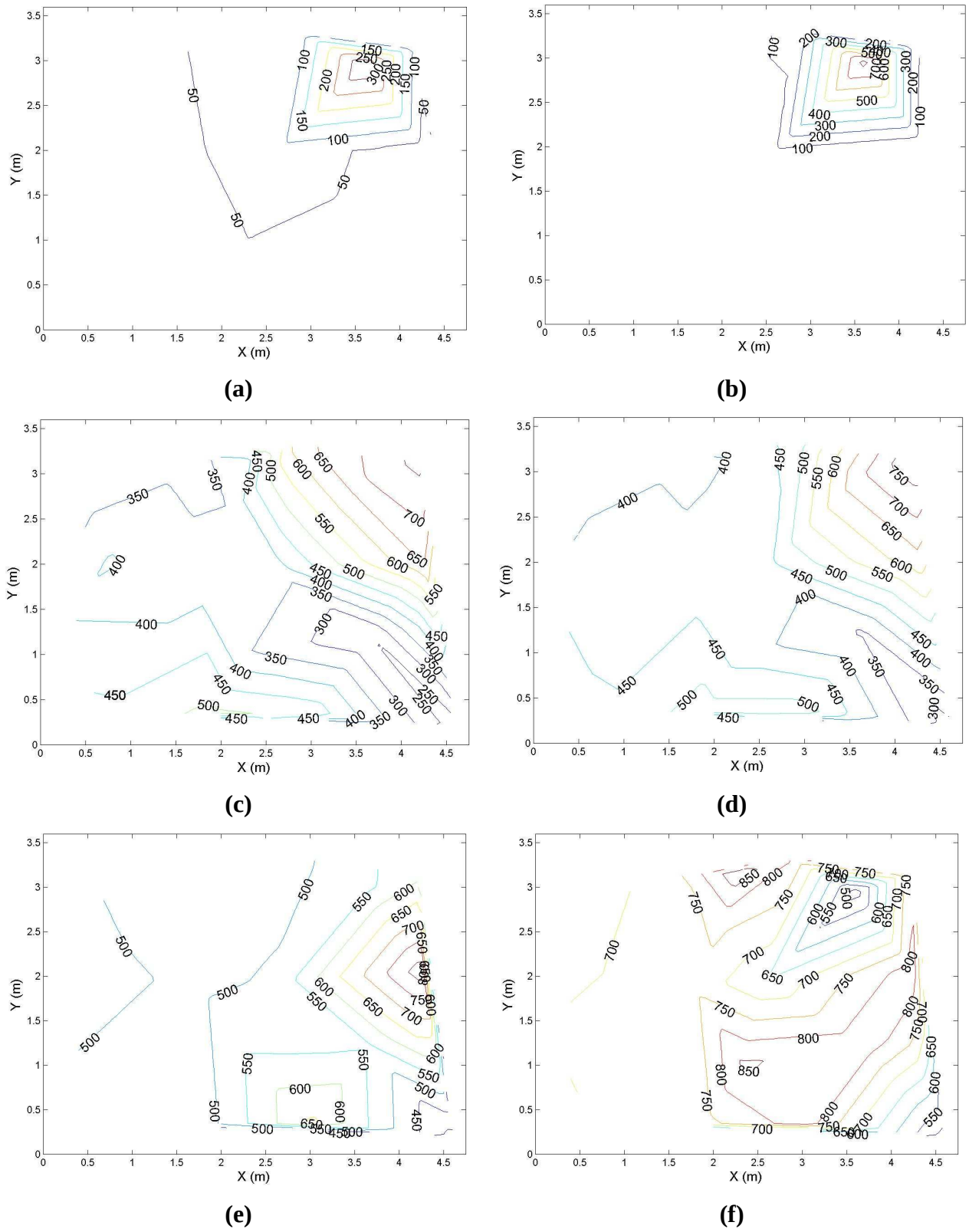

Figure D.20. The evolution of temperature contours through section HOR10 which is defined by the horizontal plane at Z = 0.85 m, at Time Steps: (a) 201 s; (b) 251 s; (c) 351 s; (d) 420 s; (e) 661 s; and, (f) 901 s from ignition of Dalmarnock Fire Test One.

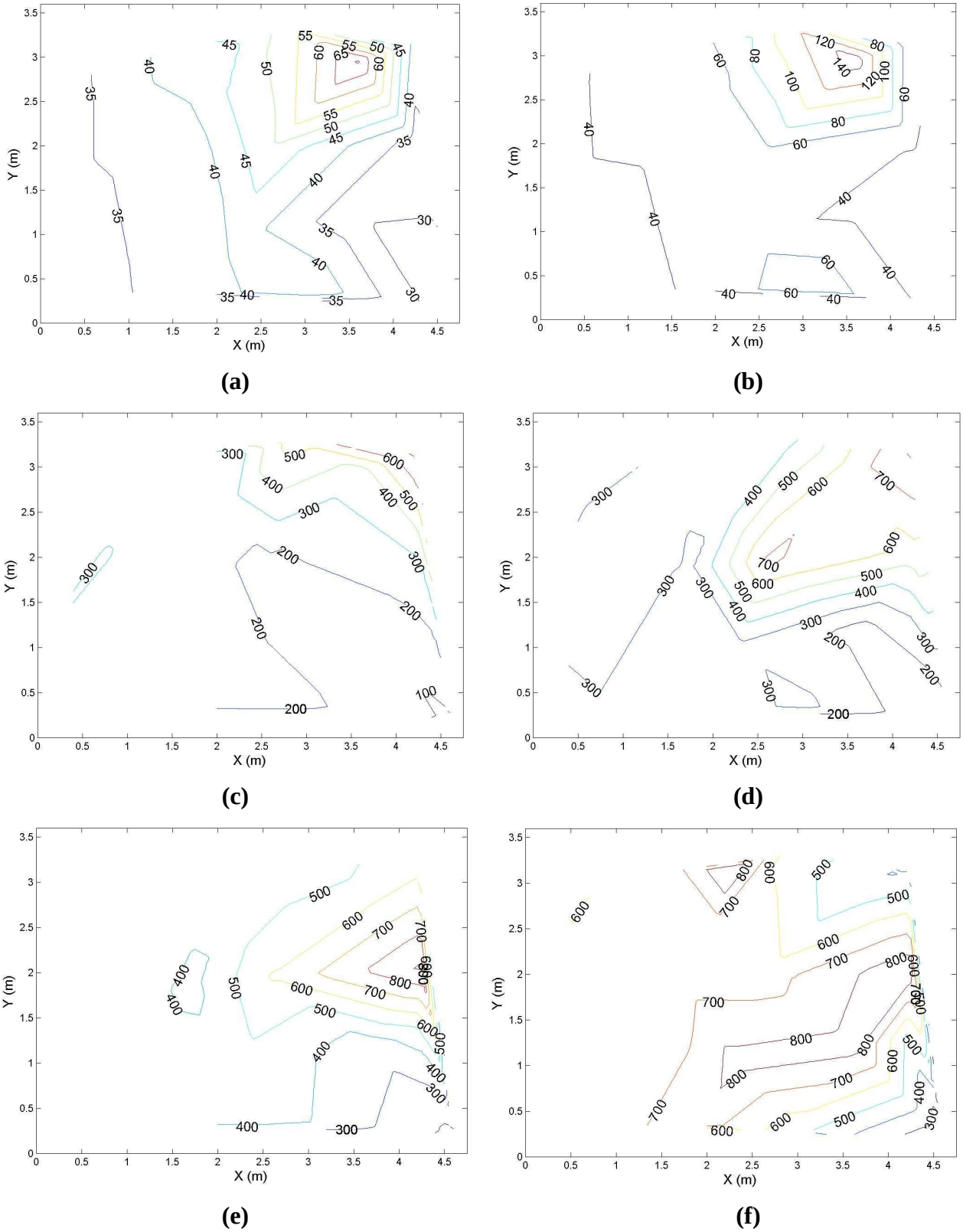

Figure D.21. The evolution of temperature contours through section HOR11 which is defined by the horizontal plane at Z = 0.45 m, at Time Steps: (a) 201 s; (b) 251 s; (c) 351 s; (d) 420 s; (e) 661 s; and, (f) 901 s from ignition of Dalmarnock Fire Test One.

External Temperature Contours

The external thermocouple trees were all aligned, hence the external temperature contours are shown in sections running parallel (PARA) and perpendicular (PERP) to the façade as well as horizontally (HOR) at each thermocouple height. The location of the parallel and perpendicular sections is illustrated in Figure D.22. The external temperature evolution at each of the section locations is shown in a series of four Time Steps after ignition, namely: at 900 s when the NW window pane had already broken out; at 1095 s when there was sustained external flaming; at 1115 s when the SW window pane had also broken out; and, at 1135 s during the period of maximum sustained external flaming. Figures D.23 – D.27 show the PARA series, Figures D.28 – D.30 show the PERP series, and Figures D.31 – D.28 show the HOR series which is numbered, in order, from the lowermost thermocouple level (below compartment window soffit) upwards. The data are presented relative to the Global Coordinate System the origin of which is located at floor level in the SW corner as shown in Figure D.22.

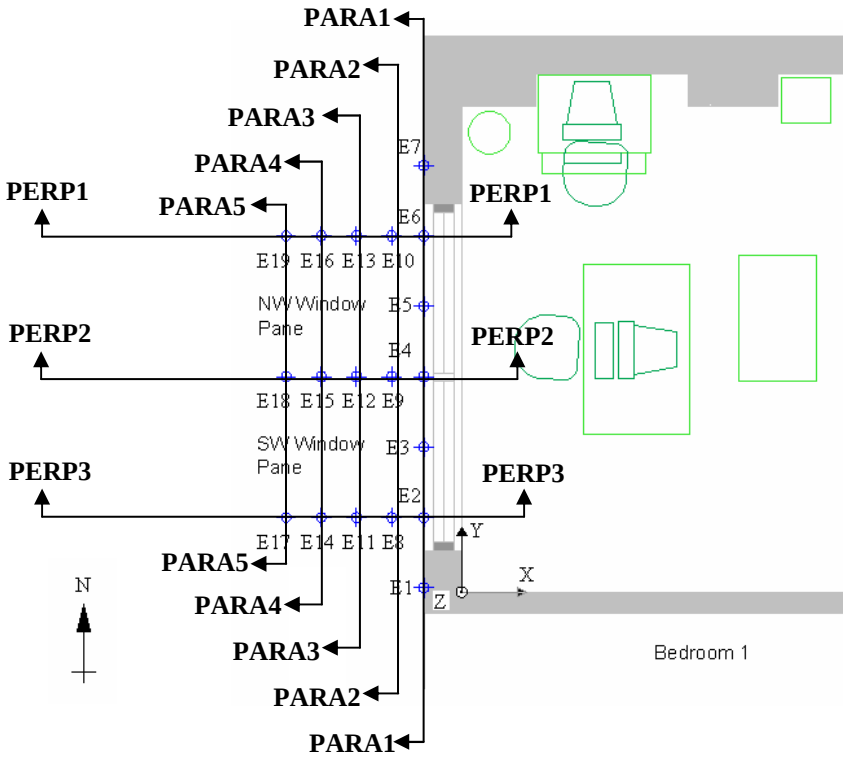

Figure D.22. Plan view of the western half of the Dalmarnock Fire Test One compartment showing some of the furniture (fire load; *cf.* Chapter 4, Figure 4.3 for the furniture item key) relative to the window. External thermocouple trees are shown beyond the compartment window and labelled correspondingly, as are the parallel (PARA) and perpendicular (PERP) sections taken through the plume. The global coordinate system origin is shown in the SW corner, at floor level.

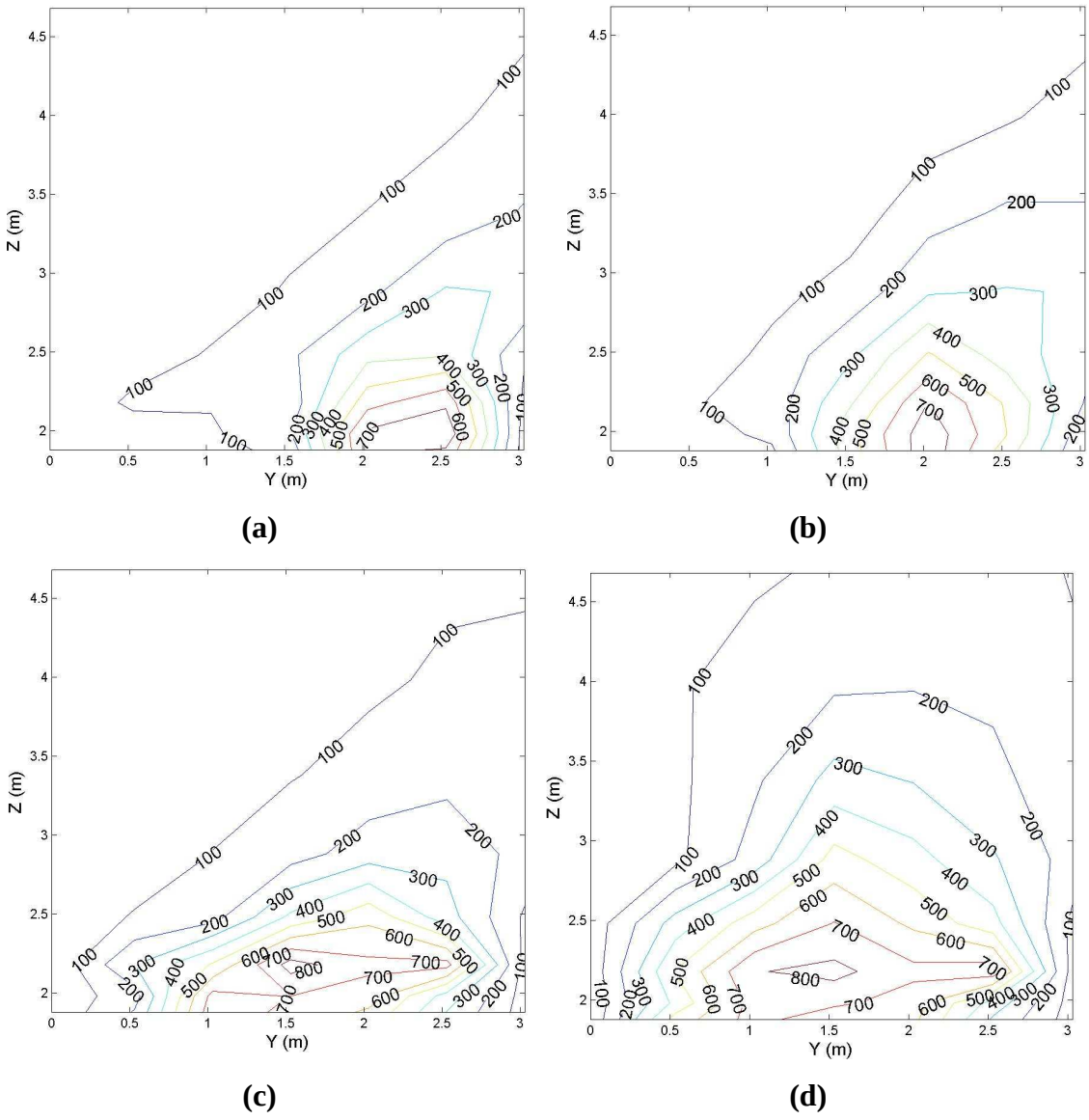

Figure D.23. The evolution of temperature contours through external section PARA1 which is defined by the horizontal plane at X = -0.27 m, at Time Steps: (a) 900 s; (b) 1095 s; (c) 1115 s; and, (d) 1135 s from the ignition of Dalmarnock Fire Test One.

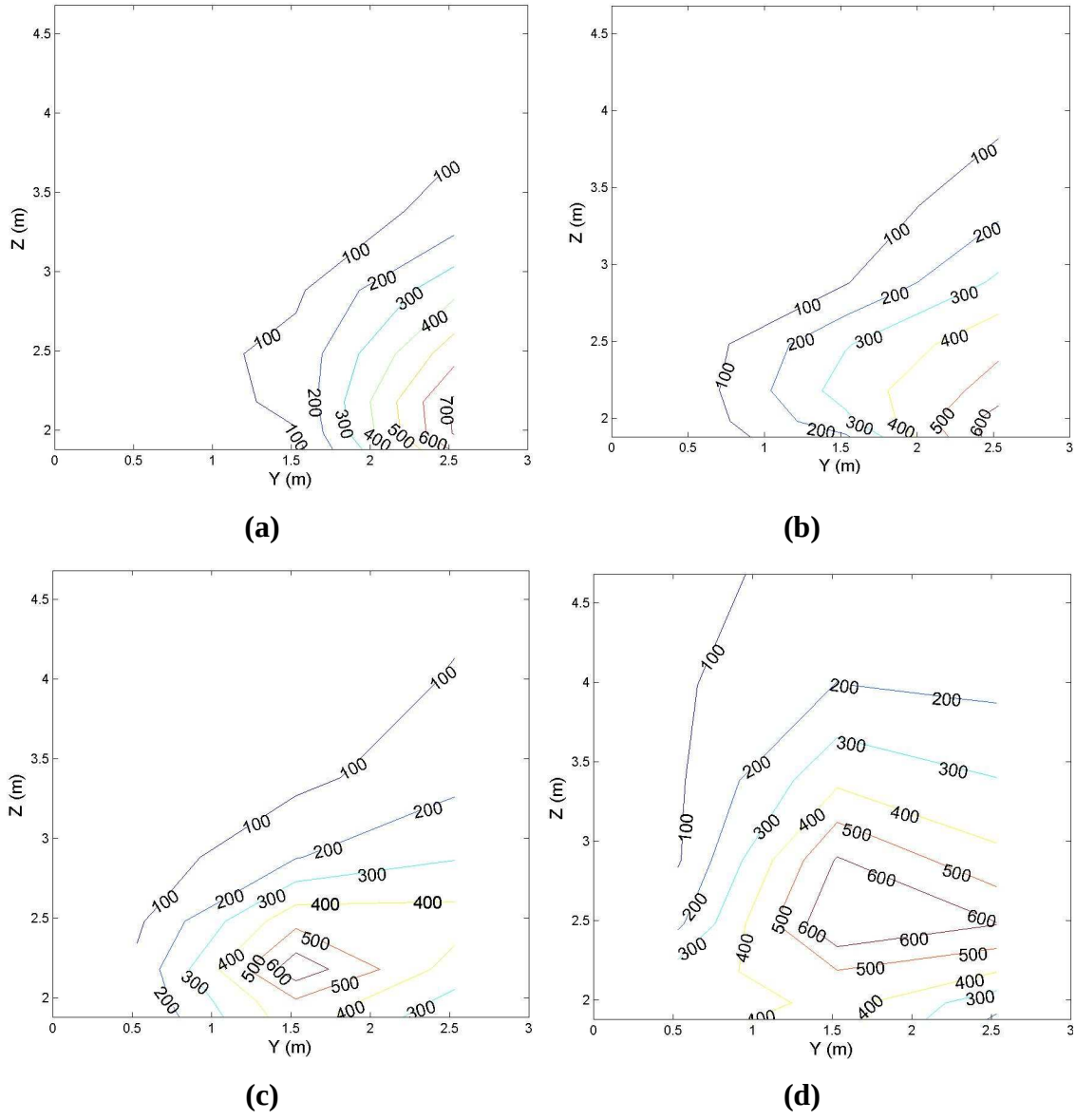

Figure D.24. The evolution of temperature contours through external section PARA2 which is defined by the horizontal plane at X = -0.50 m, at Time Steps: (a) 900 s; (b) 1095 s; (c) 1115 s; and, (d) 1135 s from the ignition of Dalmarnock Fire Test One.

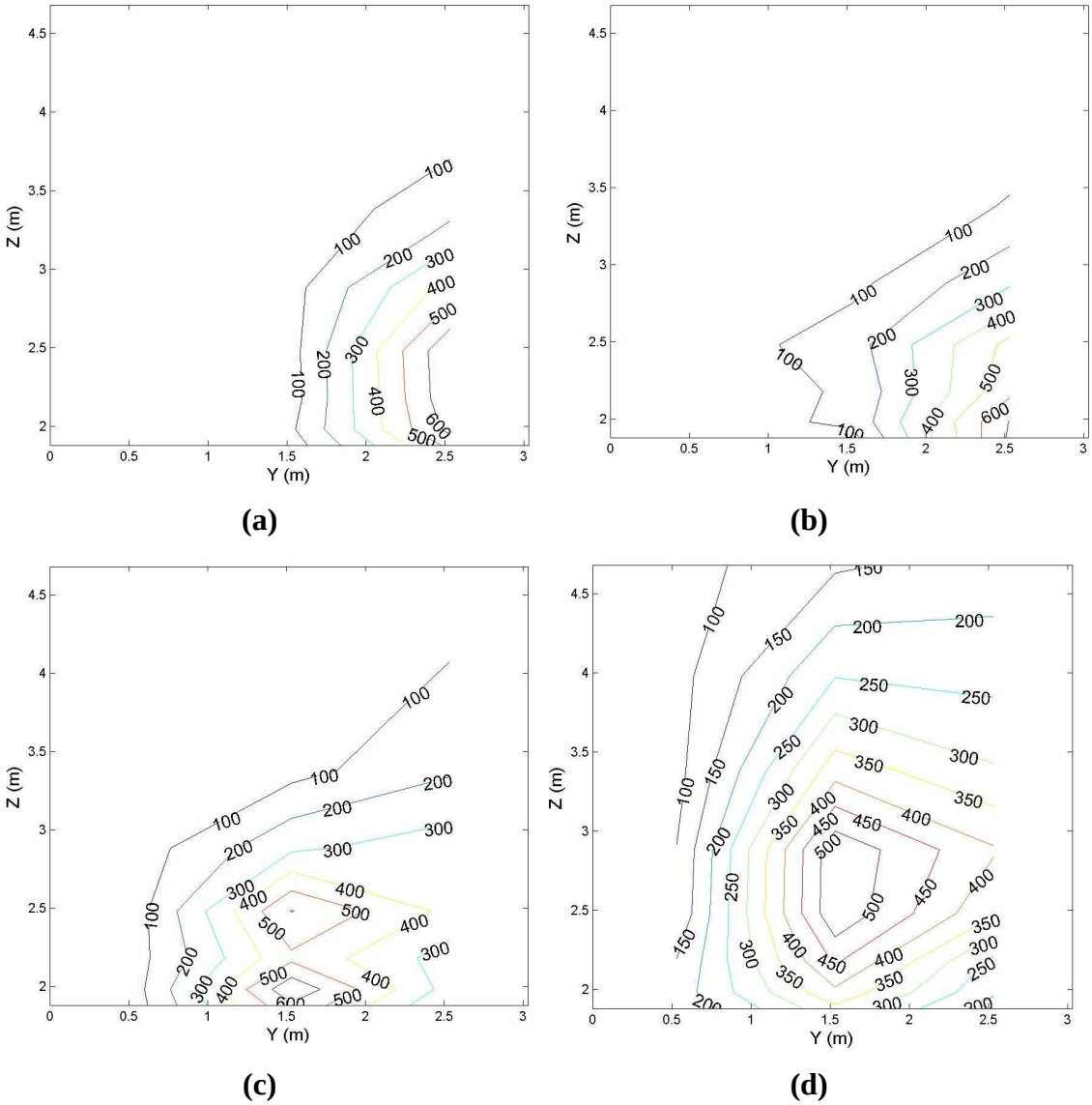

Figure D.25. The evolution of temperature contours through external section PARA3 which is defined by the horizontal plane at X = -0.75 m, at Time Steps: (a) 900 s; (b) 1095 s; (c) 1115 s; and, (d) 1135 s from the ignition of Dalmarnock Fire Test One.

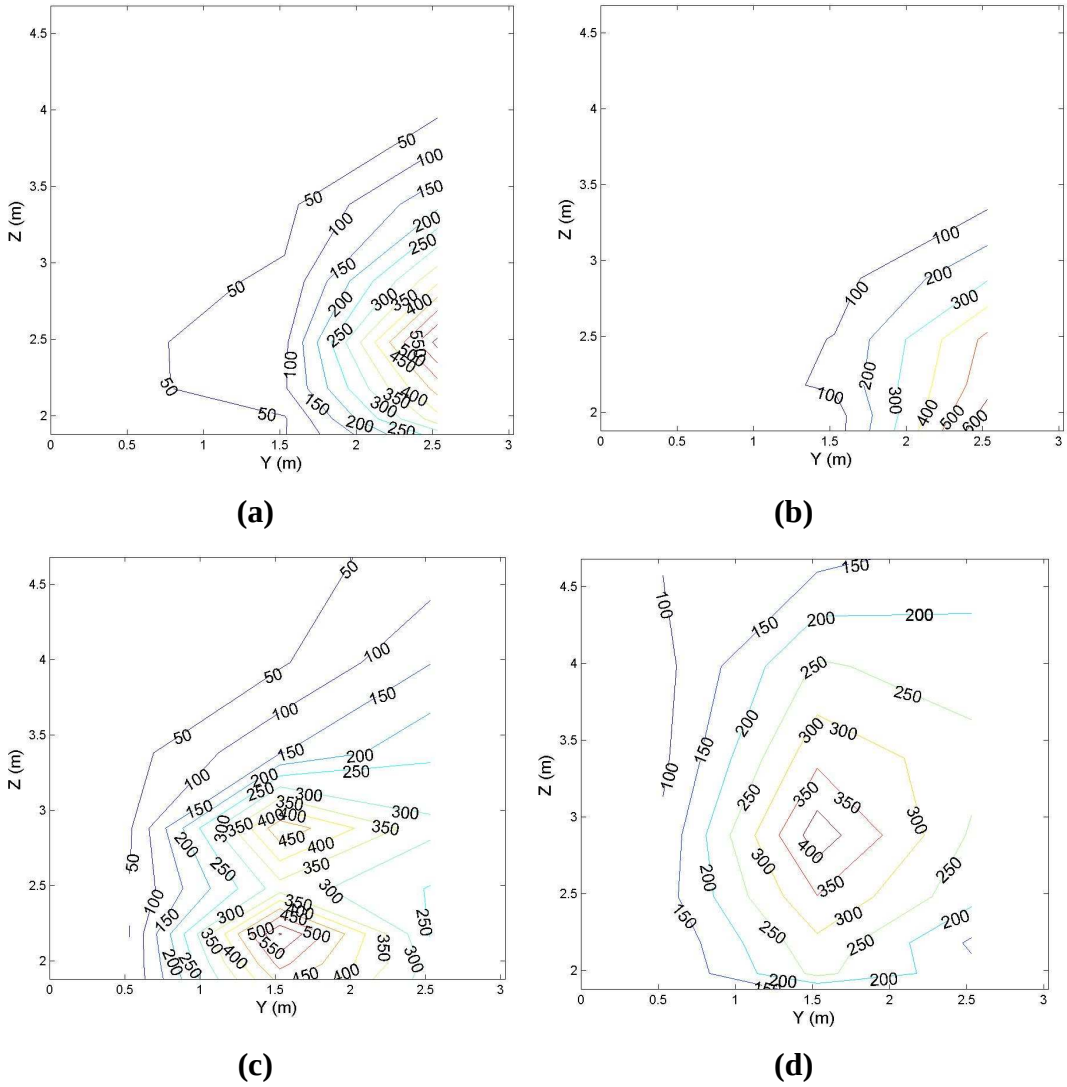

Figure D.26. The evolution of temperature contours through external section PARA4 which is defined by the horizontal plane at X = -1.00 m, at Time Steps: (a) 900 s; (b) 1095 s; (c) 1115 s; and, (d) 1135 s from the ignition of Dalmarnock Fire Test One.

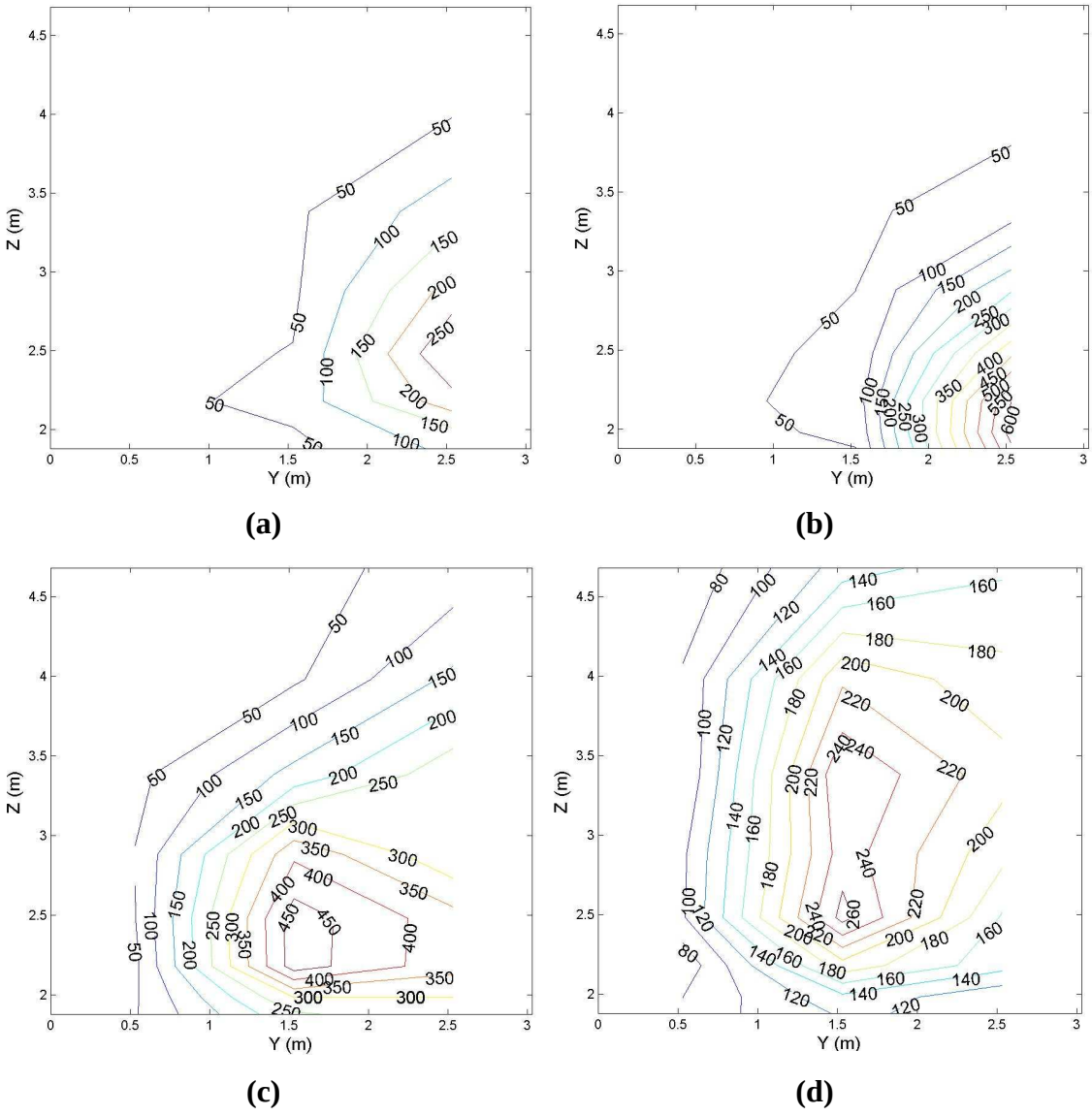

Figure D.27. The evolution of temperature contours through external section PARA5 which is defined by the horizontal plane at X = -1.25 m, at Time Steps: (a) 900 s; (b) 1095 s; (c) 1115 s; and, (d) 1135 s from the ignition of Dalmarnock Fire Test One.

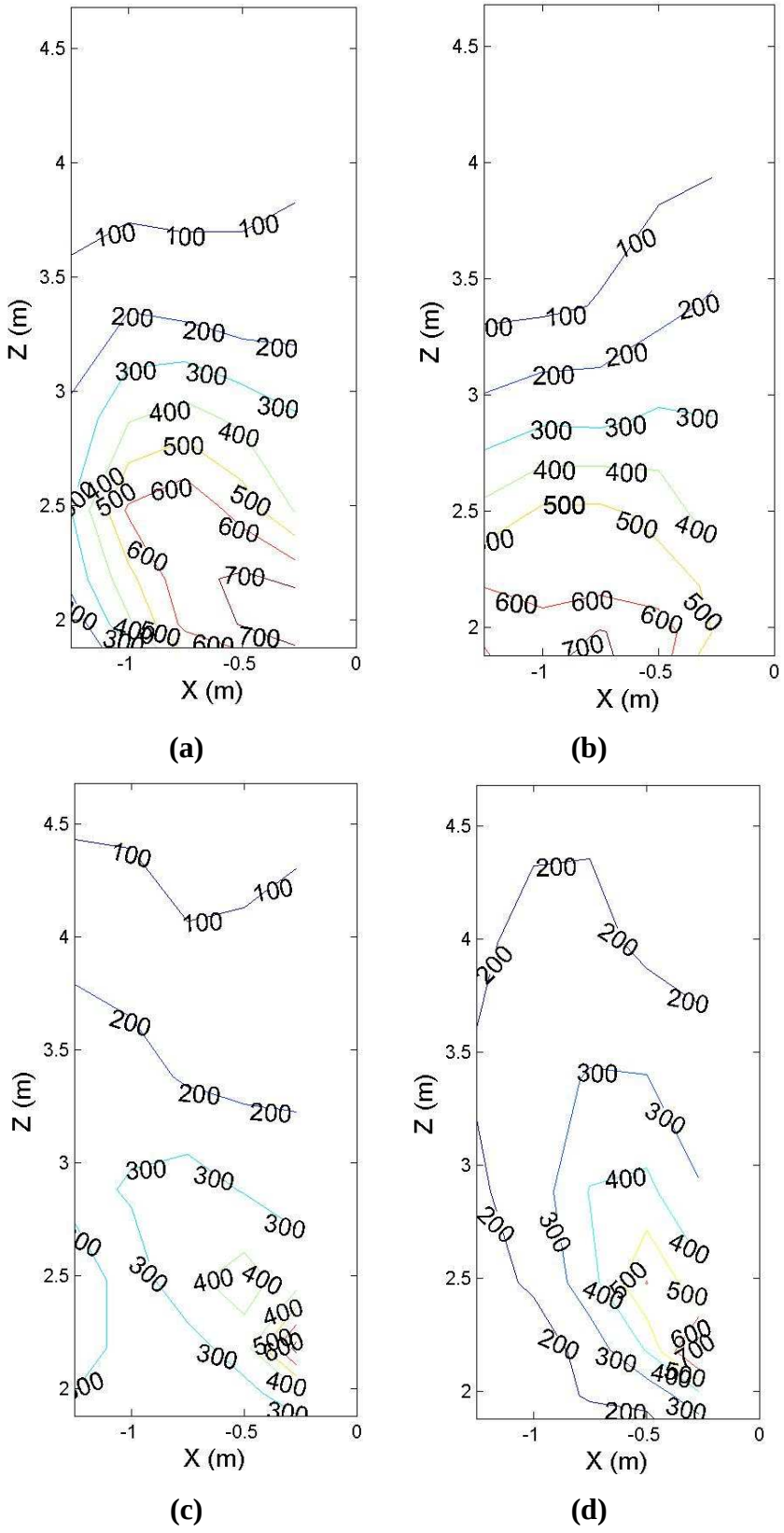

Figure D.28. The evolution of temperature contours through external section PERP1 which is defined by the horizontal plane at Y = 0.53 m, at Time Steps: (a) 900 s; (b) 1095 s; (c) 1115 s; and, (d) 1135 s from the ignition of Dalmarnock Fire Test One.

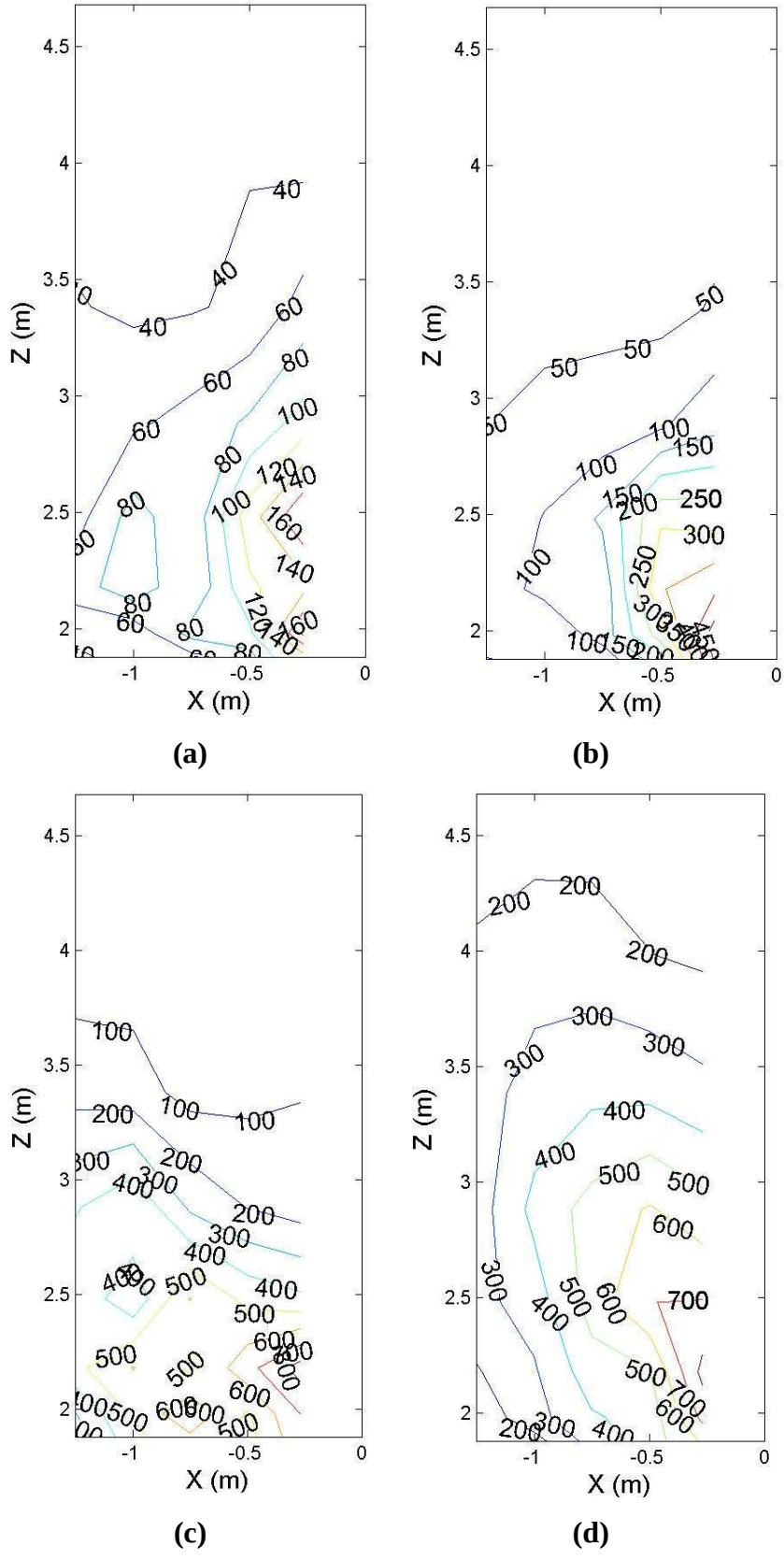

Figure D.29. The evolution of temperature contours through external section PERP2 which is defined by the horizontal plane at Y = 1.53 m, at Time Steps: (a) 900 s; (b) 1095 s; (c) 1115 s; and, (d) 1135 s from the ignition of Dalmarnock Fire Test One.

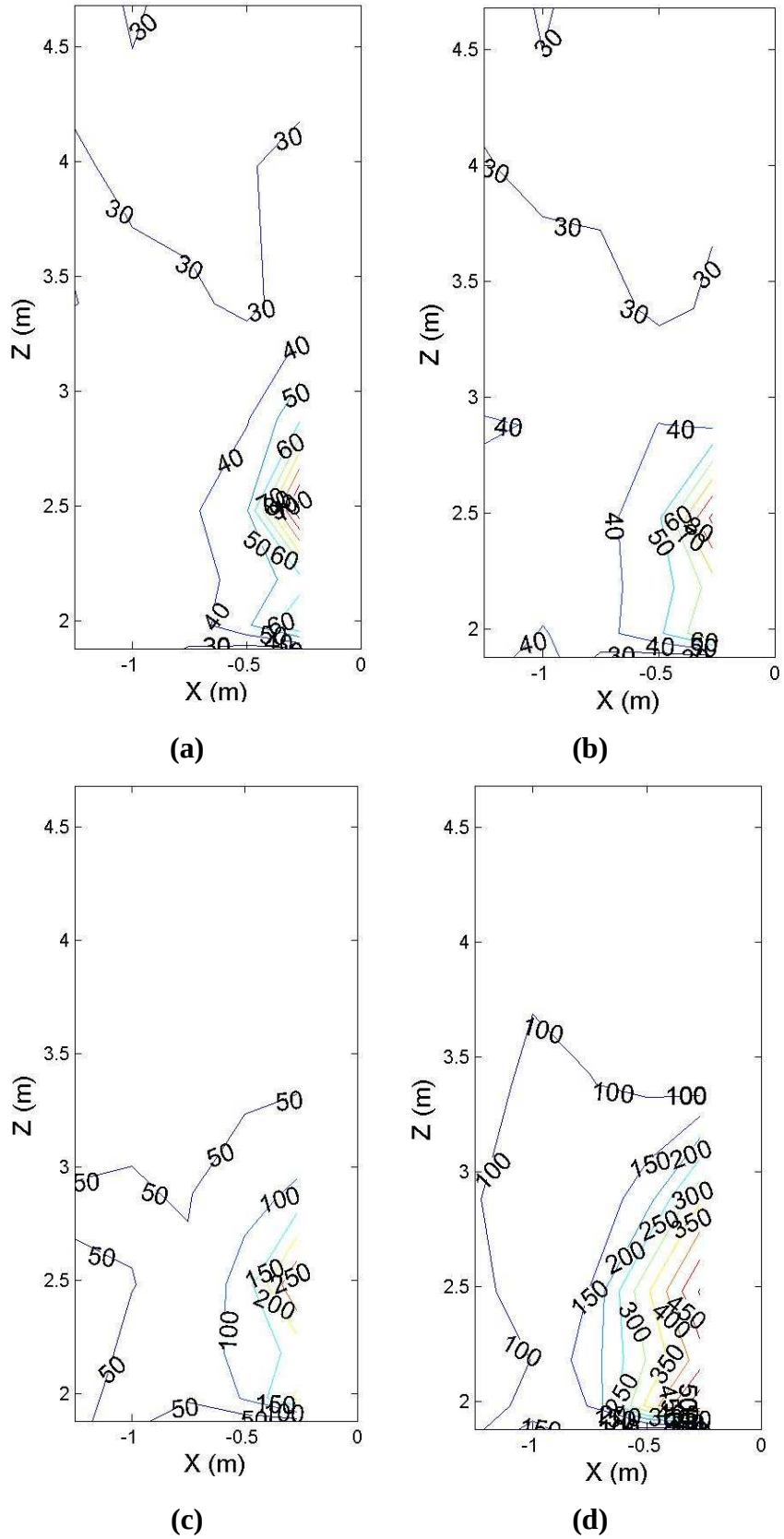

Figure D.30. The evolution of temperature contours through external section PERP3 which is defined by the horizontal plane at Y = 2.53 m, at Time Steps: (a) 900 s; (b) 1095 s; (c) 1115 s; and, (d) 1135 s from the ignition of Dalmarnock Fire Test One.

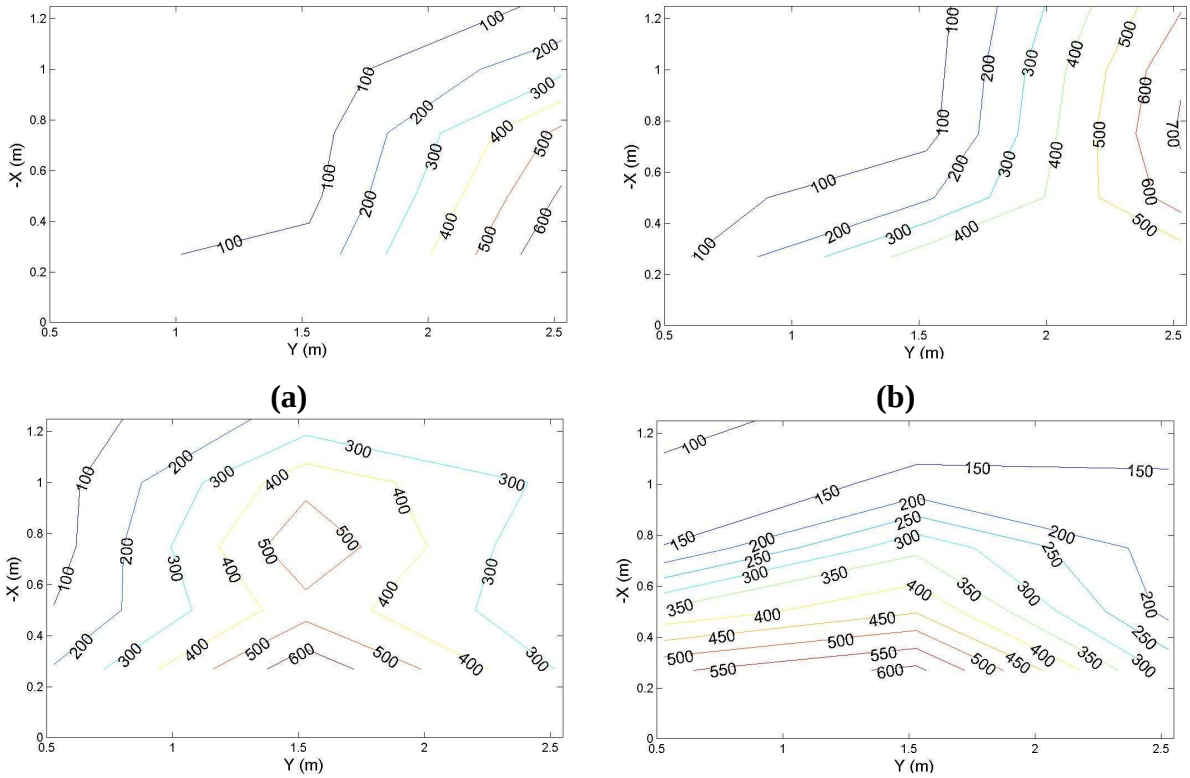

Figure D.31. The evolution of temperature contours through external section HOR1 which is defined by the horizontal plane at Z = 1.88 m, at Time Steps: (a) 900 s; (b) 1095 s; (c) 1115 s; and, (d) 1135 s.

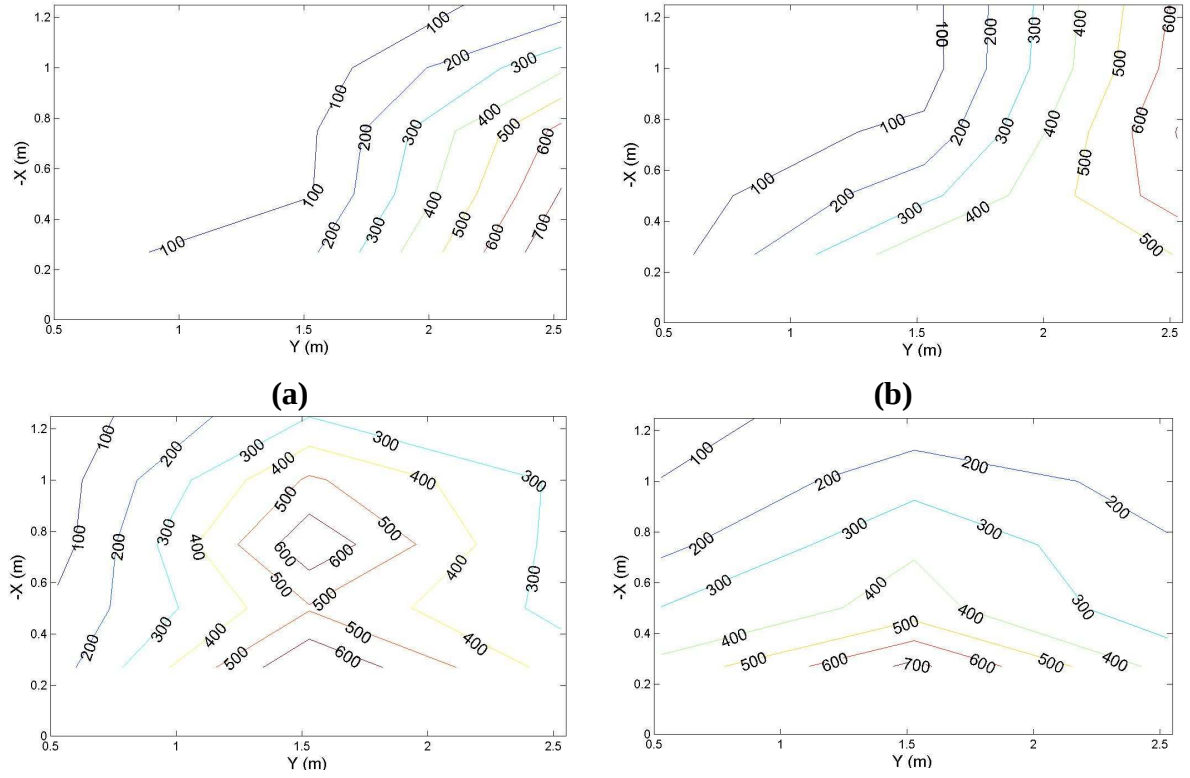

Figure D.32. The evolution of temperature contours through external section HOR2 which is defined by the horizontal plane at Z = 1.98 m, at Time Steps: (a) 900 s; (b) 1095 s; (c) 1115 s; and, (d) 1135 s.

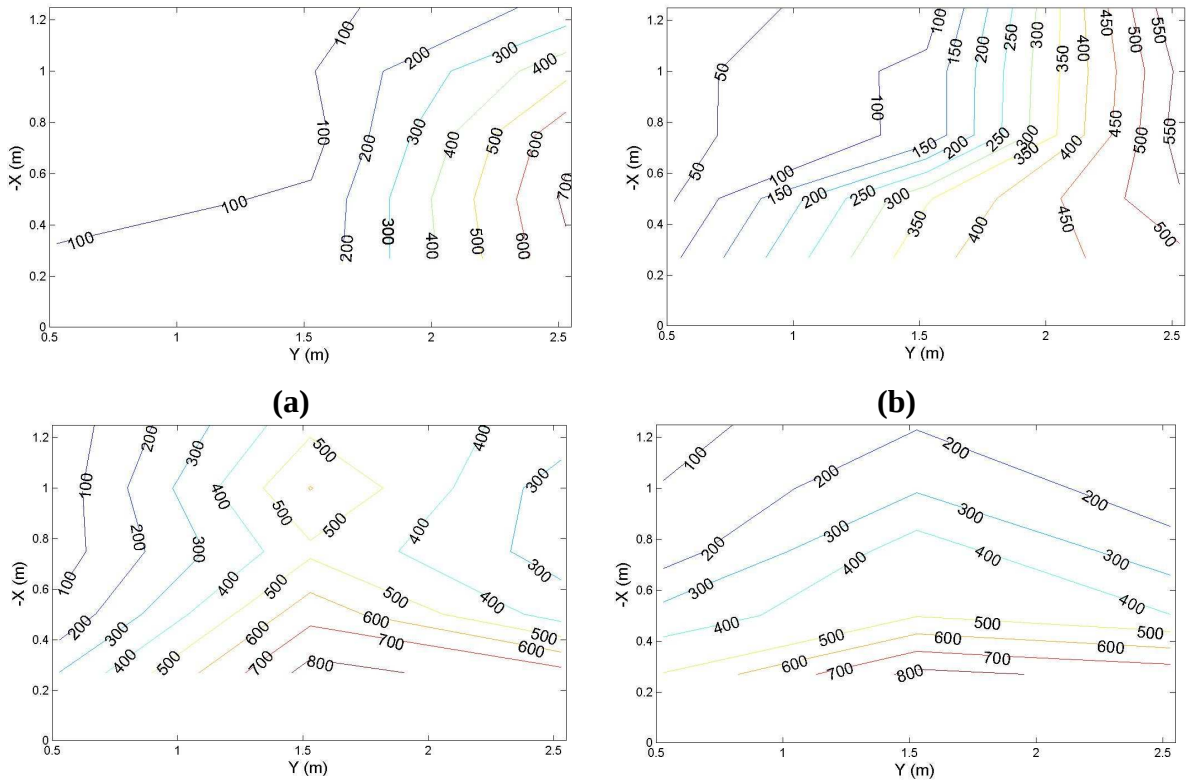

Figure D.33. The evolution of temperature contours through external section HOR3 which is defined by the horizontal plane at Z = 2.18 m, at Time Steps: (a) 900 s; (b) 1095 s; (c) 1115 s; and, (d) 1135 s.

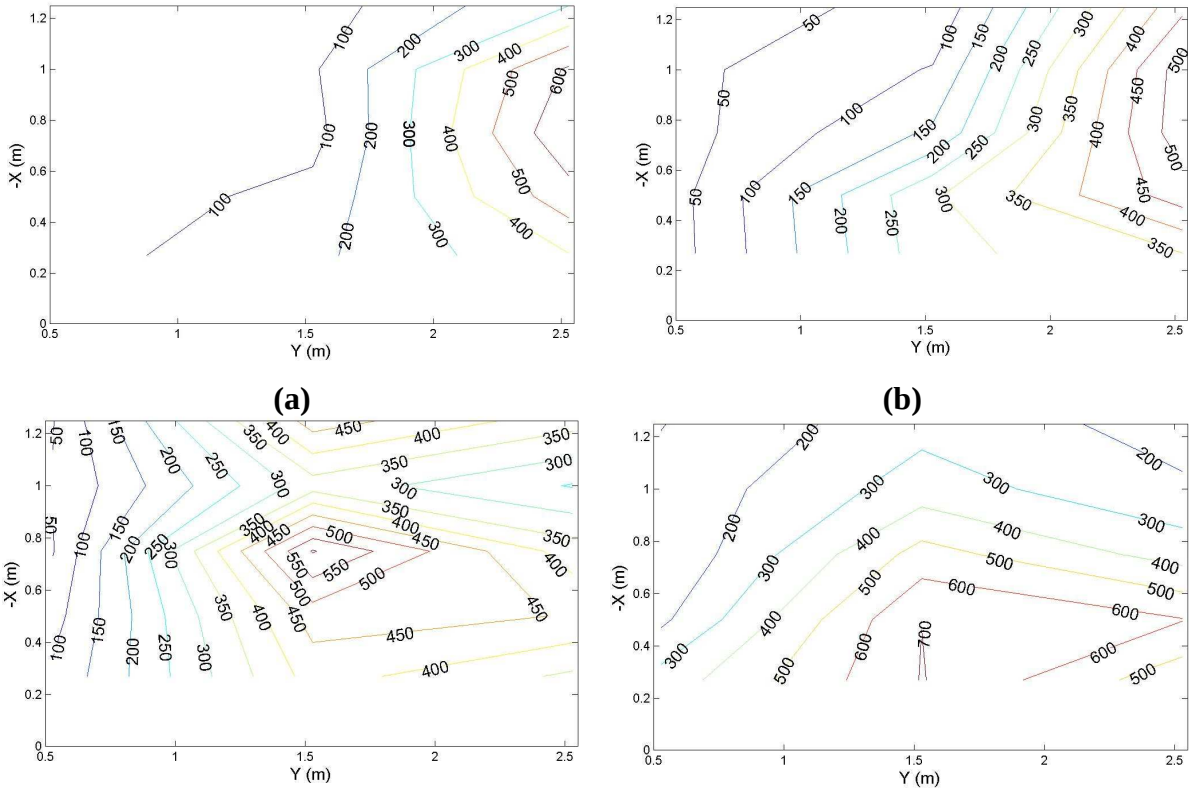

Figure D.34. The evolution of temperature contours through external section HOR4 which is defined by the horizontal plane at Z = 2.48 m, at Time Steps: (a) 900 s; (b) 1095 s; (c) 1115 s; and, (d) 1135 s.

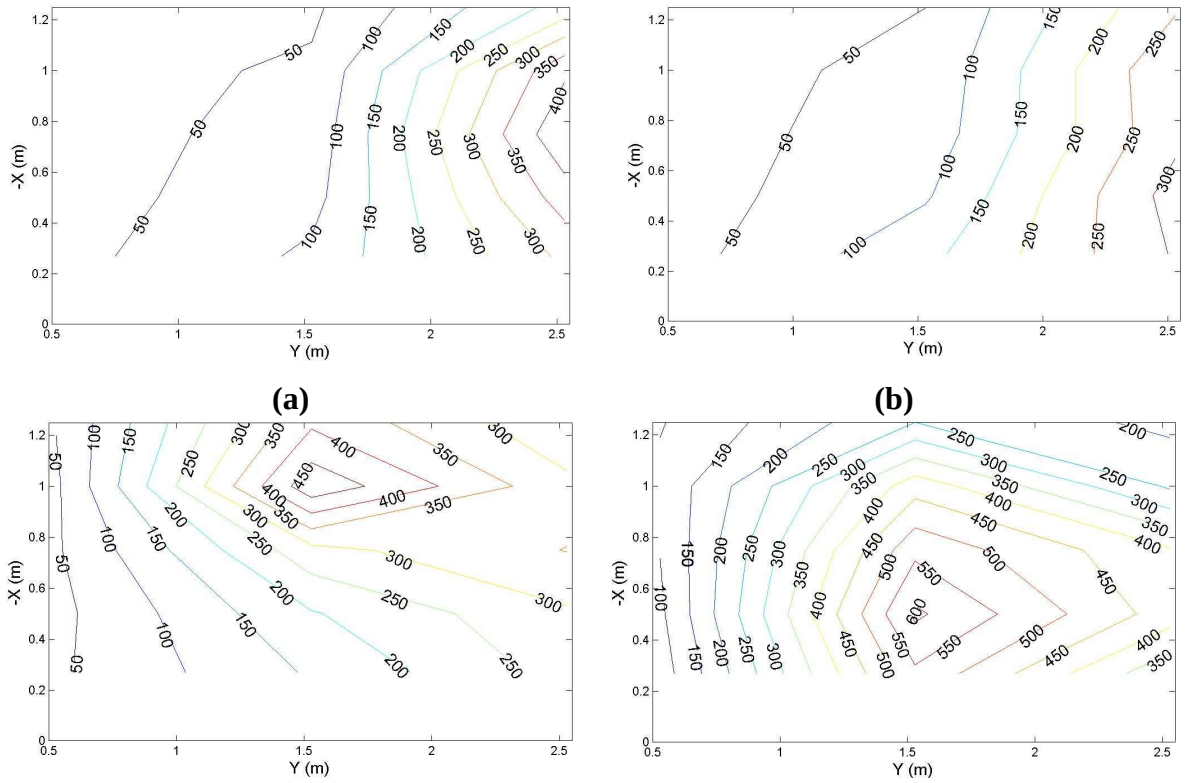

Figure D.35. The evolution of temperature contours through external section HOR5 which is defined by the horizontal plane at Z = 2.88 m, at Time Steps: (a) 900 s; (b) 1095 s; (c) 1115 s; and, (d) 1135 s.

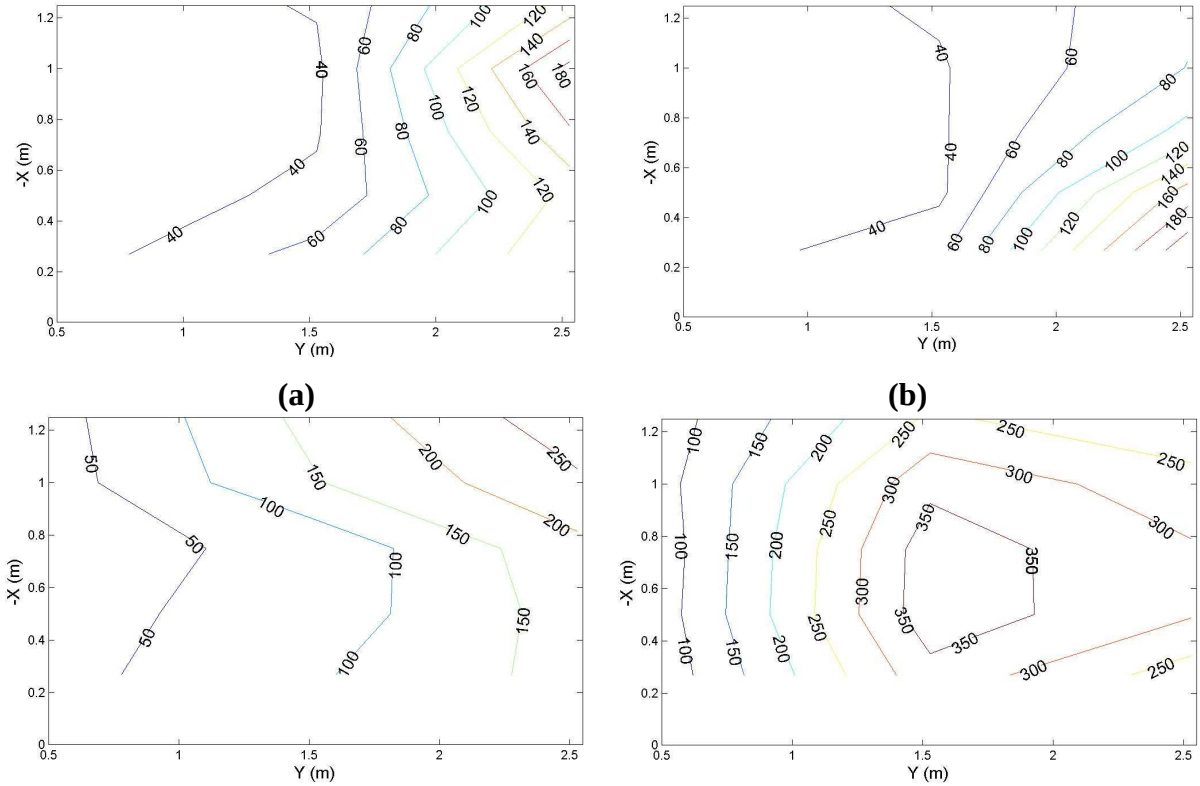

Figure D.36. The evolution of temperature contours through external section HOR6 which is defined by the horizontal plane at Z = 3.38 m, at Time Steps: (a) 900 s; (b) 1095 s; (c) 1115 s; and, (d) 1135 s.

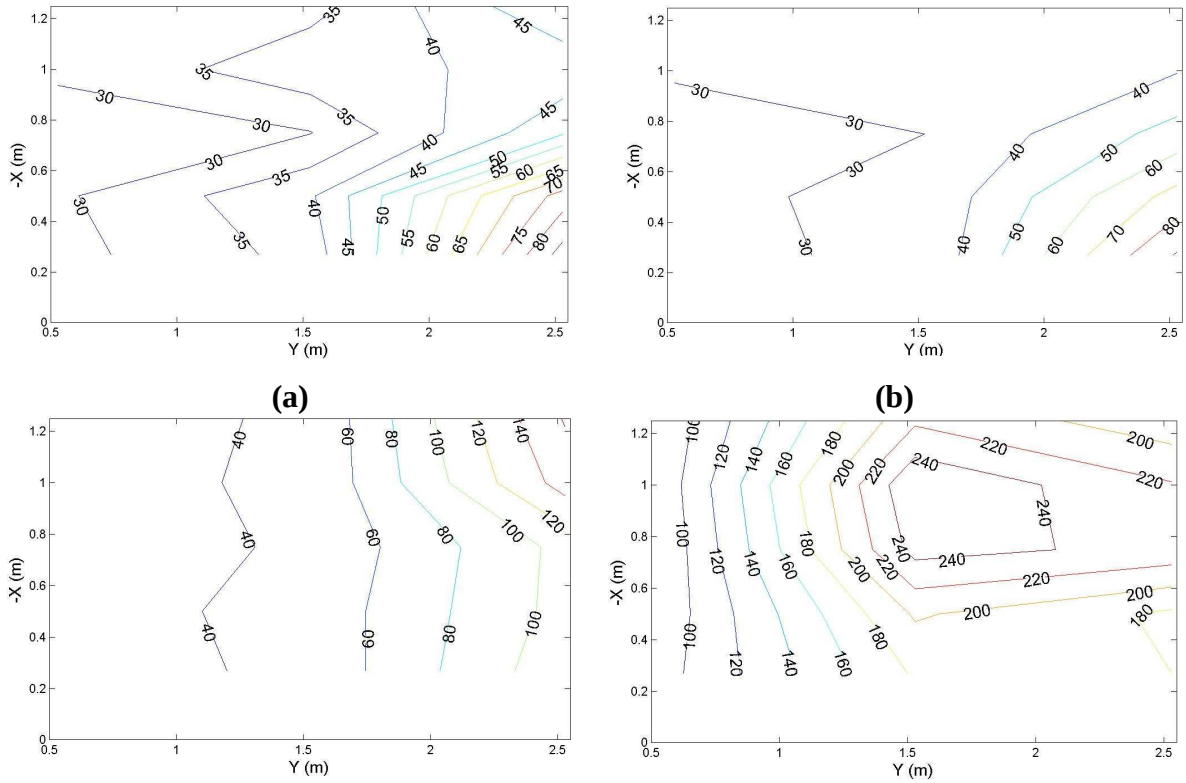

Figure D.37. The evolution of temperature contours through external section HOR7 which is defined by the horizontal plane at Z = 3.98 m, at Time Steps: (a) 900 s; (b) 1095 s; (c) 1115 s; and, (d) 1135 s.

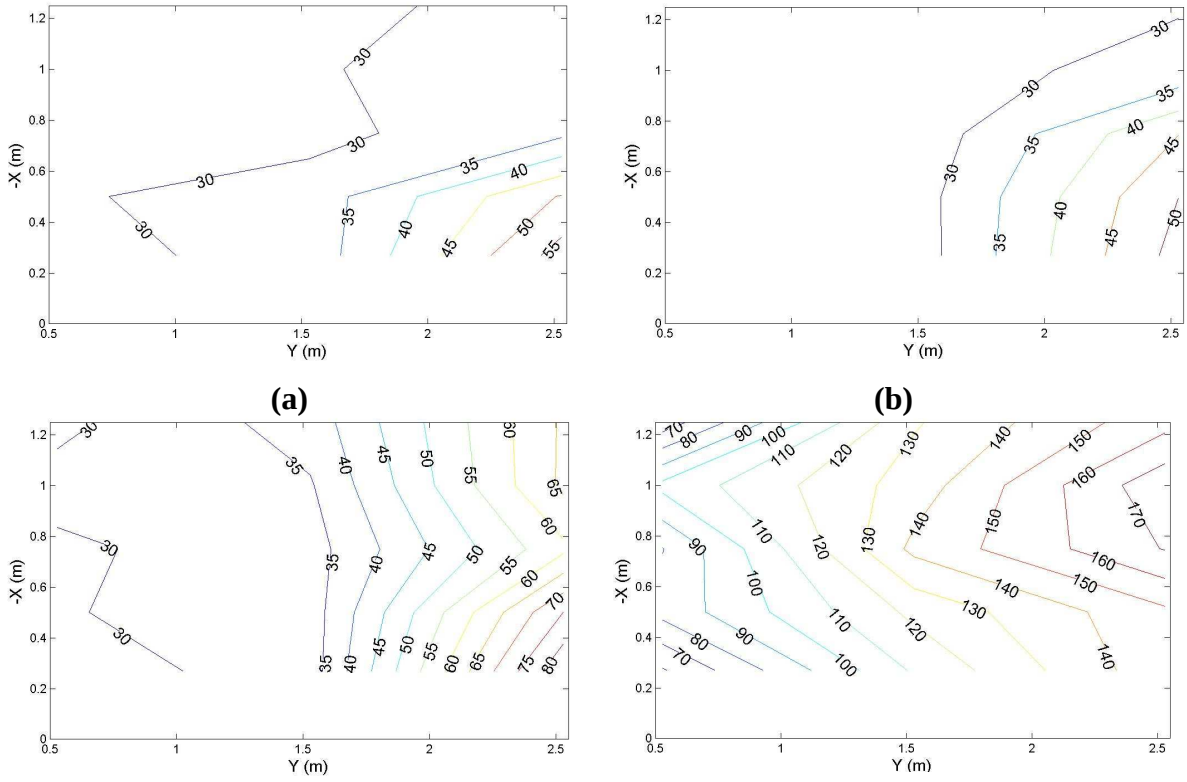

Figure D.38. The evolution of temperature contours through external section HOR8 which is defined by the horizontal plane at Z = 4.68 m, at Time Steps: (a) 900 s; (b) 1095 s; (c) 1115 s; and, (d) 1135 s.

Appendix E : Calculation of the Fire Load (density) in the Dalmarnock Fire Tests

The fire load in the Dalmarnock Fire Tests comprises of several different items of furniture as may be expected in a typical compartment used as a living room and/or office space. It is necessary to express this fire load in terms of mass of wood-equivalent, for comparison with the Law Model. While the larger items are taken into account, some of the mass values are approximated to take into account other minor items of the same composition. For some of the items, such as the bookcase, the net calorific value was obtained from large-scale calorimetry conducted on a near-identical item (full-laden with its contents) at the University of Edinburgh fire laboratory.

Material	**Net Calorific Value** (MJ/kg)	**Source**
Polypropylene	43	[2]
Polystyrene	40	[2]
Polyurethane foam	26	[2]
Particle board	18	[2]
Paper, Cardboard	17	[2]
Medium density fibreboard	41.6	[21]
Bookcase (with contents)	32.71	Lab. Experiment [122]

Table E.1. Net calorific value for different combustible materials found in the Dalmarnock Fire Test One fire load setup.

The main material the items are composed of is taken into account and the net calorific value for the respective material is taken from the literature, as listed in Table E.1. This enables a calculation of the approximate energy stored in each of the items as listed in Table E.2, which comes to a total of circa 10 GJ. Taking the heat of combustion of wood as 18.4 kJ/g [21], the Dalmarnock Fire Tests fire load is equal to **546 kg** in wood-equivalent. Given the floor areas is 17.1 m^2 and assuming a uniform fire load density throughout the floor area (as per the Law Model) the fire load density is found to be **31.91 kg/m^2** (~ 32 kg/m^2).

Item	**No. Items**	**Mass** (kg)	**Material**	**Energy** (MJ)
Sofa	1	34	Polyurethane foam	884
Bookcases (with contents)	3	53.1	(Lab. Experiments)•	5210.7
Work table	1	8.5	Particle board	153
Tiered computer desk	1	25.5	Particle board	459
Swivel chair (arms, seat, back)	2	5	Polystyrene	400
Swivel chair (seat, back)	2	1.5	Polyurethane foam	78
Comp. keyboard	2	0.46	Polystyrene	36.8
Comp. monitor	2	7	Polystyrene	560
Plastic paper trays	5	0.5	Polystyrene	100
Plastic cabinet (with contents)	1	5.7	Polypropylene	245.1
Large coffee table	1	10.5	Particle board	189
Coffee table	2	4.4	Particle board	158.4
Paper lamp (shade)	2	0.3	Paper	10.2
Floor lamp (shade)	2	0.5	Polypropylene	43
Plastic magazine box	2	1	Polypropylene	86
Magazines (box full)	2	42	Paper, cardboard	1428
Total				**10041.2**

•The bookcase and its contents are considered as a whole as net calorific values are available for the ensemble from laboratory calorimetry tests. While the bookcase comprises mainly particle board, it was laden with a number of items including: books, newspapers and magazines in cardboard filling boxes, video tapes, DVDs, *etc*.

Table E.2. Calculation of the approximate energy stored in each of the items of furniture comprising the fire load in the Dalmarnock Fire Tests.